

THESIS

MEASURING OCCUPATION SPAN AT TWO STONE CIRCLE SITES IN LARIMER
COUNTY, COLORADO

Submitted by

Halston F.C. Meeker

Department of Anthropology

In partial fulfillment of the requirements

For the Degree of Master of Arts

Colorado State University

Fort Collins, Colorado

Spring 2017

Master's Committee:

Advisor: Jason M. LaBelle

Michael Pante

Tobi Jacobi

Copyright by Halston F.C. Meeker 2017

All Rights Reserved

ABSTRACT

MEASURING OCCUPATION SPAN AT TWO STONE CIRCLE SITES IN LARIMER COUNTY, COLORADO

Stone circle sites are notorious for low artifact frequencies. This deters archaeological study because low artifact frequencies are thought to limit research potential. Two stone circle sites, Killdeer Canyon (5LR289) and T-W Diamond (5LR200) offer insight into short-term habitations, despite their low artifact frequencies. The two sites are located in northern Colorado, in the hogback zone along the Front Range of the Southern Rocky Mountains. The Colorado State University field school excavated the sites in 1982 and 1971 respectively. Artifacts from the interior of the features include lithic tools and debris, bone, and ceramics. This thesis examines each artifact class from excavated context as a proxy for understanding the length and number of occupations. Local and non-local chipped stone ratios, faunal procurement and processing strategies, and petrographic analysis are used to address how long and how many times each site was occupied. New radiocarbon dates show contemporaneity between rings at each site, dating Killdeer Canyon to the late A.D. 1600s and T-W Diamond to the late A.D. 1200s. These data demonstrate the ephemerality of the two sites but highlight potential differences in site use. While Killdeer Canyon likely represents a small group passing through an area, T-W Diamond could represent a larger group congregation, perhaps for hunting purposes. Furthermore, this thesis attests to the merit of using multiple lines of evidence to compensate for small sample sizes.

ACKNOWLEDGEMENTS

In 2013, when I first began the Master's program at CSU, I was immediately welcomed by the Center for Mountain and Plains Archaeology (CMPA) graduate students and volunteers. I cannot emphasize the importance of community in a graduate program enough, and I have yet to encounter another program that is as close and encouraging as the CMPA. It is undoubtedly because of Jason LaBelle that this sense of community and inspiration is fostered and passed down through each groups of students. I owe Jason not only for my Master's degree, but for the friendships, connections, and opportunities I have made during my program. Jason exudes a love and passion of archaeology that motivates everyone he teaches to visualize the world through an archaeological lens. Jason is an incredible advisor and was always available to help with class papers, discuss thesis research, and address other stresses, sometimes unrelated to schoolwork. It was his mentorship that helped me through the most challenging parts of the Master's program. Thank you, Dr J, I am so grateful to have been a part of the CMPA.

Thank you to the basement crew, both the graduate students who were around for my first year (Chris Johnston, Ben Perlmutter, and Kaitlyn Simcox), as well as the graduate students who came towards the end of my program (Julia Kenyon, Kate Yeske, Michelle Dinkel, and Kelton Meyer). I owe a big thank you to Aaron Whittenburg (my cohort) for being there every step of the way and always being available to bounce ideas off of, edit papers, or talk about the weather (specifically clouds). I truly appreciate the time Julia, Kate, and I spent together working on assignments and "decompressing." I also want to thank the other members of the Anthropology graduate program, I really enjoyed our Friday hangouts and hearing about the progress of each person's thesis research. I owe a big thank you, and apparently *several* beers, to Chris Johnston, who will always be a mentor. Thank you for always being available to help and for always

offering a solution, you make it seem so easy! I am so happy I had the opportunity to share an office and learn from you. Thank you, Michael Troyer, for your guidance and help as I finished my thesis. You are an excellent boss and I was excited to incorporate some of the many GIS skills you have taught me into my thesis.

I would like to thank my committee members, Jason LaBelle, Michael Pante, and Tobi Jacobi, for their helpful input on my thesis. It means a lot that you took the time to learn about my research. Thank you to the undergraduate rock stars of the Anthropology department. Particularly, thank you Lance Shockley, who volunteered hours of his time to sort artifact nodules. Also thank you to Noah Benedict who helped tremendously with conceptualizing my thesis in terms of statistics. I also want to thank Ashley Packard and Christina Burch for the fun times we shared in the basement as I worked on this thesis and they worked on their undergraduate Honor's theses.

I owe tremendous thanks to Richard Adams who was an early inspiration in my archaeological career and continually motivated me to be my best. Rich has an uncanny ability to seek his students' strengths and see that they pursue them to the best of their ability. I will forever remember our field school and I am so grateful that I had the opportunity to learn from you. Thank you!

This thesis would not have been possible without the Roberts Family, who have given CSU students tremendous opportunities in regard to archaeology and other studies. Thank you, Zach Thode, Ranch Manager for the Roberts Ranch, for allowing access to field crews and helping facilitate logistics. Thank you, Elizabeth Morris, and the 1971 and 1982 CSU field crews that excavated T-W Diamond and Killdeer Canyon.

I am also grateful for funding received from the CSU Department of Anthropology's Karen S. Greienr Fund, the Alice Hamilton Fund of the Colorado Archaeological Society, the Ward F. Weakly Memorial Fund from the Colorado Council of Professional Archaeologists; and the Dorothy Mountain Scholarship from the Loveland Archaeological Society. Thank you, to the Jim and Audrey Benedict foundation who, among this project, have helped fund countless CMPA endeavors, all of which have greatly contributed to my understanding of the Roberts Ranch and this thesis topic. Much of this research would not have been possible without you.

There are also members of the "outside" basement crew that made this thesis possible. Thank you, Erica Cheadle, Jessica Ericson (though once a basement dweller), Chelsey Oeffler, Carli Baum, and Jessica Petrie for your constant support and friendship. I know that the majority of my phone calls and text messages the past four years have been focused on my thesis, I promise to talk about other things now that my thesis is done!

I am forever grateful for my family. It is hard to put into words their unrelenting support and ability to encourage me. Their constant interest and curiosity in my research continually excited me to pursue my topic further and more in depth. Thank you, Mom and Dad, for the positive values and outlook you have instilled in me. I feel fortunate to have been raised by such wonderful people. You two are a model for acceptance, unconditional love, and generosity and I hope to carry these positive outlooks with me through each job/opportunity I have in the future. Thank you, Evan, for being such a great big brother and always knowing how to make me laugh.

Thank you, Spencer Pelton, for all of your help with research, figures, wording, ideas, etc. Your patience and support through this process has meant the world to me and I know I could not have done it without you. Thank you for always encouraging me to do my best as well as telling me when to stop! Although you're a great weekend typing partner, I cannot wait to see

the adventures that await us after graduate school. Good luck finishing your dissertation, I'll be there every step of the way as you were for me.

TABLE OF CONTENTS

ABSTRACT.....	ii
ACKNOWLEDGEMENTS.....	iii
LIST OF TABLES.....	ix
LIST OF FIGURES.....	x
CHAPTER 1: INTRODUCTION AND THEORETICAL FRAMEWORK.....	1
Statement of Objectives.....	3
Theoretical Framework.....	3
Site Overviews.....	5
History of Investigation at Killdeer Canyon (5LR289).....	7
History of Investigation at T-W Diamond (5LR200).....	12
Thesis Overview.....	16
CHAPTER 2: CHRONOLOGICAL SEQUENCE AND RING CONTEMPORANEITY.....	19
Theoretical Framework.....	19
Relative Dating Discussion.....	20
Absolute Dating Discussion.....	24
Methods – Radiocarbon and Thermoluminescence Dates.....	25
Killdeer Canyon Results – Radiocarbon and Thermoluminescence Dates.....	27
T-W Diamond Results – Radiocarbon and Thermoluminescence Dates.....	34
Discussion and Conclusion.....	40
CHAPTER 3: DEBITAGE ACCUMULATION AS A MEASURE OF OCCUPATION SPAN.....	42
Theoretical Justification for Debitage Analysis.....	42
Methods.....	45
Killdeer Canyon Debitage Results.....	45
T-W Diamond Debitage Results.....	54
Discussion and Conclusion.....	60
CHAPTER 4: FORMAL TOOL ANALYSIS AND OCCUPATION SPAN.....	62
Theoretical Justification for Tool Analysis.....	62
Methods.....	63
Killdeer Canyon Formal Tool Descriptions.....	63
Killdeer Canyon Formal Tool Analysis.....	66

T-W Diamond Formal Tool Descriptions	72
T-W Diamond Formal Tool Analysis	84
Discussion and Conclusion	91
CHAPTER 5: SUBSISTENCE AS A MEASURE OF OCCUPATION SPAN	92
Theoretical Justification for Faunal Analysis	92
Methods	96
Killdeer Canyon Results	96
T-W-Diamond Results	104
Discussion and Conclusion	110
CHAPTER 6: CERAMIC DESCRIPTION AND PETROGRAPHIC ANALYSIS	112
Theoretical Justification for Ceramic Analysis	112
Methods	113
Killdeer Canyon Ceramic Results	114
T-W Diamond Ceramic Results	117
Discussion and Conclusion	120
CHAPTER 7: CONCLUSION AND DIRECTION FOR FUTURE RESEARCH	122
REFERENCES CITED	128
APPENDIX	136
Appendix A: 5LR200 original 1970s survey area	136
Appendix B: AEON radiocarbon results	137
Appendix C: AEON sample information for submitted bone	139
Appendix D: 5LR289 debitage with provenience	140
Appendix E: 5LR289 tool attributes and metrics	145
Appendix F: 5LR289 photographs of all tools from excavated context and 2014 survey	146
Appendix G: 5LR200 debitage with provenience	150
Appendix H: 5LR200 tool attributes and metrics. Flayharty (1972) original curation number is noted in table	172
Appendix I: 5LR200 photographs of all tools from excavated context and 2014 survey	175
Appendix J: 5LR289 photographs from 1982 excavation.	188
Appendix K: 5LR200 photographs from 1971 excavation.	194
Appendix L: 5LR289 faunal data	201
Appendix M: 5LR200 faunal data.	209

LIST OF TABLES

Table 1: 5LR289 summary table of artifacts by feature. The presence of an artifact is denoted using “y” and the absence is denoted using “x.” Ambiguity in original excavation notes only suggests features that contain hearths, these are noted with a question mark.	8
Table 2: 5LR289 excavation grid size and location. Red rows indicate grid sizes that are ambiguous (written with a question mark) in original excavation notes.	10
Table 3: 5LR289 feature diameter (m) and area excavated (m ²).	11
Table 4: 5LR200 summary data from feature excavation.	13
Table 5: 5LR200 summary table of artifacts reported by Flayharty (1972:92) and Meeker (this document). “F” refers to artifact tallies from Flayharty (1972) thesis and “M” refers to artifact tallies from this analysis. The presence of an artifact is denoted using “y” and the absence is denoted using “x”.	14
Table 6: 5LR200 feature diameter (m) and area excavated (m ²). Area excavated was calculated including additional 1.6 ft. (0.8 ft. on either side of ring).	15
Table 7: 5LR289 projectile point metrics. Projectile points 5LR289.10 and 5LR289.11 do not contain provenience information but are still included in relative age discussion.	20
Table 8: 5LR200 projectile point metrics.	22
Table 9: 5LR289 radiocarbon calibration results using Calib 7.1 (Stuiver and Reimer 1993). ...	27
Table 10: 5LR289 thermoluminescence date.	33
Table 11: 5LR200 radiocarbon calibrated results using Calib 7.1 (Stuiver and Reimer 1993). ...	35
Table 12: 5LR200 thermoluminescence date.	40
Table 13: 5LR289 results from obsidian sourcing. Three flakes were sourced to Valle Grande, New Mexico. Trace elements are reported in table.	48
Table 14: 5LR289 Nodule ID and description.	54
Table 15: 5LR200 Nodule ID and description.	60
Table 16: Summary results for Killdeer Canyon and T-W Diamond. The two sites are compared relative to one another. If a site had a higher frequency or percentage of an item explored in this thesis, it received a plus. If a site had a lower frequency or percentage it received a minus, and if the two were almost equal, the sites both received an equals sign.	123

LIST OF FIGURES

Figure 1: Location of sites 5LR289 and 5LR200, Larimer County, Colorado.....	2
Figure 2: 5LR289 and 5LR200 site boundaries (red polygons).	6
Figure 3: 5LR289 Feature 5 excavation (1982). Notice entirety of interior ring has been excavated.	8
Figure 4: 5LR289 diagnostic projectile points 5LR289.001 and 5LR289.002 (left to right).	20
Figure 5: 5LR200 diagnostic projectile points with feature provenience.	22
Figure 6: 5LR289 variance comparison (F-Test, $\alpha = 0.01$) of all uncalibrated radiocarbon dates. F-Test results that show no significant difference in sigma ranges are highlighted in gray.	28
Figure 7: 5LR289 radiocarbon dates calibrated using Calib 7.1 (Stuiver and Reimer 1993). 2016 bone dates are reported in orange.	29
Figure 8: 5LR 289 Student’s t-test results (left) and Cohen’s d results (right). T-test results are significant at a 99% confidence interval.	30
Figure 9: 5LR289 probability distributions for each date. New bone dates highlighted in blue. Notice higher precision for 2016 dates.	31
Figure 10: 5LR289 summed probability distributions displaying original five radiocarbon dates (bottom) and distribution with two new bone dates (top) (Bronk Ramsey 2009).	32
Figure 11: 5LR200 variance comparison (F-Test, $\alpha = 0.01$) of all uncalibrated radiocarbon dates. F-Test results that show no significant difference in sigma ranges are highlighted in gray.	35
Figure 12: 5LR200 radiocarbon dates calibrated using Calib 7.1 (Stuiver and Reimer 1993). 2016 bone dates are reported in orange.	36
Figure 13: 5LR 200 Student’s t-test results (left) and Cohen’s d results (right). T-test results are significant at a 99% confidence interval.	37
Figure 14: 5LR200 probability distributions for each date. New bone dates highlighted in blue. Notice higher precision for 2016 dates.	38
Figure 15: 5LR200 summed probability distributions displaying original five radiocarbon dates (bottom) and distribution with two new bone dates (top) (Bronk Ramsey 2009).	39
Figure 16: Location of Killdeer Canyon, T-W Diamond in relation to Kinney Spring and Campbell Mountain quartzite.	44
Figure 17: 5LR289 normalized flake frequency by excavation area (m^2).	46
Figure 18: 5LR289 percentage of local and non-local debitage normalized by area excavated (m^2). Pie charts are weighted by flake frequency. Feature number is labeled directly above ring.	49
Figure 19: 5LR289 location in relation to the Valle Grande, New Mexico.	50
Figure 20: 5LR289 relative thickness of local and non-local debitage by feature.	51
Figure 21: 5LR289 nodule dispersal between rings normalized by excavated m^2 . Pie charts are weighted to represent the frequency of debitage.	53
Figure 22: 5LR200 normalized flake frequency by excavation area (m^2).	55

Figure 23: 5LR200 percentage of local and non-local debitage normalized by area excavated (m ²). Pie charts are weighted by flake frequency. Feature number is labeled directly above ring.	57
Figure 24: 5LR200 relative thickness of local and non-local debitage by feature.	58
Figure 25: 5LR200 nodule dispersal between rings normalized by excavated m ² . Pie charts are weighted to represent the frequency of debitage.	59
Figure 26: 5LR289 frequency of bifaces and other tools by feature. Images of tools (not to scale) are displayed in chart.	68
Figure 27: 5LR289 percentage of local and non-local tools normalized by square meters excavated. Pie charts are weighted by tool frequency. Feature number is labeled directly above ring.	69
Figure 28: 5LR289 mean per capita occupation span. Local and non-local material (x-axis) includes all tools, flakes, etc. Diagram on right depicts logged values.	70
Figure 29: 5LR289 frequency of local and non-local tools (bar chart) and percentage of local and non-local debitage with pie chart weighted by debitage frequency.	72
Figure 30: 5LR200 steatite tool fragment, likely pipe.	83
Figure 31: 5LR200 frequency of bifaces and other tools by feature. Images of tools (not to scale) are displayed in chart.	87
Figure 32: 5LR200 percentage of local and non-local tools normalized by square meters excavated. Pie charts are weighted by tool frequency. Feature number is labeled directly above ring.	88
Figure 33: 5LR200 mean per capita occupation span. Local and non-local material (x-axis) includes all tools, flakes, etc. Diagram on right depicts logged values.	89
Figure 34: 5LR200 frequency of local and non-local tools (bar chart) and percentage of local and non-local debitage with pie chart weighted by debitage frequency.	90
Figure 35: 5LR289 bone mass (g) by feature number normalized by excavation area (m ²). Feature 7 is highlighted in gray because there is no associated stone circle. The area likely represents an outside processing station.	97
Figure 36: 5LR289 species representation by feature.	98
Figure 37: 5LR289 bone tool, likely flesher. White arrow points at polished end with grooves.	100
Figure 38: Killdeer Canyon (5LR289) frequency and mass (g) of bone fragments by feature. .	101
Figure 39: 5LR289 element dispersal displayed in pie charts weighted by bone frequency normalized by area excavated (m ²). Feature number is labeled directly above pie chart.	103
Figure 40: 5LR200 bone mass (g) by feature number normalized by excavation area (m ²).	105
Figure 41: 5LR200 species representation by feature.	106
Figure 42: 5LR200 frequency and mass (g) of bone fragments by feature.	107
Figure 43: 5LR200 element dispersal displayed in pie charts weighted by bone frequency normalized by area excavated (m ²). Feature number is labeled directly above pie chart.	109

Figure 44: Figure adapted from Varien and Ortman (2005:144). Red arrow points near origin where stone circle sites would fall on scatterplot. Figure highlights the need for adapting accumulation rate methods to short-term hunter-gatherer sites..... 113

Figure 45: 5LR289 pottery sherds from Feature 7. The four sherds were selected for petrographic analysis, completed by Ownby (2015). 115

Figure 46: 5LR289 location of pottery used in thin-section analysis. Thin sections are displayed in top left corner of image. Thin-section images from Ownby (2015:17) showing shale-derived clay paste with sand temper. 117

Figure 47: 5LR200 pottery sherds from Feature 11. The five sherds were selected for petrographic analysis, completed by Ownby (2015)..... 118

Figure 48: 5LR200 location of pottery used in thin-section analysis. Thin sections are displayed in bottom left corner of image. Thin-section images from Ownby (2015:18) showing sedimentary clay paste..... 120

CHAPTER 1: INTRODUCTION AND THEORETICAL FRAMEWORK

“Stone circles” are one of the most ubiquitous prehistoric archaeological features in the Great Plains. The term subsumes a variety of feature types, from ceremonial structures such as medicine wheels (Grinnell 1922), to multiple course stone structures (Schroeder 2015) to the remains of expedient shelters, or stone circles. This thesis focuses on the Great Plains and Foothills physiographic regions, where stone circles typically refer to the foundations of hide structures, otherwise known as tipis.

This analysis uses the term “stone circle” in reference to spaced-rock features, which are the inorganic remnants of Native American habitation features, commonly referred to as ‘tipis’. The rock rings serve as guides for archaeological investigation because they roughly delineate the extents of interior, domestic space. Ethnographic images depict tipis as conical structures that are secured using rocks or wooden pegs (Banks and Snortland 1995; Kehoe 1958). Although we cannot assume all stone circles are the remnants of the iconic conical “tipi” (Brasser 1982), we can assume that the artifacts recovered from the rings can indicate differences in occupation length, use intensity, and ultimately hunter-gatherer mobility. Kehoe (1958:4), in an article examining stone circle sites in Alberta and Montana, stated “...all that can be expected from the excavation of a tipi ring are a few bone fragments, flint and obsidian (not native to the region) flakes and perhaps broken points, rough hammerstone, and an occasional grooved maul.”

In other words, stone circle sites are notorious for having small artifact assemblages. This often deters archaeological investigation because researchers assume little information can be extracted from such small datasets. This may be true, but small artifact assemblages are precisely what should be expected from residential structures that represent short architectural

occupations. In the context of the spectrum of forager residential occupation length and complexity, stone circles exist towards the simple end, while permanent residential structures fall on the other.

This study develops a suite of analytical tools to understand the number and lengths of residential occupations (here forth referred to as occupation span) at Killdeer Canyon (5LR289) and T-W-Diamond (5LR200), two stone circle sites located on the Roberts Ranch, north of Livermore, Colorado (Figure 1). To circumvent small artifact assemblages, this study employs multiple lines of evidence to explore residential use, including lithic, faunal, ceramic, and radiometric analyses. Combined, these analyses better situate these sites on a continuum of residential occupation, thereby better contextualizing these often-overlooked archaeological features.



Figure 1: Location of sites 5LR289 and 5LR200, Larimer County, Colorado.

Statement of Objectives

This thesis intends to address the following overarching question: how can we use stone circle habitation sites to understand prehistoric occupation span and Native American groups returning to place? Returning to place, or purposefully returning to the same location on the landscape, suggests groups were incorporating a particular place into seasonal rounds or returning through time for other cultural reasons. Specifically, this thesis addresses the following questions (1) What is the length of occupation on a broad spectrum ranging from short-term sites occupied for a few days to long-term sites occupied for years and (2) Do the sites represent one or many occupations at Killdeer Canyon and T-W Diamond? Specific expectations for individual artifact classes are listed at the beginning of each chapter.

Theoretical Framework

In this section, I acknowledge assumptions in my thesis. There is tremendous variation in household structure types in the archaeological record (Ranere et al. 1969; Quigg 1979). These differences vary both in time and space and are attributed to social, economic, and environmental factors (Binford 1990). Examining household features in the archaeological record is important because they frame domestic occupations and allow archaeologists to address questions regarding household construction, maintenance, and abandonment. As previously stated, stone circle site analyses provide an important delineation of interior and exterior space.

There are methods not used in this thesis that can accurately assess ring contemporaneity, most effectively artifact refit analysis. These methods were not, however, attempted because the detailed analyses were beyond the scope of this thesis. This study provides a foundation for future research and will better indicate in what rings refitting analyses will be most beneficial. Although artifact refitting is effective, I argue that analyses of all artifact classes can also

indicate occupational contemporaneity at stone circle sites. This study is a first step in understanding ring contemporaneity and occupation length. Several hypotheses are created based on the results of this thesis which can be tested in the future.

Furthermore, as is the case with other stone circle sites, Killdeer Canyon and T-W Diamond do not contain high artifact frequencies, and small sample sizes prevent comprehensive analyses. Therefore, the power of multiple broad-scale artifact analyses is used in this thesis rather than a small-scale analysis of one artifact class.

Stone circle habitation features differ from other structure types because they are designed to be relatively short-term and the exterior hides to be transportable. I examine habitation features as individual units of analysis and I assume that temporary households are not reoccupied. The assumption that rings are not reoccupied is supported by four lines of evidence: (1) the return to the same place but lack of stratified stone circles, (2) the lack of evidence of rock robbing, (3) and frequency variation between stone circle sites. The first and second lines of evidence go hand in hand. There is evidence of return to the same place through time. Two sites in particular represent the returning of Native Americans to the same place. The Smoky Hill River and Indian Village contain buried stone circle features directly under more recent features (Raynesford 1953). There is sterile ground between the features indicating that while groups returned to the same place through time, they did not maintain and camp in the same household features. If there is return to the same place, there is the potential to see multiple component, or stratified stone circle sites. Instead, sites that are occupied repeatedly contain features that have been “robbed” of rocks (Cassells and Farrington 1986; Malouf 1961) where missing rocks from stone circles are thought to have been used as weights for structures in subsequent occupations. This suggests that although subsequent occupations were returning to the same place, they were

not camping on already established rock ring surfaces. Third, there is variation in the frequency of stone circles at sites. Finnigan (1982:11) states that clusters of fifty or more stone circles automatically suggest multiple occupations based on ethnographic knowledge of band societies (Steward 1936; Williams and Wobst 1974). It is more likely that high frequencies of stone circles reflect multiple occupations rather than large group numbers. These three lines of evidence indicate that hunter-gatherer groups were returning to the same places on the landscape; however, were not camping in already established stone circle features. Thus, excavated stone circles present opportunities for examining separate occupation episodes.

This study is grounded primarily in accumulations research. Accumulation theories examine site formation processes (Nelson et al. 1994; Varien and Mills 1997) and assume that artifacts types with predictable discard rates, such as debitage and pottery, have increasing frequencies over time (Nelson et al. 1994:128). Therefore, a higher discard rate, or higher frequency of that artifact class, suggests a longer occupation span. It is important to note that artifacts can accumulate at similar rates from different occupation scenarios. For example, a site that is occupied by a small group for a long period can have a similar artifact accumulation rates as a site that is occupied by a large group for a short period. These scenarios are further complicated by the reuse of hunter-gatherer sites over time. Because the rings are treated as individual units of analysis, this thesis creates expectations regarding artifact patterning across the site to help differentiate between the two scenarios.

Site Overviews

Killdeer Canyon and T-W Diamond are located in the foothills of the Southern Rocky Mountains, within the hogback zone on the eastern side of the Medicine Bow Mountains. The

sites are situated at the ecotone of the short grass Plains and the Rocky Mountains providing the inhabitants of the area with an abundance of flora, fauna, and tool stone resources.

The sites are found one kilometer apart but separated by nearly 500 years of prehistory (Figure 2). The hogback zone provides a shield from harsh winter weather making this area habitable year round. The Roberts Ranch, where Killdeer Canyon and T-W Diamond are located, is home to hundreds of known cultural resources, some of which represent winter occupations (see Perlmutter 2015 for an example of a long term permanent occupation). Thus, the area would have been suitable for permanent residential sites, but also used by hunter-gatherer groups passing through on a seasonal basis.

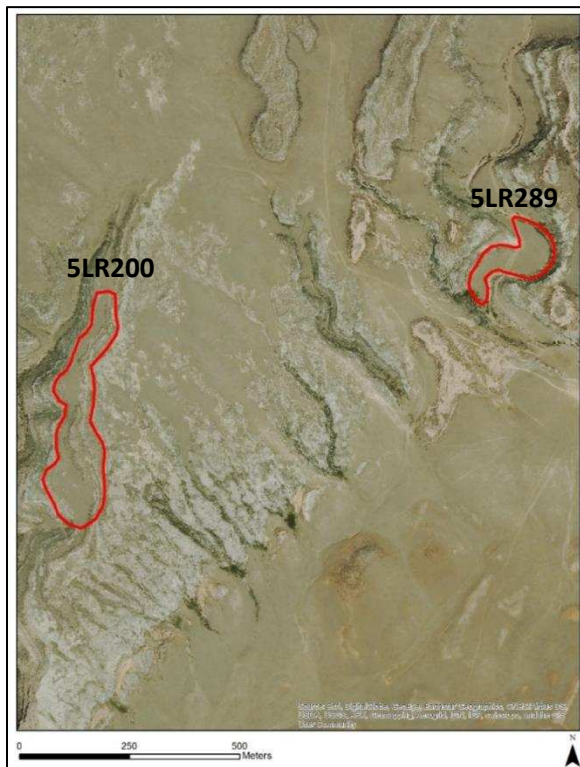


Figure 2: 5LR289 and 5LR200 site boundaries (red polygons).

History of Investigation at Killdeer Canyon (5LR289)

Howie Davidson and seven other crew members first recorded Killdeer Canyon in 1973 (see Appendix J for original excavation photos). The original site card, stored at the Archaeology Repository, CSU, noted the crew spent two hours recording the site and found at least 14 partial and complete stone circles. Concentrations of fire-cracked rock and flakes were also noted at the site.

Following the site's initial recording, the Colorado State University (CSU) archaeological field school excavated Killdeer Canyon, under the direction of Dr. Elizabeth Ann Morris, in 1982. The field school identified thirteen stone circles lining a terrace edge near a natural spring. The rings are positioned at a valley bottom, surrounded by canyon walls making the visibility of the surrounding landscape poor. The excavation yielded an assemblage consisting of chipped stone debitage, formal chipped stone tools, pottery, faunal remains, and a bone tool (Table 1). Sandstone fragments, thought at the time to be ground stone, were collected from the 1982 excavation. Although the fragments contain light polish, investigations of the site by CSU in 2014 found natural outcroppings of sandstone slabs in Spring Gulch, within the site boundary. The author did not find sufficient evidence that the collected sandstone slabs were culturally modified, but instead eroded by natural processes. Thus, ground stone is not included in this analysis as an artifact type.

Eight of the 13 rings noted in 1982 were excavated. One of the eight features did not contain rocks and was noticed when pottery was found on the surface near the edge of the terrace. Collected charcoal samples from excavation provided five radiocarbon dates for the site that are published in Morris (1989) (see Chapter 2). The site is associated with the Late Ceramic period, A.D. 1540-1860 (Gilmore 1999).

Table 1: 5LR289 summary table of artifacts by feature. The presence of an artifact is denoted using “y” and the absence is denoted using “x.” Ambiguity in original excavation notes only suggests features that contain hearths, these are noted with a question mark.

Artifacts	Provenience (by Feature)							Total
	1	2	3	4	5	6	7	
Pottery	x	x	x	x	x	x	478	478
Points	1	x	x	x	1	x	1	3
Other Tools	x	1	1	1	x	x	3	6
Flakes	29	18	19	10	46	4	62	188
Hearths	y?	y?	?	?	y?	y?	?	4?
Charcoal	x	y	x	x	y	y	x	3
Bone (g)	0.3	0.2	3.1	28.6	48.7	47.3	140.1	268.3

Under the direction of Dr. Jason LaBelle, the 2014 CSU field school revisited the site and extensively mapped and measured stone circle features using a total station and other grid-mapping techniques. These data are archived at the Center for Mountain and Plains Archaeology, Department of Anthropology, CSU.



Figure 3: 5LR289 Feature 5 excavation (1982). Notice entirety of interior ring has been excavated.

The focus of this analysis is on artifacts from the 1982 excavation. Artifact frequencies for Chapters 3-6 are standardized by square meters excavated for each ring. These methods varied slightly between Killdeer Canyon and T-W Diamond due to differences in excavation methods and are described separately. Excavation at Killdeer Canyon was not focused on the interior space of features. Excavation grids were primarily 3 x 3 meters unless otherwise noted, and included both interior and exterior space (Table 2). While interior and exterior space was excavated at Killdeer Canyon, photographs from the 1982 excavation show rings were excavated in their entirety (Figure 3). While the exact location of artifacts in grids is not known, flakes that were found within features were labeled with the feature number. Therefore, only items that contained feature provenience labeled on the artifact itself were used in this analysis.

For the purpose of this analysis, the author standardizes artifact frequencies by feature area. The 1982 field notes did not explicitly state the square meters excavated for each feature, however, based on the photographic evidence that Features 1-6 (Feature 7 is not a ring and is discussed separately) were excavated in their entirety, and because only artifacts with feature provenience were included, stone circle area is an appropriate measure for standardization. Feature 8 did not yield any artifacts with interior feature provenience and is not discussed in this analysis.

Table 2: 5LR289 excavation grid size and location. Red rows indicate grid sizes that are ambiguous (written with a question mark) in original excavation notes.

Grid Size (m)	Grid	E/W	Grid	N/S	Comments
3x3	6	E	24	S	
3x3	6	E	27	S	
3x3	9	E	24	S	
3x3	9	E	27	S	
3x3	9	E	30	S	
1x4	12	W	25	S	question mark in notes
2x2	15	W	25	S	
3x3	15	W	27	S	
1x4	16	W	30	S	question mark in notes
2x2	17	W	25	S	
2x2	17	W	27	S	
3x3	18	E	12	S	question mark in notes
3x3	18	E	15	S	question mark in notes
3x3	21	E	15	S	
3x3	21	E	18	S	question mark in notes
3x3	21	E	21	S	
3x3	21	E	24	S	
3x3	21	E	27	S	
3x3	24	E	18	S	
3x3	24	E	21	S	question mark in notes
3x3	27	E	18	S	question mark in notes
3x3	27	E	21	S	
3x3	30	E	18	S	
3x3	30	E	21	S	
3x3	30	E	24	S	
1x3	36	W	24	S	question mark in notes
3x3	39	E	6	S	
3x3	39	E	9	S	
1x1	39	W	23	S	
3x3	39	W	24	S	
3x3	42	E	9	S	
3x3	42	W	24	S	
3x3	51	W	33	S	
3x3	51	W	36	S	
3x3	54	W	33	S	
3x3	54	W	36	S	
3x3	57	W	39	S	
3x3	60	W	39	S	
Total: 303 m²					

Table 3: 5LR289 feature diameter (m) and area excavated (m²).

Feature #	Feature Diameter (m)	Area Excavated (m²)
1	7.1	39.6
2	6.1	29.2
3	6.3	31.2
4	6.7	35.2
5	6.0	28.3
6	4.3	14.5
7	NA	36.0

Original maps of Features 1-6 drawn to scale were used to calculate feature diameter (Table 3). Features 1-5 were complete circles and were measured from the exterior edges of the rock ring. Rocks drawn on the map but not obviously part of the rock ring were not included in diameter measurement. Feature 6 is a partial ring and was measured by inferring the diameter of the ring from the half circle. The plan-view map of Feature 6 shows a charcoal stain in the center of the circle, thus making it easy to infer the diameter of the complete feature. Feature 7 is not a stone ring and the meters excavated are calculated differently. While the area excavated is not explicitly stated, artifacts with both feature and grid provenience were used to calculate the extent of Feature 7 excavation. The number of grids containing artifacts labeled “Feature 7” were compared to the grid notes to calculate square meters excavated. It is the author’s best guess that Feature 7 was excavated in six 3x3 meter grids, though the final 1982 excavation map is somewhat conflicting and shows irregularly shaped grids that follow the edge of the cut bank. For the purpose of this analysis, the author relies on the original field notes rather than the shape of the grids on the later produced site map.

History of Investigation at T-W Diamond (5LR200)

T-W-Diamond was excavated by the CSU archaeological field school under the direction of Dr. Morris in the summer of 1971 (see Appendix K for original excavation photos). The site has a total of 47 stone circles and is positioned on a ridge-top with a 360-degree view of the surrounding landscape. A natural spring is located one mile east of the site. The site contains chipped stone debitage, formal chipped stone tools, pottery, faunal remains, and a soapstone pipe fragment. There are two formal publications on T-W-Diamond. The first is a Master's thesis by Ross Flayharty (1972), and the second is an article published by Flayharty and Morris (1974). Radiocarbon dates (see Chapter 2) associate the site with the Middle Ceramic period, A.D. 1150-1540 (Gilmore 1999).

The following section describes the 1971 excavation methods from Flayharty (1972). The rings were excavated by field school students in groups of 2-4; because of student's excavation inexperience. Excavation began outside of the ring in test pits and trenches and slowly progressed towards the feature. One of the main goals of excavation was to locate the living floor of features, and students were instructed on careful excavation in order to recognize any soil changes that included color, texture, artifact densities, etc. During the initial test pit and trench excavations, no naturally occurring stratigraphic levels were found so the students dug in arbitrary 0.5 ft. levels. These test pits and trenches were dug until the edge of a stone circle feature was reached and then stopped. Next, test trenches were dug at right angles in the center of the features maintaining 0.5 ft. arbitrary levels. Once the trenches were completed within the stone circle features, the students excavated the remainder of the circles in 0.25 ft. arbitrary levels. Unfortunately, no living floors were detected within the 17 rings that were tested or excavated.

Table 4: 5LR200 summary data from feature excavation.

Feature #	Fully Excavated?	Hearth?	Grid Location	Comments
1	x	x	x	Not a Feature
2	Yes	Yes	C-2, D-2, C-3, D-3	
3	"Conservative Trenches"	No	D-5	
4	Yes	Yes	C-5, D-5, C-6	
5	x	x	x	Not a Feature
6	Yes?	?	M-1	
7	Yes?	No	L-2, L-3, M-2, M-3	
8	"Partially Complete"	?	D-22, E-22	
9	Yes?	No	D-23	
10	Yes	Yes	C-18, C-19	
11	Yes?	Yes	B-21	
12	No	Yes	O-96	
13	No	No	S-92	
32	Yes	Yes	R-92	
35	No	No	Outside Grid	
38	No	No	Outside Grid	
39	No	Yes	Outside Grid	

Excavation boundaries of features were extended 0.8 ft. outside of the feature on all sides and dug to a 0.5 ft. depth. Artifact densities were noted to be greatest between 0.1-0.4 ft. (below surface). Artifacts found below this depth were noted to be a result of rodent burrows. All back dirt was screened in a ¼ inch mesh. In a later publication, Morris et al. (1983:50) noted that the areas outside of the rings contained less than one artifact per square meter with no indication of any exterior activity areas. Therefore, and unlike the rings at Killdeer Canyon, the majority of artifacts are safely assumed to be from the interior of excavated features.

Table 5: 5LR200 summary table of artifacts reported by Flayharty (1972:92) and Meeker (this document). “F” refers to artifact tallies from Flayharty (1972) thesis and “M” refers to artifact tallies from this analysis. The presence of an artifact is denoted using “y” and the absence is denoted using “x”.

Artifacts	Provenience (by Feature)																								Total			
	2		3		4		6		7		8		9		10		11		12		13		32		39		F	M
	F	M	F	M	F	M	F	M	F	M	F	M	F	M	F	M	F	M	F	M	F	M	F	M	F	M		
Pottery	x	x	x	x	x	x	x	x	x	x	x	x	x	x	x	139	139	x	x	x	x	x	x	x	x	139	139	
Points	1	x	3	1	x	x	1	2	1	x	5	4	x	x	6	1	2	4	2	1	x	x	7	5	1	29	18	
Other Tools	9	4	3	3	11	2	7	4	7	1	7	6	1	1	4	5	2	0	2	7	x	x	4	2	x	57	35	
Flakes	93	90	60	63	218	231	55	49	45	45	46	44	4	4	321	317	28	28	48	46	3	3	34	34	8	8	963	962
Hearths	1	x	x	x	1	x	?	x	x	x	?	x	x	x	1	x	1	x	1	x	x	x	1	x	1	x	7	
Charcoal	y	y	y	y	y	y	y	y	y	y	y	y	y	y	y	y	y	y	y	y	x	x	y	y	x	x		
Bone (g)	y	42.6	y	28.1	y	62.9	x	x	x	x	x	0.7	x	1.6	y	25.0	y	0.8	y	0.3	x	x	y	x	x	x	162.0	

Table 6: 5LR200 feature diameter (m) and area excavated (m²). Area excavated was calculated including additional 1.6 ft. (0.8 ft. on either side of ring).

Feature	Fully Excavated?	Diameter in feet	Diameter + 1.6 ft.	Diameter (including 1.6 ft.) in meters	Radius (m)	Total Area Excavated (m)
1		x				
2	Yes	16.5	18.1	5.5	2.8	23.9
3	"Conservative Trenches"	18.0	19.6	6.0	3.0	28.0
4	Yes	16.0	17.6	5.4	2.7	22.6
5		x				
6	Yes?	18.0	19.6	6.0	3.0	28.0
7	Yes?	16.0	17.6	5.4	2.7	22.6
8	Yes?	14.6	16.2	4.9	2.5	19.1
9	Yes?	14.5	16.1	4.9	2.5	18.9
10	Yes	17.5	19.1	5.8	2.9	26.6
11	Yes?	16.5	18.1	5.5	2.8	23.9
12	No	18.7	20.3	6.2	3.1	30.1
13	No	16.5	18.1	5.5	2.8	23.9
32	Yes	17.5	19.1	5.8	2.9	26.6
35	No	16.0	17.6	5.4	2.7	22.6
38	No	16.3	17.9	5.5	2.7	23.4
39	No	17.5	19.1	5.8	2.9	26.6

Table 4 summarizes excavation data from Flayharty (1972) and Table 5 summarizes the artifact frequencies within rings. While the excavation volume cannot be calculated because of inconsistent excavation depths that are not reported, the area excavated within each ring can be presumed using the ring diameter. As noted above, rings were excavated beginning with a trench through the center and then, if there was time, excavated 0.8 ft. from the exterior of the feature. The excavation notes in Flayharty (1972) do not explicitly state whether all rings were partially or entirely excavated, therefore, other maps and photographs are used to determine excavation completeness. In order to standardize artifact frequencies by feature, the area of stone ring was calculated. Flayharty (1972:92) notes the diameters in feet of each ring. Diameters of each ring (including the 0.8ft. excavated on each side of the feature wall) were converted to meters before the area of each ring was calculated (Table 6).

Thesis Overview

This analysis combines evidence from all artifact classes collected during the 1970s and 1980s excavations. Chapter 2 builds a chronological sequence using relative and absolute dating measures. These data are used to argue ring contemporaneity within each site. Showing ring contemporaneity provides a necessary platform for examining the site assemblages as a whole. While artifact signatures within individual rings are examined, ultimately the purpose of this thesis is to situate Killdeer Canyon and T-W Diamond on an occupation length continuum. Situating the two sites on the continuum is accomplished by examining artifact types and frequencies from a site level.

Chapter 3 addresses the number and length of occupations at each site using debitage frequency, relative thickness, and local and non-local material use. Debitage frequencies are quantified as a proxy of occupation length. This follows the assumption that the longer a group

remains on site; the more refuse, or debitage is produced. Relative thickness is used to determine local and non-local debitage size as a measure of reduction stage and local material replenishment. Lastly, percentages of local and non-local materials are used to determine the length of occupation both in individual rings and at a site level. This proxy is an appropriate measure of occupation length due to the sites proximity (within 3 kilometers) of a raw material source. Patterned local and non-local material use between rings and ring clusters supports both Killdeer Canyon and T-W Diamond as single occupation sites.

The purpose of Chapter 4 is twofold. First, all formal tools from Killdeer Canyon and T-W Diamond are described. Second, formal tools are used as a proxy for the number and length of occupations. This is accomplished using tool frequencies, local and non-local tool percentages, and the mean per capita occupation span. These data are compared to results from Chapter 3. Tool frequencies are used as a proxy for occupation length by following the assumption that more tools will be used and discarded as a group remains in one place for longer. By examining local and non-local tool percentages, it is possible to determine the degree of retooling that took place on site. Local and non-local material ratios of tools and all other artifacts are then used to establish the mean per capita occupation span as defined by Surovell (2008). Lastly, the tool data are compared to the debitage within each ring and at a site level.

Chapter 5 examines faunal remains as a measure of occupation span. This is accomplished by examining bone mass, degree of processing, species representation, bone modification, and element representation. Because there is no evidence of plant processing, bone mass is used to assess how long the occupants of the two sites could have subsisted off of fauna alone. The degree of processing is examined as a measure of occupation length following the assumption that the longer occupants remain in one location, the greater the degree of

processing. Species representation is used to make an argument for ring contemporaneity. While lithic materials come in a variety of different sized packages, fauna have an explicit number of elements. If peoples are sharing one or two animals at camp, the MNI and element distribution can be mapped between different features. This allows species and element distribution to be used as a measure for ring contemporaneity.

Chapter 6 uses petrographic analysis of pottery fragments from Killdeer Canyon and T-W Diamond to hypothesize whether vessel(s) were manufactured on or off-site. This is part of a larger project through the Center for Mountain and Plains Archaeology (see Chapter 6). These data are used as a proxy for the relative time a group would need to remain on camp to manufacture a vessel. Pottery fragments are only present in one feature at each site and could not be used to assess ring contemporaneity. The pottery styles from each site are also briefly described and discussed in terms of cultural affiliation.

CHAPTER 2: CHRONOLOGICAL SEQUENCE AND RING CONTEMPORANEITY

The purpose of this chapter is to examine all relative and absolute dating methods available for Killdeer Canyon and T-W Diamond. First, the relative dates are determined using diagnostic tools, such as projectile point types. Pottery is also a good method of relative dating and is discussed briefly in Chapter 6. Second, absolute dates are examined using a summed probability distribution to test statistical contemporaneity between features. This chapter uses preexisting radiocarbon dates, submitted in the 1970s and 1980s by Elizabeth Morris, as well as four new bone dates from Killdeer Canyon and T-W Diamond.

Theoretical Framework

This chapter tests the assumption that a single occupation site should have rings with statistically contemporaneous date ranges. The results of this chapter provide the necessary evidence for examining occupation span in the following chapters. It is important to note that statistically contemporaneous radiocarbon dates do not definitively suggest a site is one occupation. The precision of radiocarbon dating, though vastly improved from the 1970s, cannot separate occupations that occurred within a couple years of each other. Thus, the artifact analyses in this thesis are used as a secondary line of evidence, testing expectations on the artifact signatures a single versus multiple occupation site would produce (see Chapter 1).

Relative Dating Discussion

Killdeer Canyon Projectile Point Types

There are five diagnostic projectile points from Killdeer Canyon (5LR289.001, 5LR289.002, 5LR289.010, 5LR289.011, and 5LR289.212). Two contain feature provenience (5LR289.001 and 5LR289.002) and are discussed in this chapter. The following section compares point types to other types in this region. For a description of the projectile points see Chapter 4.



Figure 4: 5LR289 diagnostic projectile points 5LR289.001 and 5LR289.002 (left to right).

Table 7: 5LR289 projectile point metrics. Projectile points 5LR289.10 and 5LR289.11 do not contain provenience information but are still included in relative age discussion.

CMPA Curation Number	Feature	Max Length (mm)	Max Width (mm)	Thickness (mm)	Mass (g)
5LR289.001	7	22.8	13.9	2.9	1.1
5LR289.002	1	21.6	13.6	3.9	1.3

Both projectile points from Killdeer Canyon compare to Late Prehistoric side-notched types (Figure 4) (Kehoe 1966). Despite subtle differences in size and reduction stage, the

projectile points from Killdeer Canyon are almost identical in dimensions (Table 7). Projectile points 5LR289.001 and 5LR200.002 have nearly identical dimensions, all within one millimeter. Item 5LR289.002 looks more rounded than 5LR289.001 because of small fractures on the ears and notches. Inferring the form before the tool was broken, 5LR289.002 would have been very similar in shape to 5LR289.001. Items 5LR289.001 and 5LR289.002 are similar to side-notched point types from the Roberts Buffalo Jump (5LR100) (Johnston 2016:59) a Late Ceramic bison jump, dating to the late A.D. 1600s, approximately three kilometers southwest of Killdeer Canyon (Johnston 2016:75). Johnston (2016:75) recently submitted five bison bone samples for radiocarbon dates, four of which (165 \pm 25 RCYBP, 190 \pm 25 RCYBP, 210 \pm 25 RCYBP, and 185 \pm 25 RCYBP) came back in the late 1600s calibrated range, overlapping with Killdeer Canyon. As Johnston (2016) mentions in his analysis, a brief attempt was made to find a lithic association between the jump site and Killdeer Canyon occupants, though no artifact refits were found. Both Johnston (2016) and the author of this thesis believe this hypothesis would be worth exploring in the future. The projectile point types are also remarkably similar to the Upper Boxelder Creek Bison Kill (UBE), in Laramie County, Wyoming (Meeker et al. 2013). UBE is also a Late Prehistoric aged bison kill, likely pound site, that dates to 380 \pm 20 B.P., cal A.D. 1446-1522 (71.3%) or cal A.D. 1575-1624 (24.1%) (OxCal 4.2, Reimer et al. 2013).

T-W Diamond Projectile Point Types

Nine diagnostic projectile point and point fragments (5LR200.001, 5LR200.003, 5LR200.005, 5LR200.011, 5LR200.014, 5LR200.015, 5LR200.016, 5LR200.020, and 5LR200.026) were collected from the T-W Diamond rings. The projectile points can be separated into five sub-types, all associated with the Late Prehistoric era (Figure 5). Projectile

point metrics are summarized in Table 8. For a description of projectile point form and manufacture, see Chapter 4.

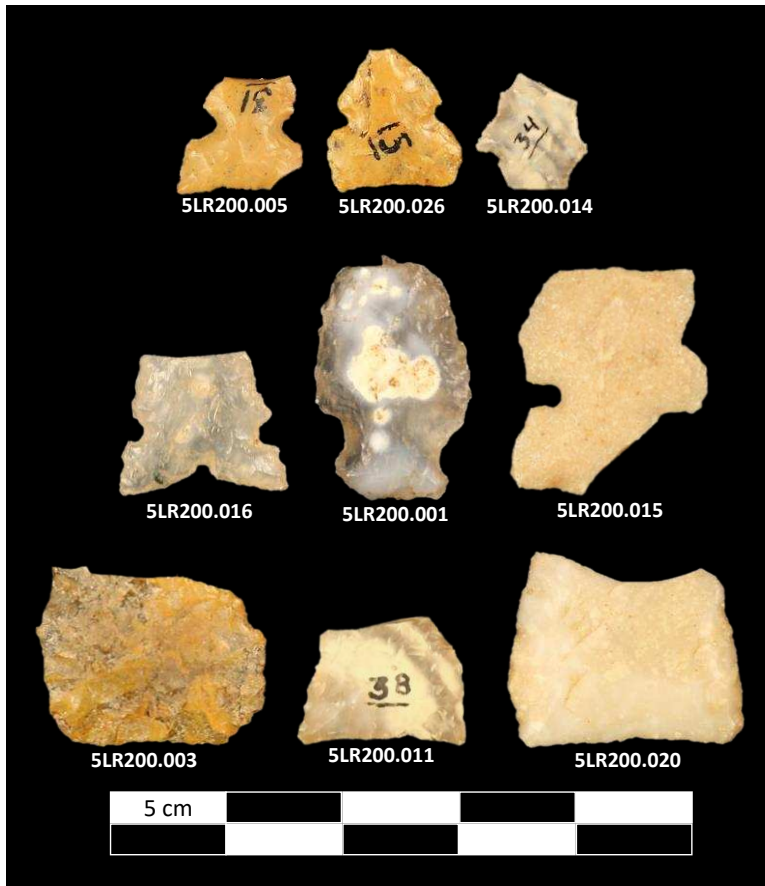


Figure 5: 5LR200 diagnostic projectile points with feature provenience.

Table 8: 5LR200 projectile point metrics.

CMPA Curation Number	Feature	Max Length (mm)	Max Width (mm)	Thickness (mm)	Mass (g)
5LR200.001	11	21.2	13.5	4.3	1.3
5LR200.003	12	15.3	20.0	3.6	1.3
5LR200.005	35	9.7	10.6	2.4	0.3
5LR200.011	32	11.2	14.4	2.1	0.4
5LR200.014	32	10.0	9.4	1.7	0.1
5LR200.015	8	20.0	16.3	3.1	1.0
5LR200.016	6	12.0	14.5	3.0	0.6
5LR200.020	32	16.8	20.1	3.4	1.5
5LR200.026	11	11.9	11.3	2.6	0.4

Items 5LR200.001 and 5LR200.014 are temporally diagnostic of a Hog Back corner-notched arrow point (Nelson 1971) and compare to corner-notched projectile points 5LR104.62 and 5LR104.104 from the Owl Canyon Rockshelter (Burgess 1981:40, Figure 10) and projectile point Type 14 from the Spring Gulch site (Kainer 1976:62). Items 5LR200.005, 5LR200.015 and 5LR200.026 are diagnostic of a side-notched arrow point type (Taylor 2006). Item 200.005 and 5LR200.026 compare to projectile point Type 1 from the Spring Gulch site (Kainer 1976:103). Item 5LR200.015 most closely resembles side-notched arrow points from the Owl Canyon Rockshelter (Burgess 1981:36, Figure 9). Items 5LR200.003, 5LR200.011, and 5LR200.020 resemble un-notched projectile points similar to Roberts Buffalo Jump (5LR100) (Johnston 2016:59). Item 5LR200.016 resembles specimen 'c' (Johnston 2016:59, Figure 4.2), a tri-notched arrow point. The Roberts Buffalo Jump dates roughly 500 years later than T-W Diamond (see radiocarbon dates in previous section) suggesting either the point typologies are not consistent with a single component occupation or these point types can co-occur much earlier, in the Middle Ceramic.

There are instances of other well-dated stratified sites where these point types occur simultaneously. The Vore site (48CK302) show side-notched, tri-notched, and un-notched projectile points co-occurring, but dating much later to A.D. 1700-1800 (Reher and Frison 1980:29). At the Glenrock Buffalo Jump (48CO304), tri-notched points do not appear until the most recent level and are dated to 210 +/-100 B.P. (Frison 1970:7) cal A.D. 1491-1603 (17.3%) or cal A.D. 1612- modern (78.1%) (OxCal 4.2, Reimer et al. 2013). The Cherokee Mountain Rock Shelter (5DA1001) contains tri-notched projectile point types (as well as side and un-notched) and dates slightly earlier, A.D. 1250-1590 (Nelson and Stewart 1973) suggesting these point types do, in some instances, occur earlier. The Murray Site (Benedict 1975:167) contains

both side and corner-notched projectile point types. Charcoal from the floor of pit no. 4, where both point types were recovered, was dated to 670 +/- 150 BP, cal A.D. 1021- 1514 (94.7%) or cal A.D. 1600-1617 (0.7%) (OxCal 4.2, Reimer et al. 2013). Although this site has a slightly earlier date, and has side and corner-notched projectile points co-occurring, there were no tri or un-notched projectile point types. The Roberts Buffalo Jump also contains side-notched, tri-notched, and un-notched types, but again dates to the late 1600s. Thus, it is not uncommon for these point types to co-occur; however, it seems rare that all point types are represented in a Middle Ceramic-aged site. This could suggest multiple occupations at T-W Diamond, or could represent an early case for these points co-occurring.

Absolute Dating Discussion

There are 14 radiocarbon dates and two thermoluminescence (TL) dates from Killdeer Canyon and T-W Diamond. Each site has seven radiocarbon dates and one TL date from a pottery sherd. This thesis contributes two new radiocarbon dates on faunal remains from each site. Bone samples were selected from different features to refine preexisting charcoal dates and test ring contemporaneity.

Faunal dates, as opposed to charcoal dates, better address site contemporaneity for the following reasons. First, bone from excavated context represents a cultural event. This means that the animal was killed during site occupation and transported back to the camp where it was consumed and discarded. Thus, dating faunal remains pinpoints the cultural occupation, or target event, whereas charcoal samples may only pinpoint the death of the tree (unless twigs or seeds are used). Dating bone is a means of solving the 'old wood problem' (Schiffer 1986). Second, many of the charcoal samples collected during the original site excavations in the early 1970s and 1980s lack detailed provenience information and do not state whether the sample was

collected from the interior or exterior of the ring. Therefore, while charcoal samples could have provided more dates, knowing the context of the radiocarbon date was of greater significance. Therefore, to address ring contemporaneity, four bone dates with feature provenience were selected from Killdeer Canyon and T-W Diamond.

Methods – Radiocarbon and Thermoluminescence Dates

Bone samples were selected from Killdeer Canyon and T-W Diamond following these criteria: (1) the sample provenience would add clarification to previously dated stone features or feature clusters, and (2) the sample was sufficient in size and mass for dating. Bone samples included a second phalanx and astragalus from Killdeer Canyon and an unidentifiable molar and radius from T-W Diamond. A molar was selected for dating because there were no other dateable bone fragments from the feature of interest. Bone and tooth samples were submitted to Aeon Laboratories, LLC for radiocarbon analysis. The results of the analysis can be found in Appendix B. The bones were measured and photographed before they were sent to Aeon (bone sample attributes can be found in Appendix C).

Because the bone samples were small, the CMPA shipped the fragments in their entirety to Aeon. Aeon selected portions of the bone that would most likely yield sufficient collagen for dating and cut the bone in their laboratory, minimizing the potential for contamination. All four samples (three bone fragments and one tooth) had sufficient collagen to radiocarbon date.

Bone samples were also analyzed for $\delta^{15}\text{N}$ and $\delta^{13}\text{C}$ content (see Appendix B). Only three samples contained sufficient collagen to perform the carbon and nitrogen analyses, the tooth fragment had no remaining collagen after producing a radiocarbon date.

There are competing methodologies for examining the statistical contemporaneity between radiocarbon dates. While OxCal has implemented a function (R_Combine) to

statistically compare calibrated radiocarbon dates using a chi-squared analysis, the function assumes that radiocarbon dates are from the same event which is not appropriate for this analysis. Instead, this analysis modifies methods developed in Long and Rippeteau (1974:210) to statistically compare two sets of uncalibrated radiocarbon dates. Whereas the relationship of statistically similar uncalibrated radiocarbon dates does not account for how dates change after calibration, the author uses this analysis as a proxy for understanding whether the rings could have been occupied at the same time. Uncalibrated radiocarbon dates are statistically compared using an f-test, t-test, and Cohan's D (effect size) analysis.

First, a variance comparison (F-Test) between all uncalibrated dates from Killdeer Canyon and T-W Diamond respectively is completed to assess which radiocarbon sigma ranges are similar enough to perform a statistical analysis. A t-test is performed at a 0.01 confidence level using sets of dates with similar sigma ranges following methods established by Long and Rippeteau (1974:210). The effect size, or the standardized difference between two means of uncalibrated radiocarbon dates, is also compared (Cohen 1988). Whereas the t-test reports a value that can be interpreted as significant or not significant, the effect size reports a raw value that is interpreted on a continuum of very small to very large. In the case of a very large effect size, the radiocarbon dates would have a greater difference between the two means. The t-test and effect size analyses complement one another and are used to highlight statistical contemporaneity between features at Killdeer Canyon and T-W Diamond. While these results are only as good as the resolution of the radiocarbon dataset, this chapter represents one line of evidence that is tested throughout this thesis using compounding lines of evidence (see Chapter 1).

Killdeer Canyon Results – Radiocarbon and Thermoluminescence Dates

Bone was selected from Killdeer Canyon to test whether the site is a short-term single occupation habitation site. This was accomplished using the following assumption: a single occupation site should have statistically contemporaneous radiocarbon dates between rings. Bone was selected from Features 4 and 7. Feature 4 is a residential structure and had never been dated. Feature 7, a possible outside activity area, contains pottery, and was a high priority for dating because the results could be compared to the petrographic analysis. Bone dates from Features 4 and 7 complemented one another because of their different locations on the site. They also helped clarify whether the differences in previously dated features reflected a poor sigma range or indicated multiple occupations. Table 9 lists the five original radiocarbon dates and the two new bone dates. Dates were calibrated using Calib 7.1 to a 2σ range (Stuiver and Reimer 1993) according to the IntCal 13 radiocarbon age calibration curves (Reimer et al. 2013).

Table 9: 5LR289 radiocarbon calibration results using Calib 7.1 (Stuiver and Reimer 1993).

Feature	Lab Number	Uncorrected Radiocarbon Age	Calibrated Date Range	Probability Distribution, 2σ	Median Probability of all Date Ranges	Material Dated
7	Beta-5129	360+/-80	AD 1416-1668	0.987	A.D. 1548	Charcoal
6a	Beta-5127	150+/-50	AD 1665-1787	0.473	A.D. 1799	Charcoal
6b	Beta-5130	260+/-50	AD 1483-1683	0.772	A.D. 1637	Charcoal
5	Beta-5128	300+/-90	AD 1432-1695	0.816	A.D. 1591	Charcoal
2	Beta-5131	170+/-50	AD 1716-1891	0.63	A.D. 1780	Charcoal
4 (2016)	Aeon-2150	225+/-25	AD 1642-1681	0.481	A.D. 1763	Bone
7 (2016)	Aeon-2151	230+/-25	AD 1641-1680	0.536	A.D. 1672	Bone

Previous radiocarbon dates generally associate the site with the Late Ceramic period A.D. 1540-1860 (Gilmore 1999) (Figure 7). There are several difficulties dating stone circle sites of this age. First, the dates on charcoal are potentially from old juniper wood, which can live up to 700 years. Second, other complications lie in the radiocarbon calibration curve for sites this age.

Third, the original dates are fairly imprecise. To examine the age and contemporaneity of the features at Killdeer Canyon, the radiocarbon dates are first tested for statistical contemporaneity. This analysis then examines the probability distributions of the calibrated date ranges to make an argument for ring contemporaneity.

Variance Comparison (5LR289)	$\alpha = 0.01$	Date	360	150	260	300	170	225	230	
	Critical F-Value: 6.6349	s	80	50	50	90	50	25	25	
	Date	s	s²	6400	2500	2500	8100	2500	625	625
	360	80	6400							
	150	50	2500	2.560						
	260	50	2500	2.560	1.000					
	300	90	8100	1.266	3.240	3.240				
	170	50	2500	2.560	1.000	1.000	3.240			
	225	25	625	10.240	4.000	4.000	12.960	4.000		
	230	25	625	10.240	4.000	4.000	12.960	4.000	1.000	

Figure 6: 5LR289 variance comparison (F-Test, $\alpha = 0.01$) of all uncalibrated radiocarbon dates. F-Test results that show no significant difference in sigma ranges are highlighted in gray.

The following null-hypothesis is tested: radiocarbon dates, before calibration, between stone circles are statistically the same. If the null hypothesis cannot be rejected, it suggests the rings at Killdeer Canyon were occupied at the same time. Figure 6 shows the variance comparison of results of all rings from Killdeer Canyon indicating which dates have similar-enough standard deviations to run t-tests. Dates that can be used in the statistical analysis are highlighted in gray (Figure 6).

Select pairs of radiocarbon dates were used in the statistical analysis based on their spatial distribution throughout the site (Figure 7). Two radiocarbon dates from Feature 6 are tested against the null hypothesis to determine if the ring represents one cultural event or two

different events (ring reoccupation). Features 6 and Feature 2 as well as Feature 2 and Feature 4 are tested against the null hypothesis to determine whether rings in different spatial locations across the site are related to the same event. Lastly, Features 4 and 7 are tested to determine whether the outside activity area (Feature 7) is related to the habitation features.



Figure 7: 5LR289 radiocarbon dates calibrated using Calib 7.1 (Stuiver and Reimer 1993). 2016 bone dates are reported in orange.

Student's t-Test Results (5LR289)	$\alpha = 0.01$		Date	360	150	260	300	170	225	230	
	t-score/p-value		s	80	50	50	90	50	25	25	
	Date	s	s ²	6400	2500	2500	8100	2500	625	625	
	360	80	6400								
	150	50	2500								
	260	50	2500								1.556/ 0.360
	300	90	8100								
	170	50	2500								1.273/ 0.420
	225	25	625								0.984/ 0.510
	230	25	625								0.141/ 0.910

Cohen's d		Date	360	150	260	300	170	225	230	
		s	80	50	50	90	50	25	25	
Date	s	s ²	6400	2500	2500	8100	2500	625	625	
360	80	6400								
150	50	2500								
260	50	2500								2.200
300	90	8100								
170	50	2500								1.800
225	25	625								1.391
230	25	625								0.200

Figure 8: 5LR 289 Student's t-test results (left) and Cohen's d results (right). T-test results are significant at a 99% confidence interval.

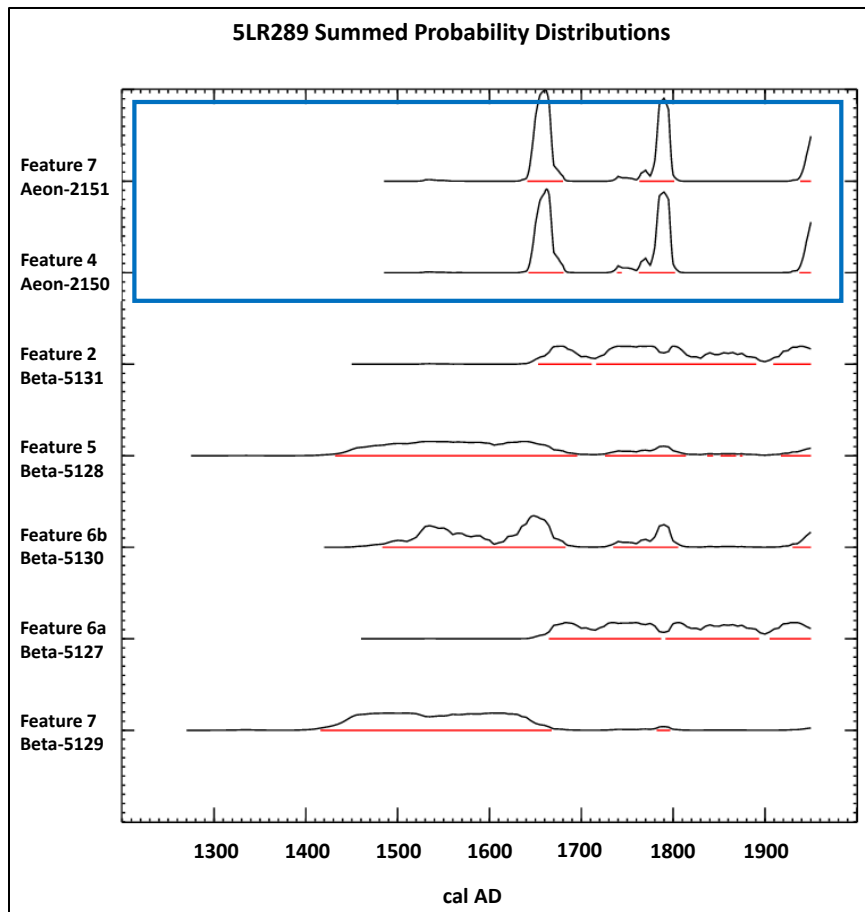


Figure 9: 5LR289 probability distributions for each date. New bone dates highlighted in blue. Notice higher precision for 2016 dates.

Figure 8 shows that at a .01 confidence level the null hypothesis cannot be rejected. All four date sets are statistically contemporaneous indicating the rings at Killdeer Canyon could have been occupied at the same time. Cohen's d analysis shows varying degrees of closeness between radiocarbon dates means. Expectedly, the two new radiocarbon dates have the highest probability that they are statistically contemporaneous as well as the smallest magnitude effect size, meaning they have the smallest difference between the two means.

Figure 9 shows the probability distributions of individual feature dates. The two new bone dates are highlighted in blue. High sigma ranges from the five preexisting charcoal dates show the degree of uncertainty with an age dispersal of over 600-years, from the early 1400s

until after European contact. Figure 10 displays the combined summed probability distributions with the original five radiocarbon dates (bottom plot) and all seven radiocarbon dates (top plot).

The two high precision bone dates help refine the summed probability distribution.

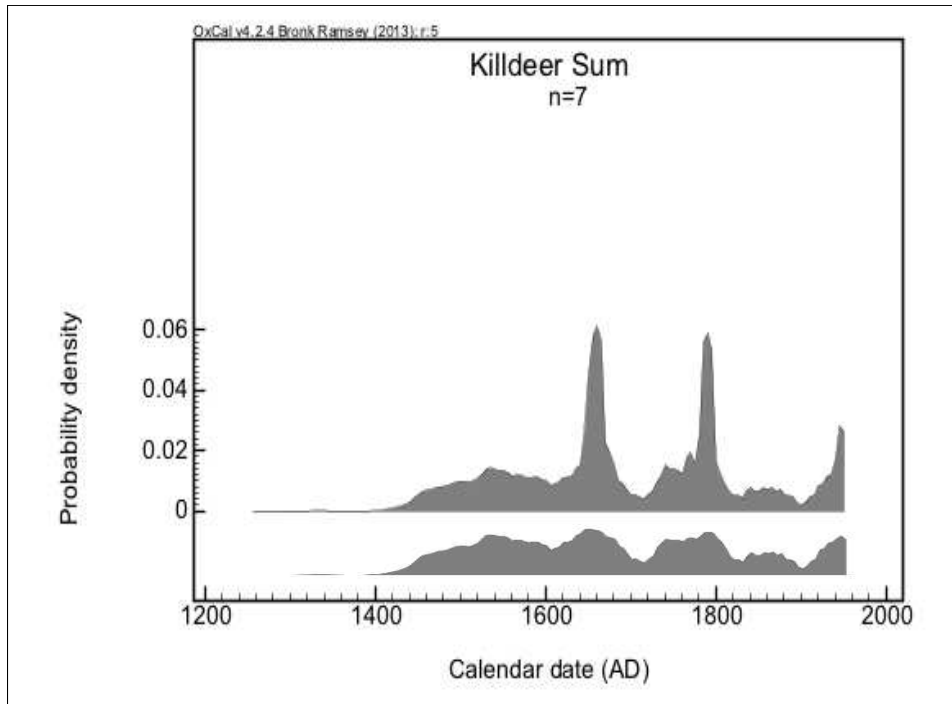


Figure 10: 5LR289 summed probability distributions displaying original five radiocarbon dates (bottom) and distribution with two new bone dates (top) (Bronk Ramsey 2009).

The probability distributions show overlap between all seven dates from Killdeer Canyon, again supporting the rings represent a single occupation. It is important to note that the two peaks do not represent two occupations at the site. Rather, the two peaks indicate the site was occupied, at a 2σ range, either between A.D. 1641-1680 or between A.D. 1763-1801. These represent non-contiguous date ranges that result from a plateau in the radiocarbon calibration curve that impact dates from the seventeenth to nineteenth centuries.

Table 10: 5LR289 thermoluminescence date.

Lab Number	Thermoluminescence Age (B.P.)	Calibrated Thermoluminescence Age (reported in Calendar years before 1950)	Uncertainty (%)	Provenience	Material Dated
Alpha-470	420	A.D. 1530	20	Feature 7	Sherd

The TL date, slightly older than the highest probability date ranges, may not be the best indication of feature age (Table 10). Problems with thermoluminescence dates have been explored by others including Benedict (1989) and Johnson et al. (1986). Specifically, James Benedict examined three different dating methods at the Caribou Lake site including TL dating on pottery sherds and radiocarbon methods (Benedict 1989:7-8). Benedict found that TL dating had a variety of cumulative errors that had to do with post depositional processes after the pot was discarded. Because the dated bone samples from Killdeer Canyon are related to cultural practices and are not as greatly impacted by cumulative errors after site abandonment, the two high probability date ranges are trusted from the radiocarbon analysis.

Statistical contemporaneity between four rings at Killdeer Canyon suggest the site could be a single occupation. This is supported by the summed probability distributions which show greater overlap in the later date ranges. A later occupation would have interesting implications for mobility and the inhabitants of Killdeer Canyon. The late 1700s date range is contemporaneous with the introduction of the horse in this area (Jacobsen and Eighmy 1980:338; Wedel 1961). Although it is outside of the scope of this thesis to examine whether the hunter-gatherers at this occupation had horses, it is probable. This would have had implications regarding group mobility as well as the materials transported into and out of camp.

T-W Diamond Results – Radiocarbon and Thermoluminescence Dates

Previous radiocarbon dates generally associate the site with the Middle Ceramic period (Table 11). Middle Ceramic dates are less affected by plateaus in the radiocarbon calibration curve; however, the T-W Diamond dates have very high sigma ranges, some in the hundreds. The samples are also from charcoal and could have problems associated with old wood.

To contribute to this dataset, bone samples were selected for dating from Features 4 and 10. Feature 4 was selected to refine the dates from rings in the northern cluster. Feature 10 was selected to refine the dates in southern cluster. Feature 10 is one of the few features containing bone in the southern portion of the site and is just north of Feature 11, the only feature on site containing pottery fragments. Feature 11 also has the earliest radiocarbon date from the site. While there was no dateable bone from Feature 11, bone was selected from Feature 10 to try to refine the date ranges for the southern ring cluster. A statistical analysis was then performed between Features 10 and 11 to test ring contemporaneity. Table 11 lists the original and newly added uncorrected and corrected radiocarbon dates. Dates were calibrated using Calib 7.1 to a 2σ range (Stuiver and Reimer 1993) according to the IntCal 13 radiocarbon age calibration curves (Reimer et al. 2013).

Again, the following null hypothesis is tested: radiocarbon dates between stone circles are statistically the same. If the null hypothesis cannot be rejected, it suggests the rings at T-W Diamond could have been occupied at the same time. Figure 11 shows the variance comparison of results of all rings from T-W Diamond indicating which dates have similar-enough standard deviations to run t-tests. Dates that can be used in the statistical analysis are highlighted in gray (Figure 11). Inconsistent sigma ranges from the charcoal dates from T-W Diamond allow less

comparisons between features than Killdeer Canyon, however, four rings across two main clusters of the site were still successfully compared.

Table 11: 5LR200 radiocarbon calibrated results using Calib 7.1 (Stuiver and Reimer 1993).

Feature	Lab Number	Uncorrected Radiocarbon Age	Calibrated Date Ranges	Probability Distribution, 2σ	Median Probability of all Date Ranges	Material Dated
2a	Beta-6848	860+/-100	cal AD 987-1297	1.000	A.D. 1157	Charcoal
2b	Beta-6849	930+/-230	cal AD 660-1425	1.000	A.D. 1071	Charcoal
4	A-1272	920+/-80	cal AD 990-1260	1.000	A.D. 1114	Charcoal
10	A-1273	780+/-220	cal AD 770-1524	0.978	A.D. 1200	Charcoal
11	A-1274	1500+/-340	B.C. 204- cal AD 1219	0.999	A.D. 510	Charcoal
4 (2016)	Aeon-2152	715+/-25	cal AD 1260-1298	0.977	A.D. 1279	Bone
10 (2016)	Aeon-2153	750+/-30	cal AD 1223-1286	1.000	A.D. 1264	Bone

		$\alpha = 0.01$	Date	860	930	920	780	1500	715	750	
		Critical F-Value: 6.6349	s	100	230	80	220	340	25	30	
Variance Comparison (5LR200)	Date	s	s ²	10000	52900	6400	48400	115600	625	900	
	860	100	10000								
	930	230	52900	5.290							
	920	80	6400	1.563	8.266						
	780	220	48400	4.840	1.093	7.563					
	1500	340	115600	11.560	2.185	18.063	2.388				
	715	25	625	16.000	84.640	10.240	77.440	184.960			
	750	30	900	11.111	58.778	7.111	53.778	128.444	1.440		

Figure 11: 5LR200 variance comparison (F-Test, $\alpha = 0.01$) of all uncalibrated radiocarbon dates. F-Test results that show no significant difference in sigma ranges are highlighted in gray.

Select pairs of radiocarbon dates were used in the statistical analysis based on their spatial distribution throughout the site (Figure 12). Two radiocarbon dates from Feature 2 are tested against the null hypothesis to determine if the ring represents one cultural event or two different events (ring reoccupation). Features 2 and 10, 10 and 11, and 4 and 10 are tested against

the null hypothesis to determine whether rings in different spatial locations across the site are related to the same event.

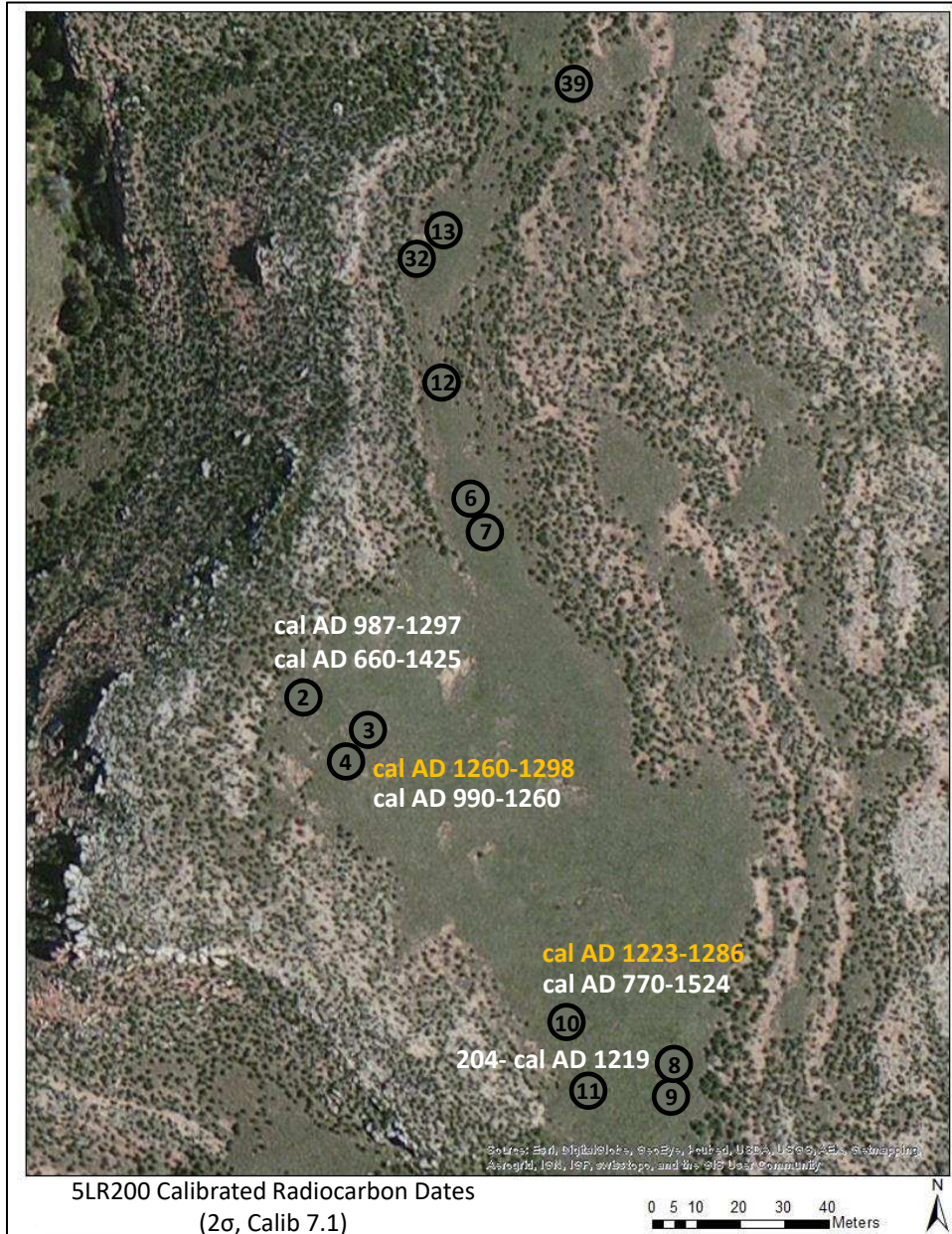


Figure 12: 5LR200 radiocarbon dates calibrated using Calib 7.1 (Stuiver and Reimer 1993). 2016 bone dates are reported in orange.

Student's t-Test Results (5LR200)	$\alpha = 0.01$		Date	860	930	920	780	1500	715	750							
	t-score/p-value		s	100	230	80	220	340	25	30							
	Date	s	s ²	10000	52900	6400	48400	115600	625	900							
	860	100	10000														
	930	230	52900								0.279/ 0.830						
	920	80	6400														
	780	220	48400									0.471/ 0.720					
	1500	340	115600											1.778/ 0.330			
	715	25	625														
	750	30	900													0.896/ 0.530	

Cohen's d		Date	860	930	920	780	1500	715	750							
		s	100	230	80	220	340	25	30							
Date	s	s ²	10000	52900	6400	48400	115600	625	900							
860	100	10000														
930	230	52900								0.395						
920	80	6400														
780	220	48400									0.667					
1500	340	115600											2.514			
715	25	625														
750	30	900														1.268

Figure 13: 5LR 200 Student's t-test results (left) and Cohen's d results (right). T-test results are significant at a 99% confidence interval.

Figure 13 shows that at a .01 confidence level the null hypothesis cannot be rejected. All four date sets are statistically contemporaneous indicating the rings at T-W Diamond were occupied at the same time. Furthermore, this suggests that the charcoal date from Feature 11 is likely not the best representation of site due to its high precision. Because of the statistical contemporaneity between the Features 10 and 11, it is best to rely on the later date ranges that associate T-W Diamond with the late 1200s. Just as Killdeer Canyon, Cohen's d analysis shows varying degrees of closeness between radiocarbon dates means. The smallest difference in means are between the dates from Feature 2.

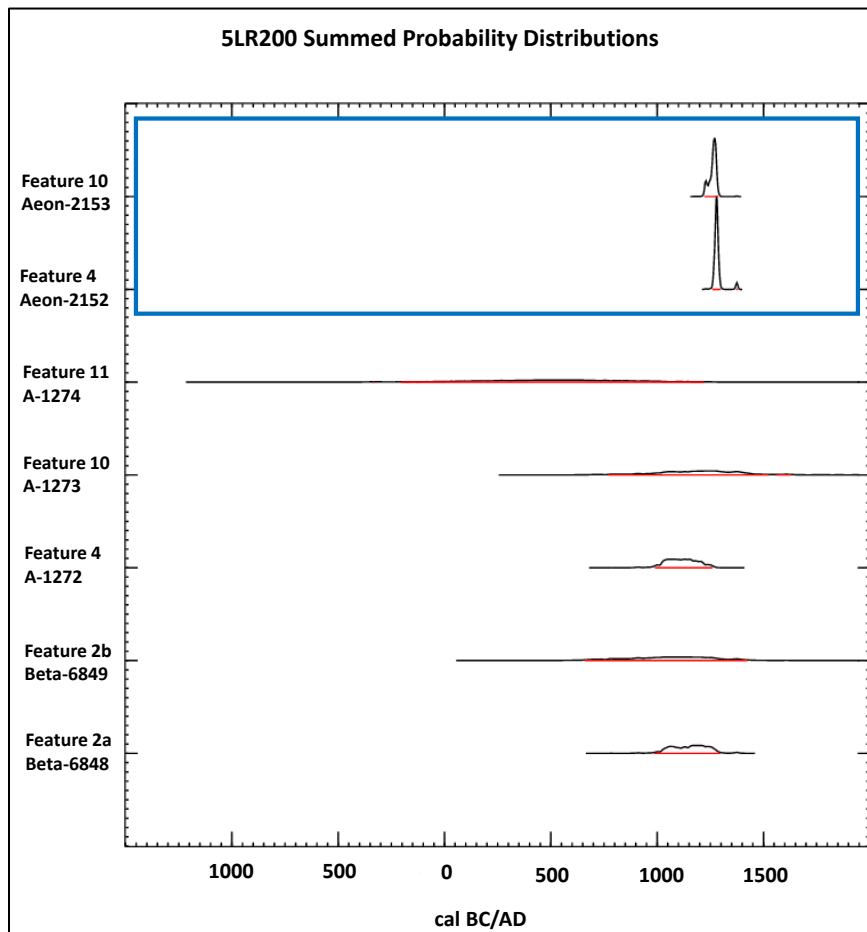


Figure 14: 5LR200 probability distributions for each date. New bone dates highlighted in blue. Notice higher precision for 2016 dates.

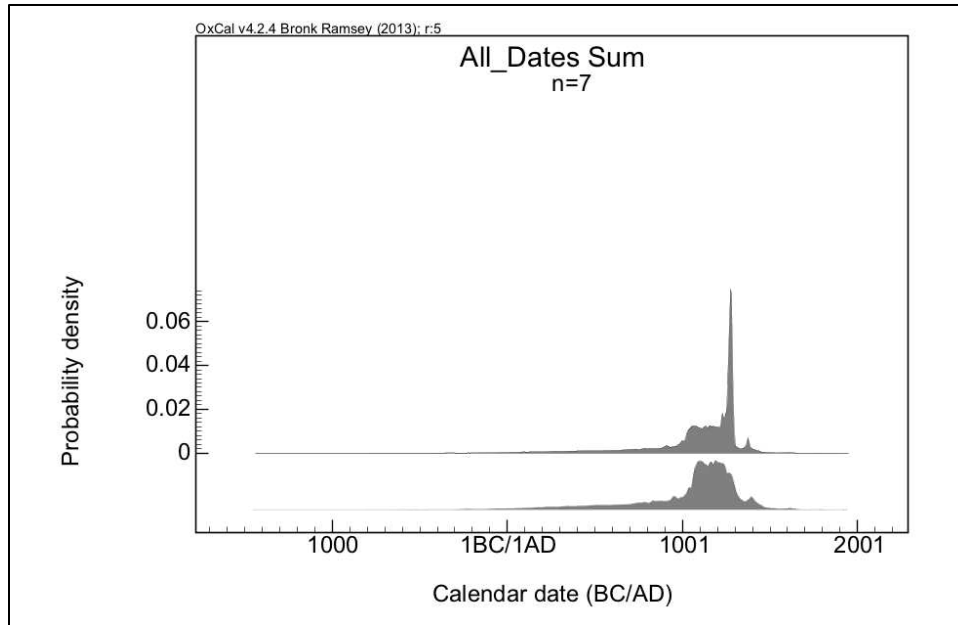


Figure 15: 5LR200 summed probability distributions displaying original five radiocarbon dates (bottom) and distribution with two new bone dates (top) (Bronk Ramsey 2009).

The summed probability distribution for the preexisting 5 radiocarbon dates, not including the two new dates shows the probability density dispersed over 1,000 years with two higher probability ages around A.D. 1000 and A.D. 1500 (Figure 14). Bone dates from Features 4 and 10 (highlighted in blue) refine the most probable occupation age to the late 1200s. While the summed probability distribution shows a greater date dispersal than Killdeer Canyon (Figure 15), the problems impacting more recent dates attributed to flattening of the radiocarbon curve are not as big an issue. The probability distributions show overlap between all seven dates from T-W Diamond, again supporting the hypothesis that the rings represent a single occupation.

Results from the radiocarbon analysis for T-W Diamond show contemporaneity between feature clusters at the site suggesting that the excavated rings represent one cultural event. Four rings have statistically contemporaneous uncalibrated radiocarbon dates suggesting that different areas of the site were occupied at the same time. This is somewhat counterintuitive to spatial interpretations of stone circle sites where separate clusters, or sites containing 50 to 100 rings

“automatically suggest different occupations” (Finnigan 1981:11). It is possible that T-W Diamond represents a group congregation, perhaps explaining why the site is situated in a highly visible area. This hypothesis will be further explored in the following chapters examining individual artifact classes.

Table 12: 5LR200 thermoluminescence date.

Lab Number	Thermoluminescence Age (B.P.)	Calibrated Thermoluminescence Age (reported in Calendar years before 1950)	Uncertainty (%)	Provenience	Material Dated
Alpha-469	430	A.D. 1520	20	Feature 11	Sherd

Again, as is the case at Killdeer Canyon, the TL date may not be the best indication of feature age (Table 12). The thermoluminescence date range for T-W Diamond spans A.D. 1430-1600, suggesting a later occupation than the highest probability radiocarbon dates. Based on Benedict’s (1989) analysis, discussed in the Killdeer Canyon section, it is best to rely more heavily on the radiocarbon analysis than the thermoluminescence date.

Discussion and Conclusion

Relative dating methods suggest Killdeer Canyon was occupied in the Late Prehistoric era. Killdeer Canyon contained only two points with feature provenience, though nearly identical metric attributes suggest the points were made at the same time and the site may have been one occupation. T-W Diamond contained several (n=5) different point types, all of which date to the Late Prehistoric era. Tri-notched and un-notched projectile points are similar to point types from the Roberts Buffalo Jump, which dates roughly 500 years after the proposed age of T-W Diamond. These data suggest either T-W Diamond was a multiple component site and the later

point types do not occur simultaneously with the dated bone, or T-W Diamond represents a case study for these point types co-occurring.

Previous radiocarbon dates generally associated Killdeer Canyon with the Late Ceramic period (A.D. 1540-1860) and T-W Diamond with the Middle Ceramic period (A.D. 1140-1540). Both sets of new dates from Killdeer Canyon and T-W Diamond add clarity to previous charcoal dates. Furthermore, four dates from each site indicate statistical contemporaneity suggesting Killdeer Canyon and T-W Diamond may have been single occupation sites. Contemporaneity using radiocarbon dates cannot, however, identify site reoccupations that occurred within a couple years or even decades. Therefore, the remaining chapters in this thesis test expectations regarding artifact signatures for single occupation sites.

CHAPTER 3: DEBITAGE ACCUMULATION AS A MEASURE OF OCCUPATION SPAN

Accumulation theories, predominantly used in Southwestern archaeology, are modified in this chapter for short-term hunter-gatherer sites. Whereas understanding the exact number of days the site was occupied is not possible, this section uses debitage as a proxy for measuring the relative occupation length (from short to long). These methods are designed to be easily applied to other short-term hunter-gatherer household sites. This section relies on the accumulation of debitage, flake size, and local and non-local material ratios to determine occupation span.

Theoretical Justification for Debitage Analysis

Debitage accumulation provides a relative measure of occupation length. Whereas lithic tools undergo a series of transformations from production to discard (Andrefsky 2005), debitage often remains in the place of tool manufacture. Thus, debitage is a valuable tool for understanding site purpose, occupation length, use-intensity, and a variety of other questions. Whereas parsing individual cultural events from multiple component sites is difficult and often not possible, stone circle excavations provide an important delineation of space and time. Debitage from the inside of a stone ring likely represents one cultural event (see Chapter 1). To determine the length of occupation and relationship between stone circles at each site, the following debitage variables are examined: raw material type, flake frequency, flake thickness, local and non-local material, and nodule dispersal.

The following expectations are used to determine occupation length: debitage frequency, relative thickness, and local and non-local material use. Local and non-local debitage ratios are particularly useful measures of occupation length in sites near raw material sources. This is because mobile hunter-gatherers can only carry a limited amount of material to a site. As the site

is inhabited longer, local material will be used to replenish expended non-local tools. A site containing a greater ratio of non-local material suggests the group was not in one place long enough to need to replenish their toolkits with local materials. Conversely, a high ratio of local to non-local raw materials suggests the inhabitants were at the site long enough to expend non-local tools and replenish their toolkits with the local material. This would manifest in higher frequencies of local materials as well as comparatively larger pieces of local debitage (Nelson 1991) which is tested using relative thickness.

Kinney Spring represents a good case study for understanding semi-permanent residential behavior. Kinney Spring is a semi-permanent Early Ceramic residential base located within two kilometers of Killdeer Canyon and T-W Diamond (Figure 16). The site, likely a winter occupation, contains primarily local tools and debitage (Perlmutter 2015). While this could result from a preference of the Campbell Mountain raw material type, this is exactly what would be expected at a long-term site near, roughly 2 kilometers, a raw material source.

Relative thickness (Ostahowski and Kelly 2015:133) is used to examine whether late stage tool manufacture and resharpening flakes are predominantly from local or non-local materials. The relative thickness is expressed as the length divided by the thickness as a measure for reduction stage. Debitage size can indicate tool manufacturing and resharpening processes that took place on site (Nelson 1991). Sites assemblages consisting mainly of smaller, non-local flakes suggest carrying costs influenced the transportation of raw materials (Shott 1986). Carrying costs can be mitigated by carrying transportable high-quality materials, such as bifaces (Kelly 1988). If high quality bifaces are transported to a site, the debitage will reflect late stage tool manufacture and resharpening instead of early stage biface/core reduction. When raw material is available, materials do not need testing before leaving the quarry site. This results in

minimally modified local chipped stone tools (Lurie 2009). Readily accessible raw materials also produce a higher ratio of local to non-local flakes.

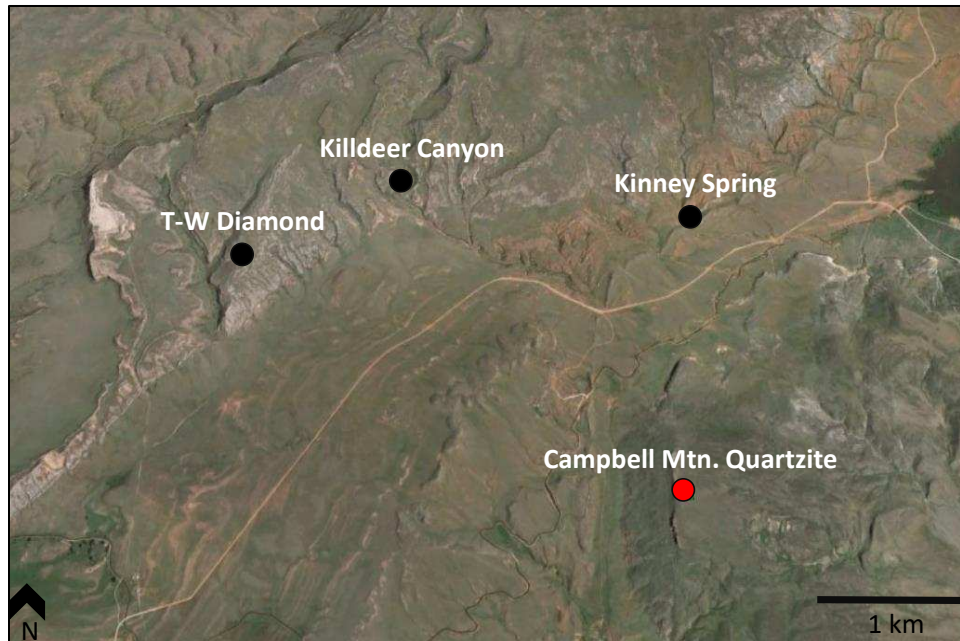


Figure 16: Location of Killdeer Canyon, T-W Diamond in relation to Kinney Spring and Campbell Mountain quartzite.

Finally, nodule dispersal is used to examine the number of occupations at each site. A single occupation should contain homogeneity in local and non-local material ratios. Furthermore, identifiable raw material nodules should be equally dispersed throughout rings. This is because a group occupying a site will have access to the same limited raw material types transported to the site. Multiple occupations should contain more heterogeneity between rings. This is because groups carry different frequencies and types of non-local materials to a site. Therefore, there should be noticeable patterns between features or feature clusters in regard to material ratios and nodule types.

Methods

The Killdeer Canyon and T-W Diamond collections are stored in the CSU Archaeological Repository. Many of the artifacts were still in their original artifact bags from the 1982 and 1971 excavations (respectively). Initially, debitage from the two sites were catalogued and flakes were individually bagged. Basic metrics (length, thickness, and mass) were measured on all flakes. Debitage was then sorted by similar nodules with help from CSU/CMPA undergraduate volunteer Lance Shockley. Raw material nodules were “sourced” (if possible) using visual and texture comparison to the CMPA raw material collection, curated at CSU, Department of Anthropology. A distinction between local and non-local materials was made based on previous research of northern Colorado tool stone (Pelton et al. 2013). For the purpose of this analysis, all quartzite is classified as local and all non-quartzite (chert, chalcedony, obsidian, petrified wood, argillite, etc.) is classified as non-local. All other materials are farther than 20 km from the study area and considered non-local for this analysis. This distance is based on Binford (1980) who differentiates between local (within 20 km) and non-local (farther than 20 km) based on the distance a person can walk in one day. Future analyses should examine different nodule types and artifact refits as a more precise measure for ring contemporaneity.

Killdeer Canyon Debitage Results

During the 1982 excavation of Killdeer Canyon, 670 pieces of chipped stone debitage were collected. One hundred eighty-eight of the 670 flakes have provenience and are used in this analysis (see Appendix D). The other 482 flakes not used in the analysis did not contain any feature provenience and are likely from excavations occurring outside of the stone rings. The raw materials range from local quartzite and chalcedony (Pelton et al. 2013) to non-local chert and

obsidian. The range of maximum length is between 5 and 52 mm. The average maximum length is 14 mm.

Debitage frequencies are examined by feature as a proxy for occupation length (Figure 17). Limited excavation provenience notes prevented calculating the density of flakes per square meter of excavation. Because the original excavation goals were to locate the household floors, debitage with feature provenience can be confidently associated with the interior of the structure. Thus, the debitage recovered from each feature is a good indication of household occupation.

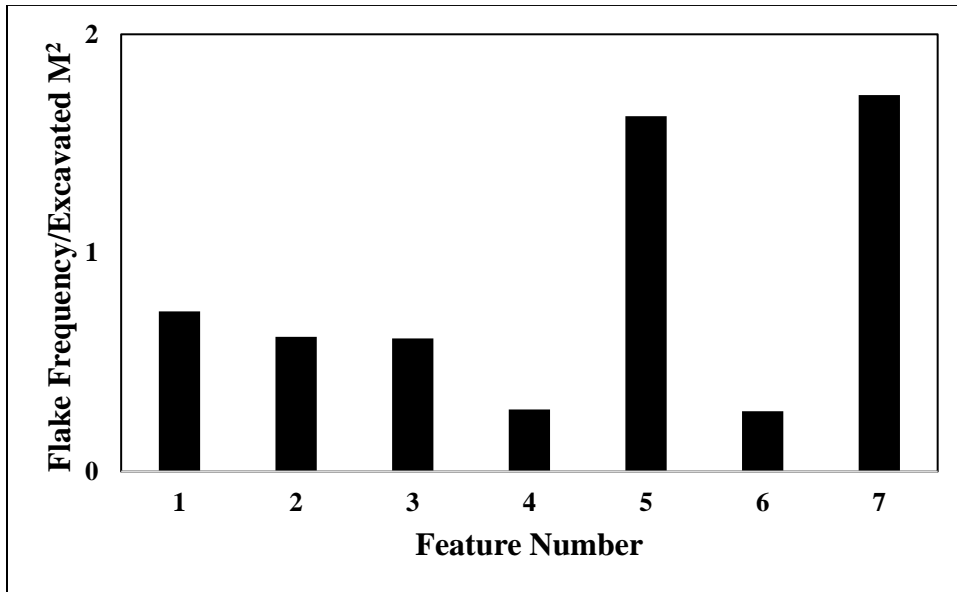


Figure 17: 5LR289 normalized flake frequency by excavation area (m²).

Feature 7 contains the highest debitage frequency (n=62) even when normalized by area excavated (1.7 flakes per m²) (Figure 17). Feature 7 lacks a rock ring suggesting it was not a habitation area. Instead, this feature may represent an outside processing area that was associated with the other rings. This is supported by the contemporaneity between radiocarbon dates from all dated features (see Chapter 2). The second highest flake frequency, Feature 5, is 46 flakes (1.6 flakes per m²). These low debitage suggest that the site was occupied temporarily,

potentially by a small group (or groups). This places the rings at Killdeer Canyon on the short-term end of the continuum.

Assuming that Killdeer Canyon was one occupation, it is possible to derive a mean debitage accumulation rate from the site assemblage. This is accomplished by dividing the total frequency of debitage by the number of features. Only using the debitage with provenience, Killdeer Canyon has a mean debitage accumulation rate of 26.9 flakes per feature. While this does not represent the entirety of the assemblage, it does represent the flakes from the interior of habitation features, and is an extremely low rate for debitage accumulation. Even taking the entire assemblage into account (n=670), and including Feature 8 which was excavated but did not yield any debitage with feature provenience, there is still less than 100 flakes per feature (n=84).

The local to non-local material ratios are generally homogenous throughout the site (Figure 18). Features contain relatively even frequencies of local and non-local materials. This suggests Killdeer Canyon was somewhere between the thresholds for short and long term (in terms of highly mobile hunter-gatherer groups). The occupants were at camp long enough to begin replenishing their toolkits with the local Campbell Mountain quartzite, however they were not on site long enough to completely exhaust non-local resources. The two features that contain the highest flake frequencies contain slightly more non-local debitage.

Differences in local and non-local material ratios can likely be attributed to rings serving different functions. It is possible that certain rings were used for lithic reduction and tool manufacture while others were used for other activities such as faunal processing. In this scenario, lithic reduction and retooling would result in more local material because exhausted non-local resources are being replenished with the local quartzite. Conversely, a ring used for

faunal processing may contain lower debitage frequencies and fewer raw material types. This is because specific task area, such as faunal processing, would use tools catered to that task that were likely produced elsewhere on site. The signature would then be limited to resharpening refuse from those specific tools (i.e. scrapers).

Table 13: 5LR289 results from obsidian sourcing. Three flakes were sourced to Valle Grande, New Mexico. Trace elements are reported in table.

Site Number	Feature	Provenience	Ti	Mn	Fe	Rb	Sr	Y	Zr	Nb	Ba	Source
5LR289	7	35S 54W L2	980	419	8652	158	7	45	169	59		Valle Grande, NM
5LR289	6	24S 39W L1	1034	465	8268	138	7	37	152	48		Valle Grande, NM
5LR289	2	21S 21E L2	959	463	8534	156	6	42	169	54		Valle Grande, NM

Previous results from energy dispersive X-Ray florescence (ED-XRF) on obsidian flakes from 5LR289 are summarized in Table 13 (Shackley 2012). These data are part of a larger project by Dr. Jason LaBelle and the CMPA sourcing obsidian artifacts from the northern Colorado Hogback region. The obsidian results show all samples source to Valle Grande, New Mexico and are from different features located across the site. These data are consistent with the ring contemporaneity analysis in Chapter 2. Furthermore, these data indicate Feature 7 was associated with the stone rings when they were occupied (Figure 19). This suggests either the occupants of Killdeer Canyon were traveling from New Mexico, or there were ties to southwestern trade networks. As mentioned in Chapter 2, it is possible Killdeer Canyon was occupied after the introduction of the horse, suggesting the inhabitant's networks and access to non-local materials would have increased and the cost of material transport would have decreased.

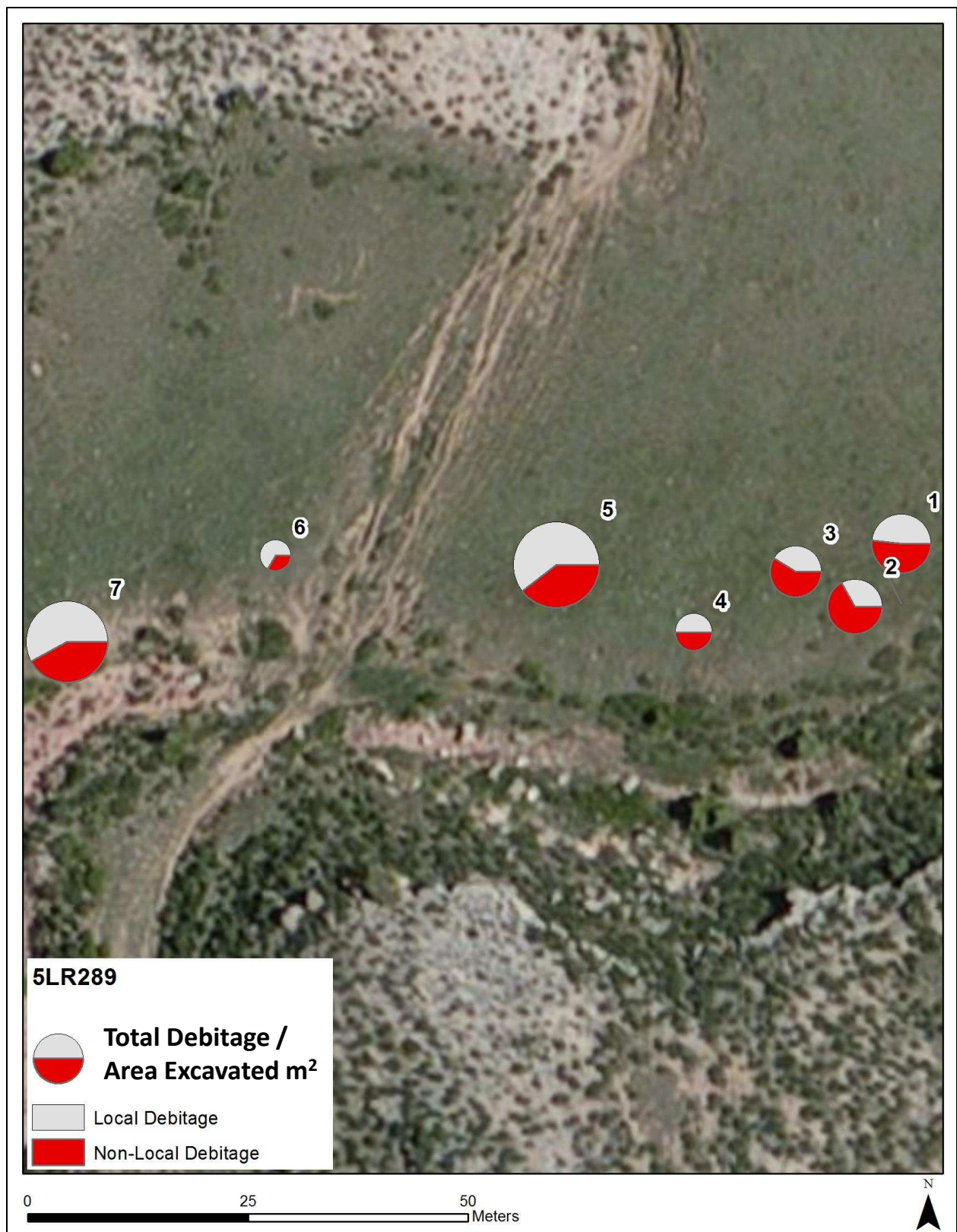


Figure 18: 5LR289 percentage of local and non-local debitage normalized by area excavated (m²). Pie charts are weighted by flake frequency. Feature number is labeled directly above ring.

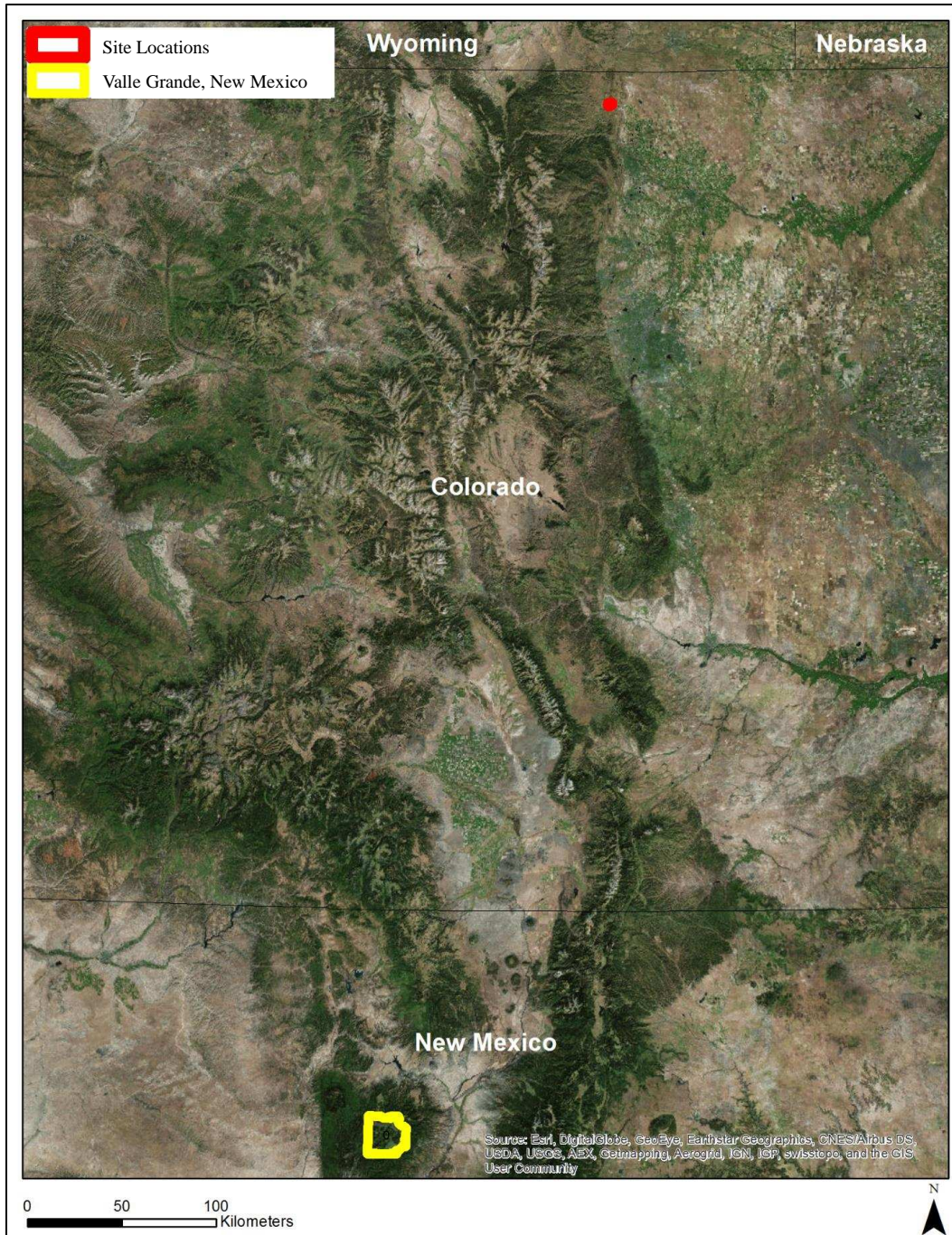


Figure 19: 5LR289 location in relation to the Valle Grande, New Mexico.

Examining the relative thickness of local and non-local debitage by feature shows no notable differences between flake size and material type (Figure 20). Overall, the findings are consistent with Nelson (1991) who stated that local flakes should be slightly larger than non-

local flakes. The two features (Feature 3 and 4) that contain a higher relative thickness, or thinner local flakes, are located on the eastern portion of the site. Although the difference is subtle, this suggests the inhabitants of these rings were participating in late stage manufacture and retouch of local tools. This could be the result of a “gearing up” by replenishing their toolkits before leaving a nearby raw material source. The presence of non-local resharpening flakes does suggest that the occupants were not camping long enough to exhaust all non-local tools. Without a refit of analysis of non-local flakes to discarded tools, however, it is probable that these flakes represent manufacture of late-stage tools that were then transported off-site.

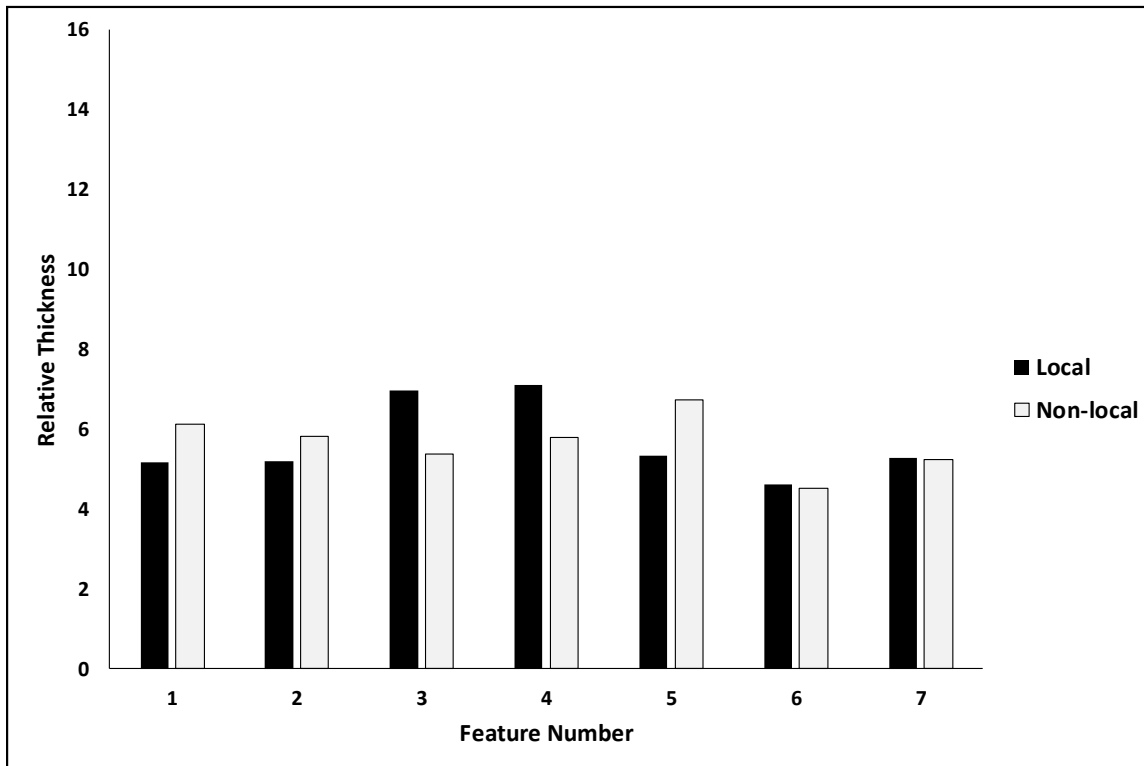


Figure 20: 5LR289 relative thickness of local and non-local debitage by feature.

To examine the number of occupations at Killdeer Canyon, debitage were sorted into nodules based on visual and texture similarities. The nodule groupings were not used to identify raw material source, rather to determine whether rings shared common material types. If Killdeer

Canyon represents one occupation, the rings should be relatively homogenous in regard to nodule dispersal. This means that the occupants had access to and were sharing the same materials during occupation.

Figure 21 shows the nodule dispersal using pie charts weighted by the total frequency of debitage. Nodule descriptions are summarized in Table 14. The nodule dispersal supports the site as a single occupation. There is homogeneity between all rings, meaning that the majority of the nodules are dispersed between rings 1-7.

The debitage analysis supports results from Chapter 2 suggesting the feature occupations were contemporaneous. Whereas Features 7 and 5 may have been associated with faunal processing or tool manufacture, Features 1-4, and 6 may have been used for different purposes that included less intensive tool manufacture. Less intensive tool manufacture would have been expected in areas used for sleeping, where spatial maintenance would have prevented the accumulation of debitage within the structure.

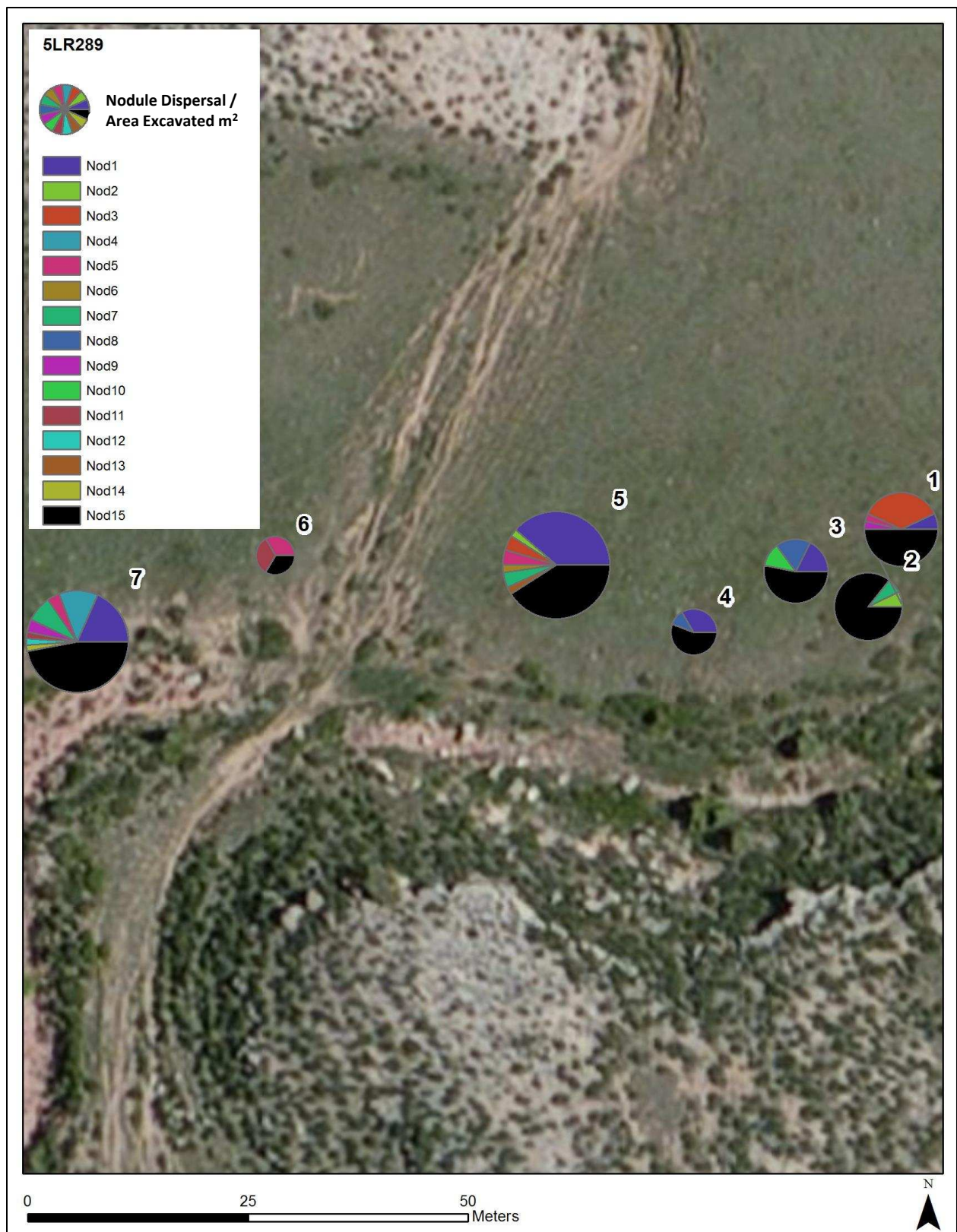


Figure 21: 5LR289 nodule dispersal between rings normalized by excavated m². Pie charts are weighted to represent the frequency of debitage.

Table 14: 5LR289 Nodule ID and description.

Nodule	Description
1	white to clear chalcedony with some white and pink inclusions
2	quartz crystal
3	chalcedony with thick and dense dendritic inclusions
4	burnt and crazed white chert
5	light pink chalcedony
6	light yellowish tan chalcedony
7	dark red chert with some dendritic inclusions
8	light tan/ off white chert
9	yellow/brown chert with dendritic inclusions
10	tan and gray mottled chert with white inclusions
11	pink and tan matte chert
12	oolitic chert
13	petrified wood
14	obsidian
15	quartzite

T-W Diamond Debitage Results

One thousand twenty-nine pieces of chipped stone debitage were collected from the 1971 excavation. Unlike Killdeer Canyon, the majority of the flakes were labeled with provenience information. Flake totals per feature were compared to Flayharty (1972) to ensure the correct number of flakes were associated with the correct features. Nine hundred sixty-two of the 1,029 flakes contained sufficient feature provenience and are used in this analysis (see Appendix G). The raw materials range from local quartzite (Pelton et al. 2013) to non-local chert and chalcedony. The range of maximum length is between 3 and 51 mm. The average maximum length is 13 mm.

Feature 10 contains 317 flakes, or 11.9 flakes per square meter (Figure 22). Feature 4 contains the second highest frequency with 231 flakes, 10.2 flakes per square meter. Using debitage as a proxy for occupation length, it is possible these features were occupied at different times and for longer periods than the other features. However, the spatial distribution of the rings, in clusters of two to three, does not make this a likely scenario. Alternatively, these

features could represent higher household use intensities or task specialization within the site. Assuming that the site was one occupation, it is possible to derive a mean debitage accumulation rate from the site assemblage. This is accomplished by dividing the total frequency of debitage by the number of features. The mean debitage accumulation per feature at T-W Diamond is 74.0. A much higher debitage accumulation rate than at Killdeer Canyon. In order to differentiate between whether higher artifact frequencies represent longer occupation spans, or more intensively used rings, the ratios of local to non-local debitage are examined.

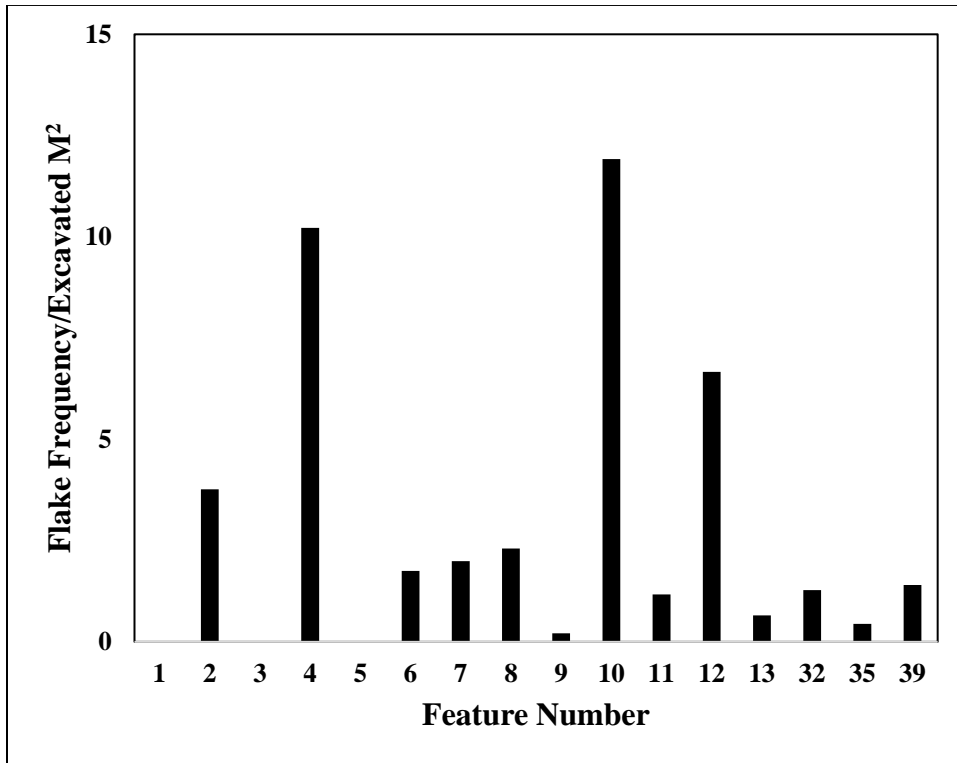


Figure 22: 5LR200 normalized flake frequency by excavation area (m²).

Examining the frequency of local to non-local debitage by feature exhibits some interesting patterns (Figure 23). The rings are clustered in groups, with two to four rings in each cluster. The percentages of local to non-local materials are similar in these clusters. For example, Features 8, 9, 10, and 11, located at the southern portion of the site contain almost entirely non-

local materials. Feature 11 is the only circle that contains pottery, and just like Killdeer, has a higher percentage of non-local debitage. Out of the 13 features examined on this map, all but two (Features 2 and 12) contain higher frequencies of non-local debitage. This suggests that the occupants of T-W Diamond were not on site long enough to exhaust their non-local resources. Based on the ratio of local to non-local material, it is possible that T-W Diamond was occupied for less time than Killdeer Canyon. The higher frequencies of debitage could instead represent a larger group transporting more material to the site.

The relative thickness of non-local raw materials is greater at all features (Figure 24). This means that the non-local debitage is consistently thinner than the local debitage, again consistent with Nelson (1991). Because the site is situated near a raw material source, local materials would not need to be conserved and flake sizes should be larger and thicker, this suggests the occupants of T-W-Diamond were conserving their non-local materials. If this is a true pattern, expedient tools should be manufactured primarily from local materials, a hypothesis tested in Chapter 4.

In order to examine the number of occupations at T-W Diamond, debitage were sorted into nodules based on visual and texture similarities. The nodule groups were not used to identify raw material source, rather to determine whether rings shared common material types. If T-W Diamond represents one occupation, the rings should be relatively homogenous in regard to nodule dispersal. This means that the occupants had access to and were sharing the same materials during occupation resulting in an even dispersal throughout the site.

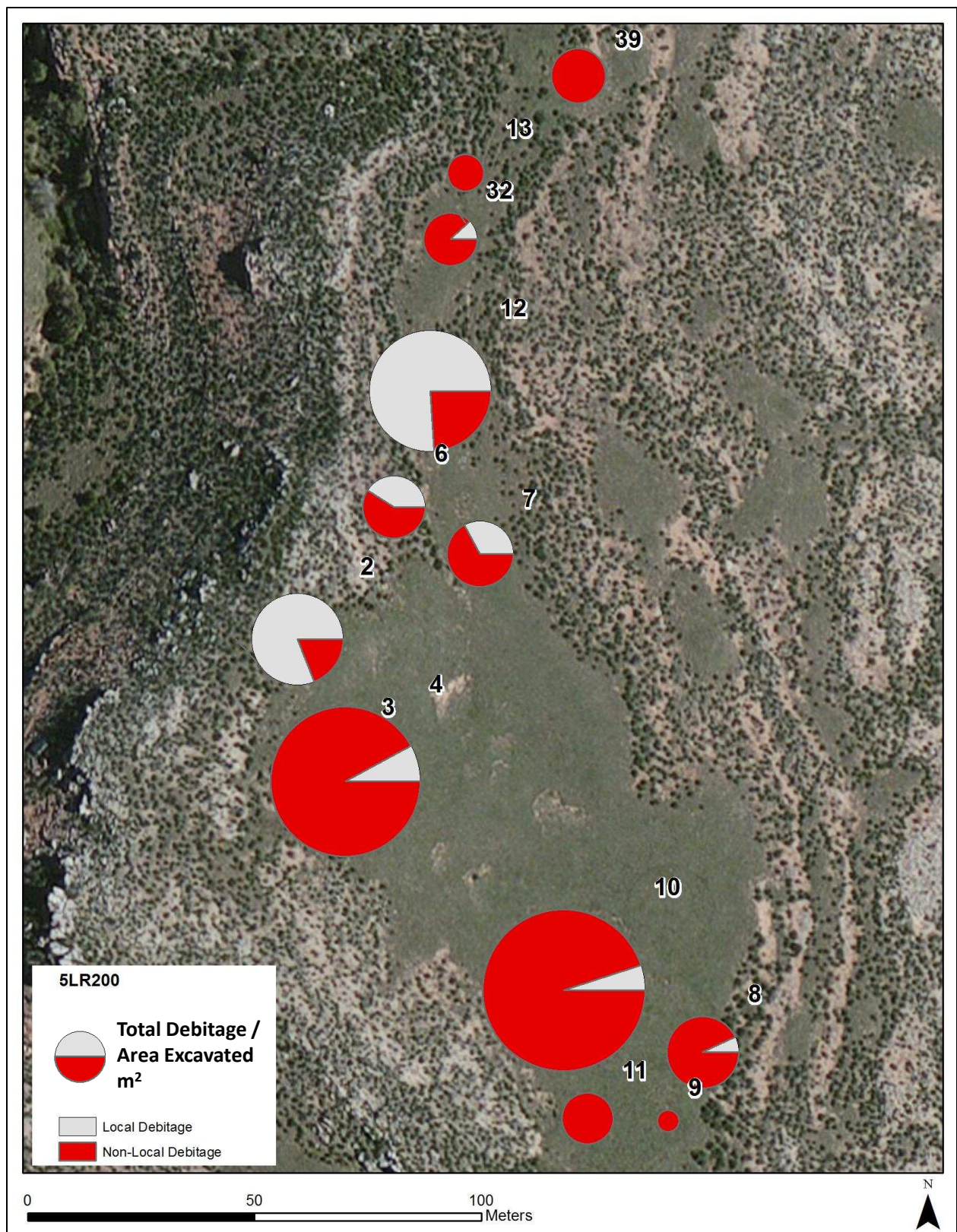


Figure 23: 5LR200 percentage of local and non-local debitage normalized by area excavated (m²). Pie charts are weighted by flake frequency. Feature number is labeled directly above ring.

Figure 25 shows the nodule dispersal using pie charts weighted by the total frequency of debitage. Nodule descriptions are summarized in Table 15. The nodule dispersal supports the site as a single occupation. There is heterogeneity between rings, meaning that the majority of the nodules are dispersed between all 13 excavated rings. In fact, there is not a single nodule type that is not present in at least two rings.

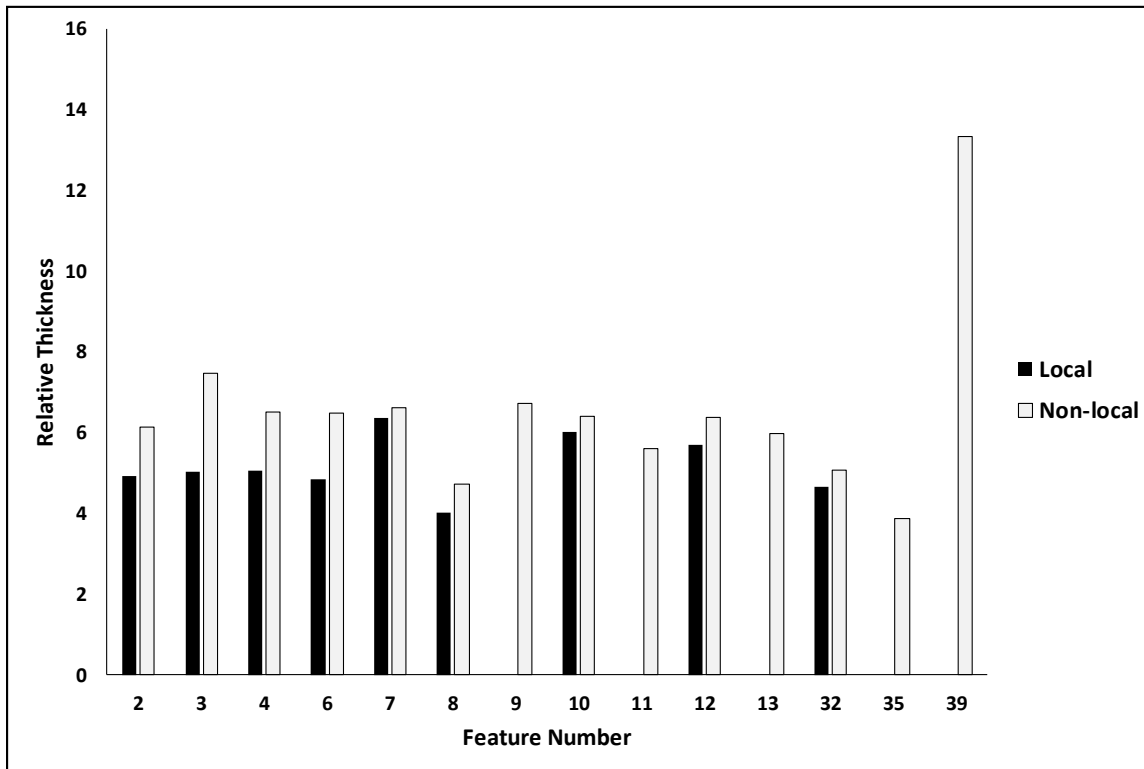


Figure 24: 5LR200 relative thickness of local and non-local debitage by feature.

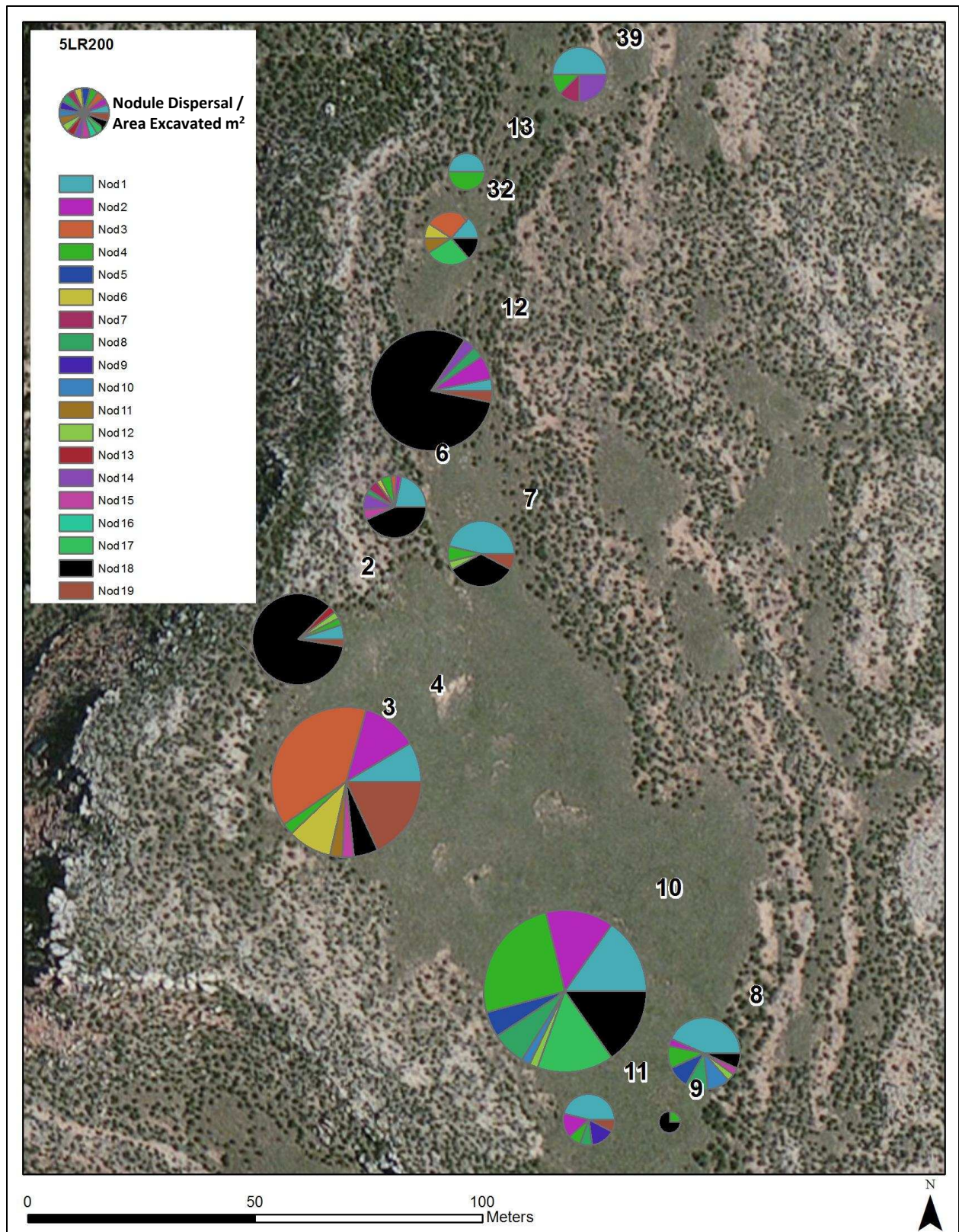


Figure 25: 5LR200 nodule dispersal between rings normalized by excavated m². Pie charts are weighted to represent the frequency of debitage.

Table 15: 5LR200 Nodule ID and description.

Nodule	Description
1	tan/light brown chert and chalcedony with some dendritic inclusions
2	darker brown chert/chalcedony with some dendritic inclusions, ranges from brown to almost black
3	light brown/tan chert/chalcedony
4	reddish brown chert
5	dark gray/black chert
6	brown, chert/chalcedony with some dendritic inclusions, similar to 2 but has distinct color difference
7	dark brown/gray matte chert
8	matte brown chert
9	matte gray to brown chert with some dendritic inclusions
10	reddish light brown chert/chalcedony
11	white matte chert/chalcedony with some inclusions
12	light tan and reddish chert with very few dendritic inclusions
13	reddish pink chert, mottled
14	light tan matte chert with dendritic inclusions
15	light gray and matte chert
16	very light tan and matte chert
17	petrified wood
18	local quartzite - reddish tan
19	white translucent chalcedony

Discussion and Conclusion

Comparing both Killdeer and T-W-Diamond reveals differences in the frequency of debitage per feature, the percentage of local to non-local debitage, and the relative thickness of the flakes. These differences can suggest patterns of household use intensity. Killdeer contains a relatively low frequency of debitage per feature, with 62 flakes representing the most-dense feature and 46 flakes representing the most-dense stone circle. On the contrary, T-W-Diamond contains a higher frequency of debitage per feature with 317 flakes in one stone circle. This could indicate differences in household use or support several site occupations. Killdeer Canyon does not show drastic differences in local and non-local material ratios. T-W-Diamond does, however, show a clear majority of features containing higher percentages of non-local materials. For every one feature at T-W Diamond that contains a higher percentage of local materials, there are 5.5 features that contain a higher percentage of non-local materials. Furthermore, the non-local materials from T-W-Diamond are smaller and thinner than the local materials.

Therefore, the two sites may represent the following scenario. Killdeer likely represents one occupation with minimal household use intensity. Feature 7 contains no structural evidence suggesting this may have been a short-term, camp during a warmer season when activities were completed outside of the tents. Based on the site's location in a valley bottom and on a small terrace, tucked away from the visibility of other groups passing by, the site probably represents a temporary campsite for a transit group. The local to non-local debitage ratios indicate some degree of tool replenishment took place, suggesting that the occupants stayed at camp long enough to seek out and use the local raw material source.

T-W-Diamond shows greater site-use intensity based on higher frequencies of debitage in some house features. T-W-Diamond likely represents a more-intensively used but shorter-term occupation. This is based on the higher frequency of debitage but low percentage of local material, as compared to Killdeer Canyon. The sites location on a ridge-top could have served as an easily recognizable area for a group congregation and suggests the occupants were not trying to conceal their location from other groups. The lack of substantial local material also suggests the inhabitants did not need to replenish their toolkits and were potentially on site for less time than the inhabitants of Killdeer Canyon.

CHAPTER 4: FORMAL TOOL ANALYSIS AND OCCUPATION SPAN

The purpose of this chapter is to a) describe the formal tools in the Killdeer Canyon and T-W Diamond assemblages and b) test assumptions regarding tool transport and occupation span at stone circle sites. Specifically, tool frequencies and raw materials are examined to test the length of occupation. In order to differentiate between one and many occupations, expectations are created for local and non-local tool dispersal patterns, the mean per capita occupation span, and patterns of local and non-local tools and debitage.

Theoretical Justification for Tool Analysis

Local and non-local tools are also a good indication of occupation length. Unlike debitage, lithic tool life spans do not exist entirely in their place of manufacture (Andrefsky 2005). Throughout the tool use life, it may be manufactured in one area, used off site, and transported to an entirely new location before the tool is replenished or discarded. Therefore, the questions that can be answered using lithic toolkits are somewhat different from those using debitage. Lithic tools do, however, provide important information regarding material transport and mobility.

Surovell (2009) developed methods for assessing occupation length per site occupant for Folsom-aged sites (Surovell 2009:58-98). Surovell (2009) argued that the mean per capita occupation span can be measured using the ratio of local and non-local raw materials to debitage to non-local tools. Ratios are used because discard rates of transported artifacts are reliant on the transported toolkit size. This analysis applies the mean per capita occupation span to each feature at Killdeer Canyon and T-W Diamond to assess the number of occupations at each site. The mean per capita occupation span should measure similarities in local and non-local resource

exhaustion rather than ring use-intensity. Therefore, the more clustered the data points, the more likely the site represents one occupation.

Because of the small sample size of tools at Killdeer Canyon and T-W Diamond, it is important to use the results from Chapter 3 to compare to the results of the formal tool analysis. The purpose of this analysis is to examine tool frequency, replenishment, and local and non-local material use.

Methods

Tools were sorted into nodules based on texture and visual comparison. The nodules were sourced to discern local from non-local materials, not to examine the distance non-local resources were transported. It is not in the scope of this analysis to examine the distance the occupants traveled or explore the possibility of trade.

Killdeer Canyon Formal Tool Descriptions

There are nine formal tools from excavated context (see Appendix E and F). For the tool analysis, artifacts were first split into categories describing their form (bifaces, unifacial tools, edge modified flakes, etc.) and then, if applicable, they were split into functional categories within the formal categories. The following section describes the functional categories, such as projectile points, first, then describes the remaining tools that were grouped by form.

Projectile Points

5LR289.1 is an all but complete projectile point made from tan-colored quartzite. The projectile point type compares to other Plains side-notched types (see Chapter 2) for a comparison of 5LR289.1 to other point types. The base form is concave and the blade form is

triangular. There is evidence of light resharpening on the blade margins. There is an impact fracture on the distal end of the projectile point suggesting it was discarded after use.

5LR289.2 is an all but complete projectile point made from gray-colored chalcedony. The projectile point type compares to other Plains side-notched types (see Chapter 2) for a comparison of 5LR289.2 to other point types. The base form is concave and the blade form is triangular. The ears, corners of the base, and tip are snap fractured. The blade margins are heavily retouched suggesting the tool was used multiple times before it was lost or discarded.

5LR289.4 is the tip of a finished biface, likely projectile point, made from brown colored quartzite. Although the tool is not diagnostic, the triangular and symmetrical blade form and small width (11 mm) suggest the tip would not have been part of a larger biface or knife. There is light resharpening on both blade margins. The fragment is snap fractured on both the distal and proximal end.

5LR289.10 is an all but complete projectile point made from purple-colored chert. The projectile point type compares to other Plains side-notched types (see Chapter 2) for a comparison of 5LR289.10 to other point types. The base form is straight concave and the blade form is triangular. There is evidence of light resharpening on the blade margins. A recent looking snap fracture on the distal end of the point suggests it was broken after it was lost.

5LR289.11 is a complete projectile point made from purple colored quartzite. The projectile point type compares to other Plains side-notched types (see Chapter 2) for a comparison of 5LR289.11 to other point types. The base form is concave and the blade form is triangular. The blade edges are heavily retouched and there is no utility remaining in the tool, suggesting it was discarded for this reason.

Bifaces

5LR289.3 is a complete hafted knife made from grayish tan-colored quartzite. The base is straight and the blade form is asymmetrical and triangular. It is possible the tool was a corner-notched dart point that was reworked into a knife. The tool is not considered a projectile point because of the asymmetrical edges. There is evidence of heavy retouch on the both blade margins.

Scrapers

5LR289.9 is a complete end scraper made from mottled purple and pink-colored chert. All edges of the scraper are modified. The distal end of the tool is at a 90-degree angle and is heavily retouched. The bulb of percussion and errature flake scars are still visible on the proximal end and ventral side of the tool. There is no evidence that the tool was hafted, such as polish or notching.

Edge Modified Flakes

This class includes all tools with at least one modified edge that do not fit within a functional category. This category includes tools 5LR289.5, 5LR289.6, 5LR289.7, and 5LR289.8. All but 5LR289.5 are made from chert. 5LR289.5 and 5LR289.6 both contain two modified edges. 5LR289.5 has an asymmetrical blade form suggesting the tool may have been used as a knife. All other margins of the tool are snap fractured. 5LR289.6 is a complete flake with two modified edges, but otherwise no shaping. 5LR289.7 and 5LR289.8 are more robust edge modified flakes, made on thicker flake blanks. 5LR289.7 contains no more than 10% cortex on the proximal end and is snap fractured on the distal end. Both lateral margins are pressure flaked. 5LR289.8 is a nicely manufactured cutting or scraping tool with a hinge fracture on one

end and a snap fracture on the other end. The tool has patterned pressure flaking on both lateral margins, one of which is steeply cut suggesting it may have been used for scraping.

Tools Found During 2014 Field School Survey, Not Included in Analysis

The following tools were found on the surface within the Killdeer Canyon boundary, but not within stone circle features, thus they were not included in the ring analysis.

5LR289.012 is a late-stage, likely projectile point, tip made from obsidian. The tool was found in an ant mound near other microdebitage. There is a snap fracture on the proximal end of the tip. While the association of the tool and the stone circle features is unclear, other obsidian artifacts from the site suggest the item was related to the site occupation.

Killdeer Canyon Formal Tool Analysis

The frequency of bifaces and other tools is displayed in Figure 26. Feature 7 contains the highest frequency of lithic tools. This feature, however, is not a stone circle, further supporting the feature as an outside processing area. Features 1-5 all contain one projectile point or other formal tool type. The low density of formal tools suggests the site was relatively short-term. Features 2, 3, and 4 contain other formal tool types, such as knives and a scraper that may have been used for processing.

Figure 27 displays the percentage of local and non-local lithic tools. There is only one local biface discarded at the site. Instead, the majority of tools discarded or left at this site are non-local materials. This indicates that the inhabitants of Killdeer Canyon were not on site long enough to need to replenish their toolkits. Instead, non-local tools were transported to the site, still contained use life, and were potentially used for animal processing and other activities. Local bifaces may have been manufactured in anticipation for a hunt or kill. On average, there is

one tool per feature at Killdeer Canyon positioning Killdeer Canyon at the far short side of the occupation length continuum.

Forty-four percent of the tools from Killdeer Canyon are local. This positions the site somewhere in the middle of the short to long continuum, suggesting the inhabitants were on site long enough to begin replenishing their toolkits with local materials. Furthermore, the majority of locally manufactured tools are bifaces. Whereas a longer-occupied site should have higher frequencies of expedient local tools (Parry and Kelly 1987) because of the proximity to a local source, the lack of expedient tools suggests Killdeer Canyon is somewhere near the middle of the continuum. The local and non-local tool data are somewhat contrary to the tool frequency results. Low tool frequencies indicate a short occupation while the percent local to non-local suggests the inhabitants were on site for a longer period. While these data may seem contradictory, the results likely indicate Killdeer Canyon inhabitants moved the majority of manufactured tools off-site.

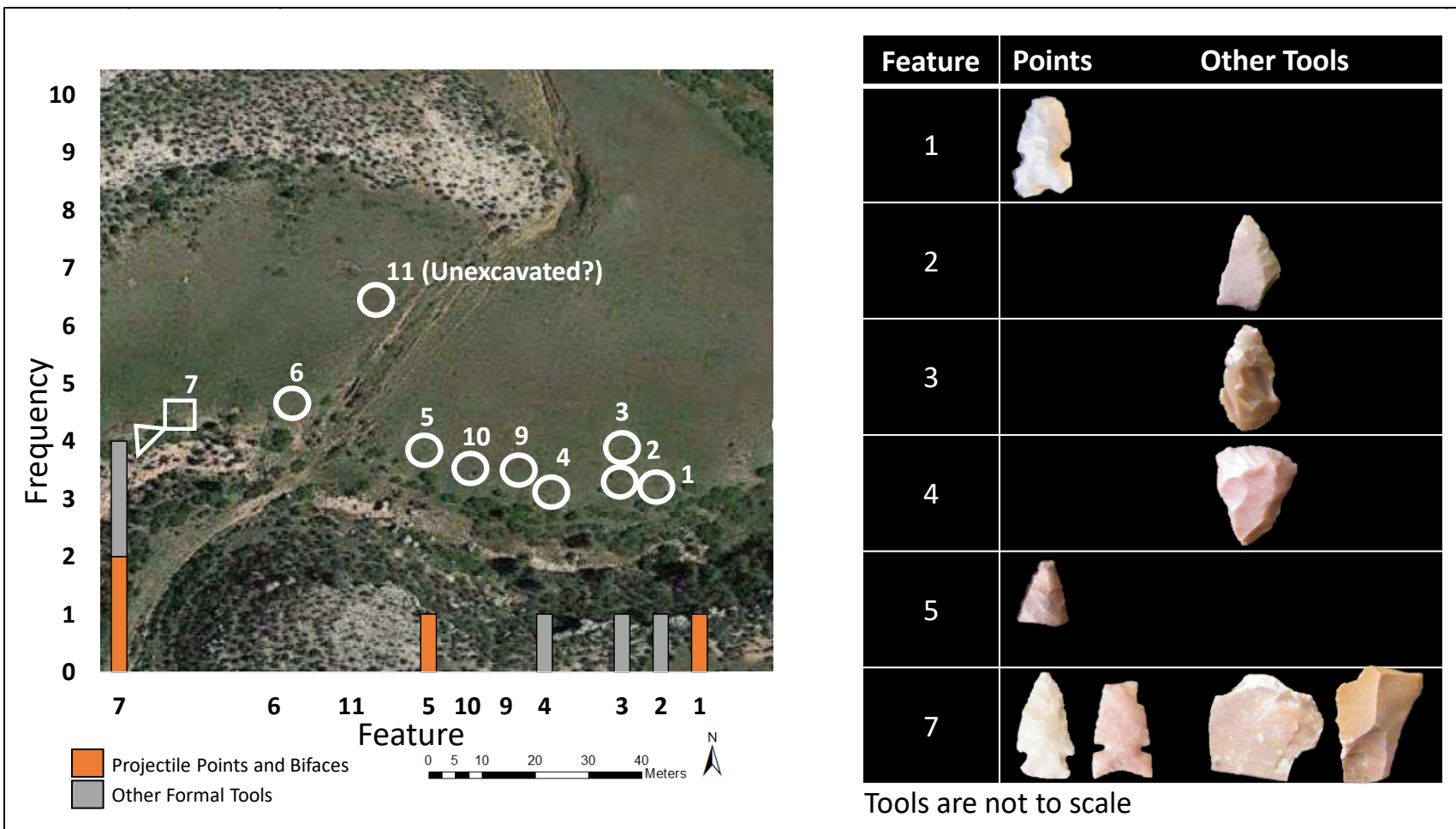


Figure 26: 5LR289 frequency of bifaces and other tools by feature. Images of tools (not to scale) are displayed in chart.

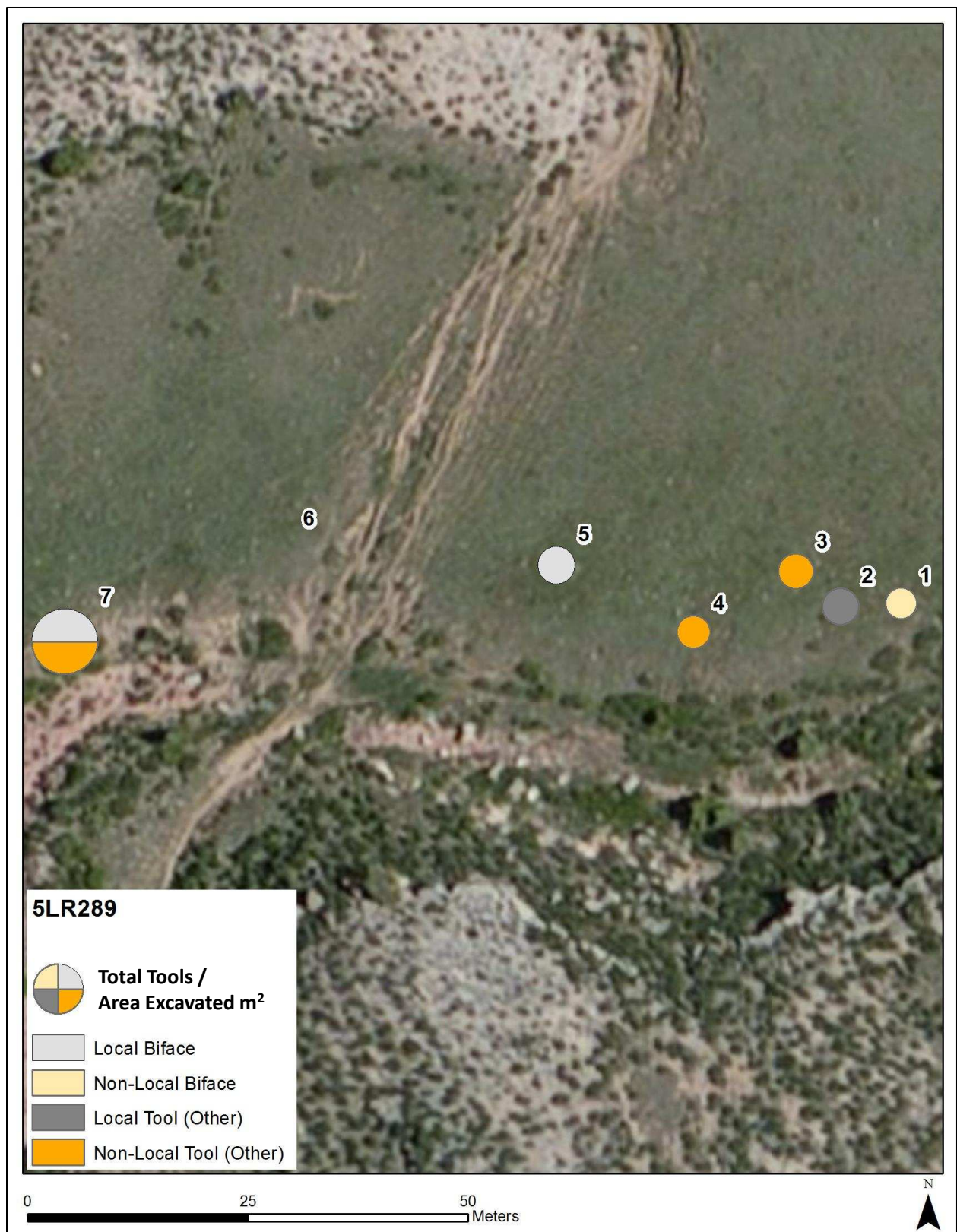


Figure 27: 5LR289 percentage of local and non-local tools normalized by square meters excavated. Pie charts are weighted by tool frequency. Feature number is labeled directly above ring.

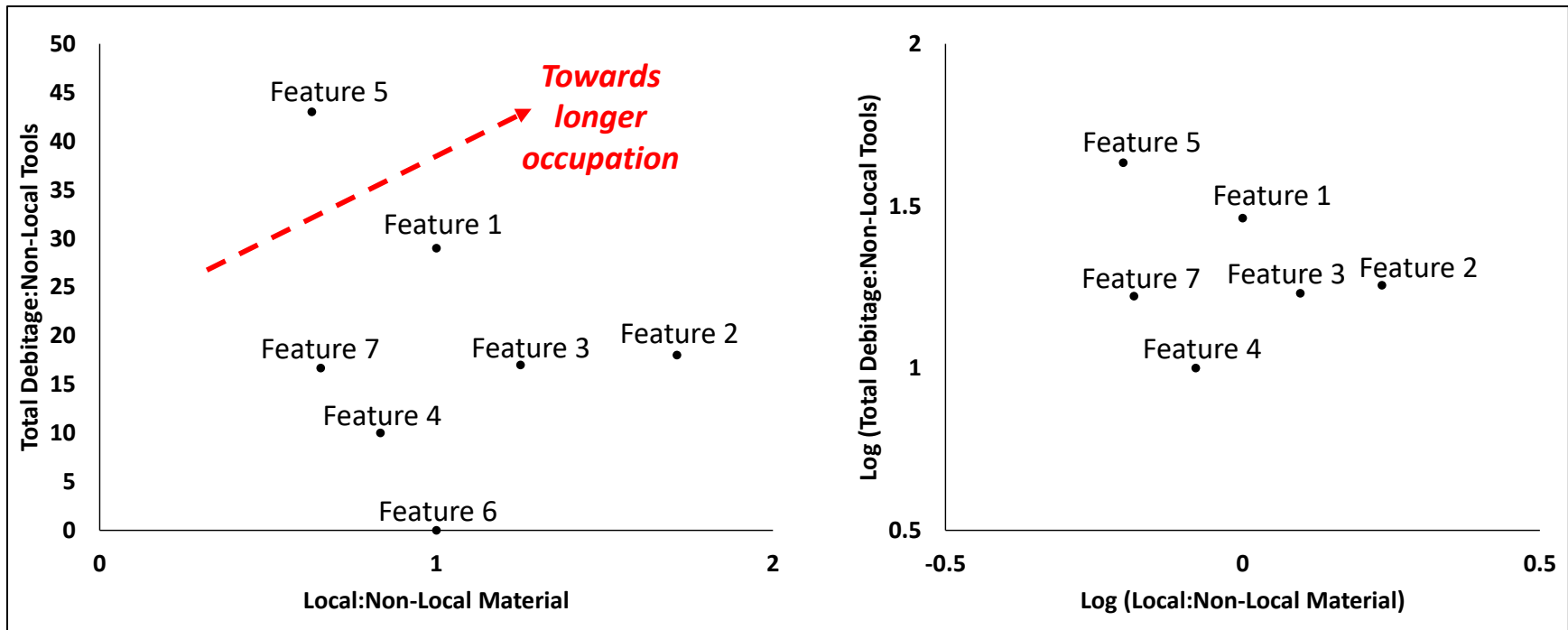


Figure 28: 5LR289 mean per capita occupation span. Local and non-local material (x-axis) includes all tools, flakes, etc. Diagram on right depicts logged values.

Features from Killdeer Canyon show similar mean per capita occupation spans (Figure 28). Feature 2 stands out farthest from the origin, suggesting it may be a longer occupied or perhaps more intensively used. When the data is logged, however, the features are clustered close together, suggesting the activities that took place in each ring and in Feature 7 may have been different, but the occupation lengths were similar. If Killdeer represents multiple occupations, there should be diversity in local to non-local material ratios between individual features. This again follows the assumption that an individual hunter-gatherer group would have access to only the materials transported to the site. Thus, the non-local materials should be replenished at roughly the same rate between rings.

Figure 29 shows the ratio of local to non-local debitage as well as the frequency of debitage using pie charts and the frequency of local and non-local tools is shown using a bar chart. Feature 2, farthest from the origin in the Figure 28 scatter plot, contains primarily all non-local debitage. Features 1 - 5 all contain one non-local tool.

Killdeer Canyon is a likely short-term occupation but ratios of local to non-local materials suggest the inhabitants were on site long enough to begin replenishing their toolkits. Patterns in material dispersal show slight differences between rings, but are overall homogenous. This suggests that the tools from Killdeer Canyon represent a single occupation rather than multiple reoccupations, supporting the results from Chapter 2 and Chapter 3.

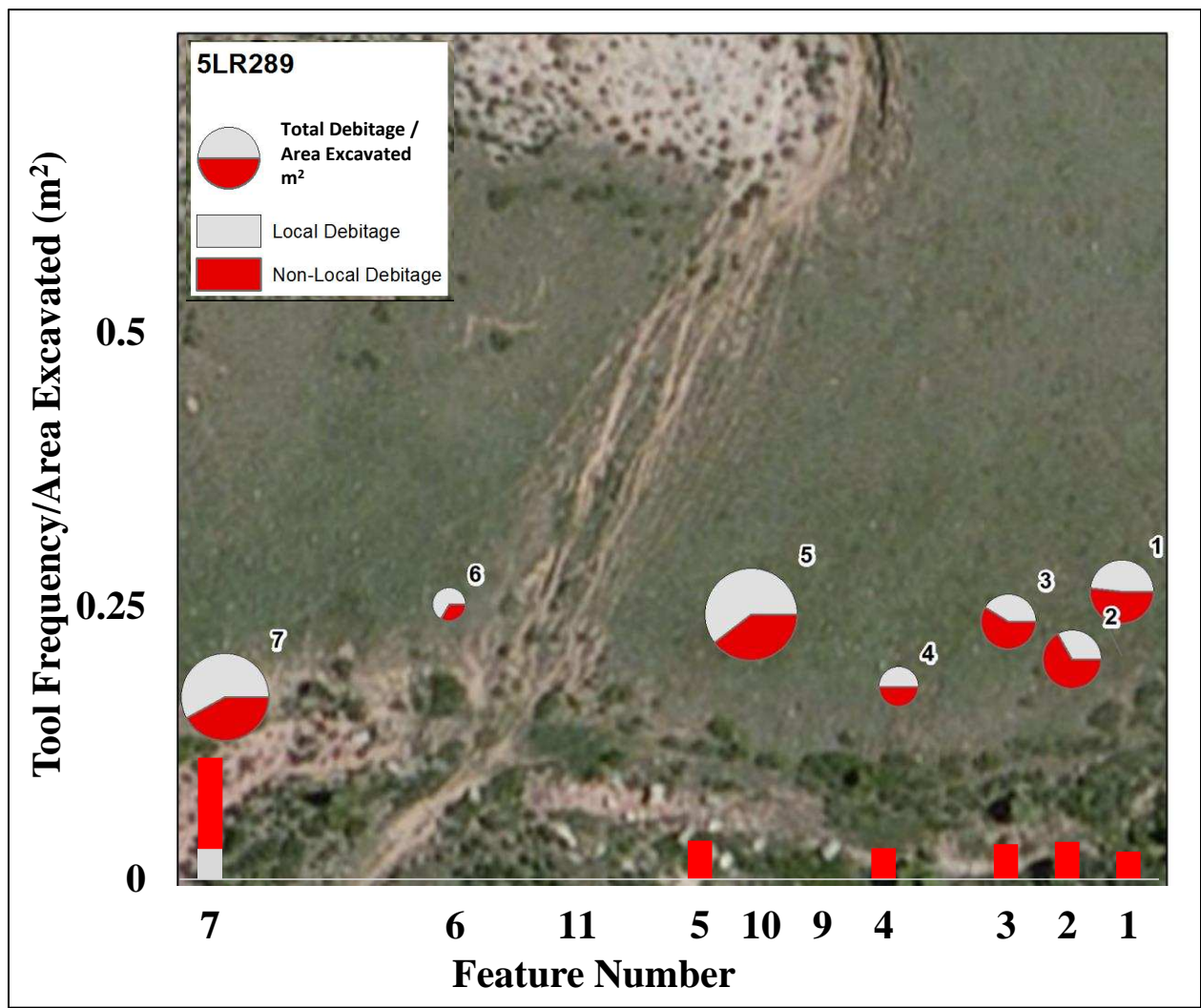


Figure 29: 5LR289 frequency of local and non-local tools (bar chart) and percentage of local and non-local debitage with pie chart weighted by debitage frequency.

T-W Diamond Formal Tool Descriptions

There are 56 tools in the T-W Diamond assemblage, 50 of which contain feature provenience (see Appendix H and I). These results are different from Flayharty’s (1972:92) original report, which had much higher tool counts. This is a result of re-cataloging the artifacts for this analysis. Many of the items originally classified as tools from the T-W Diamond site were omitted because the present author believes they are not formal tools. Higher projectile point counts originally reported in Flayharty (1972) are a result of an extensive surface survey

(see Appendix A). The original tool curation numbers (as marked on the tool) from the 1970s excavation were not reported in Flayharty (1972) but are reported here in Appendix H. Tools were split into categories first describing their form (bifaces, unifacial tools, edge modified flakes, etc.) and then, if applicable, they were split into functional categories within the formal categories.

Projectile Points

5LR200.1 is an all but complete Late Prehistoric projectile point made from white chalcedony with matte white inclusions. The projectile point is comparable to other Plains side-notched types (see Chapter 2) for a comparison of 5LR200.1 to other point types. The blade form is triangular and the lateral margins have little evidence of resharpening. There is a snap fracture on the distal margin and the tips of the ears and corners of the base are snapped off. It has a straight base. All snap fractures look recent and likely occurred after the projectile point was discarded.

5LR200.5 is the base of a Late Prehistoric projectile point made from tan and red chert with dendritic inclusions. The projectile point is comparable to other Plains side-notched types (see Chapter 2) for a comparison of 5LR200.5 to other point types. There is a hinge fracture on the distal portion of the projectile point suggesting the tool may have been broken in the haft. A corner of the base is also snapped off. The base is straight-concave.

5LR200.10 is the tip of a biface made from white and gray chert. The tip is likely from a projectile point based on the narrow point and triangular blade form; however, there is not enough of the biface to determine the tool function. The biface tip has some pot lidding and discoloration suggesting it was burnt. A snap fracture on the proximal end has the same evidence of burning suggesting it may have broken in a fire.

5LR200.14 is the midsection of a Late Prehistoric projectile point made from white and gray mottled matte chert. The projectile point is comparable to other Plains side-notched types (see Chapter 2) for a comparison of 5LR200.14 to other point types. There is one complete notch on the tool, confirming (coupled with the size and inferred neck width) that it is an arrow point. The blade form is triangular and the remaining lateral margins have no evidence of resharpening. The distal and proximal ends have recent-looking snap fractures suggesting the tool was broken after it was discarded.

5LR200.15 is the base and midsection of a Late Prehistoric projectile point made from tan quartzite. The projectile point is comparable to other Plains side-notched types (see Chapter 2) for a comparison of 5LR200.15 to other point types. The lateral margins are broken but the intact edges suggest the blade form was triangular and there is little evidence of resharpening on the intact margins near the base. Only one complete notch and side of the base are intact, but based on the inferred form, the base is straight. There are recent looking snap fractures on the proximal and distal ends suggesting the tool may have been broken after it was discarded.

5LR200.16 is the base and midsection of a Late Prehistoric projectile point made from white chalcedony with matte white inclusions. The projectile point is comparable to Plains tri-notched types (see Chapter 2) for a comparison of 5LR200.16 to other point types. One ear is missing and there is a snap fracture on the distal end of the tool. The blade form is triangular and the lateral margins close to the base show little evidence of resharpening. The base is concave and there is a notch at its center.

5LR200.17 is the tip of a projectile point made from tan and red petrified wood. There is light resharpening on the lateral margins of the tool. The tip is snap fractured on the proximal and distal ends but based on the small size and triangular blade form was part of a projectile point.

5LR200.21 is the tip of a biface made from tan chert. The biface tip is narrow and the blade form is symmetrical suggesting that the tool may have functioned as a projectile point. There is minimal resharpening on the lateral margins. There is a recent snap fracture on the proximal end of the tool suggesting it was broken after site abandonment.

5LR200.25 is the tip of a projectile point made from red chert. There is moderate resharpening on the lateral margins of the tool. The tip is snap fractured on the proximal end, but based on the small size and triangular blade form of the tool, it likely functioned as a projectile point.

5LR200.26 is an all but complete Late Prehistoric projectile point made from brown chert with dendritic inclusions. The projectile point is comparable to Plains side-notched types (see Chapter 2) for a comparison of 5LR200.26 to other point types. Only the tip of the projectile point is snap fractured off. The blade form is triangular. The tool has been resharpened all the way down to the base and has no remaining use life. The tool was likely discarded for this reason. The base is straight-concave.

Unnotched Points and Preforms

Unnotched projectile points are differentiated from projectile point preforms by determining whether the base is finished. A finished base is classified as a shaped margin that has been pressure flaked to be thinned.

5LR200.2 is an all but complete arrow point preform made from brown chert with dendritic inclusions. Based on its maximum width, the finished projectile point would have had a neck width less than 1 cm suggesting it is a Late Prehistoric aged tool. The projectile point preform is made from chert with material flaws in the medial portion preventing bifacial thinning on one face. The blade form is triangular and there is no resharpening. The proximal end of the preform is shaped to be concave but is not basally thinned, suggesting the tool was not finished.

5LR200.3 is the proximal end of a projectile point preform made from tan and brown petrified wood. Based on its maximum width, the finished projectile point would have had a neck width less than 1 cm, suggesting it is a Late Prehistoric aged tool. The projectile point preform is bifacially thinned; however, the broken platform from the flake is still visible on one of the lateral margins suggesting the tool is not finished and is a preform rather than a finished unnotched projectile point. The blade form is triangular and there is no resharpening. The proximal end of the preform is shaped to be straight.

5LR200.6 is an all but complete projectile point preform made from white chalcedony. Based on its maximum width, the finished projectile point would have had a neck width less than 1 cm, suggesting it is a Late Prehistoric aged tool. The projectile point preform is bifacially thinned. The blade form is triangular and there is no resharpening suggesting it is a preform rather than a finished projectile point. The proximal end of the preform is shaped to be straight.

5LR200.8 is an all but complete projectile point preform made from light tan chert with dendritic inclusions. Based on its maximum width, the finished projectile point would have had a neck width less than one centimeter suggesting it is a Late Prehistoric aged tool. The projectile point preform is bifacially thinned. The blade form is triangular and there is no resharpening suggesting it is a preform rather than a finished projectile point. The proximal end of the preform

is shaped to be straight concave. The distal end of the projectile point preform has a recent-looking snap fracture that likely occurred after site abandonment.

5LR200.11 is the base of an unnotched projectile point made from white and gray mottled chert. Based on the maximum width of the basal portion of the tool (less than one centimeter), the projectile point dates to the Late Prehistoric period. The blade form is triangular and the base is straight-concave. The projectile point is bifacially thinned, symmetrical, and has a finished base suggesting it is a finished projectile point and not a preform. There is no evidence of resharpening on the basal margins of the tool. There is a recent snap fracture on the distal end of the tool suggesting it was broken after site abandonment.

5LR200.18 are three glued portions of the midsection of an unnotched projectile point made from gray quartzite. Based on its maximum width, the projectile point dates to the Late Prehistoric period. The blade form is triangular and the base is straight-concave. The projectile point is bifacially thinned, symmetrical, and has a finished base suggesting it is a finished projectile point and not a preform. There is light resharpening on the lateral margins. There is an old impact fracture on the distal margin of the tool as well as multiple recent snap fractures suggesting the tool was discarded after use and broken again after site abandonment.

5LR200.20 is the base of a projectile point preform made from white chert. The maximum width of the base is 20.1 mm, larger than the other projectile point preforms on the site. The blade form is triangular and the base is straight-concave. The preform is bifacially thinned but has no evidence of resharpening suggesting it is not a finished projectile point. There is a recent snap fracture on the distal end of the base suggesting the tool was broken after site abandonment.

5LR200.44 is an all but complete finished unnotched projectile point made from matte gray chert. The maximum width of the base is 11.2 mm suggesting the finished projectile point would have had a neck width smaller than 1 cm associating it with the Late Prehistoric. The blade form is rectangular and the base is straight. The tool is bifacially thinned and has light resharpening along the lateral margins. There is a recent snap fracture on the distal end of the tool suggesting it was broken after site abandonment.

Other Bifaces

5LR200.4 is the end of a late stage biface made from matte gray chert. The lateral margins are bifacially thinned and there is no evidence of resharpening. The blade form is triangular and the tool is symmetrical suggesting it may have been the midsection of a projectile point; however, there is not enough of the tool remaining to know its function. Pot lids on in the cross-section of a snap fracture suggest the tool was broken during burning.

5LR200.12 is the lateral margin of a biface made from light-gray quartzite. The remaining lateral margin of the biface is medially thinned and shows no evidence of resharpening suggesting the tool may have been an earlier stage. All other portions of the tool have been snap fractured.

5LR200.22 is the lateral margin of a biface made from brown chert with dendritic inclusions. The fragment is hinge fractured on the medially edge suggesting it may have broken away from the biface during use.

5LR200.24 is the tip of a biface made from white and pink chert. The tip is blunt suggesting the tool may have functioned as a perforator. A snap fracture on the proximal end of the biface likely occurred during burning based on crazing and discoloration occurring on the tools surface and cross-section.

5LR200.33 is an early stage biface made from tan quartzite. There is no evidence of resharpening and the edges are just beginning to be medially thinned. There are large flake scars removed from both faces of the tool suggesting it may have functioned as a bifacial core.

5LR200.36 is the end of an early stage biface made from light-gray quartzite. The lateral margins are bifacially thinned and there is no evidence of resharpening. There is an old snap fracture on the medial portion of the tool suggesting the tool was broken during use or manufacture and discarded.

5LR200.39 are two glued fragments of a late stage biface end made from light-gray quartzite. The raw material is similar to 5LR200.36 and 5LR200.41. Discoloration on the end of the biface suggests portions of the tool were subjected to burning. The discoloration occurs on the cross-sections of the fragment suggesting the tool may have broken from burning. The medial fragment is snap fractured on the proximal and distal ends but refits to the end. The end fragment is snap fractured on all edges except for the lateral margin.

5LR200.41 is a margin fragment of a late stage biface made from light-gray quartzite. The raw material is similar to 5LR200.36 and 5LR200.39. The margin is medially thinned but there is no evidence of resharpening. The tool is snap fractured on all other margins. It is possible the tool is part of the same biface as 5LR200.39.

5LR200.43 is the margin of a bimarginal tool made from orange and brown petrified wood. The edge is medially thinned and may have functioned as a knife. There is moderate resharpening along the intact edge. All other margins of the tool have been hinge fractured.

5LR200.55 is the margin of a biface made from red chert. The intact margin is heavily retouched suggesting the tool was a finished biface. The fragment is the result of a hinge fracture that likely occurred while the tool was in use.

5LR200.56 is similar to 5LR200.55 in the breakage pattern and raw material type. The fragment is the margin of a biface made from red chert. The intact margin is heavily retouched suggesting the tool was a finished biface. The fragment is the result of a hinge fracture that likely occurred while the tool was in use.

The following tool classes (scrapers, non-bifacial cutting tools, and cores) are described by group. Individual metrics can be found in Appendix H. Tools were sorted based on similarities in form.

Scrapers

The assemblage includes one complete scraper (5LR200.37) and one scraper fragment (5LR200.54). 5LR200.37 is a unifacially retouched scraper made from white, gray, and pink mottled chalcedony. The tool has edge modification on the entirety of both lateral and the distal margins. There is cortex present on the dorsal surface. 5LR200.54 is a small fragment of a retouched margin of a scraper made from tan chert with dendritic inclusions. The tool likely broke during use based step fractures on the proximal end. Furthermore, the flake scars on the distal end are polished, possibly from use, suggesting it was broken before the tool was resharpened.

Non-Bifacial Cutting Tools (Microliths)

This specific tool class was determined based on similarities in tool form. Tools in this class are nearly identical blades-like flakes (as described by Lee et al. (2016:138)) with at least one modified edge. Tools 5LR200.45, 5LR200.46, 5LR200.47, 5LR200.48, 5LR200.49, 5LR200.50, 5LR200.50, 5LR200.51, and 5LR200.52 are included in this group. All tools in this class, with the exception of 5LR200.48 and 5LR200.52, are twice as long as they are wide.

5LR200.48 and 5LR200.52 are snap fractured and would have been longer when they were complete. The majority of tools, with the exception of 5LR200.50 and 5LR200.51, still contain their platform and bulb of percussion. 5LR200.50 and 5LR200.51 are the distal fragments of flakes. Of the eight tools in this class, three are quartzite (5LR200.47, 5LR200.48, and 5LR200.51). Tools 5LR200.45 and 5LR200.46 are tan chalcedony with many dark dendritic inclusions, likely from the same nodule. All other chert tools are from different nodules.

Notched Flakes

Two flakes (5LR200.29 and 5LR200.30) contain two successive notches on one lateral margin. Both tools contain no other edge modification. 5LR200.29 is made from tan chert with small dendritic inclusions. 5LR200.30 is made from a reddish tan chert with dendritic inclusions, possibly from the same nodule as 5LR200.29. Both tools are snap fractured on one margin.

Unifacial Perforators

5LR200.9 and 5LR200.28 are both manufactured on flake blanks and contain at least one modified edge that comes to a point. 5LR200.28 is manufactured from a tan chalcedony with dendritic inclusions and 5LR200.9 is manufactured from a pinkish tan chalcedony. 5LR200.28 is complete and contains modification on all edges of the tool, forming a triangle with three points that may have been used as a perforator. 5LR200.9 is snap fractured on two edges and only contains one margin worked into a perforator.

Other Unifacial Tools

5LR200.7, 5LR200.13, 5LR200.19, 5LR200.23, 5LR200.27, 5LR200.34, 5LR200.35, 5LR200.40, 5LR200.42, and 5LR200.53 were grouped into this tool class based on the presence of at least two modified edges, suggesting the tool was intentionally shaped for a function. All

tool fragments contain at least one snap fracture and are small in size making it difficult to assign a tool function. 5LR200.13 and 5LR200.35 are manufactured from local quartzite. The rest of the tools are chert and 5LR200.34 is chalcedony.

Cores

The assemblage includes three cores (5LR200.31, 5LR200.32, and 5LR200.38) from two different nodule types. Tools 5LR200.31 and 5LR200.32 are grayish-red chert with small black dendritic inclusions. The cores are multidirectional and no longer contain useable material. 5LR200.38 is also a multidirectional core made from local quartzite. The core also contains no useable material. The three cores are similar in dimension, within one cm in maximum length and width.

Steatite Pipe or Sucking Tube Fragment

5LR200.57 is the end of a round, narrow, and hollow artifact made from dark gray mottled steatite (Figure 30). The artifact is potentially a pipe fragment made from dark gray mottled steatite. The fragment has part of the rim but is split horizontally in two. Frison and Norman (1993) documented several steatite and sandstone pipes from the southern Bighorn Basin in north-central Wyoming. More recent research by Packard (2015) documented steatite distribution in northern Colorado and indicated that the T-W Diamond steatite fragment is at least 200 km from its place of manufacture. The diameters range from 8 – 17 mm (proximal barrel diameter), most of them larger than the 12.4 measured maximum width of 5LR200.57.



Figure 30: 5LR200 steatite tool fragment, likely pipe.

Tools Found During 2014 Field School Survey, Not Included in Analysis

The following tools were found on the surface within the T-W Diamond boundary, but not within stone circle features, thus they were not included in the ring analysis.

5LR200.1114 is an all but complete corner-notch projectile point made from gray chalcedony. The base is convex and the blade form is triangular. One ear is recently snap fractured, which likely occurred after the tool was discarded. There is evidence of light resharpening on both blade margins. The tip of the projectile point is blunt and contains an impact fracture that travels down one blade margin suggesting it was lost or discarded after use.

5LR200.1115 is a midsection of a finished biface made from red chert with dendritic inclusions. All other tool margins are snap fractured. The intact edge is medially thinned with even flake scars on either side suggesting the finished tool was nicely made. The blade form is straight making it difficult to determine the tools original function.

5LR200.1116 is a possible scraper made from local gray quartzite. The tool is lightly retouched on two adjacent margins. The edge of the tool is angled greater than 45 degrees

suggesting it was modified for scraping and not cutting. Other margins contain snap fractures likely from bovid trample since the tool was on the surface.

5LR200.1117 is a bimarginal tool with asymmetrical margins made from matte tan chert with dendritic inclusions. The tool was likely used as a knife based on the asymmetrical edges. Both margins are medially thinned, however, the ventral surface contains no modification. The proximal and distal end of the tool are recently snap fractured which likely occurred after the tool was discarded. There is no evidence of resharpening on either of the margins.

T-W Diamond Formal Tool Analysis

T-W Diamond contains slightly more discarded projectile points and bifaces (n=29) than other tools (n=21) (Figure 31). On average, there are four tools per feature positioning T-W Diamond on the short-term side of the occupation length continuum.

Features 2, 4, and 9 only contain tools that are not bifaces or projectile points. Figure 31 also shows a noticeable pattern in raw material types between the two tool classes. Projectile points and bifaces are made out of more diverse materials than the artifacts in the other tool category. Although this cannot be tested, there appears to be more aesthetic selection of raw material for the formal tools from T-W Diamond.

T-W Diamond contains primarily non-local bifaces and other tools (Figure 32). Only Features 2, 8, and 12 contain locally manufactured tools. Feature 2 is the only feature containing expedient tools (n=2) manufactured from local quartzite; Features 8 and 12 both contain local bifaces. Again, this suggests the occupants of T-W Diamond were not at the site long enough to replenish their toolkits entirely with local materials. As mentioned in Chapter 3, a short-term site near a raw material area should lack expedient local tools. This is the pattern at T-W Diamond, suggesting the occupants were gearing up for their next move, rather than staying on site long

enough to use expedient tools from a local material source. Seventy-four percent of the tools are non-local, situating T-W Diamond on the far short-end of the occupation length continuum.

Examining the mean per capita occupation span at T-W Diamond, there is more diversity than seen at Killdeer Canyon. The majority of the features are clustered near the origin; however, a few stand out (Figure 33). Feature 2 is the farthest from the origin. This indicates it may have been the longest occupied. Features 7 and 10 are also outside of the cluster of features by the origin; however, they do not stand out as far as Feature 2. While this might suggest Feature 2 represents a different component, the radiocarbon dates are not different from other ring date ranges. Instead, Feature 2 may be associated with tool manufacture, causing a higher frequency of local material than expected. Future efforts should focus on refit analyses between Feature 2 and other clusters. A positive refit would prove the rings are contemporaneous and that the differences in mean per capita occupation manifest from task specialization.

Figure 34 shows the ratio of local and non-local debitage using pie charts skewed by frequency as well as the frequency of local and non-local tools using a bar chart. The distribution of local and non-local material shows a majority of non-local materials. Features 2 and 12 contain the most local debitage and Feature 12 contains the highest frequency of local tools. It is possible Features 2 and 12 are part of a different occupation than the other rings in this analysis based on their higher frequencies of local materials. However, the rings are located within different clusters suggesting the differences in local and non-local materials could actually represent task specialization. While Features 4 and 10 contain the most debitage, Features 2 and 12 could have been primary lithic reduction areas where new tools were being manufactured from local material. Features 4 and 10 could represent an intensive processing area where transported tools were used, reworked, and discarded first. T-W Diamond could represent a

short-term single occupation site based on ratios of local to non-local materials suggesting the inhabitants were not on site for a long period and did not need to replenish most of their non-local tools.

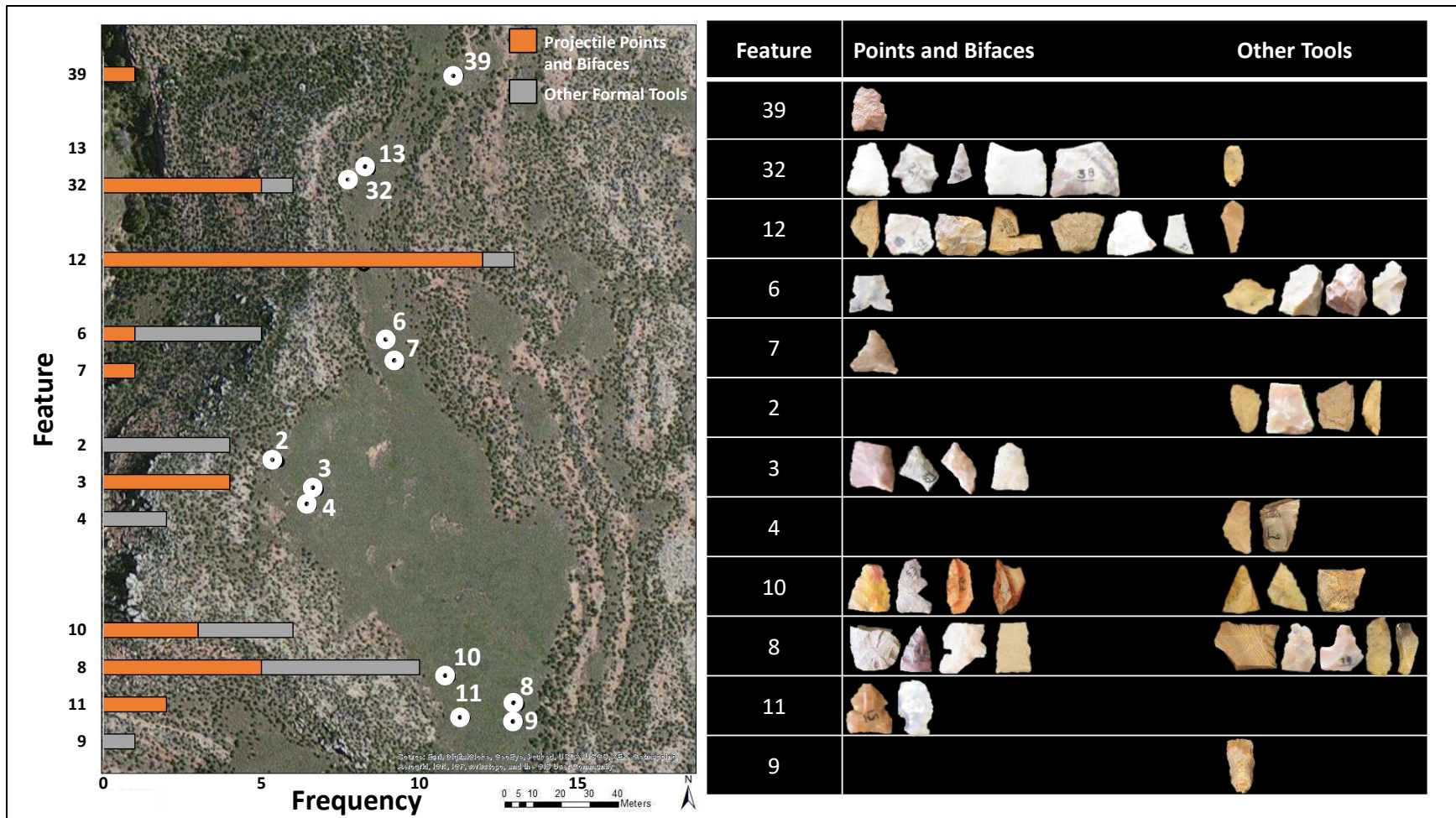


Figure 31: 5LR200 frequency of bifaces and other tools by feature. Images of tools (not to scale) are displayed in chart.

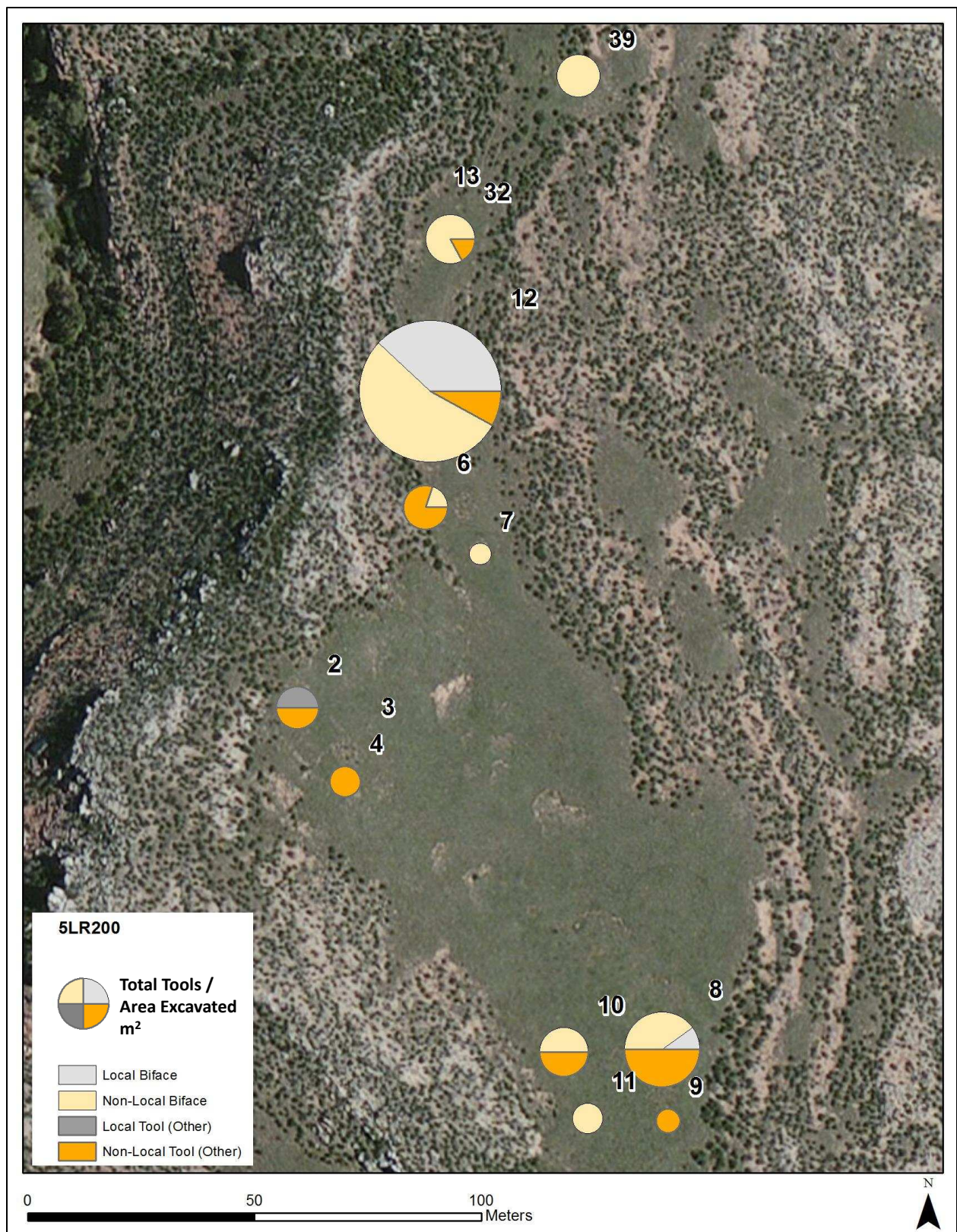


Figure 32: 5LR200 percentage of local and non-local tools normalized by square meters excavated. Pie charts are weighted by tool frequency. Feature number is labeled directly above ring.

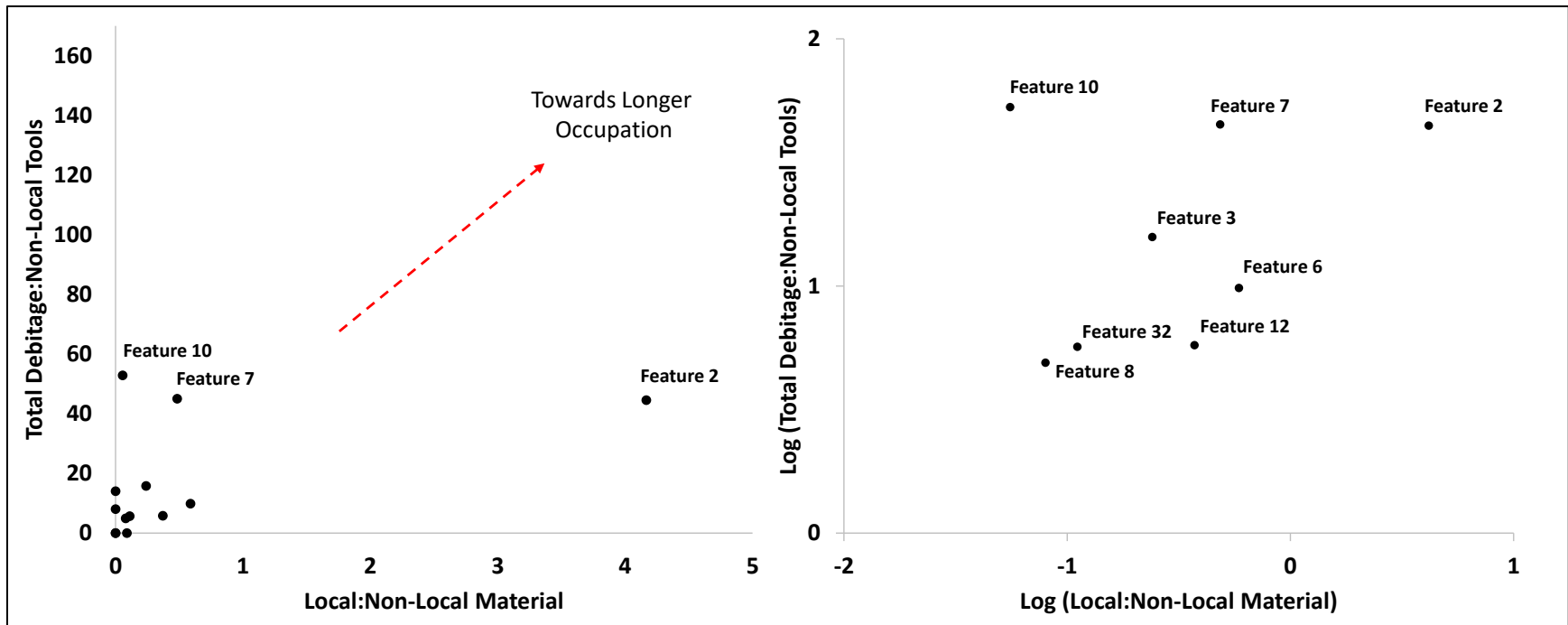


Figure 33: 5LR200 mean per capita occupation span. Local and non-local material (x-axis) includes all tools, flakes, etc. Diagram on right depicts logged values.

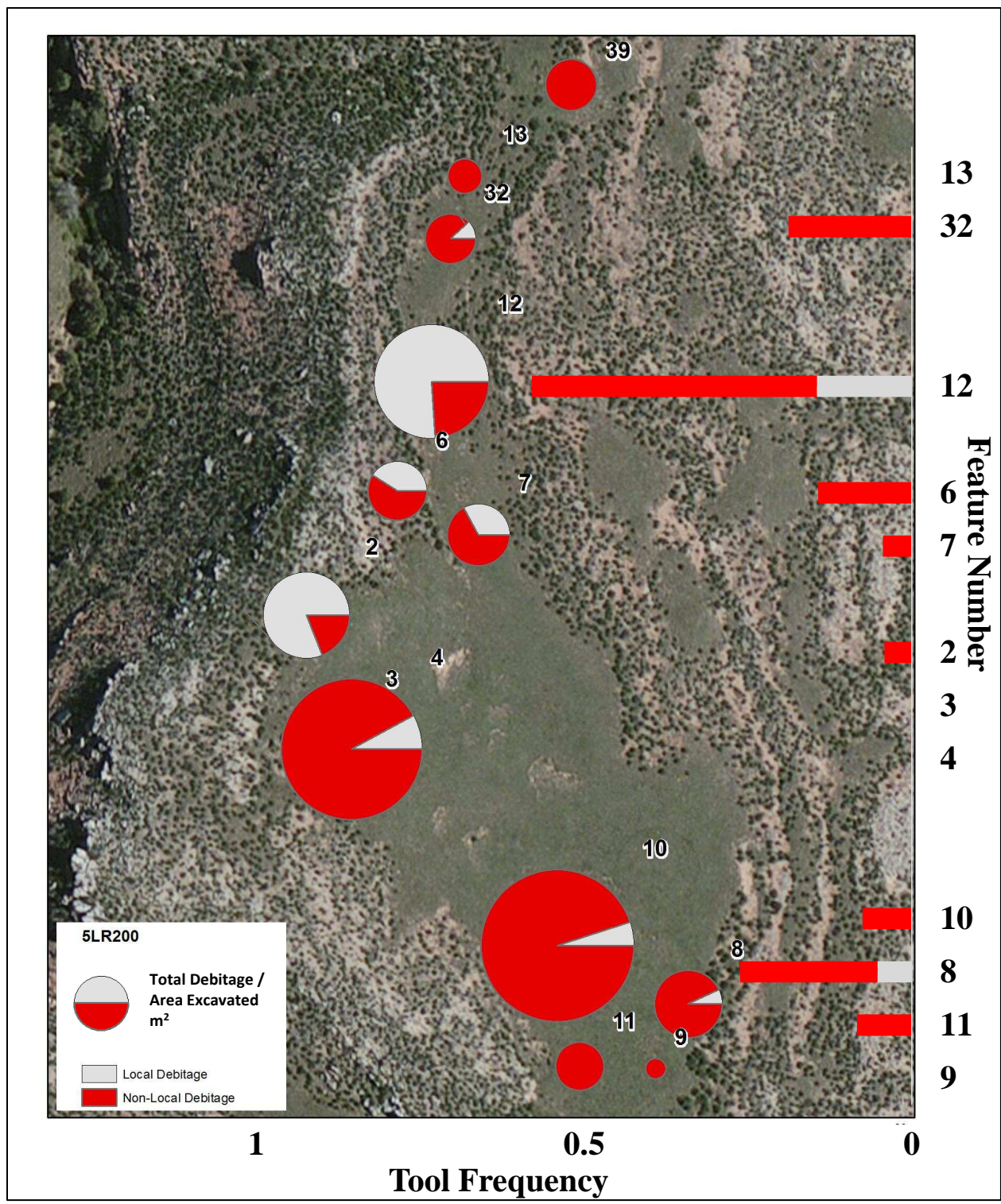


Figure 34: 5LR200 frequency of local and non-local tools (bar chart) and percentage of local and non-local debitage with pie chart weighted by debitage frequency.

Discussion and Conclusion

Comparing the two sites, the closeness of artifact types and raw material use is evident at Killdeer, suggesting it is a single occupation. Again, this chapter supports Killdeer was occupied relatively longer than some of the features at T-W Diamond. There is primarily non-local tool discard at the Killdeer Canyon and T-W Diamond sites. The small sample size at Killdeer Canyon, and similarity of occupation length between stone circle features suggest the site was one occupation. The moderate sample size and similarity between stone circle occupation lengths at T-W Diamond suggest this site was also one occupation, but the high frequency of non-local material indicates it was occupied for less time than Killdeer Canyon. While this could be a result of T-W Diamond being farther from the Campbell Mountain material source, it is unlikely an added kilometer distance would not be significant enough to impact the toolkit replenishing strategies. The mean per capita occupation span also supports the hypothesis that T-W Diamond was occupied for less time. While features from both sites are clustered near the origin, the Killdeer Canyon stone circles plot slightly farther from the origin than the rings from T-W Diamond suggesting they were occupied for longer.

CHAPTER 5: SUBSISTENCE AS A MEASURE OF OCCUPATION SPAN

This chapter uses faunal remains from individual rings as a proxy for occupation span at Killdeer Canyon and T-W Diamond. This is accomplished by examining bone mass, degree of processing, species representation, bone modification, and element representation.

Theoretical Justification for Faunal Analysis

Occupation length is examined using total bone, processing intensity, species representation, and modification. This assumes that bone fragments will increase with occupation length because a group staying in one place for a long period will require more food to feed their camp.

Species representation and diversity can be used as a proxy for measuring occupation length. This reflects residential versus logistical mobility patterns (Binford 1980). A site that is organized around residential mobility may contain a low diversity of taxa because hunter-gatherer groups would be more reliant on procuring one species. A site that is organized around logistical mobility should have higher frequencies of taxa because animals would be hunted within a radius of the camp and brought back to the base camp for further processing. The latter group organization limits mobility thus increasing the diversity of resources. Following this assumption, a residential camp would be in one place for a shorter period than a logistical camp. Measuring the diversity of taxa will be used as a proxy for understanding occupation length. This assumes that species diversity will increase with occupation length. Occupation length can be visualized on a continuum using different site types with known occupation lengths. Bison kills can be viewed on the very short end of the continuum.

Bison jumps represent a moment in time where a herd is driven off a cliff and processed. The purpose of these kills is to yield a lot of meat in a short period, thus, the efforts of the hunter-gatherers are focused on the procurement of one species. The Roberts Buffalo Jump (5LR100) (Johnston 2016) is an example of a Late Ceramic-aged jump located within two kilometers of Killdeer Canyon and T-W Diamond. Conversely, more permanent residential sites, such as Kinney Spring (5LR144c) (Perlmutter 2015) can be viewed on the other end of the continuum.

Morris (1981:215) summarized a kilocalorie study using bison meat/jerky. The study found that 1.2lbs of bison meat is a sufficient supply for daily caloric intake. Buffalo bulls range between 1,600-1,800 lbs. and buffalo cows range between 800-900 lbs. If a 1,000 lbs. bison is processed, the deboned meat yield would be around 425 lbs. (National Bison Association 2016). For a group of five, a 1,000 lbs. bison would theoretically last for 70 days, or just over two months. Based on the number of rings at each site (Killdeer = six excavated rings/ one processing area and T-W Diamond = 17 excavated rings) it is very likely that more than five people were occupying each site. Although the exact number of occupants can only be hypothesized by methods not examined in this thesis (ring diameter, ethnographic records, number of processing vs. domestic structures, etc.) if there were three people in each tipi, that would suggest the number of occupants at Killdeer Canyon was around 20 and the number of occupants at T-W Diamond was around 50. One bison would have lasted the Killdeer occupants just over two weeks (18 days) and the T-W Diamond occupants around one week. Although this is a hypothetical instance, without evidence for other intensive processing tools, such as ground stone, the MNI of bison is a good indication of relative occupation length.

Faunal processing and modification are used as a proxy for occupation length in the following manner. While other tasks such as lithic reduction are known to take place inside of structures, bone processing presents an interesting dilemma for studying its accumulation within rings, as the majority of processing probably took place outside of stone features. While a probably outside processing area was identified during excavation at Killdeer Canyon, no outside activity areas were found at T-W Diamond (see Chapter 1). If there are unexcavated processing locales at T-W Diamond this would likely impact the faunal study in the following way. While small fragments of bone may have been discarded in rock rings, the larger and more preliminary processing debris could be elsewhere. These results would then suggest T-W Diamond was occupied for less time.

As occupations length increases, processing intensity of bone will also increase. Highly processed faunal remains include bone fragments smaller than 6 cm, cut and percussion marked bones, and bone tools (Scheiber and Reher 2007). Furthermore, the represented elements will indicate the utility of materials being processed. In an intensively used ring, hunter-gatherers have more time to process a greater diversity of elements for different tasks. This includes using animal hides and furs for shelter and clothing production/maintenance, as well as manufacturing of bone tools for completing these tasks. A low intensity ring might only process high utility elements for a single task, such as consumption, and discard the remaining unmodified elements. This phenomenon is seen in other archaeological sites such as the Kaplan-Hoover bison jump (Todd et al. 2001) where only the high utility elements on the most accessible bison were processed.

To differentiate between one versus many short-term occupations, the following expectations are tested. Counter to the lithic analysis in this study, if a site contains multiple

short-term occupations, there should be no recognizable pattern of skeletal element distribution between ring clusters. Because the number of elements are known within a species, patterning of element dispersal between rings might suggest food sharing, a phenomenon that could only take place during a single occupation. If a site contains multiple occupations, these expectations should be patterned in ring clusters throughout the site. In this scenario, occupation spans may differ between occupations, thus different ring clusters should show different element compositions. This assumes that related peoples will camp close to one another and clustered rings with similar faunal signatures should represent one occupation.

Within ring clusters, a group should have been practicing similar food preparation strategies. It is possible that there was some degree of task specialization within these clusters, which could cause some rings to have different faunal signatures. In other words, if a group killed a bison, even if the elements were distributed unequally throughout the rings, other variables such as species type and relative age should be more similar within the cluster than between other clusters. This phenomenon is noted by O'Brien (2013) at the Eden Farsen site and attributed to unequal food sharing. Conversely, a site that contains multiple occupations can have greater homogeneity between all rings. This is because there are a set number of elements within once species. If small groups are returning to an area repeatedly through time, and hunting bison, it is possible that unrelated rings will contain similar elements.

It should be noted that there are more precise methods of faunal analysis, such as anatomical refit analysis, that can demonstrate ring contemporaneity. These methods, however, are outside the scope of this analysis. Future research should test expectations created in this chapter with more precise measures such as these.

Methods

Individual bone fragments were sorted and given catalog numbers. Only bone from excavated context was included in this analysis. Stone rings were used to separate the bone into units of analysis. Faunal specimens were sorted and analyzed by feature number. Maximum length (mm) and weight (g) were collected for each bone fragment. Identifiable specimens were coded for species, element, portion, segment, side, and age if possible. Identifiable fragments were compared to the Department of Anthropology faunal comparative collection.

Killdeer Canyon Results

The Killdeer Canyon assemblage consists of 271 bone and tooth fragments (see Appendix L). There are 284.7 grams (total) of faunal remains from excavated context at the Killdeer Canyon site and 268.3 grams have feature provenience (Figure 35). Fragments range from less than one gram to 49 grams and the average mass of the bone fragments is 3 grams. Bone fragment length, on average, is 18.0 mm, though bone mass is more heavily relied on because bone fragments vary in their deterioration rate. Feature 7, a probable outside processing area, contains the highest bone mass.

Features 5 and 6 contain the second highest masses of bone fragments. These features are located on the western portion of the site and are separated from other ring clusters further east. An ephemeral wash down-cuts the terrace on a roughly north/south axis between Features 5 and 6 suggesting that there may have once been other stone circles located between the two features. Alternatively, features 5 and 6 may have represented processing structures and been purposefully isolated from other habitation structures. A decrease in bone mass in rings farthest from Feature 7 suggests the site may have been organized with habitation structures, used for sleeping,

situated away from the processing area. This is supported by a lack of other lithic debris in Features 1-3 (see Chapters 3 and 4).

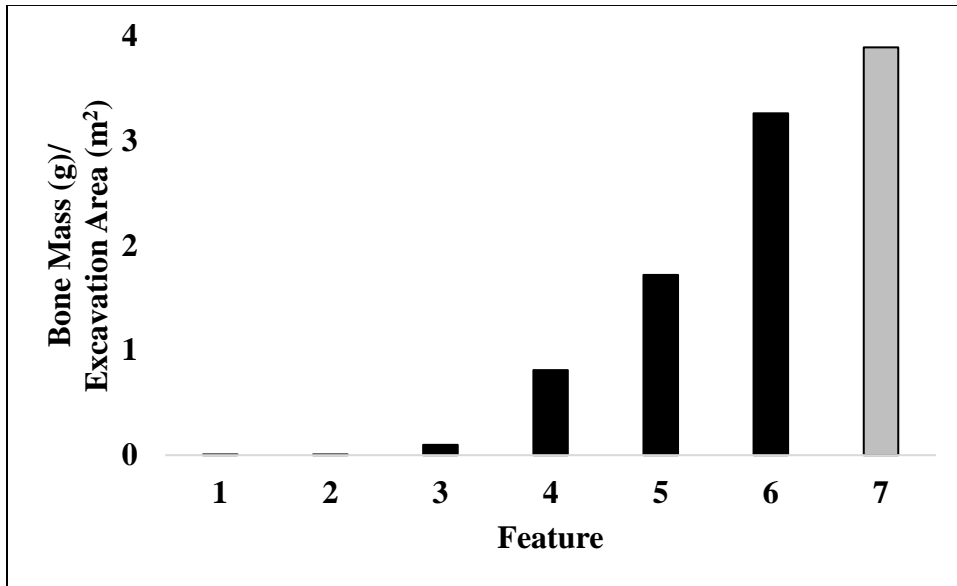


Figure 35: 5LR289 bone mass (g) by feature number normalized by excavation area (m²). Feature 7 is highlighted in gray because there is no associated stone circle. The area likely represents an outside processing station.

The species representation at Killdeer Canyon is not diverse. Features 4, 5, 6, and 7 all contain adult *Bison bison* (MNI=1). Features 4, 5, and 6 all contain juvenile bison increasing the MNI (MNI=2). Feature 7 contains likely intrusive rodent (Figure 36). The lack of other more intensive processing units, such as ground stone, and lack of species diversity supports the hypothesis that the occupants of Killdeer Canyon were on site for a very short period. The dispersal of adult and juvenile bison between rings and low MNI supports the site as a single occupation, although anatomical refitting would be necessary to confirm contemporaneity.

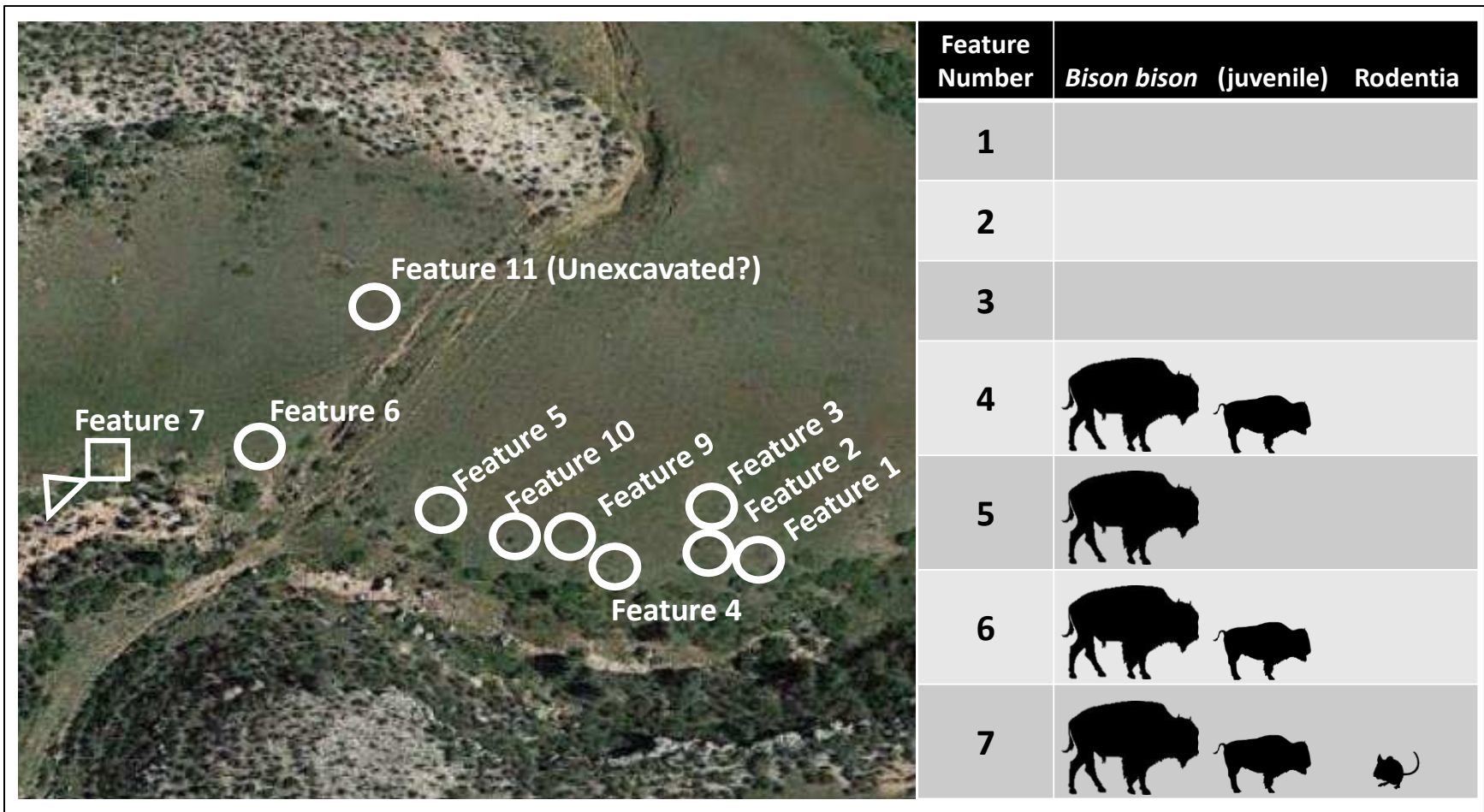


Figure 36: 5LR289 species representation by feature.

Processing intensity was measured using the maximum length of fragments as well as the bone frequency and mass (g). Maximum length (mm) ranges from 3 mm to 108 mm. The average length of bone fragments in the assemblage is 18.03 mm, the median is 12.3 mm, and the mode is 15.7 mm.

The frequency and mass (g) of bone per feature can be spatially compared to examine the processing intensity. A higher mass (g) of bone but smaller frequency indicates the elements are larger. Conversely, a lower mass (g) but higher frequency of bone indicates the elements are smaller. Killdeer Canyon's Features 1, 3, and 7 all contain smaller bone fragments. Features 4, 5, and 6 all contain larger bone fragments (Figure 38).

The small sizes of bone fragments are consistent with longer occupations, as defined by Scheiber and Reher (2007). This is at odds with the expectations created for short-term stone circle sites. This is likely a result of one or a combination of three reasons. First, it is possible taphonomic processes have eroded much of the bone in this shallowly buried stone circle site, making fragments much smaller and more brittle. Second, it is possible that the size of bone fragments is not a good indication for occupation length and instead simply reflects a need for more intense use of the animal. Third, it is possible that smaller bone fragments should be expected within a household structure because animals are not necessarily processed but consumed inside. Thus, most fragments recovered from interior spaces should be smaller and more consistent with the signature seen at other long term residential sites.



Figure 37: 5LR289 bone tool, likely flesher. White arrow points at polished end with grooves.

Killdeer Canyon contained one spirally fractured femur, zero cut marked bone, and zero carnivore modified bone. There is one bone tool from excavated context, however it contains no provenience. The bone tool is 108.03 mm long, 16.78 wide, and 6.01 thick. There is heavy polish on the distal end and at least two intentional grooves engraved on the dorsal surface of the distal end (Figure 37). The tool likely functioned as a flesher, or processing tool. The function of the grooves is unknown, but they are likely not a result of use wear based on the patterning of the incisions and deepness of the grooves which can be seen without any magnification.

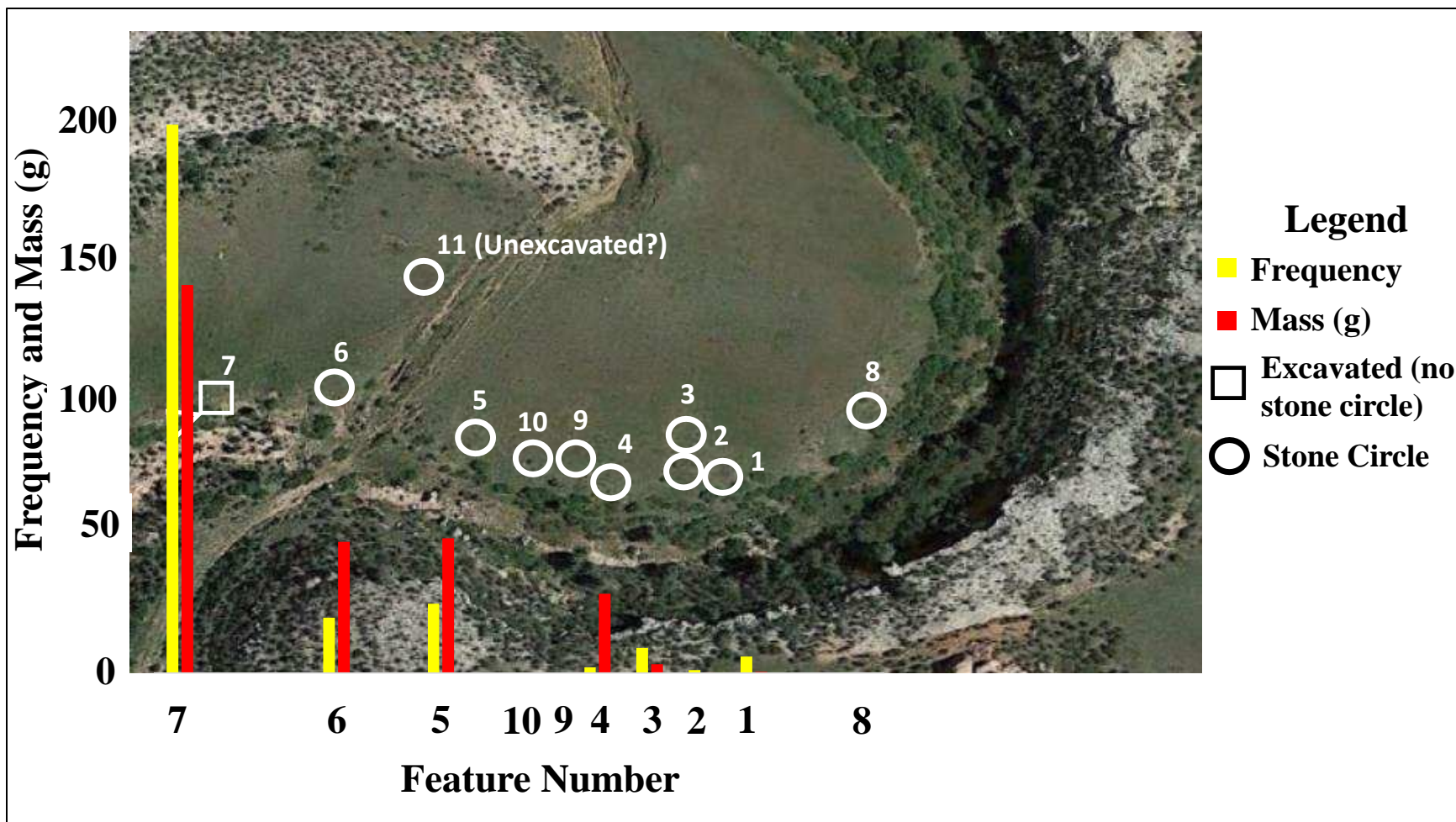


Figure 38: Killdeer Canyon (5LR289) frequency and mass (g) of bone fragments by feature.

To examine the number of occupations, element representations from each feature are plotted using pie charts (Figure 39). Feature 7 contains the highest diversity of elements. This supports the hypothesis that Feature 7 was the primary outdoor processing area where animals would be disarticulated before they were distributed to different rings. Feature 5 is the only other ring which contains more than one element representation. Features 2 and 3 bone fragments were too small to identify; however, Feature 2 contains the only cranial element representation out of any of the ring features. The proximity of the rings as well as contemporaneous radiocarbon dates (see Chapter 2) all support the site as a single occupation. Thus, the near lack of faunal remains in Features 1, 2, 3 but high frequency and diversity of elements in Feature 7 may indicate designated areas for task specialization. Features 6 and 4 all contain only one element; however, Feature 6 contains more than 50% of unidentifiable fragments, suggesting there may be other elements present. The only recognizable cranial elements outside of Feature 7 are in Feature 2 which otherwise has very little bone.

Killdeer Canyon most likely represents a very short-term and single occupation site. Killdeer Canyon also contains a low species diversity, with only bison (MNI=2) and likely intrusive rodent. The processing intensity is consistent with what Scheiber and Reher (2007) defined as highly processed bone, however, other circumstances, including taphonomy or simply the need to process the bison in their entirety, may have occurred. The presence of one bone tool suggests there was more animal processing, perhaps for clothing or structure maintenance that occurred on site. It is unknown whether the bone tool was transported on site or manufactured from the procured faunal remains.

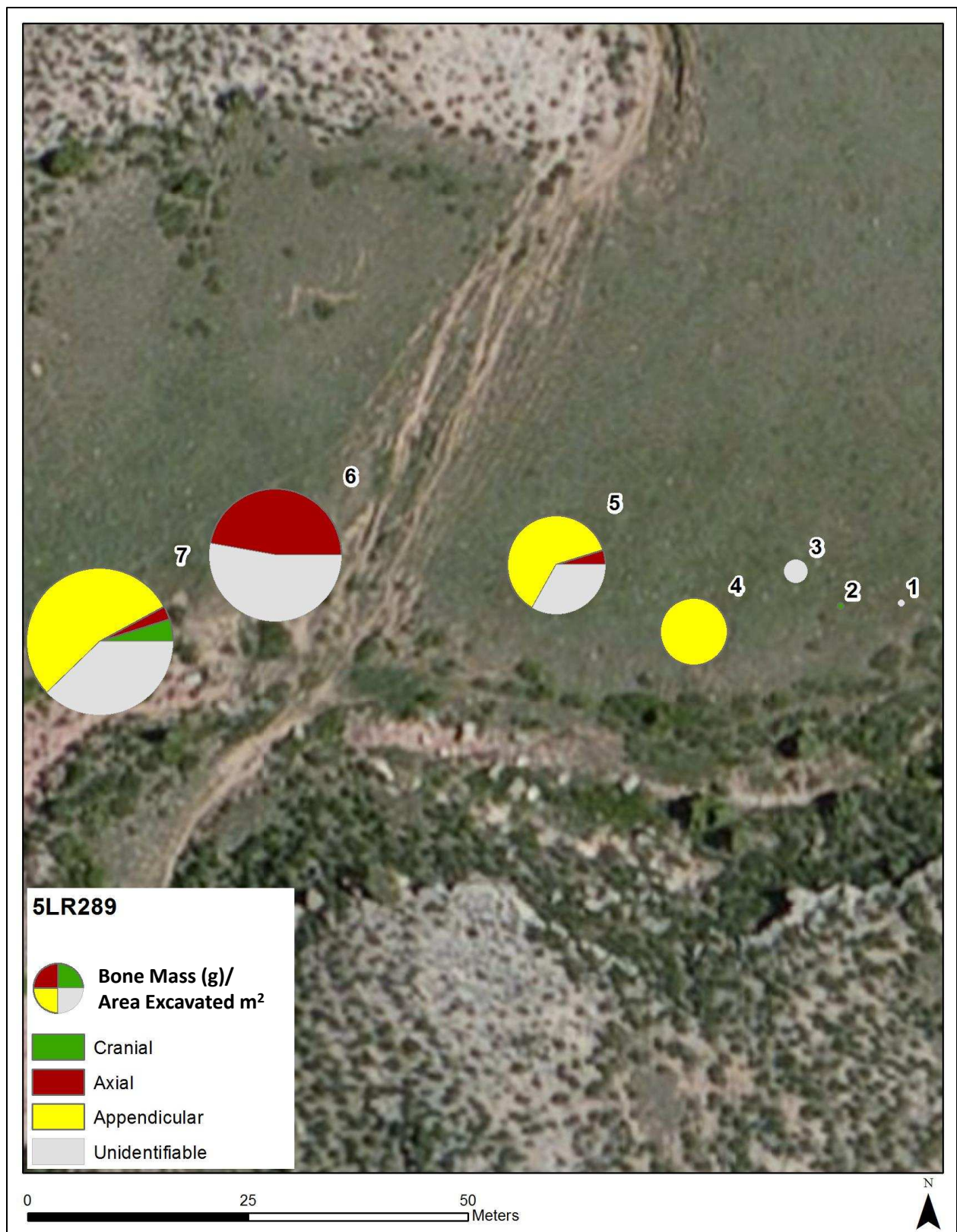


Figure 39: 5LR289 element dispersal displayed in pie charts weighted by bone frequency normalized by area excavated (m²). Feature number is labeled directly above pie chart.

The element representation suggests Killdeer Canyon was a single component site with some task specialization in rings. Features 1, 2, and 3 contain almost no faunal remains, while Feature 7 contains the greatest diversity and mass (g) of faunal elements. Features 4, 5, and 6 all contain either axial or appendicular elements suggesting there may have been unequal dispersal of elements, although, high frequencies of unidentifiable elements make this difficult to determine.

T-W-Diamond Results

The T-W-Diamond assemblage contains 180 bone fragments (see Appendix M). There are 219.3 grams of faunal remains from the site and 162.0 grams have feature provenience (Figure 40). The fragments range from less than 1 gram to 42 grams. The average mass of the bone fragments are 2 grams, excluding the bones from a small rodent. Maximum length (mm) ranges from 4 mm to 140 mm with an average length of 20.5 mm.

Feature 4 contains the highest bone mass, with Feature 2 containing the second highest bone mass. Both features are in a visual cluster of Features 2, 3, and 4. This area may suggest a bone processing area or may indicated food sharing between rings. The latter hypothesis will be explored in the following section.

There is a low species diversity at T-W Diamond. Features 2, 3, and 4 contain adult *Bison bison* (MNI=1) (Figure 41). Feature 10 contains fetal bison bone again increasing the number of individual represented (MNI=2) for the site. The fetal bison bone was visually compared to fetal cow using the CSU Department of Anthropology comparative collection. The presence of fetal bison bone suggests the stone circle was occupied sometime around April during calving season (Frison and Reher 1970:46).

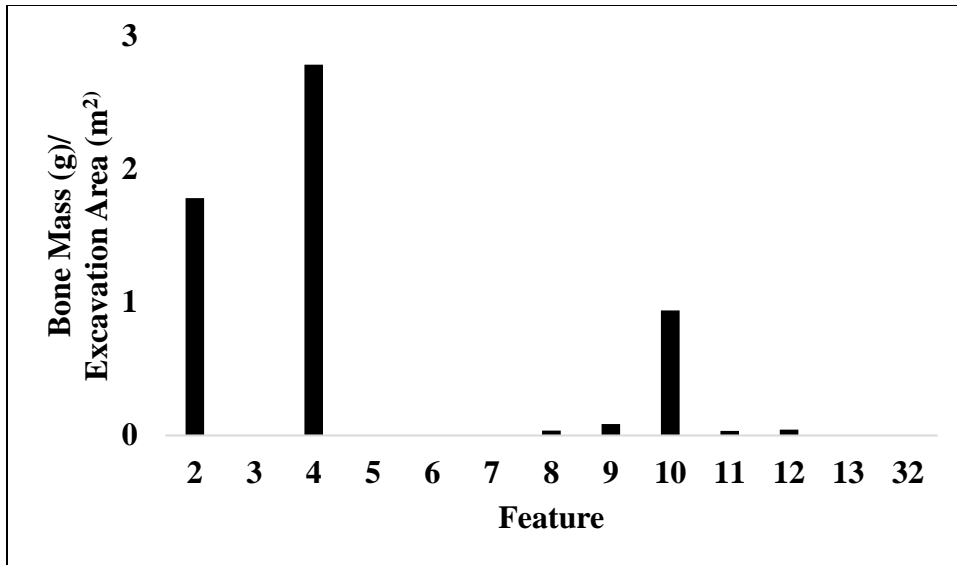


Figure 40: 5LR200 bone mass (g) by feature number normalized by excavation area (m²).

Feature 10 also contains intrusive rodent. The rodent skeleton is complete suggesting it was not procured and processed during the occupation of Feature 10. Lastly, the first phalanx of an Artiodactyla (c.f., *Odocoileus* sp.) was collected during excavation; however, there is no provenience to a specific excavated feature.

To explore the processing intensity, the average length of bone as well as the mass and frequency are compared. The mean maximum length of bone fragments is 20.5 mm, the median is 14.7 mm, and the mode is 6.76 mm. T-W-Diamond's Features 2, 3, 4 all contain comparatively larger elements than Features 8, 9, 10, and 11 (Figure 42). The two clusters of rings suggest either different occupation episodes or different distributions of faunal elements. This hypothesis will be further explored by examining the element and species representation in these clusters to determine the number of occupations.

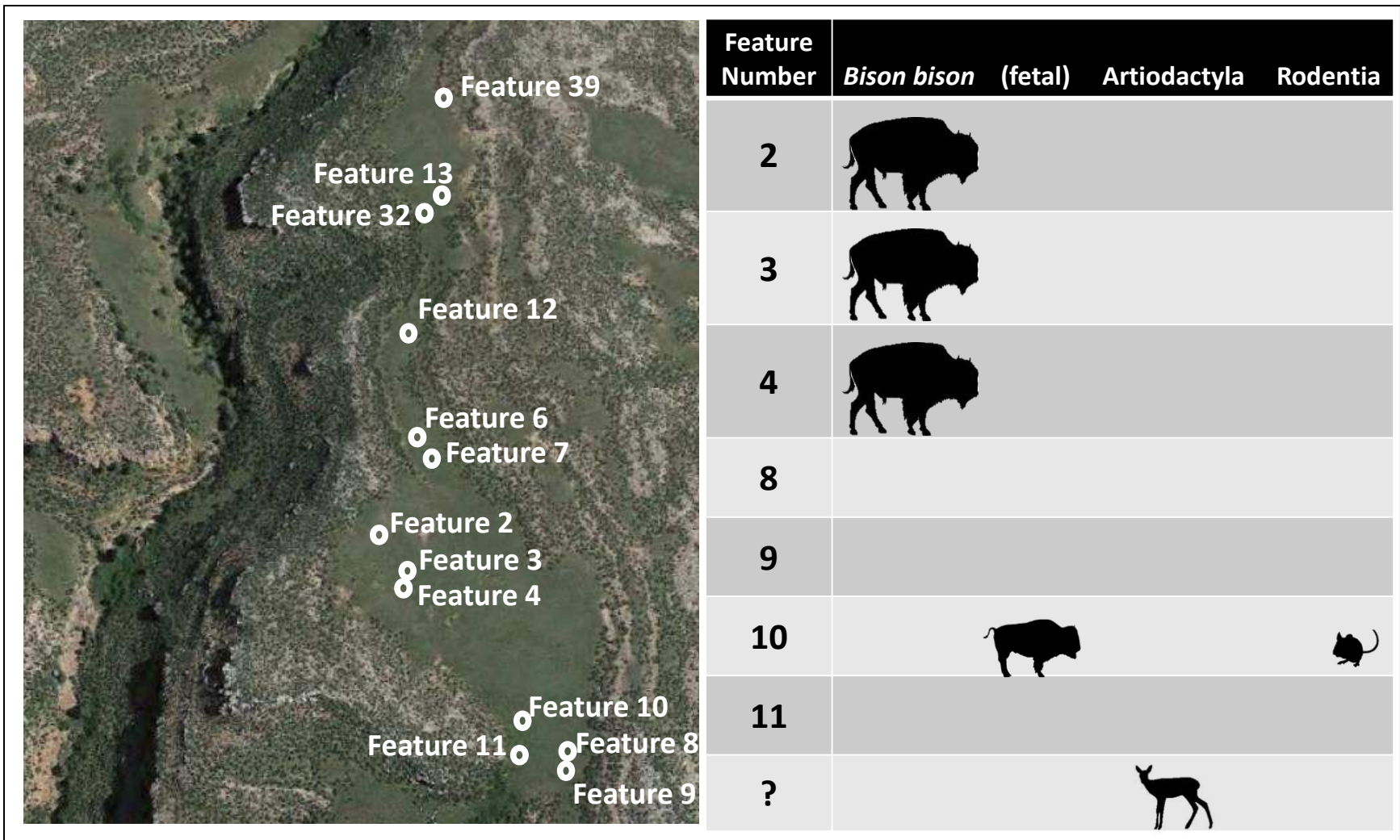


Figure 41: 5LR200 species representation by feature.

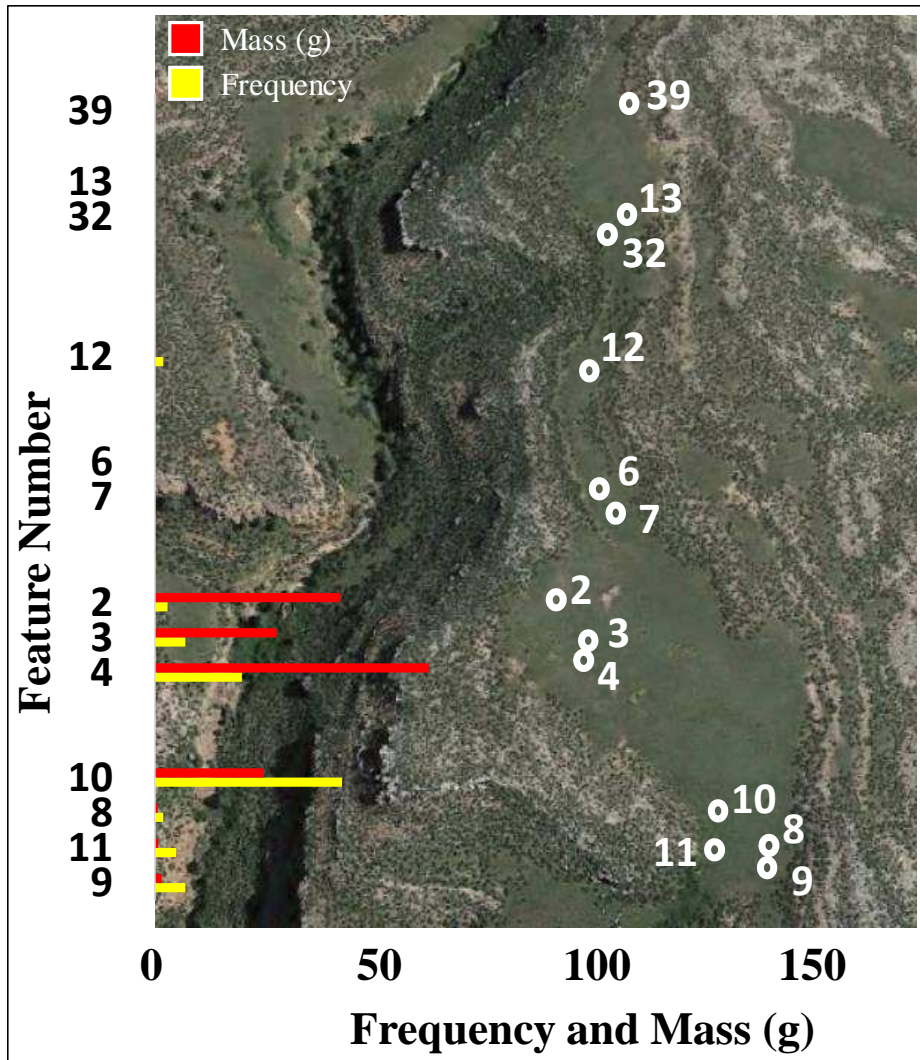


Figure 42: 5LR200 frequency and mass (g) of bone fragments by feature.

The dispersal of elements is used to examine the number of occupations. Features 2, 3, and 4 all contain appendicular skeletal elements (Figure 43). Features 8, 9, and 10 all contain cranial elements. The spatial clustering of these element representations are visually evident. Features 2, 3, and 4 are in a cluster of three separated from other ring clusters. Features 8, 9, and 10 are in a cluster at the southern-most portion of the site. Feature 12 is the only other ring to contain faunal material; however, the fragments were too small to identify any skeletal element representations.

O'Brien (2013) examined food sharing between household structures at the Late Prehistoric Eden-Farson site in Wyoming. Despite the pronghorn kill containing a much higher frequency of bone, the concept of food sharing should be applied to other site types, such as stone circle sites. O'Brien (2013) observed the unequal distribution of faunal material within residential structures that are associated with the same occupation. If T-W-Diamond's features represent a single residential occupation, then then spatial clusters could represent unequal food distribution.

T-W-Diamond contained no modified bone fragments. The low frequency of spirally fractured and cut marked bone is likely attributed to the high degree of processing and smaller bone fragments. Furthermore, many of the bone fragments are burnt suggesting cut marks might be present but not identified.

T-W Diamond most likely represents a short-term and single occupation site. Killdeer Canyon also contains a low species diversity, with only bison (MNI=2), a deer phalanx with no feature provenience, and likely intrusive rodent. The processing intensity is consistent with what Scheiber and Reher (2007) defined as highly processed bone, however, just as Killdeer Canyon, other circumstances may have contributed to more intensive bone processing.

The element representation suggests T-W Diamond was a single component site with strong evidence for food sharing. There is a pattern of element dispersal between Features 2, 3, 4 and 8, 9, 10, and 11. Although it is possible that these clusters were occupied by two separate components, the probability of two temporally separate groups catching the same species but bringing completely different elements back to camp seems unlikely. It is more likely that T-W Diamond shows evidence of a group gathering and food sharing.

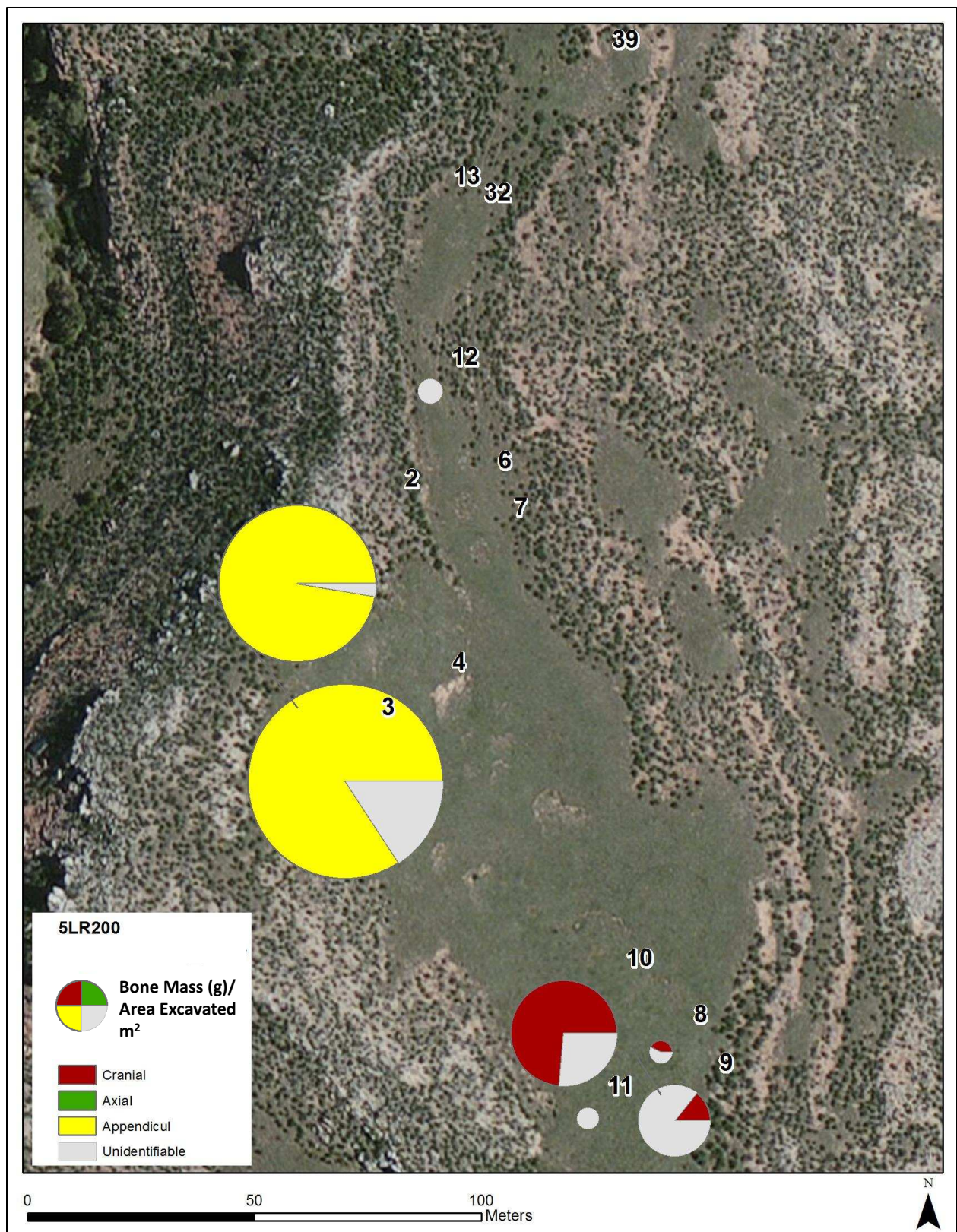


Figure 43: 5LR200 element dispersal displayed in pie charts weighted by bone frequency normalized by area excavated (m²). Feature number is labeled directly above pie chart.

Discussion and Conclusion

The following variables were examined as a measure of occupation span: (1) bone fragment frequency, (2) species representation, (3) processing intensity, (4) cultural and carnivore modification, and (5) element dispersal. Both Killdeer Canyon and T-W-Diamond primarily contain bison bone. Fetal bison bone at T-W-Diamond suggests the site was occupied sometime around April. Bison and deer bone is common in other excavated stone circle sites (Reher 1983; Smith et al. 1995). This suggests that the occupants at these sites were not intensively procuring other species near the sites and likely only present at these campsites for a short period.

There is a high degree of bone processing at Killdeer Canyon and T-W-Diamond. A T-Test at a 95% confidence interval shows no significant difference between the maximum length of bone at Killdeer Canyon and T-W-Diamond ($p= 0.1765$). Features either contain less than 3 grams of faunal remains or between 25 and 65 grams of fauna. This suggests that either bone at either site is deteriorating at a similar rate, or, the hunter-gatherers who occupied the site participated in similar subsistence strategies. Because the two sites are in opposite settings on the landscape, Killdeer Canyon at a valley bottom and T-W Diamond on a ridge top, it would not be expected that the same taphonomic processes would be effecting bone deterioration. Therefore, the latter option is more likely, suggesting that the inhabitants of the sites were participating in similar subsistence procurement and processing strategies. Killdeer Canyon and T-W-Diamond likely suggest at least similar subsistence strategies regarding the MNI of bison present at each site.

The element representations are not clearly divided among stone circles at Killdeer Canyon. Feature 7, at Killdeer Canyon, contains the highest diversity of elements suggesting this

area served as the primary outside processing area. The element representation at T-W-Diamond is highly patterned and shows a clear visual distinction between two clusters of rings. This suggests either different occupations were present at the site or the rings were occupied simultaneously and partook in unequal food sharing. This hypothesis will be further explored using other results from lithic, ceramic, and radiocarbon analyses.

The species representation is similar between Killdeer Canyon and T-W-Diamond. Both sites contain primarily bison bone which is consistent with other excavated stone circle sites in Wyoming. A low species diversity suggests the sites were not occupied for a long period. Finally, the taphonomic analysis yielded only one spirally fractured bison bone at the Killdeer Canyon site. The lack of cut marks is attributed to the high degree of fragmentation.

CHAPTER 6: CERAMIC DESCRIPTION AND PETROGRAPHIC ANALYSIS

The purpose of this chapter is to briefly describe the pottery styles and frequencies at Killdeer Canyon and T-W Diamond as well as discuss the site's role in a larger petrographic study by the Center for Mountain and Plains Archaeology. Pottery fragments, specifically cookware, are used as a measure for occupation length. Because pottery was only found in one feature at each site, this chapter cannot address spatial patterning regarding the number of occupation. Instead, this analysis relies on the results of the petrographic analysis to examine similarities in pottery manufacture.

Theoretical Justification for Ceramic Analysis

The following assumptions are tested: because mobility patterns will influence the production of pottery, highly mobile Plains hunter-gatherers should (1) have a low frequencies and mass of pottery on site and (2) have primarily non-locally produced vessels. The first assumption is based on accumulation theories largely used by the Southwest (also discussed in Chapter 2 regarding debitage accumulation). Figure 44 is adapted from Varien and Ortman (2005:144) showing a positive relationship between the length of occupation and an increase in sherds associated with cooking (Varien and Ortman 2005:137). In regard to short-term hunter-gatherer sites, this presents a problem. While permanent sites in the southwestern United States can be easily measured using cookware accumulation, the two stone circle sites in this analysis would barely register on the plot (red arrow, Figure 44). A very short-term occupation (perhaps a few days) would not be on camp long enough to manufacture or even require pottery. Although a vessel can be manufactured in as little as two days (Ellwood 2002), if the inhabitants are not on site long enough to require a cooking vessel, there would be no need for local pottery

manufacture. If the inhabitants at Killdeer Canyon and T-W Diamond were only processing bison before moving to the next location, high frequencies of more intensive processing techniques, such as pottery manufacture, would not be expected.

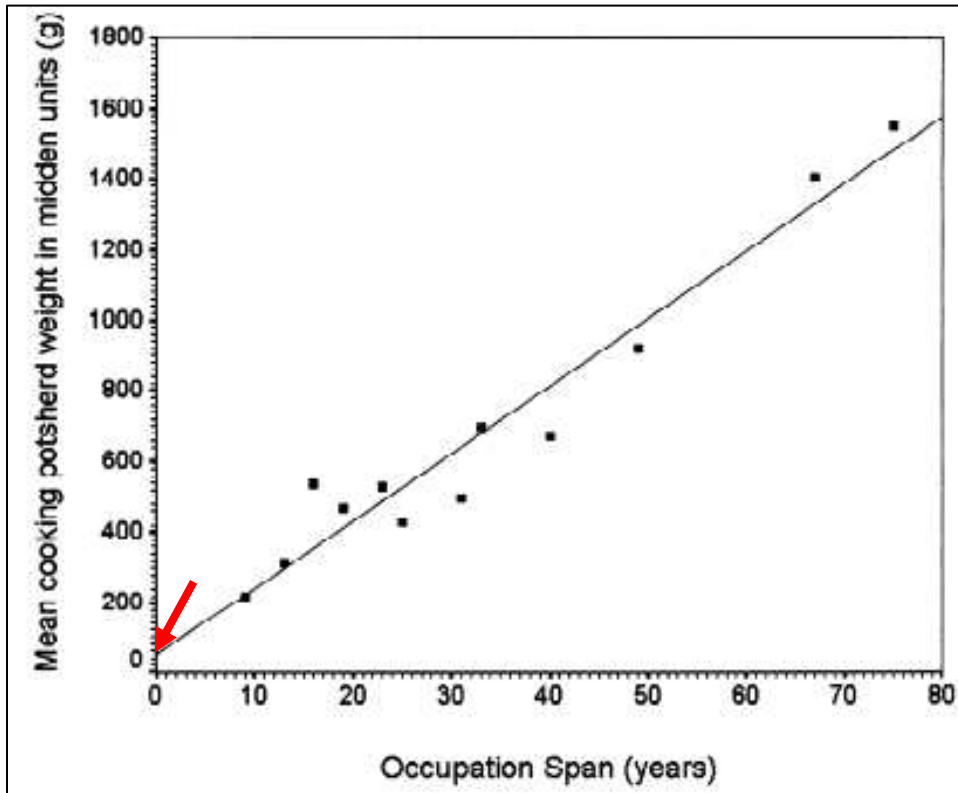


Figure 44: Figure adapted from Varien and Ortman (2005:144). Red arrow points near origin where stone circle sites would fall on scatterplot. Figure highlights the need for adapting accumulation rate methods to short-term hunter-gatherer sites.

Methods

As part of a larger project through the Center for Mountain and Plains Archaeology and Desert Archaeology, pottery sherds from Killdeer Canyon (n=4) and T-W Diamond (n=5) were submitted for petrographic analysis. In sum, the project analyzed 40 pottery sherds from 10 different sites, ranging from the Early Ceramic to Late Ceramic era (AD 150-1860) (Gilmore 1999). All the sites included in the analysis were well-dated and regionally specific to the northern Colorado Hogback zone.

Petrographic analysis examines the mineralogical content of pottery fragments through polarized light microscopy (Reedy 1993). It can be used to examine similarities between different ceramic fragments as well as similarities to clays in the surrounding area. Other petrographic studies have examined the shaping techniques (indicated by internal alignment of pores), the degree of firing, and the location of manufacture (local or non-local) (Reedy 1993). This chapter tests petrography results against assumptions regarding pottery manufacture and occupation length. Pottery surface treatments and radiocarbon dates from nearby sites are briefly discussed as a comparison to Killdeer Canyon and T-W Diamond. This chapter also briefly summarizes the results of the petrographic analysis as it directly relates to occupation span at Killdeer Canyon and T-W Diamond, but for more information, the reader can consult Ownby (2015).

Killdeer Canyon Ceramic Results

In sum, there are 478 pottery fragments from Killdeer Canyon (129.9 grams). The pottery fragments are stylistically plain and undecorated (Figure 45). All pottery fragments from Killdeer Canyon with provenience are from Feature 7 suggesting the sherds are from one vessel.



Figure 45: 5LR289 pottery sherds from Feature 7. The four sherds were selected for petrographic analysis, completed by Ownby (2015).

Plain and undecorated ceramics are generally attributed to two different pottery types in this region. Mulloy (1958) originally defined the Intermountain Ware tradition which includes vessels with a flower pot-shape and flat bottom. Dismal River, generally associated with the Apache (Brunswig 1995), contains olla-shaped vessels with a wide mouth and slight to moderately flared rim (Gunnerson 1968:175-176). Five restored vessels from the Lovitt site (25CH1), a Dismal River site located in southwestern Nebraska, exhibit a very fine sand paste or grit (Gunnerson 1968:175-176). The pottery fragments from Killdeer Canyon are small, and no refit analysis was attempted to determine vessel morphology, thus radiocarbon dates are used to discuss possible cultural affiliation. Proto-Apache Athapaskan, or Dismal River pottery are generally associated with A.D. 1650-1750 (Brunswig 2012), though more recent data from the Colorado mountains and foothills suggest earlier sites also contained Dismal River Pottery (Brunswig 2012). Nonetheless, A.D. 1650-1750 is the same period that Killdeer Canyon is occupied. Brunswig (2012:20) notes that the Plains Apaches were sharing the eastern plains, foothills, and Front Range with other protohistoric and historic groups. These groups included

the Ute tribes of which were living in more permanent residences in the intermontane of the Colorado Rockies (Brunswig 2012:20).

The Killdeer Canyon sherds are manufactured from shale clay with granitic sand (Ownby 2015:22) (Figure 46). The sand is likely from Middle Proterozoic deposits, from the Upper and Middle Pennsylvanian Fountain Formation deposits (Ownby 2015:22). None of the sherds compared to locally collected sediment samples suggesting that the vessel was manufactured off-site. Brunswig (2012:24) notes differences between Apachean and Ute ceramic manufacture and temper. Some of the more notable differences include: Ute pottery is coil-built and often contains fingertip and fingernail indentations whereas Apachean pottery is almost always constructed from accretion (Brunswig 2012:24). Temper inclusions most noticeably differ with mica temper being included in Apachean ceramics and not Ute ceramics. While the radiocarbon dates at Killdeer Canyon are consistent with Dismal River, there is little evidence of mica use in the temper, other than the use of granitic sand which can contain mica. Future research should compare pottery construction methods and surface treatments to Apachean ceramic sites identified in Brunswig's (2012) analysis.

The low frequency, provenience, and petrographic analysis suggest only one or two vessels were transported to Killdeer Canyon and discarded in Feature 7. The pottery mass (130 grams) is just 20 grams less than the pottery from T-W Diamond, also presumed to be one vessel. This suggests the occupants were not intensively processing and cooking food on site, supporting the site as a single and short-term occupation. Transported pottery and obsidian from New Mexico suggest the occupants either traveled a long distance or, more likely, had much broader trade connections. While it is possible the vessel was carried a long distance to the site,

because pottery is fragile, it is perhaps more conceivable that the group camping at Killdeer Canyon procured non-local materials through trade networks.



Figure 46: 5LR289 location of pottery used in thin-section analysis. Thin sections are displayed in top left corner of image. Thin-section images from Ownby (2015:17) showing shale-derived clay paste with sand temper.

T-W Diamond Ceramic Results

There are 139 pottery fragments from T-W Diamond (154.4 grams). The pottery fragments are stylistically smooth and some fragments have punctate markings (Figure 47). All pottery fragments from T-W Diamond were found in Feature 11 suggesting they are part of one or two vessels. In the Northeastern region of Colorado, pottery from the Middle Ceramic era is associated with Upper Republican culture (Ellwood 2002). This designation is based largely on

sherds with small and narrow cord-impressed patterns, some of which are obliterated (Ellwood 2002). Upper Republican pottery corresponds with A.D. 1000-1400 in this region (Ellwood 2002), during the same period T-W Diamond is occupied. T-W Diamond does not, however, contain any cord-marked pottery fragments. Instead, the fragments are plain ware or punctate and compare to pottery Type II from Bayou Gulch, a multiple component Plains Woodland (A.D. 900 and 1100) site located in the foothills south of Denver (Ellwood 1987). Ellwood (1987:122-123) notes that of the three types recognized at Bayou Gulch, Type II resembles more of a category than a type with the common element being the plain surface. Type II pottery is the most variable category Ellwood (1987) notes from Bayou Gulch.



Figure 47: 5LR200 pottery sherds from Feature 11. The five sherds were selected for petrographic analysis, completed by Ownby (2015).

Plain and punctate pottery sherds were also recovered from the Caribou Lake site (5GA22) and both surface treatments are thought to be from the same component (Benedict 1985). The pottery sherds likely date to 665 \pm 80 B.P. (Benedict 1989), cal A.D. 1219-1424 (95.4%) (OxCal 4.2, Reimer et al. 2013) corresponding with the same time T-W Diamond is occupied. These styles are typically associated with the Ute (Brunswig 2012; Buckles 1971).

Previous analysis by Flayharty and Morris (1974:165) suggested that the T-W Diamond ceramics are part of a flat bottom Intermountain vessel and are associated with the Shoshone.

While this is a tentative association, the presence of potential Intermountain Ware at T-W Diamond, along with several other sites along the Colorado Front Range, could represent the southern-most expansion of the Shoshone (Eighmy 1995; Ellwood 2002). A steatite fragment from T-W Diamond further supports the occupants had northern ties, perhaps to Shoshone territory in Wyoming. This is in opposition to the group occupying Killdeer Canyon that likely traveled north from New Mexico (based on the presence of obsidian from the Valle Grande). No analysis was completed to confirm vessel morphology.

The T-W Diamond sherds used in the petrographic analysis contain an identical paste and are manufactured from secondary clay deposits from sedimentary formation erosion (Ownby 2015:21) (Figure 48). The sand is likely from Owl Canyon Formation, the Glendo Shale Member, or the Red Hill Shale Member; these formations are all found within 5km of the site (Ownby 2015:21). This suggests that the pottery may have been locally manufactured on site or near T-W Diamond.

The frequency, manufacture, and petrographic analysis suggest the ceramics from T-W Diamond represent one vessel. The low frequencies of pottery indicate the inhabitants were not intensively processing and cooking food. This supports the hypothesis that the T-W Diamond inhabitants were not on site for longer than a few days or weeks. It is possible the vessel was manufactured locally, within 5 kilometers, although it is important to note that this does not necessarily suggest on site. Instead, this may suggest the inhabitants of T-W Diamond did not have as extensive trade networks as did the inhabitants of Killdeer Canyon.

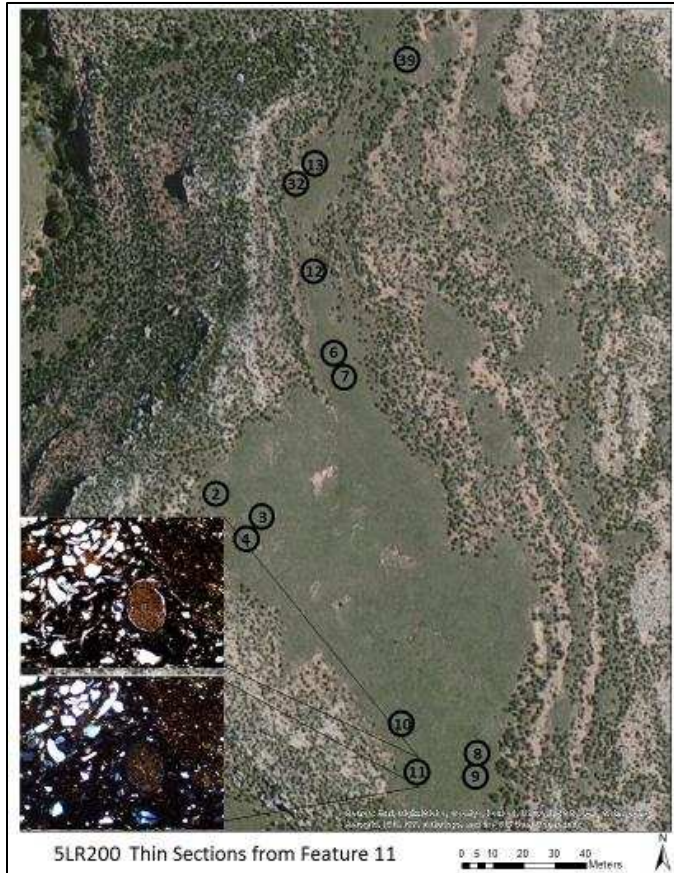


Figure 48: 5LR200 location of pottery used in thin-section analysis. Thin sections are displayed in bottom left corner of image. Thin-section images from Ownby (2015:18) showing sedimentary clay paste.

Discussion and Conclusion

The pottery from Killdeer Canyon and T-W Diamond both support the sites as short-term occupations. Both sites contain pottery from only one feature. The petrographic analysis suggests the pottery from Killdeer Canyon was manufactured from non-local sources suggesting Killdeer Canyon peoples may have either traveled a long distance or had extensive trade networks. The petrographic analysis from T-W Diamond suggests the pottery was manufactured on or near the site suggesting the group remained on site longer than the occupants of Killdeer Canyon. This is contradictory to other analyses completed in this thesis suggesting that the Killdeer occupants were on site longer than the T-W Diamond occupants. Although it is not in the scope of this

thesis to discuss the use of horses, the possibility that Killdeer Canyon occupants may have had access to horses would have greatly increased their network systems as well as their long-distance transportation capacities. It is best to not put too much weight on the whether a single vessel was manufactured on or off site. The low frequencies of pottery present at the site, and contemporaneity between rings, suggest both sites were not occupied long enough to intensify their foraging and cooking strategies.

CHAPTER 7: CONCLUSION AND DIRECTION FOR FUTURE RESEARCH

Stone circles delineate time and space in the hunter-gatherer record. This thesis addresses occupation span at Killdeer Canyon and T-W Diamond by examining each artifact class from excavated context. Furthermore, this analysis demonstrates the merit of using multiple lines of evidence to compensate for small sample sizes.

Projectile point types associate the sites with the Late Prehistoric era. The two projectile points with feature provenience from Killdeer Canyon are side-notched types. The types from T-W Diamond include side-notched, tri-notched, and un-notched point forms. These point forms generally occur in the Late Ceramic period and T-W Diamond could represent one of the earliest occurrences of all three types in this region. This also may be an indication that T-W Diamond represents multiple occupations, however, radiocarbon ages confidently associate the site with the Middle Ceramic period.

Radiocarbon analyses were used to test ring contemporaneity between features. As part of this research, four new bone samples were submitted for radiocarbon dating. The dates from the bone samples greatly refine the age estimates for the two sites, dating Killdeer Canyon to the Late Ceramic era and T-W Diamond to the Middle Ceramic era. There is statistical contemporaneity between rings (examining uncalibrated dates) at each respective site. While radiocarbon dates are not precise enough to examine repeated human occupation, the radiocarbon analysis supports the sites could have been one occupation.

Table 16: Summary results for Killdeer Canyon and T-W Diamond. The two sites are compared relative to one another. If a site had a higher frequency or percentage of an item explored in this thesis, it received a plus. If a site had a lower frequency or percentage it received a minus, and if the two were almost equal, the sites both received an equals sign.

Relative Occupation Span			
		Killdeer Canyon	T-W Diamond
Lithic Debitage	Frequency	-	+
	Percent Local	+	-
	Relative Thickness	+	-
Lithic Tools	Frequency	-	+
	Percent Local	+	-
	Occupation Span	+	-
Faunal Remains	Mass	+	-
	Frequency	+	-
	Species Diversity	=	=
	MNI	=	=
Ceramics	Frequency	=	=
	Locally Manufactured	-	+

Table 16 summarizes the results of all measures examined in this thesis (discussed below). The two sites are measured comparatively to one another as a general proxy for occupation length. More green cells suggest the site was occupied for a longer period while more red cells suggest the site was occupied for less time. Killdeer Canyon has six green cells while T-W Diamond only has three. The results of this thesis suggest Killdeer Canyon was occupied (slightly) longer than T-W Diamond.

The debitage analysis found differences in ring use intensity based on flake frequencies. Local to non-local debitage ratios suggest that the sites were used differently and occupied for different lengths, though both relatively short-term. Higher frequencies of debitage and higher ratios of non-local to local material at T-W Diamond suggest the site was more intensively used, but occupied for less time than Killdeer Canyon. Killdeer Canyon contains less non-local to local

debitage suggesting that the occupants were on site long enough to begin replenishing their toolkits with the local material.

The lithic tool analysis showed differences in tool frequencies per site. Whereas Killdeer Canyon, on average, contained 0.7 tools per feature, T-W Diamond contained 4 tools per feature. Both sites contained primarily non-local tools. Tool types included basic hunting and expedient processing tools with little evidence for intensive processing (such as ground stone) or hide/clothing production (needles, drills, etc.). As seen in thedebitage chapter, the higher frequencies of tools at T-W Diamond may reflect a larger group of people congregating on site rather than a longer occupation or multiple occupations.

The faunal analysis found an MNI of two bison at each site. The low MNI and lack of other processing tools suggests the occupants of Killdeer Canyon and T-W Diamond could not have sustained a camp longer than a few weeks, depending on the number of people. Again, this attests to the ephemerality of the camps. The element analysis revealed interesting dispersal patterns at both sites. Killdeer Canyon contained some evidence of unequal element dispersal as well as a possible outside processing area. The element analysis at T-W Diamond shows strong evidence for unequal food sharing between ring clusters. This could have resulted from a congregation of kin groups staying at the site temporarily. In order to test this hypothesis, a refit analysis should be conducted using faunal elements.

The pottery analysis found that accumulation rates are similar between Killdeer Canyon and T-W Diamond. Pottery types at Killdeer Canyon may suggest a tie to Dismal River, however, more analysis needs to be completed on pottery surface treatments and vessel form. The pottery at T-W Diamond looks similar to Intermountain ware, suggesting a possible Ute connection, though previous analyses by Flayharty and Morris (1974) suggest the vessel may

have Shoshone ties. The petrographic analysis conducted by the Center for Mountain and Plains Archaeology through Desert Archaeology found that the Killdeer Canyon vessel was likely manufactured non-locally while the T-W Diamond vessel was manufactured locally.

While Kehoe's (1958) statement that "...all that can be expected from the excavation of a tipi ring are a few bone fragments, flint and obsidian (not native to the region) flakes and perhaps broken points, rough hammerstone, and an occasional grooved maul" is largely correct, this thesis demonstrated that valuable information can still be gathered from small assemblages. The purpose of this thesis was to show how stone circle sites could be examined to address occupation length and ultimately understand Native American's reuse of landscapes. The Roberts Ranch is a bountiful landscape with access to resources year round, yet hunter-gatherers were still using the area as a temporary camp throughout the Late Prehistoric. It is the author's hope that this analysis is applied to other stone circle sites in the region to help build an understanding of ephemeral residential sites, as analysis of this site type is woefully underrepresented in the archaeological literature.

This analysis proposed new methods for examining short-term hunter gatherer residential sites. Stone circle sites are notorious for containing small assemblages; thus, this thesis relied on using multiple lines of evidence to compensate for small sample sizes. In terms of the artifact analysis, this study was coarse and established several hypotheses that can be tested by future projects. First, radiocarbon dates suggest ring contemporaneity at each site. This is supported by artifact signatures found in each of these rings. However, ring contemporaneity cannot be proven until more intensive analyses are explored. Future research should examine artifact refits, both lithic and faunal, between rings. The identification of artifact refits between rings will prove that the occupants of each site inhabited the rings at the same time.

Finally, this thesis calls for more intensive analyses of stone circle sites to build our understanding of temporary structure use. Stone circles are the most common Plains and Foothill hunter-gatherer structure type and as such present an opportunity to understand similarities and differences in occupation span.

Challenges Encountered

Perhaps one of the most challenging aspects of working with legacy projects is the nature of the field notes. Whereas data collection today is largely standardized, digitized, and backed up using digital libraries, field notes from 1970s and early 1980s excavations pose some challenges.

Both sites were excavated by field schools which led to variation in field note quality and quantity. Students wrote all unit, level, and provenience information in their personal field books which often got intertwined in other miscellaneous day to day impressions of the site.

Provenience was also written on some artifact bags that, through time were mismatched or combined. This resulted in some data loss from Killdeer Canyon and T-W Diamond.

Specifically, this analysis was affected by missing provenience of artifacts from Killdeer Canyon. While the debitage is still present in the Colorado State University Archaeological Repository, missing provenience on flakes limits the information that can be learned.

Although these challenges were frustrating at times, the author must stress the importance of revisiting old excavation assemblages. As technology changes, so does the information that can be learned from sites. For example, advances in radiocarbon dating allowed new radiocarbon date precisions to be narrowed to less than thirty years. This is substantially more precise than some of the original radiocarbon dates which had ranges of upwards of 200 years. The purpose of this thesis is not to discredit the work that has already been completed on both sites, rather to add to the information that we already know. This thesis would not have been possible without

contributions of Elizabeth Morris and Ross Flayharty and it is the author's hope that future research will add to this dataset.

REFERENCES CITED

- Andrefsky, William Jr.
2005 *Lithics: Macroscopic Approaches to Analysis*. Cambridge University Press, New York.
- Banks, Kimball M., and J. Signe Snortland
1995 Every Picture Tells a Story: Historic Images, Tipi Camps, and Archaeology. *Plains Anthropologist* 40(152):125-144.
- Benedict, James B.
1975 The Murray Site: A Late Prehistoric Game Drive System in the Colorado Rocky Mountains. *Plains Anthropologist* 20(69):161-174.
1985 *Arapaho Pass: Glacial Geology and Archaeology at the Crest of the Colorado Front Range*. Research Report No. 3, Center for Mountain Archaeology, Ward, Colorado.
1989 Age of Punctate Pottery from the Caribou Lake Site: Comparison of Three Physical Dating Methods. *Southwestern Lore* 55(2):1-10.
- Binford, Lewis R.
1980 Willow Smoke and Dogs' Tails: Hunter-Gatherer Settlement Systems and Archaeological Site Formation. *American Antiquity* 45(1):4-20.
1990 Mobility, Housing, and Environment: A Comparative Study. *Journal of Anthropological Research* 46(2):119-152.
- Brasser, Ted J.
1982 The Tipi as an Element in the Emergence of Historic Plains Indian Nomadism. *Plains Anthropologist* 27(98):309-321.
- Bronk Ramsey, Christopher
2009 Bayesian Analysis of Radiocarbon Dates. *Radiocarbon* 51(1):337-167.
- Brunswig, Robert H.
2012 Apachean Archaeology of Rocky Mountain National Park, Colorado, and the Colorado Front Range. In *From Land of Ever Winter to the American Southwest: Athapaskan Migrations and Ethnogenesis*, edited by Deni J. Seymour, pp. 20-36. The University of Utah Press, Salt Lake City.
- Brunswig, Robert H.
1995 Apachean Ceramics East of Colorado's Continental Divide: Current Data and New Directions. In *Archaeological Pottery of Colorado: Ceramic Clues to the Prehistoric and Protohistoric Lives of the State's Native Peoples*, edited by Robert H. Brunswig, Bruce Bradley, and Susan M. Chandler, pp. 172-202. CCPA Occasional Papers No. 2, Colorado Council of Professional Archaeologists, Denver.

- Buckles, William Gayl
1971 *The Uncompahgre Complex: Historic Ute Archaeology and Prehistoric Archaeology on the Uncompahgre Plateau in West Central Colorado*. Unpublished Ph.D. dissertation, Department of Anthropology, University of Colorado, Boulder.
- Burgess, Robert J.
1981 *Cultural Ecological Investigations in the Owl Canyon Rockshelter (5LR104)*. Unpublished Master's thesis, Department of Anthropology, Colorado State University, Fort Collins.
- Cassells, Steve and Robert Noel Farrington
1986 Excavations at the Indian Mountain Site, 5BL876: A Multi-Component Stone Circle Site in Colorado's Northeastern Foothills. *Plains Anthropologist* 31(112):129-139.
- Cohen, Jacob
1988 *Statistical Power Analysis for the Behavioral Sciences*. Academic Press, New York.
- Eighmy, Jeffrey
1995 Intermountain Pottery in Colorado. In *Archaeological Pottery of Colorado: Ceramic Clues to the Prehistoric and Protohistoric Lives of the State's Native Peoples*, edited by Robert Brunswig, Bruce Bradley, and Susan Chandler, pp. 162-171. Colorado Council of Professional Archaeologists Occasional Papers No. 2, Denver.
- Ellwood, Priscilla B.
2002 *Native American Ceramics of Eastern Colorado*. Natural History Inventory of Colorado No. 21. University of Colorado Museum, Boulder.
- Ellwood, Priscilla B.
1987 Bayou Gulch (5DA265) Ceramics. *Plains Anthropologist* 32(116):113-139.
- Finnigan, James T.
1981 *Tipi Ring and Plains Prehistory: A Reassessment of Their Archaeological Potential*. Master's thesis, University of Saskatchewan, Department of Anthropology and Archaeology.
- Flayharty, Ross A.
1972 *T-W-Diamond, A Tipi Ring Site in Northern Colorado*. Unpublished Master's thesis, Department of Anthropology, Colorado State University, Fort Collins.
- Flayharty, Ross A. and Elizabeth A. Morris
1974 T-W-Diamond, A Stone Ring Site in Northern Colorado. *Plains Anthropologist* 19(65):161-172.
- Frison, George C., and Zola Van Norman
1993 Carved Steatite and Sandstone Tubes: Pipes for Smoking or Shaman's Paraphernalia. *Plains Anthropologist* 38(143):163-176.

- Frison, George C., and Lawrence C. Todd (editors)
 1987 *The Horner Site: The Type Site of the Cody Cultural Complex*. Academic Press, Orlando.
- Gilmore, Kevin P.
 1999 Late Prehistoric Stage (A.D. 150-1540). In *Colorado Prehistory: A Context for the Platte River Basin*, edited by Marcia Tate, Mark L. Chenault, Bonnie Clark, Terri McBride, and Margaret Wood, pp. 175-308. Colorado Council of Professional Archaeologists, Denver.
- Grinnell, George Bird
 1922 The Medicine Wheel. *American Anthropologist* 24(3):299-310.
- Gunnerson, James H.
 1968 Plains Apache Archaeology: A Review. *Plains Anthropologist* 13(41):167-189.
- Jacobsen, R. Brooke and Jeffrey L. Eighmy
 1980 A Mathematical Theory of Horse Adoption on the North American Plains. *Plains Anthropologist* 25(90):333-341.
- Johnson, R.A., J.J. Stipp, M.A. Tamers, Georges Bonani, Martin Suter, and Willy Wolfli
 1988 Archaeologic Sherd Dating: Comparison of Thermoluminescence Dates with Radiocarbon Dates by Beta Counting and Accelerator Techniques. *Radiocarbon* 28(2A):719-725.
- Johnston, M. Chris
 2016 *Running of the Buffalo: Investigations of the Roberts Ranch Buffalo Jump (5LR100), Northern Colorado*. Master's thesis, Colorado State University, Department of Anthropology.
- Kainer, Ronald E.
 1976 *Archaeological Investigations at the Spring Gulch Site (5LR252)*, Master's thesis, Colorado State University, Department of Anthropology.
- Kehoe, Thomas F.
 1958 Tipi Rings: The "Direct Ethnological" Approach Applied to an Archaeological Problem. *American Anthropologist* 60:861-873.
 1966 The Small Side-Notched Point System on the Northern Plains. *Plains Anthropologist* 31(6):827-841.
- Kelly, Robert L.
 1988 The Three Sides of a Biface. *American Antiquity* 53(4):717-734.

- Lee, Craig M., Michael Neeley, Mark D. Mitchell, Marcel Kornfeld, and Crae O'Connor
2016 Microcores and Microliths in Northwestern Plains and Rocky Mountain Front Lithic Assemblages. *Plains Anthropologist* 61(238):136-158.
- Lurie, Rochelle
1989 Lithic Technology and Mobility Strategies: The Koster Site Middle Archaic. In *Time, Energy and Stone Tools*, edited by Robin Torrence, pp. 46-56. Cambridge University Press, Cambridge.
- Long, Austin and Bruce Rippeteau
1974 Testing Contemporaneity and Averaging Radiocarbon Dates. *American Antiquity* 39(2):205-215.
- Malouf, Carling
1961 The Tipi Rings of the High Plains. *American Antiquity* 26(3):381-389.
- Meeker, Halston F.C., Christopher M. Johnston, and Jason LaBelle
2013 *What Once Was Lost, But Now is Found: The Archaeology of the Upper Boxelder Creek Bison Kill, Laramie County, Wyoming*. Poster presented at the 70th Annual Meeting of the Plains Anthropological Conference, Saskatoon, Canada.
- Morris, Elizabeth Ann
1989 Considerations of Tipi Ring Data from a Colorado Point of View: A Trial Application of HRAF Attributes. In *Household and Communities: Proceeding of the Twenty-first Annual Conference of the Archaeological Association of the University of Calgary*, edited by Scott MacEachern, David J.W. Archer, and Richard D. Garvin, pp. 237-242. University of Calgary Archaeological Association, Calgary.
- Morris, Elizabeth Ann, Daniel Mayo, Richard C. Blakeslee, and Patrick W. Bower
1983 Current Perspectives on Stone Ring Structures in Northeastern Colorado. *Plains Anthropologist* 28(102), Part 2: Memoir 19: FROM MICROCOSM TO MACROCOSM: Advances in Tipi Ring Investigation and Interpretation: 45-58.
- Morris, Elizabeth Ann, W. Max Witkind, Ralph L. Dix, and Judith Jacobson
1981 Nutritional Content of Selected Aboriginal Foods in Northeastern Colorado: Buffalo (Bison Bison) and Wild Onions (*Allium* SPP.) *Journal of Ethnobiology* 1(2):213-220.
- Mulloy, William
1958 *A Preliminary Historical Outline for the Northwestern Plains*. University of Wyoming Publications 22:1-235.
- National Bison Association (NBA)
2016 Bison FAQs. <http://www.bisoncentral.com/faqs>
- Nelson, Charles E.
1971 The George W. Lindsay Ranch Site, 5JF11. *Southwestern Lore*, 37(1):1-14.

- Nelson, Charles E. and Bruce G. Stewart
1973 Cherokee Mountain Rock Shelter. *Plains Anthropologist* 18(62):328-335.
- Nelson, Ben A., Timothy A. Kohler, and Keith W. Kintigh
1994 Demographic Alternatives: Consequences for Current Models of Southwestern Prehistory. in *Understanding Complexity in the Prehistoric Southwest*. Proceedings Volume XVI, Santa Fe Institute, Studies in the Sciences of Complexity, edited by George J. Gumerman and Murray Gell-Mann, pp. 113-146. Addison-Wesley Publishing Company, Reading, Massachusetts.
- Nelson, M.C.
1991 The Study of Technological Organization. *Archaeological Method and Theory* 3:57-100.
- O'Brien, Matthew J.
2013 *The Socioeconomic Organization of Communal Hunting: An Archaeological Examination of Shoshone Collective Action*. PhD Dissertation, Department of Anthropology, University of New Mexico.
- Ostahowski, Brian E. and Robert L. Kelly
2015 Alm Rockshelter Lithic Debitage Analysis: Implications for Hunter-Gatherer Mobility Strategies in the Big Horn Mountains, Wyoming. In *Lithics in the West*, edited by Douglas H. MacDonald, William Andrefsky, Jr., and Pei-Lin Yu, pp. 120-141. University of Montana Press, Missoula.
- Ownby, Mary F.
2015 *Petrographic Analysis of Sand and Pottery from Northern Colorado: Petrographic Report No. 2015-02, Desert Archaeology, Inc.* Manuscript on file, Center for Mountain and Plains Archaeology, Colorado State University, Fort Collins.
- Packard, Ashley N.
2015 *Steatite Vessels in Northern Colorado and the Concept of Prehistoric Borders*. Unpublished Undergraduate Honors Thesis, Department of Anthropology, Colorado State University, Fort Collins.
- Parry, W. and Robert L. Kelly
1987 Expedient Core Technology and Sedentism. In *The Organization of Core Technology*, edited by J.K. Johnson, and C.A. Morrow, pp. 285-304. Westview Press, Boulder, Colorado.
- Pelton, Spencer R., Jason M. LaBelle, Chris Davis, and Cherise Bunn
2013 *The Spring Canyon Site, a Large Campsite at the Base of the Foothills of Larimer County, Colorado*. Manuscript on file at the Center for Mountain and Plains Archaeology, Department of Anthropology. Colorado State University, Fort Collins.

Perlmutter, Benjamin

2015 *Bringing it All Back Home: Early Ceramic Period Residential Occupation at the Kinney Spring Site (5LR144C), Larimer County, Colorado*. Unpublished Master's thesis, Department of Anthropology, Colorado State University, Fort Collins.

Quigg, Michael J.

1979 Comments on the Significance of Stone Circle Excavations in Alberta. *Plains Anthropologist* 24(85):261-266.

Ranere, A.J., J.C. Ranere, and J. Lortz

1969 The Monida Pass Tipi Ring Site. *Tebawa* 12(1):39-46.

Raynesford, Howard

1953 Unpublished manuscript on *The Smoky Hill River and Fremont's Indian Village*. Archived at the Kansas Historical Society Archeological Inventory.

Reedy, Chandra L.

1993 Thin-Section Petrography in Studies of Cultural Materials. *Journal of the American Institute for Conservation* 33(2):115-129.

Reher, Charles A.

1982 Analysis of Spatial Structure in Stone Circle Sites. *Plains Anthropologist* 28(102): Memoir 19:192-222.

Reher, Charles A. and George C. Frison

1980 The Vore Site, 48CK302: A Stratified Buffalo Jump in the Wyoming Black Hills. *Plains Anthropologist* Memoir 16.

Reimer, P.J., E. Bard, A. Bayliss, J.W. Beck, P.G. Blackwell, C. Bron, Ramsey, P.M. Grootes, T.P. Guilderson, H. Hafliadason, I. Hajdas, C. Hatt, T.J. Heaton, D.L. Hoffman, A.G. Hogg, K.A. Hughen, K.F. Kaiser, B. Kromer, S.W. Manning, M. Niu, R.W. Reimer, D.A. Richards, E.M. Scott, J.R. Southon, R.A. Staff, C.S.M. Turney, and J. van der Plicht

2013 IntCal13 and Marine 13 Radiocarbon Age Calibration Curves, 0-50,000 Years cal BP. *Radiocarbon* 55(4):1869-1887.

Scheiber, Laura L. and Charles A. Reher

2007 The Donovan Site (5LO204): An Upper Republican Animal Processing Camp on the High Plains. *Plains Anthropologist* 52(203):337-364.

Schroeder, Bryon Alan

2015 *It Takes a Village: Placing Middle Rocky Mountain High Altitude Residential Sites of the Late Prehistoric Firehold Phase into a Broader Regional Context*. PhD Dissertation, Department of Anthropology, University of Montana.

Schiffer, Michael B.

1986 Radiocarbon Dating and the "Old Wood" Problem: The Case of the Hohokam Chronology. *Journal of Archaeological Science* 13:13-30.

Shackley, M. Steven

2012 *An Energy-Dispersive X-Ray Fluorescence Analysis of Obsidian Artifacts from Archaeological Sites in Larimer and Jefferson Counties, Colorado*. Letter Report, 3 March 2012. On file, Center for Mountain and Plains Archaeology, Colorado State University, Fort Collins.

Shott, Michael

1986 Technological Organization and Settlement Mobility: An Ethnographic Examination. *Journal of Anthropological Research* 42(1):15-51.

Smith, S. Craig, Lance M. McNees, and Thomas P. Reust

1995 Site Structure of Two Buried Stone Circle Sites, Southern Wyoming. *Plains Anthropologist* 40(151):5-21.

Steward, Julian.

1936 The Economic and Social Basis of Primitive Bands. In *Essays in Anthropology Presented to Alfred L. Kroeber*, edited by R.H. Lowie, pp.331-350. University of California Press, Freeport.

Stuiver, M. and Reimer, P.J.

1993 Extended 14C Data Base and Revised CALIB 3.0 14C Age Calibration Program, *Radiocarbon* 35:215-230.

Surovell, Todd A.

2009 *Toward a Behavioral Ecology of Lithic Technology: Cases from Paleoindian Archaeology*. The University of Arizona Press, Tucson.

Taylor, Jeb

2006 *Projectile Points of the High Plains: New Perspectives of Typology Based on Examinations of Original Type Site Specimens*. Sheridan Books, Chelsea, Michigan.

Todd, Lawrence C., David C. Jones, Robert S. Walker, Paul Burnett, and Jeffrey Eighmy

2001 Late Archaic Bison Hunters in Northern Colorado: 1997-1999 Excavations at the Kaplan-Hoover Bone Bed (5LR3953). *Plains Anthropologist* 46(176):125-147.

Varién, Mark D. and Barbara J. Mills

1997 Accumulations Research: Problems and Prospects for Estimating Site Occupation Span. *Journal of Archaeological Method and Theory* 4(2):141-191.

Varién, Mark D. and Scott G. Ortman

2005 Accumulations Research in the Southwest United States: Middle-Range Theory for Big-Picture Problems. *World Archaeology* 37(1):132-155.

Wedel, Waldo R.

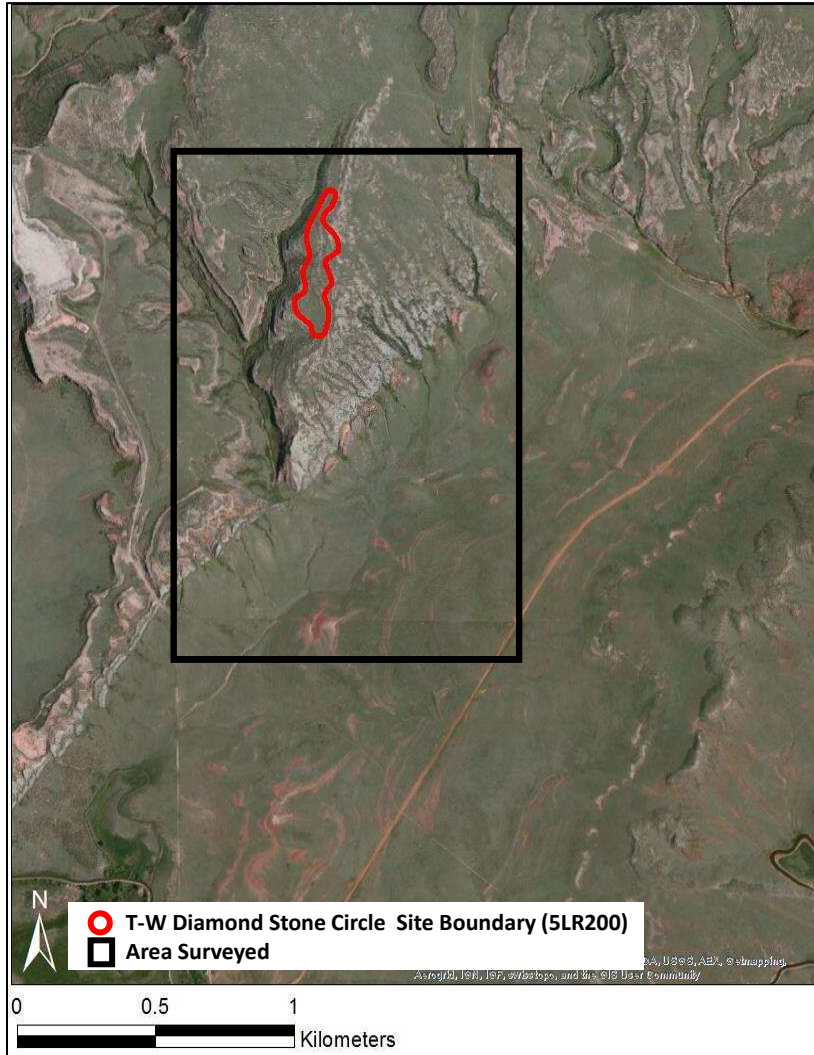
1961 *Prehistoric Man on the Great Plains*. University of Oklahoma Press, Norman.

Williams, Bobby Joe., and H. Martin Wobst

1974 A Model of Band Society. *Memoirs of the Society for American Antiquity* 29:1-138.

APPENDIX

Appendix A: 5LR200 original 1970s survey area. All surface artifacts from the black rectangle were reported as part of Flayharty (1972). Artifacts reported in this thesis are within boundaries of stone rings (red polygon) and only include items from excavation. Surface artifacts from the original survey are curated at the Colorado State University Archaeological Repository, Department of Anthropology.



Appendix B: AEON radiocarbon results



Radiocarbon Analysis

2016-03-08

Report for:

Hallie Meeker
710 City Park Av, APT A110
Fort Collins, CO 80521

Aeon #	Sample	Material	Pretreat	Yield µg C	Yield % C	δ ¹³ C ‰	F ¹⁴ C	±	¹⁴ C age Years BP	±
2150	5LR289-Sample 1	bone	gelatin	1076	34.9	-13.9	0.9725	0.0031	225	25
2151	5LR289-Sample 2	bone	gelatin	914	42.5	-12.3	0.9715	0.0031	230	25
2152	5LR200-Sample 3	bone	gelatin	878	41.9	-13.0	0.9150	0.0028	715	25
2153	5LR200-Sample 4	bone	gelatin	992	42.0	-15.5	0.9110	0.0033	750	30

Notes

Item	Description
Aeon #	The unique identifier for each radiocarbon analysis performed by Aeon. Use this number for publication: e.g., "Aeon-137"
Sample	The customer-provided sample identifier.
Material	The type of material targeted for analysis. A sub-sample of this type is selected from the total material submitted to Aeon.
Pretreat	The chemical pretreatment protocol applied to the sub-sample. ABA = acid-base-acid; ABOX = acid-base-strong oxidation
Yield	The amount of sample carbon analyzed for ¹⁴ C and the percentage of carbon in the sub-sample ¹⁾ .
δ¹³C	The relative difference between the ¹³ C/ ¹² C ratio of the test sample ²⁾ and that of the VPDB standard, expressed in per mille.
F¹⁴C	The ¹⁴ C activity ratio ³⁾ , corrected for isotopic fractionation and normalized to δ ¹³ C = -25‰.
¹⁴C age	The conventional radiocarbon age, based on the "Libby" 5568-year half-life.
±	The 1σ uncertainty for the value to the left.

¹⁾ the sub-sample is the portion of the total submitted material that is subjected to pretreatment.

²⁾ the test sample is the analyzed portion of the carbon extracted from the sub-sample.

³⁾ relative to "Modern" as defined by the Oxalic Acid I standard.

References

Stuiver, M., Polach, H., 1977. Discussion: Reporting of ¹⁴C data. Radiocarbon 19 (3), 355-363.
van der Plicht, J., Hogg, A., 2006. A note on reporting radiocarbon. Quaternary Geochronology 1 (4), 237-240.



**Supplemental
Analysis**
for bone samples
2016-03-08

Report for:
Hallie Meeker
710 City Park Av, APT A110
Fort Collins, CO 80521

Sample	before pretreatment			RGY %	after pretreatment		
	%C	%N	C:N		%C	%N	C:N
5LR289-Sample 1	13.19	4.11	3.74	10.1	43.91	16.02	3.20
5LR289-Sample 2	11.96	3.50	3.99	16.5	45.54	16.43	3.23
5LR200-Sample 3	11.99	3.36	4.16	11.4	46.44	16.55	3.27
5LR200-Sample 4	4.26	0.28	17.74	10.1	44.62	16.42	3.17

Sample	$\delta^{13}\text{C}$ ‰	$\delta^{15}\text{N}$ ‰
5LR289-Sample 1	-13.9	7.4
5LR289-Sample 2	-12.7	7.8
5LR200-Sample 3	-12.3	7.2
5LR200-Sample 4	-13.9	8.6

Notes

Item	Description
Sample	The customer-provided sample identifier.
%C	carbon content, % of test sample mass (nominal: 43.1 ± 6.3% after pretreatment)
%N	nitrogen content, % of test sample mass (nominal: >0.5% before pretreatment, 15.5 ± 2.3% after pretreatment)
C:N	ratio of carbon atoms to nitrogen atoms (nominal: <11.0 before pretreatment, 3.25 ± 0.17 after pretreatment)
RGY	residual gelatin yield (nominal: >0.5 %)
$\delta^{13}\text{C}$	The $^{13}\text{C}/^{12}\text{C}$ ratio of the pretreated material. This value may differ from that obtained for the AMS test sample.
$\delta^{15}\text{N}$	The $^{15}\text{N}/^{14}\text{N}$ ratio of the pretreated material.

Appendix C: AEON sample information for submitted bone

Site	AEON sample #	Thesis #	Item	Grid	E/W	Grid	N/S	Feature	Level	Count	Mass (g)	Max Length (mm)	Element	Portion	Segment	Side	PF	DF	Skeletal Portion	Species	LI (mm)	Lm (mm)	Wp (mm)	Wd (mm)	DI (mm)	Dm (mm)
5LR289	1	35.1	bone	9	E	24	S	4	3	1	17.1	44.4	PHS	US	US	N	3	3	AP	Bison						
5LR289	2	37.1	bone	51	W	33	S	7	2	1	48.5	67.8	AS	CO	CO	R	5	5	AP	Bison	68.9*, measured by inferring extension of intact edge, following the trend of the bone	67.2	43.2	42.1	38.7	31.2* bone is highly weathered on edge, this measurement is smaller than it should be
Site	AEON sample #	Thesis #	Item	Grid	Trench			Feature	Level	Count	Mass (g)	Max Length (mm)	Element	Portion	Segment	Side	PF	DF	Skeletal Portion	Species						
5LR200	3	33.3	bone	C5	NA			4	NA	1	25.8	89.7	RD	PR	CD?	R	0	5	AP	Adult Bison						
5LR200	4	34.2	tooth	C18-19	NA			10	2	1	2.5	32.4	MUN	NA	NA	NA	NA	NA	CR	Fetal Bison						

Appendix D: 5LR289 debitage with provenience.

CPMA Curation Number	HFM Item #	Item	Grid	E/W	Grid	N/S	Level	Max Length (mm)	Max Thickness (mm)	Raw Mat	Cortex	Burning	Mass (g)
5LR289.013	1.1	FK	18	E	15	S	1	21.51	2.84	CH	N	N	0.90
5LR289.014	1.2	FK	18	E	15	S	1	20.38	2.86	QTZ	N	NA	0.90
5LR289.015	1.3	FK	18	E	15	S	1	14.72	2.34	QTZ	N	NA	0.30
5LR289.016	1.4	FK	18	E	15	S	1	12.37	2.75	QTZ	N	NA	0.40
5LR289.017	1.5	FK	18	E	15	S	NA	11.87	2.62	QTZ	N	NA	0.30
5LR289.018	1.6	FK	18	E	15	S	NA	8.25	1.50	QTZ	N	NA	0.10
5LR289.019	1.7	FK	18	E	15	S	NA	8.71	2.94	QCL	N	N	0.20
5LR289.020	1.8	FK	18	E	12	S	1	26.57	11.17	QCL	N	N	6.00
5LR289.021	2.1	FK	21	E	18	S	NA	8.36	2.42	QCL	N	N	0.20
5LR289.022	3.1	FK	57	W	39	S	2	12.01	2.49	CH	N	N	0.30
5LR289.023	4.1	FK	54	W	36	S	NA	10.74	2.50	CH	Y	N	0.20
5LR289.024	4.2	FK	54	W	36	S	3	30.89	6.17	QTZ	N	NA	3.90
5LR289.025	6.1	FK	60	W	39	S	1	11.97	5.37	QCL	N	N	0.80
5LR289.026	6.2	FK	60	W	39	S	NA	8.91	3.39	QCL	N	N	0.20
5LR289.027	6.3	FK	60	W	39	S	3	12.47	1.51	QTZ	N	NA	0.10
5LR289.028	7.1	FK	9	E	24	S	NA	16.90	3.25	QTZ	N	NA	0.30
5LR289.029	7.2	FK	9	E	24	S	NA	10.41	1.38	CH	N	N	0.01
5LR289.030	7.3	FK	9	E	24	S	NA	8.00	1.19	CHAL	N	N	0.01
5LR289.031	9.1	FK	27	E	21	S	NA	11.02	1.71	QTZ	N	NA	0.10
5LR289.040	9.11	FK	27	E	21	S	NA	9.02	1.91	CHAL	N	N	0.10
5LR289.041	9.12	FK	27	E	21	S	1	16.59	4.06	QTZ	N	NA	0.50
5LR289.042	9.13	FK	27	E	21	S	NA	10.18	1.98	CH	N	N	0.20
5LR289.043	9.14	FK	27	E	21	S	NA	10.18	1.93	QTZ	N	NA	0.10
5LR289.044	9.15	FK	27	E	21	S	NA	8.21	2.10	QTZ	N	NA	0.01
5LR289.045	9.16	FK	27	E	21	S	NA	7.16	0.99	CHAL	N	N	0.01
5LR289.046	9.17	FK	27	E	21	S	NA	5.39	0.68	QTZ	N	NA	0.01
5LR289.032	9.2	FK	27	E	21	S	1	11.26	2.52	QTZ	N	NA	0.20
5LR289.033	9.3	FK	27	E	21	S	1	14.37	2.74	QTZ	N	NA	0.40
5LR289.034	9.4	FK	27	E	21	S	1	14.75	2.34	CHAL	N	N	0.30
5LR289.035	9.5	FK	27	E	21	S	1	20.20	2.86	CHAL	N	N	0.40
5LR289.036	9.6	FK	27	E	21	S	NA	12.13	2.56	CHAL	N	N	0.20
5LR289.037	9.7	FK	27	E	21	S	NA	11.30	1.54	CHAL	N	N	0.10
5LR289.038	9.8	FK	27	E	21	S	NA	10.48	2.01	CHAL	N	N	0.10
5LR289.039	9.9	FK	27	E	21	S	NA	9.47	1.58	CHAL	N	N	0.10
5LR289.047	10.1	FK	27	E	18	S	1	13.98	1.84	CH	N	N	0.20
5LR289.048	10.2	FK	30	E	18	S	1	17.56	3.90	QTZ	N	NA	1.20
5LR289.049	10.3	FK	30	E	18	S	1	12.91	2.92	QTZ	N	NA	0.40
5LR289.050	10.4	FK	27	E	18	S	1	12.94	1.84	QTZ	N	NA	0.20
5LR289.055	11.1	FK	39	W	24	S	1	11.79	1.78	CH	N	N	0.30

CPMA Curation Number	HFM Item #	Item	Grid	E/W	Grid	N/S	Level	Max Length (mm)	Max Thickness (mm)	Raw Mat	Cortex	Burning	Mass (g)
5LR289.056	11.2	FK	39	W	24	S	NA	8.25	1.79	QTZ	N	NA	0.01
5LR289.057	11.3	ANG	39	W	24	S	NA	7.64	3.12	CHAL	N	N	0.20
5LR289.058	11.4	ANG	39	W	24	S	1	19.68	8.81	QCL	N	N	2.50
5LR289.051	11.5	FK	30	E	24	S	1	13.26	2.88	QTZ	N	NA	0.30
5LR289.052	11.6	FK	30	E	24	S	1	13.56	2.59	QTZ	N	NA	0.60
5LR289.053	11.7	FK	30	E	24	S	NA	10.63	2.55	QTZ	N	NA	0.10
5LR289.054	11.8	FK	30	E	24	S	NA	9.16	1.53	CH	N	N	0.01
5LR289.059	12.1	FK	51	W	36	S	NA	10.85	2.37	CH	N	Y	0.20
5LR289.060	13.1	FK	12	W	27	S	1	14.00	2.78	CHAL	N	N	0.50
5LR289.061	13.2	FK	12	W	27	S	1	15.43	2.82	QTZ	N	NA	0.20
5LR289.062	13.3	FK	12	W	29?	S	1	15.77	3.67	QTZ	N	NA	1.20
5LR289.063	14.1	FK	30	E	18	S	1	21.84	3.39	CHAL	N	N	0.50
5LR289.064	14.2	FK	27	E	18	S	1	17.54	4.24	QTZ	N	NA	1.10
5LR289.066	15.1	FK	60	W	39	S	1	26.68	6.19	CH	N	N	2.20
5LR289.067	15.2	FK	60	W	39	S	1	15.68	6.38	CH	N	Y	0.90
5LR289.068	15.3	FK	60	W	39	S	1	14.82	7.29	CH	N	Y	1.30
5LR289.069	15.4	FK	60	W	39	S	1	14.94	2.00	QTZ	N	NA	0.30
5LR289.070	15.5	FK	60	W	39	S	1	15.79	3.43	QTZ	N	NA	0.50
5LR289.071	15.6	FK	60	W	39	S	1	12.70	2.95	QTZ	N	NA	0.40
5LR289.072	15.7	FK	60	W	39	S	1	10.18	2.56	QTZ	N	NA	0.20
5LR289.073	15.8	FK	60	W	39	S	1	12.88	2.55	QTZ	N	NA	0.20
5LR289.074	15.9	FK	60	W	39	S	1	11.07	6.37	CH	N	Y	0.70
5LR289.075	16.1	FK	60	W	39	S	NA	14.25	3.10	CH	N	N	0.20
5LR289.076	16.2	ANG	60	W	39	S	1	9.99	9.33	QCL	N	N	1.10
5LR289.077	16.3	ANG	60	W	39	S	NA	13.41	3.92	QCL	N	N	0.40
5LR289.078	16.4	ANG	60	W	39	S	NA	9.27	3.42	QCL	N	N	0.30
5LR289.079	16.5	FK	60	W	39	S	NA	8.18	2.43	QTZ	N	NA	0.10
5LR289.080	16.6	FK	57	W	39	S	1	12.19	4.16	QTZ	N	NA	0.40
5LR289.081	16.7	FK	57	W	39	S	1	10.01	1.98	QTZ	N	NA	0.10
5LR289.082	17.1	FK	60	W	39	S	2	12.78	2.46	CH	N	N	0.10
5LR289.091	17.11	ANG	60	W	39	S	2	22.16	5.83	QCL	N	N	4.30
5LR289.083	17.2	FK	60	W	39	S	2	14.31	2.91	QTZ	N	N	0.40
5LR289.084	17.3	FK	60	W	39	S	NA	10.85	2.32	CH	N	N	0.10
5LR289.085	17.4	FK	60	W	39	S	2	12.73	2.35	QTZ	Y	NA	0.20
5LR289.086	17.5	FK	60	W	39	S	1	21.63	8.16	CH	N	Y	4.50
5LR289.087	17.6	ANG	60	W	39	S	2	20.35	5.65	QCL	N	N	1.90
5LR289.088	17.7	ANG	60	W	39	S	2	15.93	4.96	QCL	N	N	0.90
5LR289.089	17.8	FK	60	W	39	S	2	10.28	5.24	CH	N	N	0.50
5LR289.090	17.9	ANG	60	W	39	S	NA	8.64	6.38	QCL	N	N	0.40
5LR289.093	18.1	FK	21	E	21	S	3	20.69	5.63	QTZ	N	NA	1.50

CPMA Curation Number	HFM Item #	Item	Grid	E/W	Grid	N/S	Level	Max Length (mm)	Max Thickness (mm)	Raw Mat	Cortex	Burning	Mass (g)
5LR289.094	18.2	FK	21	E	21	S	3	25.08	4.45	QTZ	N	NA	2.50
5LR289.095	18.3	FK	21	E	21	S	3	10.36	3.39	QCL	N	N	0.50
5LR289.096	18.4	ANG	21	E	21	S	3	18.45	8.15	QCL	N	N	2.30
5LR289.097	18.5	FK	21	E	21	S	1	12.96	3.44	QTZ	N	NA	0.70
5LR289.098	18.6	FK	21	E	21	S	1	10.20	2.51	QTZ	N	NA	0.10
5LR289.099	18.7	FK	21	E	21	S	2	7.47	1.21	QTZ	N	NA	0.01
5LR289.100	18.8	ANG	21	E	21	S	2	18.65	11.07	QCL	N	N	3.70
5LR289.101	18.9	FK	21	E	21	S	2	9.95	1.53	QTZ	N	NA	0.01
5LR289.102	19.1	FK	21	E	15	S	1	15.65	1.44	QTZ	N	NA	0.30
5LR289.103	19.2	FK	21	E	15	S	1	16.82	2.83	QTZ	N	NA	0.70
5LR289.104	19.3	FK	21	E	15	S	1	18.88	2.93	CH	N	N	0.80
5LR289.105	19.4	FK	21	E	15	S	1	12.35	2.07	CH	N	N	0.20
5LR289.106	19.5	FK	21	E	15	S	1	11.34	1.10	QTZ	N	NA	0.10
5LR289.107	19.6	FK	21	E	15	S	NA	11.94	2.42	CHAL	N	N	0.20
5LR289.108	19.7	FK	21	E	15	S	NA	7.79	1.91	CH	N	N	0.10
5LR289.109	19.8	FK	21	E	15	S	NA	9.41	0.94	QTZ	N	NA	0.01
5LR289.110	19.9	FK	21	E	15	S	NA	6.27	1.73	CH	N	N	0.01
5LR289.112	20.1	FK	30	E	21	S	1	17.79	2.81	QTZ	N	NA	0.80
5LR289.113	20.2	ANG	30	E	21	S	1	15.43	12.18	QCL	N	N	3.80
5LR289.114	21.1	FK	15	W	25	S	1	21.52	2.89	QTZ	N	NA	0.70
5LR289.123	21.11	FK	15	W	25	S	NA	9.58	1.31	CH	N	Y	0.01
5LR289.124	21.12	FK	15	W	25	S	NA	9.56	1.14	CH	N	Y	0.01
5LR289.125	21.13	FK	15	W	25	S	NA	10.68	1.47	CH	N	Y	0.10
5LR289.126	21.14	FK	15	W	25	S	NA	11.30	1.51	CH	N	Y	0.01
5LR289.127	21.15	FK	15	W	25	S	NA	10.80	1.63	CH	N	Y	0.01
5LR289.128	21.16	FK	15	W	25	S	NA	11.49	1.50	CH	N	Y	0.10
5LR289.129	21.17	FK	15	W	25	S	NA	9.01	1.12	CH	N	Y	0.01
5LR289.130	21.18	FK	15	W	25	S	NA	8.43	1.30	CH	N	Y	0.01
5LR289.131	21.19	FK	15	W	25	S	NA	7.47	1.72	CH	N	Y	0.01
5LR289.115	21.2	FK	15	W	25	S	1	15.02	4.33	QTZ	N	NA	0.70
5LR289.132	21.21	FK	15	W	25	S	NA	6.55	1.03	CH	N	Y	0.01
5LR289.133	21.22	FK	15	W	25	S	NA	8.82	1.54	CH	N	Y	0.01
5LR289.134	21.23	FK	15	W	25	S	NA	6.86	1.13	CH	N	Y	0.01
5LR289.135	21.24	FK	15	W	25	S	NA	7.47	0.91	CH	N	Y	0.01
5LR289.136	21.25	FK	15	W	25	S	NA	5.70	0.80	CH	N	Y	0.01
5LR289.137	21.26	FK	15	W	25	S	NA	9.24	0.97	CH	N	Y	0.01
5LR289.138	21.27	FK	15	W	25	S	NA	11.18	1.95	QTZ	N	NA	0.30
5LR289.139	21.28	FK	15	W	25	S	NA	12.22	3.28	QTZ	N	NA	0.20
5LR289.140	21.29	FK	15	W	25	S	NA	13.07	1.80	QCL	N	N	0.10
5LR289.116	21.3	FK	15	W	25	S	1	29.18	5.17	QTZ	N	NA	4.20

CPMA Curation Number	HFM Item #	Item	Grid	E/W	Grid	N/S	Level	Max Length (mm)	Max Thickness (mm)	Raw Mat	Cortex	Burning	Mass (g)
5LR289.141	21.31	FK	15	W	25	S	NA	7.30	1.40	CHAL	N	N	0.01
5LR289.142	21.32	FK	15	W	25	S	NA	9.12	0.97	QTZ	N	NA	0.01
5LR289.143	21.33	FK	15	W	25	S	NA	7.20	1.21	QTZ	N	NA	0.01
5LR289.144	21.34	FK	15	W	25	S	NA	7.02	1.10	CH	N	N	0.01
5LR289.145	21.35	FK	15	W	25	S	NA	6.38	0.52	CH	N	N	0.01
5LR289.146	21.36	ANG	15	W	25	S	NA	29.41	8.66	QCL	N	N	4.30
5LR289.147	21.37	ANG	15	W	25	S	NA	19.92	6.87	QCL	N	N	1.10
5LR289.117	21.4	FK	15	W	25	S	1	25.08	7.37	QTZ	Y	NA	3.60
5LR289.118	21.5	FK	15	W	25	S	NA	12.53	3.39	QTZ	N	NA	0.50
5LR289.119	21.6	FK	15	W	25	S	NA	10.70	2.12	CHAL	N	N	0.20
5LR289.120	21.7	FK	15	W	25	S	NA	11.81	1.81	QTZ	N	NA	0.20
5LR289.121	21.8	FK	15	W	25	S	NA	12.38	2.80	QTZ	N	NA	0.30
5LR289.122	21.9	FK	15	W	25	S	NA	11.56	1.98	CH	N	Y	0.20
5LR289.150	22.1	FK	54	W	33	S	NA	17.83	2.16	CH	N	N	0.40
5LR289.159	22.11	FK	54	W	33	S	NA	7.47	1.48	CH	N	Y	0.01
5LR289.160	22.12	FK	54	W	33	S	NA	7.70	1.49	CH	N	N	0.01
5LR289.161	22.13	FK	54	W	33	S	NA	5.32	1.04	QTZ	N	NA	0.01
5LR289.151	22.2	FK	54	W	33	S	NA	11.99	1.61	QTZ	N	NA	0.20
5LR289.152	22.3	FK	54	W	33	S	NA	14.21	2.07	CH	N	N	0.40
5LR289.153	22.4	FK	54	W	33	S	NA	10.48	1.28	QTZ	N	NA	0.10
5LR289.154	22.5	FK	54	W	33	S	NA	13.89	2.54	QTZ	N	NA	0.30
5LR289.155	22.6	FK	54	W	33	S	NA	8.82	1.78	CH	N	Y	0.10
5LR289.156	22.7	FK	54	W	33	S	NA	13.84	1.09	CH	N	Y	0.01
5LR289.157	22.8	FK	54	W	33	S	NA	8.23	1.06	CH	N	N	0.01
5LR289.158	22.9	FK	54	W	33	S	NA	8.06	0.83	CH	N	N	0.01
5LR289.163	23.1	FK	15	W	27	S	1	21.29	3.69	CHAL	N	N	1.60
5LR289.164	23.2	FK	15	W	27	S	1	23.47	7.60	QTZ	N	NA	2.10
5LR289.165	23.3	FK	15	W	27	S	1	33.80	6.54	QTZ	N	NA	3.50
5LR289.166	23.4	FK	15	W	27	S	1	21.87	3.54	QTZ	N	NA	1.20
5LR289.167	23.5	FK	15	W	27	S	1	24.62	3.42	QTZ	N	NA	1.10
5LR289.168	23.6	FK	15	W	27	S	1	47.94	11.05	PW	Y	N	12.50
5LR289.169	23.7	FK	15	W	27	S	1	12.59	2.98	QTZ	N	NA	0.30
5LR289.170	23.8	FK	15	W	27	S	1	13.48	2.12	CH	N	N	0.20
5LR289.171	23.9	FK	15	W	27	S	NA	12.21	1.65	CH	N	N	0.10
5LR289.172	24.1	FK	18	E	12	S	2	10.36	2.01	CH	N	N	0.30
5LR289.173	24.2	FK	18	E	12	S	2	10.55	2.31	QTZ	N	NA	0.20
5LR289.174	25.1	FK	54	W	33	S	1	24.44	3.70	CHAL	Y	N	1.80
5LR289.175	25.2	FK	54	W	33	S	1	37.90	9.55	QTZ	Y	NA	5.50
5LR289.176	25.3	FK	54	W	33	S	1	51.21	9.54	QTZ	N	NA	13.70
5LR289.177	25.4	FK	54	W	33	S	1	37.64	26.17	CHAL	Y	N	12.80

CMPA Curation Number	HFM Item #	Item	Grid	E/W	Grid	N/S	Level	Max Length (mm)	Max Thickness (mm)	Raw Mat	Cortex	Burning	Mass (g)
5LR289.178	25.5	FK	54	W	33	S	2	22.23	3.78	QTZ	N	NA	1.30
5LR289.179	25.6	FK	54	W	33	S	2	13.75	3.48	CHAL	N	N	0.60
5LR289.180	25.7	ANG	54	W	33	S	1	22.56	11.09	QCL	N	N	5.70
5LR289.181	25.8	ANG	54	W	33	S	NA	17.75	11.75	QCL	N	N	4.50
5LR289.182	25.9	ANG	54	W	33	S	NA	17.05	6.05	QCL	N	N	2.10
5LR289.183	26.1	FK	21	E	18	S	1	14.71	3.27	QTZ	N	NA	0.60
5LR289.184	26.2	FK	21	E	18	S	3	23.01	4.01	QTZ	N	NA	1.50
5LR289.185	26.3	FK	21	E	18	S	2	21.52	3.21	QTZ	N	NA	1.00
5LR289.186	26.4	FK	21	E	18	S	3	13.55	2.29	QTZ	N	NA	0.30
5LR289.187	26.5	FK	21	E	18	S	1	11.23	1.93	CH	N	N	0.20
5LR289.188	26.6	FK	21	E	18	S	1	10.28	1.93	QTZ	N	NA	0.10
5LR289.189	26.7	FK	21	E	18	S	1	9.64	2.18	QTZ	N	NA	0.10
5LR289.190	26.8	FK	21	E	18	S	1	11.88	3.00	QCL	N	N	0.30
5LR289.191	27.1	FK	9	E	24	S	2	21.31	3.01	QTZ	N	NA	1.10
5LR289.192	27.2	FK	9	E	24	S	3	18.16	4.52	CHAL	Y	N	0.90
5LR289.193	27.3	FK	9	E	24	S	3	15.03	2.31	QTZ	N	NA	0.40
5LR289.194	27.4	FK	9	E	24	S	NA	18.17	3.44	CHAL	N	N	0.40
5LR289.195	27.5	FK	9	E	24	S	NA	11.02	2.01	CHAL	N	N	0.20
5LR289.196	27.6	FK	9	E	24	S	NA	11.24	0.97	QTZ	N	NA	0.10
5LR289.197	27.7	FK	9	E	24	S	3	12.71	2.45	QTZ	N	NA	0.30
5LR289.198	28.1	FK	51	W	33	S	1	11.28	1.84	QTZ	N	NA	0.10
5LR289.199	28.2	FK	51	W	33	S	NA	13.48	1.93	CH	N	N	0.30
5LR289.200	28.3	FK	51	W	33	S	NA	14.28	2.00	CH	Y	N	0.10
5LR289.201	28.4	FK	51	W	33	S	NA	5.80	0.64	CH	N	N	0.01
5LR289.202	28.5	ANG	51	W	33	S	NA	10.27	5.50	CH	Y	N	0.50
5LR289.203	28.6	FK	51	W	33	S	NA	10.57	1.81	OB	N	N	0.20
5LR289.207	29.1	FK	54	W	33	S	1	38.30	6.70	CH	N	N	7.60
5LR289.208	30.1	FK	54	W	36	S	1	10.08	2.32	QTZ	N	NA	0.30
5LR289.209	31.1	ANG	42	E	9	S	1	25.50	10.53	QCL	N	N	4.70
5LR289.210	32.1	FK	21	E	27	S	1	10.23	1.72	CHAL	N	N	0.10
5LR289.211	33.1	FK	12	W	33	S	1	11.37	2.30	CH	N	N	0.20

Appendix E: 5LR289 tool attributes and metrics.

CMPA Curation Number	HFM Original Item #	Grid	E/W	Grid	N/S	Level	Feature	Max Length (mm)	Max Width (mm)	Thickness (mm)	Raw Material	Color of Raw Mat	Mass (g)	Tool Type	Complete?	Base	Notch	Fracture Type
5LR289.1	1.1	54	W	33	S	2	7	22.8	13.9	2.9	qtz	red	1.1	projectile point	abc	concave	side	impact
5LR289.2	1.2	30	E	21	S	1	1	21.6	13.6	3.9	chal	white	1.3	projectile point	abc	concave	side	hinge
5LR289.3	1.3	51	W	36	S	2	7	37.3	19.2	5.5	qtz	tan	3.8	knife	co	straight	corner	
5LR289.4	1.6	12	W	27	S	1	5	14	11	2.6	qtz	brown	0.4	projectile point	tip			snap
5LR289.5	1.7	21	E	21	S	1	2	22.4	12.9	2.5	qtz	brown	0.8	unifacial tool	abc			snap
5LR289.6	1.8	18	E	12	S	1	3	38	21.5	6.4	ch	brown	4.1	unifacial tool	abc			snap
5LR289.7	1.9	60	E	39	S	2	7	25.3	27.1	9.2	ch	brown	6.7	edge modified/unifacial	end			snap
5LR289.8	1.11	54	W	33	S	1	7	58.1	44.5	8.3	ch	brown	22	unifacial edge modified knife?	midsection			snap and hinge
5LR289.9	1.12	9	E	27	S	2	4	28.1	23	8.4	ch	pink	6.4	scraper	co			
5LR289.10	1.4							16.8	13.6	3.3	ch	white purple	0.7	projectile point	abc	straight concave	side	snap
5LR289.11	1.5							12.7	11.8	3.2	qtz	purple	0.4	projectile point	co	concave	side	
5LR289.12								27.9	22.9	8.3	ch	tan and pink	6.5	projectile point	tip			

Appendix F: 5LR289 photographs of all tools from excavated context and 2014 survey.





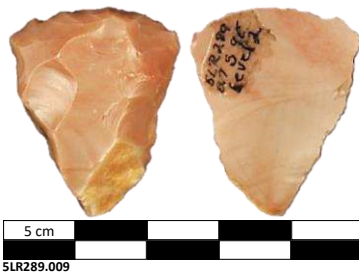
5 cm
5LR289.006



5 cm
5LR289.007



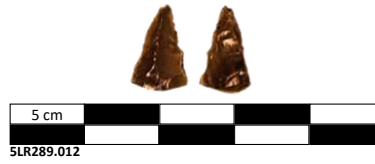
5 cm
5LR289.008



Below are Tools Collected in 2014 by the Colorado State University Field School

Not Used in this Analysis

Curated in the CSU Archaeological Repository, Department of Anthropology



Appendix G: 5LR200 debitage with provenience.

CMPA Curation Number	HFM Item #	Item	Grid	Level	Max Length (mm)	Max Thickness (mm)	Raw Mat	Cortex	Burning	Mass (g)
5LR200.58	1.1	FK	D5	1	27.83	3.38	CH	N	N	2.90
5LR200.59	1.2	FK	D5	NA	21.43	2.38	CH	N	N	0.60
5LR200.60	1.3	FK	D5	NA	17.85	2.79	CH	N	N	1.10
5LR200.61	1.4	FK	D5	NA	21.01	5.12	CH	N	Y	1.40
5LR200.62	1.5	FK	D5	1	32.07	12.13	QTZ	N	NA	7.00
5LR200.63	1.6	FK	D5	NA	17.31	2.61	CHAL	N	N	0.50
5LR200.64	1.7	FK	D5	NA	16.11	3.62	CHAL	Y	N	0.90
5LR200.65	1.8	FK	D5	1	18.76	5.22	QTZ	N	NA	1.70
5LR200.66	1.9	FK	D5	NA	21.76	2.92	CHAL	N	N	0.60
5LR200.67	1.11	FK	D5	1	20.69	3.40	CH	N	N	1.10
5LR200.68	1.12	FK	D5	1	15.26	6.01	CH	N	N	0.60
5LR200.69	1.13	FK	D5	NA	17.06	3.16	CH	N	N	0.60
5LR200.70	1.14	FK	D5	1	14.75	2.43	CHAL	N	N	0.30
5LR200.71	1.15	FK	D5	1	20.94	5.20	QTZ	N	NA	2.50
5LR200.72	1.16	FK	D5	NA	15.30	2.86	QTZ	N	NA	0.60
5LR200.73	1.17	FK	D5	NA	33.22	9.78	CH	N	Y	8.00
5LR200.74	1.18	FK	D5	1	21.19	4.56	CH	Y	N	1.00
5LR200.75	1.19	FK	D5	1	18.72	3.18	CH	N	N	0.70
5LR200.76	1.21	FK	D5	1	14.26	3.02	CH	N	N	0.80
5LR200.77	1.22	FK	D5	1	27.92	4.22	CH	N	N	2.80
5LR200.78	1.23	FK	D5	1	36.83	8.26	CH	N	N	5.30
5LR200.79	1.24	FK	D5	1	16.40	2.98	CHAL	N	N	0.40
5LR200.80	1.25	FK	D5	1	18.50	2.35	CH	N	N	0.60
5LR200.81	1.26	FK	D5	NA	19.56	3.12	CH	N	N	0.90
5LR200.82	1.27	FK	D5	1	19.08	0.20	CH	N	N	0.20
5LR200.83	1.28	FK	D5	1	20.77	3.52	CH	N	N	0.70
5LR200.84	1.29	FK	D5	1	9.03	2.28	CHAL	N	N	0.01
5LR200.85	1.31	FK	D5	NA	15.30	2.59	CH	N	N	0.50
5LR200.86	1.32	FK	D5	1	11.98	2.92	CH	N	N	0.30
5LR200.87	1.33	FK	D5	1	22.46	3.78	CH	N	N	1.00
5LR200.88	1.34	FK	D5	1	13.62	2.73	CH	N	N	0.30
5LR200.89	1.35	FK	D5	1	13.27	4.03	CH	N	N	0.50
5LR200.90	1.36	FK	D5	1	16.83	2.08	CH	N	N	0.30
5LR200.91	1.37	FK	D5	NA	11.70	2.56	CH	N	Y	0.30
5LR200.92	1.38	FK	D5	NA	11.98	2.44	QTZ	N	N	0.10
5LR200.93	1.39	FK	D5	1	13.74	2.23	CH	N	N	0.20
5LR200.94	1.41	FK	D5	1	9.35	1.56	CH	N	N	0.10
5LR200.95	1.42	FK	D5	1	15.48	3.24	CH	N	Y	0.60
5LR200.96	1.43	FK	D5	1	13.30	3.81	CHAL	Y	N	0.70
5LR200.97	1.44	FK	D5	1	11.58	1.72	QTZ	N	NA	0.20
5LR200.98	1.45	FK	D5	1	13.02	2.72	CH	N	N	0.30
5LR200.99	1.46	FK	D5	S	24.03	3.51	CH	N	N	0.70
5LR200.100	1.47	FK	D5	1	14.95	1.63	CH	N	N	0.20
5LR200.101	1.48	FK	D5	1	8.99	1.90	CH	N	N	0.20
5LR200.102	1.49	FK	D5	1	12.56	1.46	CHAL	N	N	0.20
5LR200.103	1.51	FK	D5	1	12.86	1.35	CHAL	N	N	0.20
5LR200.104	1.52	FK	D5	S	9.84	1.71	CHAL	N	N	0.10

CMPA Curation Number	HFM Item #	Item	Grid	Level	Max Length (mm)	Max Thickness (mm)	Raw Mat	Cortex	Burning	Mass (g)
5LR200.105	1.53	FK	D5	1	10.92	1.92	QTZ	N	NA	0.20
5LR200.106	1.54	FK	D5	1	8.32	1.06	QTZ	N	NA	0.01
5LR200.107	1.55	FK	D5	NA	11.68	2.00	QTZ	N	NA	0.20
5LR200.108	1.56	FK	D5	1	9.11	1.34	CHAL	N	N	0.10
5LR200.109	1.57	FK	D5	NA	13.45	2.28	CH	N	N	0.10
5LR200.110	1.58	FK	D5	1	8.29	3.49	QTZ	N	NA	0.20
5LR200.111	1.59	FK	D5	NA	9.56	2.44	CH	N	Y	0.20
5LR200.112	1.61	FK	D5	NA	7.87	2.27	CH	N	Y	0.01
5LR200.113	1.62	FK	D5	NA	7.05	1.56	CH	N	Y	0.01
5LR200.114	1.63	FK	D5	NA	9.74	1.77	CHAL	N	N	0.01
5LR200.115	1.64	FK	D5	1	15.33	1.79	CH	N	N	0.30
5LR200.116	2.1	FK	M3	1	33.00	5.16	CHAL	N	N	3.20
5LR200.117	2.2	FK	M3	1	23.01	3.37	QTZ	N	NA	1.20
5LR200.118	2.3	FK	M3	1	22.03	3.98	CHAL	N	N	2.10
5LR200.119	2.4	FK	M3	1	15.61	2.24	QTZ	N	NA	0.40
5LR200.120	2.5	FK	M3	1	21.03	2.65	CHAL	N	N	0.70
5LR200.121	2.6	FK	M3	1	20.81	3.08	QTZ	N	NA	1.30
5LR200.122	2.7	FK	M3	NA	12.38	2.34	QTZ	N	NA	0.30
5LR200.123	2.8	FK	M3	NA	13.37	3.44	CH	N	N	0.50
5LR200.124	2.9	FK	M3	NA	15.43	1.74	CH	N	Y	0.30
5LR200.125	2.11	FK	M3	NA	14.89	1.58	CHAL	N	N	0.10
5LR200.126	2.12	FK	M3	NA	14.14	2.77	QTZ	N	NA	0.50
5LR200.127	2.13	FK	M3	NA	15.98	3.16	CH	N	N	0.40
5LR200.128	2.14	FK	M3	NA	11.38	2.11	QTZ	N	NA	0.30
5LR200.129	2.15	FK	M3	NA	11.45	2.01	QTZ	N	NA	0.20
5LR200.130	2.16	FK	M3	1	14.73	3.95	CHAL	N	N	0.70
5LR200.131	2.17	FK	M3	1	9.19	1.48	CHAL	N	N	0.10
5LR200.132	2.18	FK	M3	1	10.24	2.65	CHAL	N	N	0.20
5LR200.133	2.19	FK	M3	NA	11.13	1.77	QTZ	N	NA	0.10
5LR200.134	2.21	FK	M3	NA	12.89	1.66	CHAL	N	N	0.10
5LR200.135	2.22	FK	M3	NA	12.27	2.05	QTZ	N	NA	0.10
5LR200.136	2.23	FK	M3	NA	10.13	2.05	CH	N	Y	0.01
5LR200.137	2.24	FK	M3	NA	9.98	1.30	QTZ	N	NA	0.10
5LR200.138	2.25	FK	M3	NA	11.37	1.34	CHAL	N	N	0.10
5LR200.139	2.26	FK	M3	NA	7.29	1.63	CH	N	Y	0.10
5LR200.140	2.27	FK	M3	NA	11.04	2.02	CH	N	N	0.10
5LR200.141	2.28	FK	M3	NA	9.83	1.16	CHAL	N	N	0.01
5LR200.142	2.29	ANG	M3	NA	8.12	4.44	CH	N	Y	0.20
5LR200.143	2.31	FK	M3	NA	6.50	1.21	QTZ	N	NA	0.01
5LR200.144	2.32	FK	M3	NA	6.69	0.89	CHAL	N	N	0.01
5LR200.145	2.33	FK	M3	NA	10.24	0.86	CH	N	N	0.01
5LR200.146	2.34	FK	M3	NA	8.84	0.75	CH	N	N	0.01
5LR200.147	2.35	FK	M3	NA	10.72	1.82	CHAL	N	N	0.01
5LR200.148	2.36	FK	M3	NA	6.28	1.45	CH	N	N	0.01
5LR200.149	2.37	FK	M3	NA	5.89	1.36	CH	N	N	0.01
5LR200.150	2.38	FK	M3	NA	5.84	0.83	QTZ	N	NA	0.01
5LR200.151	2.39	FK	M3	NA	7.48	1.12	CHAL	N	N	0.01
5LR200.152	2.41	FK	M3	NA	6.20	1.24	CH	N	N	0.01
5LR200.153	2.42	FK	M3	NA	5.58	0.84	QTZ	N	NA	0.01

CMPA Curation Number	HFM Item #	Item	Grid	Level	Max Length (mm)	Max Thickness (mm)	Raw Mat	Cortex	Burning	Mass (g)
5LR200.154	2.43	FK	M3	NA	5.42	0.87	CH	N	N	0.01
5LR200.155	2.44	FK	M3	NA	5.32	1.31	CH	N	N	0.01
5LR200.156	2.45	FK	M3	NA	6.10	0.80	QTZ	N	NA	0.01
5LR200.157	2.46	FK	M3	NA	6.84	0.76	CH	N	N	0.01
5LR200.158	2.47	FK	M3	NA	4.54	0.69	CH	N	N	0.01
5LR200.159	2.48	FK	M3	NA	4.83	0.37	CH	N	N	0.01
5LR200.160	2.49	FK	M3	NA	23.93	3.64	QTZ	N	NA	1.70
5LR200.161	3.1	FK	M1	2	18.76	5.54	QTZ	N	NA	1.20
5LR200.162	3.2	FK	M1	1	29.04	7.64	QTZ	N	NA	3.20
5LR200.163	3.3	FK	M1	1	18.25	2.59	CH	N	N	1.10
5LR200.164	3.4	FK	M1	1	13.43	2.92	CH	N	N	0.40
5LR200.165	3.5	FK	M1	1	16.94	4.63	QTZ	N	NA	0.70
5LR200.166	3.6	FK	M1	1	15.71	7.08	QTZ	N	NA	0.90
5LR200.167	3.7	FK	M1	1	19.94	6.41	QTZ	N	NA	1.50
5LR200.168	3.8	FK	M1	1	15.57	3.93	CHAL	N	N	0.60
5LR200.169	3.9	FK	M1	1	20.49	5.59	QTZ	N	NA	1.90
5LR200.170	3.11	FK	M1	1	19.67	4.75	CHAL	N	N	0.70
5LR200.171	3.12	FK	M1	1	14.40	4.50	QTZ	N	NA	0.70
5LR200.172	3.13	FK	M1	1	18.47	5.39	CH	N	N	1.70
5LR200.173	3.14	FK	M1	1	23.62	4.02	CH	N	Y	1.00
5LR200.174	3.15	FK	M1	1	15.54	4.24	QTZ	N	NA	0.80
5LR200.175	3.16	FK	M1	1	14.94	3.43	CH	N	Y	0.40
5LR200.176	3.17	FK	M1	1	18.94	2.04	QTZ	N	NA	0.40
5LR200.177	3.18	FK	M1	1	14.13	2.24	QTZ	N	NA	0.40
5LR200.178	3.19	FK	M1	1	10.43	3.79	QTZ	N	NA	0.30
5LR200.179	3.21	FK	M1	1	11.69	2.54	QTZ	N	NA	0.20
5LR200.180	3.22	FK	M1	1	10.17	2.20	CH	N	N	0.10
5LR200.181	3.23	FK	M1	1	11.54	3.85	CH	N	N	0.20
5LR200.182	3.24	FK	M1	1	10.31	1.73	CH	N	N	0.10
5LR200.183	3.25	FK	M1	1	11.18	2.60	QTZ	N	NA	0.30
5LR200.184	3.26	FK	M1	1	14.56	1.95	CHAL	N	N	0.20
5LR200.185	3.27	FK	M1	NA	12.87	2.41	QTZ	N	NA	0.30
5LR200.186	3.28	FK	M1	1	10.37	1.99	CHAL	N	N	0.10
5LR200.187	3.29	FK	M1	NA	10.41	1.25	QTZ	N	NA	0.01
5LR200.188	3.31	FK	M1	1	13.06	2.14	QTZ	N	NA	0.20
5LR200.189	3.32	FK	M1	1	8.98	2.07	CH	N	N	0.10
5LR200.190	3.33	FK	M1	1	13.99	3.04	CH	N	Y	0.30
5LR200.191	3.34	ANG	M1	1	9.31	4.97	CH	N	Y	0.30
5LR200.192	3.35	FK	M1	1	13.58	1.42	CH	N	N	0.10
5LR200.193	3.36	FK	M1	1	8.50	2.30	QTZ	N	NA	0.01
5LR200.194	3.37	FK	M1	1	11.95	1.74	CH	N	N	0.10
5LR200.195	3.38	FK	M1	1	9.30	2.34	CH	N	N	0.10
5LR200.196	3.39	FK	M1	1	9.79	0.68	CH	N	N	0.01
5LR200.197	3.41	FK	M1	NA	7.56	1.62	CH	N	N	0.01
5LR200.198	3.42	FK	M1	1	9.96	2.76	CH	N	N	0.10
5LR200.199	3.43	FK	M1	1	8.37	2.00	CH	N	N	0.01
5LR200.200	3.44	FK	M1	NA	7.60	1.21	CH	N	N	0.01
5LR200.201	3.45	FK	M1	1	7.32	1.74	QTZ	N	NA	0.01
5LR200.202	3.46	FK	M1	1	7.08	1.47	QTZ	N	NA	0.01

CMPA Curation Number	HFM Item #	Item	Grid	Level	Max Length (mm)	Max Thickness (mm)	Raw Mat	Cortex	Burning	Mass (g)
5LR200.203	3.47	FK	M1	NA	4.48	1.75	CH	N	N	0.01
5LR200.204	3.48	FK	M1	NA	7.78	1.71	CHAL	N	N	0.01
5LR200.205	3.49	FK	M1	2	23.44	4.85	CH	N	N	1.20
5LR200.206	3.51	FK	M1	2	15.76	2.14	CH	N	N	0.40
5LR200.207	3.52	FK	M1	2	14.39	2.36	CH	N	N	0.20
5LR200.208	3.53	FK	M1	2	13.86	4.05	CH	N	Y	0.30
5LR200.209	3.54	FK	M1	2	13.36	1.83	QTZ	N	NA	0.10
5LR200.210	4.1	FK	NA	NA	19.71	3.84	CH	N	Y	1.10
5LR200.211	4.2	FK	NA	NA	16.16	6.15	CH	Y	N	1.70
5LR200.212	5.1	FK	NA	NA	15.67	2.52	CH	N	N	0.50
5LR200.213	5.2	FK	NA	NA	12.54	1.62	CH	N	N	0.10
5LR200.214	5.3	FK	NA	NA	20.04	4.74	CH	Y	Y	1.50
5LR200.215	5.4	FK	NA	NA	16.97	5.27	CH	N	N	1.00
5LR200.216	5.5	FK	NA	NA	15.84	3.05	CH	N	N	0.40
5LR200.217	5.6	ANG	NA	NA	15.95	5.46	CH	N	Y	0.80
5LR200.218	5.7	FK	NA	NA	29.61	5.22	CHAL	N	N	1.90
5LR200.219	5.8	FK	NA	NA	16.34	2.39	CH	N	N	0.01
5LR200.220	6.1	FK	R92	NA	17.22	6.06	PW	N	N	0.70
5LR200.221	6.2	FK	R92	2	18.16	4.65	QTZ	N	NA	1.60
5LR200.222	6.3	FK	R92	2	25.82	5.66	QTZ	N	NA	2.00
5LR200.223	6.4	FK	R92	2	22.12	2.34	CH	N	N	1.10
5LR200.224	6.5	FK	R92	2	18.39	4.64	CH	N	N	1.10
5LR200.225	6.6	FK	R92	6"	21.07	7.62	PW	N	N	2.10
5LR200.226	6.7	FK	R92	2	22.14	5.88	CH	N	N	2.80
5LR200.227	6.8	FK	R92	2	20.11	4.79	CH	N	N	0.90
5LR200.228	6.9	FK	R92	2	16.44	2.80	CH	N	N	0.30
5LR200.229	6.11	FK	R92	NA	16.71	1.72	CHAL	N	N	0.10
5LR200.230	6.12	FK	R92	2	12.96	5.95	CH	Y	N	0.30
5LR200.231	6.13	ANG	R92	2	12.54	6.12	CHAL	N	N	1.00
5LR200.232	6.14	ANG	R92	2	16.05	6.72	CHAL	N	N	1.50
5LR200.233	6.15	FK	R92	2	15.26	3.32	CH	N	N	0.50
5LR200.234	6.16	FK	R92	2	19.16	2.31	PW	N	N	0.50
5LR200.235	6.17	FK	R92	NA	14.11	2.92	CH	N	N	0.40
5LR200.236	6.18	FK	R92	NA	13.54	2.96	QTZ	N	NA	0.30
5LR200.237	6.19	FK	R92	NA	12.88	2.02	CH	N	N	0.01
5LR200.238	6.21	FK	R92	2	10.94	1.95	QTZ	N	NA	0.01
5LR200.239	6.22	FK	R92	NA	13.12	4.73	CH	N	N	0.01
5LR200.240	6.23	FK	R92	NA	14.02	2.28	PW	Y	N	0.30
5LR200.241	6.24	FK	R92	NA	8.69	1.26	CHAL	N	N	0.01
5LR200.242	6.25	FK	R92	2	10.58	2.77	PW	N	N	0.20
5LR200.243	6.26	FK	R92	NA	10.05	1.66	PW	N	N	0.10
5LR200.244	6.27	FK	R92	NA	8.59	2.04	PW	N	N	0.01
5LR200.245	6.28	FK	R92	NA	6.93	1.62	CH	N	N	0.01
5LR200.246	6.29	FK	R92	NA	12.71	2.15	CHAL	N	N	0.01
5LR200.247	6.31	FK	R92	2	9.33	1.61	CHAL	N	N	0.01
5LR200.248	6.32	FK	R92	NA	11.87	3.04	CHAL	N	Y	0.30
5LR200.249	6.33	FK	R92	2	11.59	2.24	PW	N	N	0.20
5LR200.250	6.34	FK	R92	NA	9.71	1.52	PW	N	N	0.01
5LR200.251	6.35	FK	R92	NA	8.37	1.26	PW	N	N	0.01

CMPA Curation Number	HFM Item #	Item	Grid	Level	Max Length (mm)	Max Thickness (mm)	Raw Mat	Cortex	Burning	Mass (g)
5LR200.252	6.36	FK	R92	NA	7.55	2.44	PW	N	N	0.01
5LR200.253	6.37	FK	R92	NA	8.29	1.14	CH	N	N	0.01
5LR200.254	7.1	FK	E22	4"	16.05	3.73	CH	N	Y	0.50
5LR200.255	7.2	FK	E22	NA	18.52	2.64	CH	N	Y	0.50
5LR200.256	7.3	FK	E22	NA	13.98	3.17	CH	N	Y	0.40
5LR200.257	7.4	FK	E22	4"	28.52	5.21	QTZ	N	NA	3.20
5LR200.258	7.5	FK	E22	.2	15.17	2.82	CHAL	N	N	0.40
5LR200.259	7.6	FK	E22	.2	16.97	2.93	CHAL	N	N	0.70
5LR200.260	7.7	FK	E22	2"	21.82	2.18	CHAL	N	Y	0.60
5LR200.261	7.8	FK	E22	NA	15.48	4.08	CH	N	Y	0.60
5LR200.262	7.9	FK	E22	NA	11.70	2.55	CH	N	Y	0.40
5LR200.263	7.11	FK	E22	NA	12.07	1.85	CHAL	N	N	0.20
5LR200.264	7.12	FK	E22	.2	14.26	5.11	CHAL	N	N	1.00
5LR200.265	7.13	FK	E22	NA	13.45	5.80	CHAL	N	Y	1.20
5LR200.266	7.14	FK	E22	NA	14.80	3.62	CH	N	Y	0.20
5LR200.267	7.15	FK	E22	NA	10.91	1.59	CH	N	Y	0.10
5LR200.268	7.16	FK	E22	4"	12.08	5.71	CHAL	N	Y	0.70
5LR200.269	7.17	FK	E22	NA	9.27	1.41	CHAL	N	N	0.10
5LR200.270	7.18	FK	E22	NA	10.17	2.81	CH	Y	N	0.20
5LR200.271	7.19	FK	E22	NA	8.61	4.68	CH	Y	N	0.20
5LR200.272	7.21	FK	E22	NA	8.61	1.75	CHAL	N	Y	0.10
5LR200.273	7.22	FK	E22	NA	4.97	1.48	CH	N	Y	0.01
5LR200.274	8.1	FK	O96	1	25.28	7.74	QTZ	N	NA	1.70
5LR200.275	8.2	FK	O96	2	25.42	4.05	CH	N	N	1.80
5LR200.276	8.3	FK	O96	2	24.82	4.66	QTZ	N	NA	0.90
5LR200.277	8.4	FK	O96	2	19.72	3.27	QTZ	N	NA	0.90
5LR200.278	8.5	FK	O96	1	16.01	3.53	QTZ	N	NA	0.90
5LR200.279	8.6	FK	O96	NA	15.79	2.73	QTZ	N	NA	0.40
5LR200.280	8.7	FK	O96	2	12.82	2.41	QTZ	N	NA	0.40
5LR200.281	8.8	FK	O96	2	23.80	3.68	QTZ	N	NA	0.90
5LR200.282	8.9	FK	O96	2	18.42	2.56	QTZ	N	NA	0.40
5LR200.283	8.11	FK	O96	2	15.51	2.04	QTZ	N	NA	0.40
5LR200.284	8.12	FK	O96	2	13.31	2.00	QTZ	N	NA	0.30
5LR200.285	8.13	FK	O96	S	19.30	4.20	QTZ	N	NA	0.60
5LR200.286	8.14	FK	O96	2	14.10	2.16	QTZ	N	NA	0.30
5LR200.287	8.15	FK	O96	2	16.13	2.73	QTZ	N	NA	0.50
5LR200.288	8.16	FK	O96	2	15.43	3.23	QTZ	N	NA	0.50
5LR200.289	8.17	FK	O96	2	15.16	2.31	QTZ	N	NA	0.30
5LR200.290	8.18	FK	O96	2	10.34	1.94	QTZ	N	NA	0.20
5LR200.291	8.19	FK	O96	2	12.68	2.19	QTZ	N	NA	0.20
5LR200.292	8.21	FK	O96	NA	12.08	1.94	QTZ	N	NA	0.10
5LR200.293	8.22	FK	O96	2	8.52	1.87	QTZ	N	NA	0.10
5LR200.294	8.23	FK	O96	NA	9.49	1.84	CH	N	N	0.10
5LR200.295	8.24	FK	O96	2	10.72	1.90	CHAL	N	N	0.20
5LR200.296	8.25	FK	O96	NA	8.26	1.11	QTZ	N	NA	0.10
5LR200.297	8.26	FK	O96	NA	9.43	1.62	QTZ	N	NA	0.01
5LR200.298	8.27	FK	O96	NA	9.57	2.80	QTZ	N	NA	0.10
5LR200.299	8.28	FK	O96	NA	14.36	2.35	QTZ	N	NA	0.20
5LR200.300	8.29	FK	O96	NA	11.26	1.98	QTZ	N	NA	0.30

CMPA Curation Number	HFM Item #	Item	Grid	Level	Max Length (mm)	Max Thickness (mm)	Raw Mat	Cortex	Burning	Mass (g)
5LR200.301	8.31	FK	O96	2	10.03	1.41	CHAL	N	N	0.01
5LR200.302	8.32	FK	O96	2	11.15	1.81	QTZ	N	NA	0.20
5LR200.303	8.33	FK	O96	2	10.27	2.09	QTZ	N	NA	0.20
5LR200.304	8.34	FK	O96	2	14.62	2.14	QTZ	N	NA	0.30
5LR200.305	8.35	FK	O96	2	13.78	2.48	QTZ	N	NA	0.20
5LR200.306	8.36	FK	O96	NA	7.95	1.12	QTZ	N	NA	0.01
5LR200.307	8.37	ANG	O96	NA	9.27	3.79	CH	N	Y	0.30
5LR200.308	8.38	FK	O96	NA	9.94	2.05	QTZ	N	NA	0.10
5LR200.309	8.39	FK	O96	NA	8.37	1.00	QTZ	N	NA	0.01
5LR200.310	8.41	FK	O96	NA	9.26	2.15	QTZ	N	NA	0.10
5LR200.311	8.42	FK	O96	NA	6.36	1.46	QTZ	N	NA	0.01
5LR200.312	8.43	FK	O96	NA	8.84	1.26	CH	N	N	0.01
5LR200.313	8.44	FK	O96	NA	7.58	1.48	CH	N	N	0.01
5LR200.314	8.45	FK	O96	NA	8.09	2.02	QTZ	N	NA	0.10
5LR200.315	8.46	FK	O96	NA	6.19	1.09	CH	N	N	0.01
5LR200.316	8.47	FK	O96	NA	5.78	0.98	CH	N	N	0.01
5LR200.317	8.48	FK	O96	NA	8.58	1.18	CH	N	N	0.01
5LR200.318	8.49	FK	O96	NA	7.33	1.46	CH	N	N	0.01
5LR200.319	8.51	FK	O96	NA	7.81	1.37	QTZ	N	NA	0.01
5LR200.320	9.1	FK	D6	NA	16.37	3.50	QTZ	N	NA	0.90
5LR200.321	9.2	FK	D6	NA	22.20	2.90	CHAL	N	N	0.70
5LR200.322	9.3	FK	D6	2	17.06	3.86	QTZ	N	NA	1.10
5LR200.323	9.4	FK	D6	NA	19.55	2.97	CHAL	Y	N	1.00
5LR200.324	9.5	FK	D6	1	15.65	2.73	CH	N	N	0.80
5LR200.325	9.6	FK	D6	1	21.52	2.84	CHAL	N	N	0.80
5LR200.326	9.7	FK	D6	NA	14.06	2.62	CHAL	N	N	0.30
5LR200.327	9.8	FK	D6	NA	12.87	2.08	CHAL	N	N	0.30
5LR200.328	9.9	FK	D6	NA	15.15	3.17	CHAL	N	N	0.30
5LR200.329	9.11	FK	D6	NA	13.14	4.13	QTZ	N	NA	0.30
5LR200.330	9.12	FK	D6	NA	9.52	2.55	CHAL	N	N	0.10
5LR200.331	9.13	FK	D6	NA	8.52	2.13	CHAL	N	N	0.10
5LR200.332	9.14	FK	D6	NA	10.77	0.98	CHAL	N	N	0.01
5LR200.333	9.15	FK	D6	NA	8.91	0.68	CHAL	N	N	0.01
5LR200.334	9.16	FK	D6	NA	6.60	1.16	CH	N	N	0.01
5LR200.335	9.17	FK	D6	NA	6.86	1.78	CH	N	N	0.01
5LR200.336	9.18	FK	D6	NA	9.19	1.31	CHAL	N	N	0.01
5LR200.337	9.19	FK	D6	NA	5.38	0.95	CHAL	N	N	0.01
5LR200.338	9.21	FK	D6	1	10.31	1.66	CHAL	N	N	0.10
5LR200.339	10.1	FK	D4	1	29.83	6.42	QTZ	N	NA	3.70
5LR200.340	10.2	FK	D4	2	19.76	5.20	CH	N	N	1.10
5LR200.341	10.3	FK	D4	S	22.28	3.16	QTZ	N	NA	1.40
5LR200.342	10.4	FK	D4	2	50.59	10.71	CH	N	Y	14.00
5LR200.343	10.5	FK	D4	4	17.54	3.72	QTZ	N	NA	1.00
5LR200.344	10.6	FK	D4	1	18.46	4.74	QTZ	N	NA	1.20
5LR200.345	11.1	FK	C6	S	31.82	4.46	CHAL	N	N	2.90
5LR200.346	11.2	FK	C6	S	24.81	4.37	CHAL	N	N	2.00
5LR200.347	11.3	FK	C6	S	16.47	6.09	CH	N	N	1.60
5LR200.348	11.4	FK	C6	1	16.74	3.96	CH	N	N	1.10
5LR200.349	11.5	FK	C6	NA	21.67	5.22	CH	N	N	2.50

CMPA Curation Number	HFM Item #	Item	Grid	Level	Max Length (mm)	Max Thickness (mm)	Raw Mat	Cortex	Burning	Mass (g)
5LR200.350	11.6	FK	C6	NA	26.77	8.32	CH	N	N	2.30
5LR200.351	11.7	FK	C6	NA	31.71	5.90	CH	N	N	3.70
5LR200.352	11.8	FK	D6	NA	32.65	5.93	CHAL	N	N	4.10
5LR200.353	11.9	FK	C6	NA	22.66	3.64	CHAL	N	N	1.50
5LR200.354	11.11	FK	C6	1	16.52	2.64	CHAL	N	N	0.30
5LR200.355	11.12	FK	C6	NA	24.79	4.19	CH	Y	N	1.20
5LR200.356	11.13	FK	C6	2"	19.56	5.72	CHAL	Y	N	1.30
5LR200.357	11.14	FK	C6	NA	19.30	3.37	CHAL	Y	N	0.80
5LR200.358	11.15	FK	C6	NA	22.73	7.80	CH	N	Y	2.60
5LR200.359	11.16	FK	C6	NA	17.06	2.51	CHAL	N	N	0.40
5LR200.360	11.17	FK	C18	NA	21.42	2.37	PW	N	N	0.70
5LR200.361	11.18	FK	C6	1	22.11	4.05	CH	N	N	0.80
5LR200.362	11.19	FK	C6	S	15.99	4.62	CH	N	N	1.00
5LR200.363	11.21	FK	C6	NA	16.54	4.71	CHAL	N	N	0.80
5LR200.364	11.22	FK	C6	1	20.74	3.34	CHAL	N	N	0.90
5LR200.365	11.23	FK	C6	NA	21.63	6.43	CH	N	Y	1.80
5LR200.366	11.24	FK	C6	NA	14.74	2.52	CHAL	N	N	0.50
5LR200.367	11.25	FK	C6	NA	15.52	3.31	CHAL	N	N	0.70
5LR200.368	11.26	FK	C6	1	17.37	2.42	CH	N	N	0.60
5LR200.369	11.27	FK	C6	NA	22.31	5.51	CHAL	Y	N	1.20
5LR200.370	11.28	FK	D6/D7	4-6'	23.25	2.86	CHAL	N	N	0.80
5LR200.371	11.29	FK	C6	1	20.42	2.65	CH	N	N	0.60
5LR200.372	11.31	FK	C6	NA	23.66	6.18	CH	N	N	1.40
5LR200.373	11.32	FK	C6	NA	14.54	3.85	CH	N	N	0.60
5LR200.374	11.33	FK	C6	NA	13.87	2.52	CHAL	N	N	0.50
5LR200.375	11.34	FK	C6	NA	12.57	3.43	CHAL	Y	N	0.50
5LR200.376	11.35	FK	C6	NA	11.12	1.66	CHAL	N	N	0.20
5LR200.377	11.36	FK	C6	NA	21.47	2.41	CHAL	N	N	1.10
5LR200.378	11.37	FK	C6	NA	16.57	1.92	CHAL	N	N	0.30
5LR200.379	11.38	FK	C6	S	13.50	2.47	CH	N	N	0.20
5LR200.380	11.39	FK	C6	NA	14.88	2.13	CHAL	N	N	0.40
5LR200.381	11.41	FK	C6	1	12.44	2.86	CH	N	N	0.30
5LR200.382	11.42	FK	C6	NA	18.59	1.82	CHAL	Y	N	0.40
5LR200.383	11.43	ANG	C6	NA	13.87	4.13	CHAL	N	N	0.50
5LR200.384	11.44	FK	C6	1	17.38	3.99	CH	N	Y	0.70
5LR200.385	11.45	FK	C6	1	19.14	3.81	CH	N	N	0.70
5LR200.386	11.46	FK	C6	NA	12.99	2.63	CHAL	N	N	0.20
5LR200.387	11.47	FK	C6	NA	12.72	3.04	CHAL	N	N	0.20
5LR200.388	11.48	FK	C6	1	14.25	2.43	CH	N	N	0.20
5LR200.389	11.49	FK	C6	NA	17.72	2.86	CH	N	N	0.40
5LR200.390	11.51	FK	C6	NA	11.51	1.77	CHAL	N	N	0.10
5LR200.391	11.52	FK	C6	1	13.00	1.99	QTZ	N	NA	0.30
5LR200.392	11.53	FK	C6	1	13.91	4.00	CH	N	N	0.50
5LR200.393	11.54	FK	C6	NA	15.05	2.10	CHAL	N	N	0.20
5LR200.394	11.55	FK	C6	NA	14.06	1.78	CH	N	N	0.30
5LR200.395	11.56	FK	C6	1	15.15	2.51	CH	N	N	0.40
5LR200.396	11.57	FK	C6	NA	15.09	2.40	CH	N	N	0.30
5LR200.397	11.58	FK	C6	NA	11.17	3.53	CH	N	N	0.40
5LR200.398	11.59	FK	C6	1	11.61	2.15	QTZ	N	NA	0.20

CMPA Curation Number	HFM Item #	Item	Grid	Level	Max Length (mm)	Max Thickness (mm)	Raw Mat	Cortex	Burning	Mass (g)
5LR200.399	11.61	FK	C6	NA	12.80	1.92	CHAL	N	N	0.20
5LR200.400	11.62	FK	C6	NA	15.18	2.58	CHAL	N	N	0.30
5LR200.401	11.63	FK	C6	1	14.57	1.99	QTZ	N	NA	0.20
5LR200.402	11.64	FK	C6	1	11.07	2.22	CHAL	N	N	0.20
5LR200.403	11.65	FK	C6	NA	21.87	2.65	CHAL	N	N	0.50
5LR200.404	11.66	FK	C6	NA	8.54	2.55	CHAL	N	N	0.20
5LR200.405	11.67	FK	C6	1	13.66	2.23	CHAL	N	N	0.30
5LR200.406	11.68	FK	C6	S	15.01	2.73	CH	N	N	0.30
5LR200.407	11.69	FK	C6	NA	15.79	2.87	CH	N	N	0.20
5LR200.408	11.71	FK	C6	NA	16.15	1.58	CHAL	N	N	0.10
5LR200.409	11.72	FK	C6	NA	10.11	3.41	CHAL	N	N	0.40
5LR200.410	11.73	FK	C6	NA	13.41	3.65	CHAL	Y	N	0.20
5LR200.411	11.74	FK	C6	NA	17.09	3.17	CHAL	N	N	0.40
5LR200.412	11.75	FK	C6	NA	12.71	2.02	CHAL	N	N	0.10
5LR200.413	11.76	FK	C6	NA	12.77	4.75	CHAL	Y	N	0.50
5LR200.414	11.77	FK	C6	NA	13.85	2.95	CHAL	N	N	0.30
5LR200.415	11.78	FK	C6	NA	13.98	2.23	CHAL	N	N	0.20
5LR200.416	11.79	FK	C6	NA	12.74	1.73	CHAL	N	N	0.20
5LR200.417	11.81	FK	C6	NA	14.93	3.08	CHAL	N	N	0.20
5LR200.418	11.82	FK	C6	NA	13.26	3.99	CHAL	N	Y	0.30
5LR200.419	11.83	FK	C6	NA	11.08	4.40	CHAL	N	N	0.20
5LR200.420	11.84	FK	C6	NA	11.50	2.51	CHAL	N	N	0.20
5LR200.421	11.85	FK	C6	NA	11.91	1.59	CH	N	N	0.01
5LR200.422	11.86	FK	C6	NA	10.34	1.68	CH	Y	N	0.10
5LR200.423	11.87	FK	C6	NA	13.63	2.65	CH	N	N	0.20
5LR200.424	11.88	FK	C6	NA	12.67	3.01	CHAL	N	N	0.30
5LR200.425	11.89	FK	C6	NA	12.43	1.31	CHAL	N	N	0.10
5LR200.426	11.91	FK	C6	NA	10.06	1.41	CHAL	N	N	0.10
5LR200.427	11.92	FK	C6	NA	14.84	1.46	CHAL	N	N	0.20
5LR200.428	11.93	ANG	C6	NA	18.90	2.36	CHAL	N	N	0.20
5LR200.429	11.94	FK	C6	NA	10.04	1.52	CHAL	N	N	0.10
5LR200.430	11.95	FK	C6	NA	10.29	1.46	CHAL	N	N	0.10
5LR200.431	11.96	FK	C6	NA	8.83	0.69	CHAL	N	N	0.01
5LR200.432	11.97	FK	C6	NA	10.92	1.35	CHAL	N	N	0.01
5LR200.433	11.98	FK	C6	NA	17.08	2.66	CHAL	N	N	0.50
5LR200.434	11.99	FK	C6	NA	11.09	1.74	CHAL	N	N	0.10
5LR200.435	11.101	FK	C6	1	14.26	2.81	CHAL	N	N	0.01
5LR200.436	11.102	FK	C6	NA	14.82	3.34	CHAL	N	N	0.20
5LR200.437	11.103	FK	C6	NA	9.34	1.88	CHAL	N	N	0.10
5LR200.438	11.104	FK	C6	NA	9.36	2.32	CH	N	N	0.10
5LR200.439	11.105	FK	C6	NA	14.75	1.67	CHAL	N	N	0.20
5LR200.440	11.106	FK	C6	1	12.88	4.77	CHAL	N	N	0.20
5LR200.441	11.107	FK	C6	NA	6.49	1.32	CHAL	N	N	0.01
5LR200.442	11.108	FK	D6	NA	14.44	2.97	CHAL	N	N	0.20
5LR200.443	11.109	FK	C6	NA	18.83	2.23	CHAL	Y	N	0.20
5LR200.444	11.111	FK	C6	NA	10.91	1.58	CHAL	N	N	0.10
5LR200.445	11.112	FK	C6	1	9.22	1.85	CHAL	N	N	0.01
5LR200.446	11.113	FK	C6	NA	10.19	0.92	CHAL	N	N	0.01
5LR200.447	11.114	FK	C6	NA	9.71	2.56	CHAL	N	N	0.10

CMPA Curation Number	HFM Item #	Item	Grid	Level	Max Length (mm)	Max Thickness (mm)	Raw Mat	Cortex	Burning	Mass (g)
5LR200.448	11.115	FK	C6	S	11.56	2.24	CH	N	N	0.10
5LR200.449	11.116	FK	C6	I	10.40	1.91	CHAL	N	N	0.10
5LR200.450	11.117	FK	C6	NA	12.14	2.76	PW	N	N	0.20
5LR200.451	11.118	FK	C6	NA	14.24	2.56	CH	N	Y	0.20
5LR200.452	11.119	FK	C6	NA	9.01	2.69	CH	N	N	0.10
5LR200.453	11.121	FK	C6	NA	9.50	2.13	CHAL	N	N	0.20
5LR200.454	11.122	FK	C6	NA	10.36	3.45	CH	Y	N	0.30
5LR200.455	11.123	FK	C6	NA	6.52	0.91	CHAL	N	N	0.01
5LR200.456	11.124	FK	C6	NA	8.41	1.41	CHAL	N	N	0.01
5LR200.457	11.125	FK	C6	NA	5.73	1.17	CHAL	N	N	0.01
5LR200.458	11.126	FK	C6	NA	4.94	0.41	CHAL	N	N	0.01
5LR200.459	11.127	FK	C6	NA	5.60	0.86	CHAL	N	N	0.01
5LR200.460	11.128	FK	C6	NA	8.01	1.26	CHAL	N	N	0.01
5LR200.461	11.129	FK	C6	NA	6.02	0.65	CHAL	N	N	0.01
5LR200.462	11.131	FK	C6	NA	11.82	0.46	CHAL	N	N	0.01
5LR200.463	11.132	FK	C6	NA	5.61	0.57	CHAL	N	N	0.01
5LR200.464	11.133	FK	C6	NA	8.63	0.97	CHAL	N	N	0.01
5LR200.465	11.134	FK	C6	NA	6.82	1.16	CHAL	N	N	0.01
5LR200.466	11.135	FK	C6	NA	6.15	1.42	CHAL	N	N	0.01
5LR200.467	11.136	FK	C6	I	9.99	1.82	CH	N	Y	0.10
5LR200.468	11.137	FK	C6	NA	6.83	0.42	CHAL	N	N	0.01
5LR200.469	11.138	FK	C6	NA	6.68	1.16	CHAL	N	N	0.01
5LR200.470	11.139	FK	C6	NA	8.29	1.15	CHAL	N	N	0.01
5LR200.471	11.141	FK	C6	NA	8.32	1.86	QTZ	N	N	0.01
5LR200.472	11.142	FK	C6	NA	6.26	1.48	CHAL	N	N	0.01
5LR200.473	11.143	FK	C6	NA	12.50	0.97	CHAL	N	N	0.01
5LR200.474	11.144	FK	C6	NA	11.41	0.64	CHAL	N	N	0.01
5LR200.475	11.145	FK	C6	I	9.60	1.95	QTZ	N	N	0.20
5LR200.476	11.146	FK	C6	NA	9.21	1.04	CHAL	N	N	0.01
5LR200.477	11.147	FK	C6	NA	12.05	1.22	CH	N	N	0.01
5LR200.478	11.148	FK	C6	NA	10.02	1.14	CHAL	N	N	0.01
5LR200.479	11.149	FK	C6	NA	10.40	2.45	CHAL	N	N	0.20
5LR200.480	11.151	FK	C6	NA	9.83	1.64	CHAL	N	N	0.01
5LR200.481	11.152	FK	C6	NA	9.17	1.12	CH	N	N	0.01
5LR200.482	11.153	FK	C6	NA	5.09	1.25	CH	N	N	0.01
5LR200.483	11.154	FK	C6	NA	4.71	0.65	CHAL	N	N	0.01
5LR200.484	11.155	FK	C6	I	8.23	1.56	CHAL	N	N	0.01
5LR200.485	11.156	FK	C6	NA	6.12	1.36	CHAL	N	N	0.01
5LR200.486	11.157	FK	C6	NA	4.47	1.04	CHAL	Y	N	0.01
5LR200.487	11.158	FK	C6	NA	7.18	0.76	CHAL	N	N	0.01
5LR200.488	11.159	FK	C6	NA	11.38	3.54	CHAL	N	N	0.20
5LR200.489	11.161	FK	C6	NA	13.04	1.57	CHAL	N	Y	0.01
5LR200.490	11.162	FK	C6	NA	10.09	2.72	CHAL	N	Y	0.20
5LR200.491	11.163	FK	C6	NA	9.86	1.23	CHAL	N	N	0.01
5LR200.492	11.164	FK	C6	NA	8.65	1.71	CHAL	N	N	0.01
5LR200.493	11.165	FK	C6	NA	10.88	1.21	CHAL	N	N	0.01
5LR200.494	11.166	FK	C6	NA	7.81	0.42	CHAL	N	N	0.01
5LR200.495	11.167	FK	C6	NA	7.32	1.41	CHAL	N	N	0.01
5LR200.496	11.168	FK	C6	NA	8.37	1.54	CHAL	N	N	0.01

CPMA Curation Number	HFM Item #	Item	Grid	Level	Max Length (mm)	Max Thickness (mm)	Raw Mat	Cortex	Burning	Mass (g)
5LR200.497	11.169	FK	C6	NA	9.04	1.32	CHAL	N	N	0.01
5LR200.498	11.171	FK	C6	NA	7.14	1.32	CHAL	N	N	0.01
5LR200.499	11.172	FK	C6	NA	10.47	2.40	CHAL	N	N	0.10
5LR200.500	11.173	FK	C6	NA	9.71	1.15	CHAL	N	N	0.01
5LR200.501	11.174	FK	C6	NA	14.02	1.68	CHAL	N	N	0.10
5LR200.502	11.175	FK	C6	NA	11.04	2.04	CH	N	Y	0.10
5LR200.503	11.176	FK	C6	NA	7.25	1.39	CHAL	N	N	0.01
5LR200.504	11.177	FK	C6	NA	11.96	2.50	CH	Y	N	0.20
5LR200.505	11.178	FK	C6	NA	10.86	1.58	CHAL	N	N	0.01
5LR200.506	11.179	FK	C6	1	8.59	1.43	CHAL	N	N	0.01
5LR200.507	11.181	ANG	C6	NA	11.10	5.22	CHAL	N	Y	0.20
5LR200.508	11.182	FK	C6	NA	10.28	1.69	CHAL	N	N	0.01
5LR200.509	11.183	FK	C6	NA	10.38	2.22	CHAL	N	Y	0.10
5LR200.510	11.184	FK	C6	NA	7.48	1.71	CHAL	N	Y	0.01
5LR200.511	11.185	FK	C6	NA	8.66	2.47	CHAL	Y	N	0.01
5LR200.512	11.186	FK	C6	NA	8.24	1.63	CHAL	N	N	0.01
5LR200.513	11.187	FK	C6	NA	9.37	1.24	CHAL	N	N	0.01
5LR200.514	11.188	FK	C6	NA	8.44	1.43	QTZ	N	N	0.01
5LR200.515	11.189	FK	C6	NA	7.16	0.99	CHAL	N	N	0.01
5LR200.516	11.191	FK	C6	NA	7.89	0.95	CH	N	N	0.01
5LR200.517	11.192	FK	C6	NA	7.87	1.53	CHAL	N	N	0.01
5LR200.518	11.193	FK	C6	NA	14.28	0.68	CHAL	N	N	0.01
5LR200.519	11.194	FK	C6	NA	7.86	0.81	CHAL	N	N	0.01
5LR200.520	11.195	FK	C6	NA	7.41	1.12	CHAL	N	N	0.01
5LR200.521	11.196	FK	C6	NA	8.14	1.07	CHAL	N	N	0.01
5LR200.522	11.197	FK	C6	NA	6.52	1.67	CHAL	N	N	0.01
5LR200.523	11.198	FK	C6	NA	7.96	0.89	CHAL	N	N	0.01
5LR200.524	11.199	ANG	C6	NA	7.09	3.03	CHAL	N	N	0.01
5LR200.525	11.201	FK	C6	NA	7.69	0.75	CHAL	N	N	0.01
5LR200.526	11.202	FK	C6	NA	9.44	1.16	CHAL	N	N	0.01
5LR200.527	11.203	FK	C6	NA	10.57	1.55	CHAL	Y	N	0.01
5LR200.528	11.204	FK	C6	NA	5.97	1.97	CHAL	N	N	0.01
5LR200.529	11.205	FK	C6	NA	9.17	1.97	CHAL	N	N	0.01
5LR200.530	11.206	FK	C6	NA	5.29	0.79	CHAL	N	N	0.01
5LR200.531	11.207	FK	C6	NA	4.33	0.47	CHAL	N	N	0.01
5LR200.532	11.208	FK	C6	NA	5.92	0.89	CHAL	N	N	0.01
5LR200.533	11.209	FK	C6	NA	8.81	0.81	CHAL	N	N	0.01
5LR200.534	11.211	FK	C6	NA	7.86	0.40	CHAL	N	N	0.01
5LR200.535	11.212	FK	C6	NA	5.86	1.37	CHAL	N	N	0.01
5LR200.536	11.213	FK	C6	NA	4.58	1.01	CHAL	N	N	0.01
5LR200.537	11.214	FK	C6	NA	6.04	1.69	CH	N	N	0.01
5LR200.538	11.215	FK	C6	NA	7.49	1.84	CHAL	N	N	0.01
5LR200.539	11.216	FK	C6	NA	4.86	0.32	CHAL	N	N	0.01
5LR200.540	11.217	FK	C6	NA	7.71	1.56	CHAL	N	N	0.01
5LR200.541	11.218	FK	C6	NA	5.18	0.81	QTZ	N	NA	0.01
5LR200.542	11.219	FK	C6	NA	4.72	1.03	CHAL	N	N	0.01
5LR200.543	11.221	FK	C6	NA	6.39	0.88	CHAL	N	N	0.01
5LR200.544	11.222	FK	C6	NA	5.27	1.08	CHAL	N	N	0.01
5LR200.545	11.223	FK	C6	NA	5.00	0.41	CHAL	N	N	0.01

CMPA Curation Number	HFM Item #	Item	Grid	Level	Max Length (mm)	Max Thickness (mm)	Raw Mat	Cortex	Burning	Mass (g)
5LR200.546	12.1	FK	D3	NA	14.69	3.03	CHAL	Y	N	0.50
5LR200.547	12.2	FK	D3	2	19.13	4.36	QTZ	N	NA	0.60
5LR200.548	12.3	FK	D3	2	18.05	4.02	QTZ	N	NA	1.10
5LR200.549	12.4	FK	D2	1	20.07	3.18	QTZ	N	NA	1.00
5LR200.550	12.5	FK	D3	1	17.63	4.61	QTZ	N	NA	0.90
5LR200.551	12.6	FK	D2	1	19.99	7.79	QTZ	Y	NA	1.40
5LR200.552	12.7	FK	D2	1	16.09	2.84	CH	N	N	0.70
5LR200.553	12.8	FK	D3	2	23.98	3.12	QTZ	N	NA	1.10
5LR200.554	12.9	FK	D2	1	15.49	3.28	QTZ	N	NA	0.50
5LR200.555	12.11	FK	D2	1	13.09	3.71	QTZ	N	NA	0.50
5LR200.556	12.12	FK	D2	1	11.81	2.49	QTZ	N	NA	0.30
5LR200.557	12.13	FK	D2	1	18.96	6.09	QTZ	N	NA	1.00
5LR200.558	12.14	FK	D2	1	20.82	2.51	QTZ	N	NA	0.90
5LR200.559	12.15	FK	D2	1	14.06	2.94	QTZ	N	NA	0.40
5LR200.560	12.16	FK	D2	3	9.94	1.75	QTZ	N	NA	0.10
5LR200.561	12.17	FK	D3	2	14.58	3.22	CHAL	Y	N	0.50
5LR200.562	12.18	FK	D3	2	12.10	2.51	QTZ	N	NA	0.30
5LR200.563	12.19	FK	D2	NA	11.07	1.78	QTZ	N	NA	0.20
5LR200.564	12.21	FK	D2	1	13.88	1.69	QTZ	N	NA	0.30
5LR200.565	12.22	FK	D2	1	12.18	2.79	QTZ	N	NA	0.30
5LR200.566	12.23	FK	D2	NA	16.66	3.66	QTZ	N	NA	1.20
5LR200.567	12.24	FK	D2	NA	14.86	4.65	QTZ	N	NA	0.60
5LR200.568	12.25	FK	D2	1	11.82	2.76	QTZ	N	NA	0.20
5LR200.569	12.26	FK	D2	1	13.29	2.95	QTZ	N	NA	0.20
5LR200.570	12.27	FK	D2	1	9.83	1.49	QTZ	N	NA	0.10
5LR200.571	12.28	FK	D2	1	14.64	3.29	QTZ	N	NA	0.40
5LR200.572	12.29	FK	D2	NA	10.57	2.20	CH	N	N	0.20
5LR200.573	12.31	FK	D2	1	8.40	1.45	QTZ	N	NA	0.01
5LR200.574	12.32	FK	D2	1	14.29	2.66	QTZ	N	NA	0.40
5LR200.575	12.33	FK	D2	1	9.11	1.89	QTZ	N	NA	0.10
5LR200.576	12.34	FK	D2	1	10.58	1.85	QTZ	N	NA	0.20
5LR200.577	12.35	FK	D2	3	13.47	2.65	QTZ	N	NA	0.30
5LR200.578	12.36	FK	D2	NA	10.09	2.44	QTZ	N	NA	0.20
5LR200.579	12.37	FK	D2	NA	9.15	2.03	QTZ	N	NA	0.20
5LR200.580	12.38	FK	D2	NA	8.03	1.64	CH	N	N	0.10
5LR200.581	12.39	FK	D2	1	12.98	3.47	QTZ	N	NA	0.30
5LR200.582	12.41	FK	D2	1	10.46	1.74	CHAL	N	N	0.10
5LR200.583	12.42	FK	D2	1	10.60	1.42	QTZ	N	NA	0.10
5LR200.584	12.43	FK	D2	1	10.62	2.42	CH	N	N	0.20
5LR200.585	12.44	FK	D2	3	9.17	1.86	QTZ	N	NA	0.10
5LR200.586	12.45	FK	D2	1	11.57	1.92	CH	N	N	0.01
5LR200.587	12.46	FK	D2	1	9.68	1.27	CH	N	N	0.01
5LR200.588	12.47	FK	D2	1	17.46	2.18	QTZ	N	NA	0.40
5LR200.589	12.48	FK	D2	1	9.27	1.70	QTZ	N	NA	0.10
5LR200.590	12.49	FK	D2	1	9.73	2.17	QTZ	N	NA	0.01
5LR200.591	12.51	FK	D2	NA	9.76	2.31	QTZ	N	NA	0.01
5LR200.592	12.52	FK	D2	1	9.91	1.71	CH	N	N	0.01
5LR200.593	12.53	FK	D2	1	7.75	1.78	QTZ	N	NA	0.01
5LR200.594	12.54	FK	D2	NA	7.86	2.01	QTZ	N	NA	0.10

CMPA Curation Number	HFM Item #	Item	Grid	Level	Max Length (mm)	Max Thickness (mm)	Raw Mat	Cortex	Burning	Mass (g)
5LR200.595	12.55	FK	D2	1	11.39	2.09	QTZ	N	NA	0.01
5LR200.596	12.56	FK	D2	1	8.99	1.63	QTZ	N	NA	0.10
5LR200.597	12.57	FK	D2	NA	6.59	1.13	QTZ	N	NA	0.01
5LR200.598	12.58	FK	D2	NA	7.45	0.73	CHAL	N	N	0.01
5LR200.599	12.59	FK	D3	2	21.17	4.95	QTZ	N	NA	0.80
5LR200.600	12.61	FK	D3	NA	14.44	2.78	CH	N	N	0.40
5LR200.601	12.62	FK	D3	2	11.67	2.98	QTZ	N	NA	0.20
5LR200.602	12.63	FK	D3	2	14.86	2.66	QTZ	N	NA	0.30
5LR200.603	12.64	FK	D3	NA	11.28	1.54	CHAL	N	N	0.10
5LR200.604	12.65	FK	D3	2	9.80	1.94	QTZ	N	NA	0.10
5LR200.605	12.66	FK	D3	NA	8.64	1.20	CH	N	N	0.01
5LR200.606	12.67	FK	D3	2	17.63	2.80	QTZ	N	NA	0.40
5LR200.607	12.68	FK	D3	1	27.85	9.05	QTZ	N	NA	4.40
5LR200.608	12.69	FK	D3	6"	17.47	3.01	QTZ	N	NA	0.50
5LR200.609	12.71	FK	D3	NA	15.25	2.63	QTZ	N	NA	0.60
5LR200.610	12.72	FK	D3	1	23.25	5.88	QTZ	N	NA	2.20
5LR200.611	12.73	FK	D3	NA	12.32	3.21	QTZ	N	NA	0.30
5LR200.612	13.1	FK	A5	1	19.43	3.87	QTZ	N	NA	0.70
5LR200.613	13.2	FK	A5	1	15.66	3.89	QTZ	N	NA	1.00
5LR200.614	13.3	FK	A5	1	22.95	6.14	QTZ	N	NA	2.10
5LR200.615	13.4	FK	A5	1	22.50	4.82	QTZ	N	NA	1.60
5LR200.616	13.5	FK	A5	1	33.21	9.58	QTZ	N	NA	6.30
5LR200.617	13.6	FK	A5	1	36.83	7.00	QTZ	N	NA	2.60
5LR200.618	13.7	FK	A5	1	18.45	3.27	QTZ	N	NA	0.90
5LR200.619	13.8	FK	A5	S	20.34	4.32	QTZ	N	NA	1.40
5LR200.620	13.9	FK	A5	1	14.14	5.72	CH	N	N	1.10
5LR200.621	13.11	FK	A5	1	18.75	4.96	QTZ	N	NA	0.80
5LR200.622	13.12	FK	A5	1	13.38	2.48	QTZ	N	NA	0.20
5LR200.623	13.13	FK	A5	S	17.14	2.49	QTZ	N	NA	0.60
5LR200.624	13.14	FK	A5	S	22.67	4.02	CH	N	N	1.80
5LR200.625	13.15	FK	A5	1	31.58	4.85	QTZ	N	NA	1.90
5LR200.626	13.16	FK	A5	1	11.04	2.52	CH	N	N	0.40
5LR200.627	13.17	FK	A5	1	16.44	4.08	CHAL	N	Y	0.90
5LR200.628	13.18	FK	A5	1	14.56	2.38	QTZ	N	NA	0.50
5LR200.629	13.19	FK	A5	S	37.87	8.99	QTZ	N	NA	4.40
5LR200.630	13.21	FK	A5	1	17.99	4.59	QTZ	N	NA	0.70
5LR200.631	13.22	FK	A5	1	23.24	4.05	QTZ	N	NA	1.00
5LR200.632	13.23	FK	A5	1	23.72	5.89	QTZ	N	NA	1.70
5LR200.633	13.24	FK	A5	1	15.32	5.14	QTZ	N	NA	1.20
5LR200.634	13.25	FK	A5	1	12.60	2.40	QTZ	N	NA	0.20
5LR200.635	13.26	FK	A5	1	10.20	2.01	CHAL	N	Y	0.10
5LR200.636	13.27	FK	A5	1	16.54	3.79	QTZ	N	NA	0.60
5LR200.637	13.28	FK	A5	1	21.40	3.52	CH	N	Y	1.10
5LR200.638	13.29	FK	A5	1	15.74	2.54	QTZ	N	NA	0.40
5LR200.639	13.31	FK	A5	1	10.14	1.70	QTZ	N	NA	0.01
5LR200.640	13.32	FK	A5	1	16.16	4.33	CH	N	N	0.50
5LR200.641	13.33	FK	A5	1	12.09	2.25	CH	Y	N	0.20
5LR200.642	13.34	FK	A5	1	5.19	1.79	QTZ	N	NA	0.01
5LR200.643	13.35	FK	A5	1	11.80	2.14	QTZ	N	NA	0.20

CMPA Curation Number	HFM Item #	Item	Grid	Level	Max Length (mm)	Max Thickness (mm)	Raw Mat	Cortex	Burning	Mass (g)
5LR200.644	13.36	FK	A5	1	12.62	2.39	QTZ	N	NA	0.30
5LR200.645	13.37	FK	A5	1	11.86	2.13	CHAL	N	N	0.20
5LR200.646	13.38	FK	A5	1	14.63	2.92	CH	N	N	0.40
5LR200.647	13.39	FK	A5	1	13.14	3.18	QTZ	N	NA	0.40
5LR200.648	13.41	FK	A5	1	12.42	2.09	CH	Y	N	0.30
5LR200.649	13.42	FK	A5	1	11.81	3.67	QTZ	N	NA	0.20
5LR200.650	13.43	FK	A5	1	9.86	0.97	QTZ	N	NA	0.01
5LR200.651	13.44	FK	A5	1	11.52	1.90	CH	N	N	0.10
5LR200.652	13.45	FK	A5	1	21.54	0.92	CHAL	N	Y	0.10
5LR200.653	13.46	FK	A5	1	11.44	1.00	CHAL	N	N	0.10
5LR200.654	13.47	FK	A5	1	9.91	1.58	QTZ	N	NA	0.10
5LR200.655	13.48	FK	A5	1	8.62	1.96	QTZ	N	NA	0.01
5LR200.656	14.1	FK	C5	NA	14.43	3.67	QTZ	N	NA	0.60
5LR200.657	14.2	ANG	C5	1	25.35	8.41	QTZ	N	NA	3.20
5LR200.658	14.3	FK	C5	NA	26.80	3.96	QTZ	N	NA	2.60
5LR200.659	14.4	FK	C5	1	31.31	2.87	CH	N	N	1.00
5LR200.660	14.5	FK	C5	1	18.80	4.66	QTZ	Y	NA	1.00
5LR200.661	14.6	FK	C5	1	12.60	4.08	QTZ	N	NA	0.40
5LR200.662	14.7	FK	C5	2	13.64	2.08	CH	N	NA	0.20
5LR200.663	14.8	FK	C5	S	14.01	2.17	CH	N	N	0.20
5LR200.664	14.9	FK	C5	S	10.66	2.18	QTZ	N	NA	0.20
5LR200.665	14.11	FK	C5	NA	13.91	2.31	QTZ	N	NA	0.30
5LR200.666	14.12	FK	C5	1	12.52	1.91	QTZ	N	NA	0.20
5LR200.667	14.13	FK	C5	1	12.46	2.72	QTZ	N	NA	0.20
5LR200.668	15.1	FK	C23	1	19.90	5.79	CH	N	Y	1.40
5LR200.669	15.2	FK	C23	3	17.79	2.93	CHAL	N	N	0.90
5LR200.670	15.3	FK	C23	NA	13.76	2.18	CHAL	N	N	0.20
5LR200.671	15.4	FK	C23	NA	9.04	0.82	CHAL	N	N	0.01
5LR200.672	16.1	FK	B21	0-3'	22.70	10.06	CH	Y	Y	2.10
5LR200.673	16.2	FK	B21	0-3'	19.19	10.17	CH	Y	Y	1.80
5LR200.674	16.3	FK	B21	0-2'	15.76	3.05	CH	N	N	0.40
5LR200.675	16.4	FK	B21	NA	14.28	2.31	CHAL	N	N	0.20
5LR200.676	16.5	FK	B21	NA	8.71	2.88	CHAL	N	N	0.10
5LR200.677	16.6	FK	B21	NA	11.81	1.64	CH	N	Y	0.10
5LR200.678	16.7	FK	B21	NA	11.62	2.16	CHAL	N	N	0.20
5LR200.679	16.8	FK	B21	NA	12.47	1.71	CHAL	N	N	0.10
5LR200.680	16.9	FK	B21	NA	13.81	1.92	CH	N	N	0.01
5LR200.681	16.11	FK	B21	NA	16.85	4.13	CHAL	N	N	0.40
5LR200.682	16.12	FK	B21	1	10.38	2.08	CHAL	N	N	0.20
5LR200.683	16.13	FK	B21	1	12.08	2.02	CHAL	N	N	0.20
5LR200.684	16.14	FK	B21	NA	11.38	2.99	CHAL	N	N	0.30
5LR200.685	16.15	FK	B21	NA	16.16	2.48	CH	N	N	0.30
5LR200.686	16.16	FK	B21	NA	9.96	1.92	CH	N	N	0.10
5LR200.687	16.17	FK	B21	NA	10.82	2.41	CH	N	NA	0.30
5LR200.688	16.18	FK	B21	0-3'	11.14	2.04	CHAL	N	N	0.30
5LR200.689	16.19	FK	B21	NA	9.50	1.60	CHAL	N	N	0.10
5LR200.690	16.21	FK	B21	NA	10.90	1.73	CH	N	N	0.20
5LR200.691	16.22	FK	B21	NA	9.24	1.15	CH	N	N	0.01
5LR200.692	16.23	FK	B21	NA	14.34	1.90	CHAL	N	N	0.20

CMPA Curation Number	HFM Item #	Item	Grid	Level	Max Length (mm)	Max Thickness (mm)	Raw Mat	Cortex	Burning	Mass (g)
5LR200.693	16.24	FK	B21	NA	8.08	1.23	CHAL	N	N	0.01
5LR200.694	16.25	FK	B21	1	8.53	2.18	CHAL	N	N	0.10
5LR200.695	16.26	FK	B21	NA	9.92	1.63	CHAL	N	N	0.10
5LR200.696	16.27	FK	B21	NA	13.88	2.05	CHAL	N	N	0.20
5LR200.697	16.28	FK	B21	NA	12.41	1.27	CHAL	N	N	0.01
5LR200.698	16.29	FK	B21	NA	10.52	1.39	CHAL	N	N	0.01
5LR200.699	16.31	FK	B21	NA	9.28	3.67	CH	N	N	0.10
5LR200.700	17.1	FK	B5	2	24.31	6.74	QTZ	N	NA	4.80
5LR200.701	17.2	FK	B5	1	20.98	5.13	QTZ	N	NA	1.40
5LR200.702	17.3	FK	B5	2	17.60	4.07	QTZ	N	NA	0.90
5LR200.703	17.4	FK	B5	NA	13.70	5.09	QTZ	N	NA	0.60
5LR200.704	17.5	FK	B5	2	14.21	2.56	CHAL	N	N	0.40
5LR200.705	17.6	FK	B5	NA	9.82	2.51	CHAL	N	N	0.20
5LR200.706	17.7	FK	B5	1	9.96	1.58	CH	N	N	0.10
5LR200.707	17.8	FK	D5	1	19.10	3.90	QTZ	N	NA	1.00
5LR200.708	17.9	FK	D5	1	16.78	2.33	QTZ	N	NA	0.40
5LR200.709	17.11	FK	D5	1	17.71	4.23	QTZ	N	NA	1.00
5LR200.710	17.12	FK	D5	1	11.67	3.75	CHAL	N	Y	0.40
5LR200.711	17.13	FK	D5	1	10.74	3.15	CH	N	Y	0.20
5LR200.712	18.1	ANG	D22	1	24.54	12.99	QTZ	N	NA	5.10
5LR200.713	18.2	ANG	D22	NA	15.48	4.82	CH	N	N	1.10
5LR200.714	18.3	FK	D22	1	21.65	3.57	CH	Y	N	1.60
5LR200.715	18.4	FK	D22	1	20.68	4.96	CH	N	N	1.30
5LR200.716	18.5	FK	D22	NA	23.67	4.04	CHAL	N	N	1.50
5LR200.717	18.6	FK	D22	NA	21.42	7.39	CHAL	N	N	2.90
5LR200.718	18.7	FK	D22	NA	14.94	3.67	CHAL	N	N	0.20
5LR200.719	18.8	FK	D22	1	18.04	2.92	CH	Y	N	0.80
5LR200.720	18.9	FK	D22	NA	24.44	2.70	CH	N	Y	1.40
5LR200.721	18.11	ANG	D22	1	16.64	6.67	CH	N	Y	2.00
5LR200.722	18.12	FK	D22	NA	20.04	3.59	CHAL	N	N	0.60
5LR200.723	18.13	ANG	D22	NA	13.10	5.05	CH	N	N	0.50
5LR200.724	18.14	FK	D22	NA	15.67	3.75	CHAL	N	N	0.60
5LR200.725	18.15	FK	D22	NA	17.38	2.18	CHAL	N	N	0.20
5LR200.726	18.16	FK	D22	1	12.30	2.68	CH	N	N	0.50
5LR200.727	18.17	FK	D22	NA	14.47	2.11	CHAL	N	N	0.30
5LR200.728	18.18	ANG	D22	NA	8.40	5.67	CH	N	Y	0.30
5LR200.729	18.19	FK	D22	1	9.13	2.18	CH	N	Y	0.20
5LR200.730	18.21	FK	D22	NA	10.28	1.93	CH	N	Y	0.20
5LR200.731	18.22	FK	D22	NA	12.44	3.67	CH	N	N	0.20
5LR200.732	18.23	FK	D22	NA	10.13	2.16	QTZ	N	NA	0.20
5LR200.733	18.24	FK	D22	NA	8.01	2.50	CH	N	Y	0.01
5LR200.734	18.25	FK	D22	NA	9.18	2.20	CH	N	N	0.10
5LR200.735	18.26	FK	D22	NA	6.14	1.07	CH	N	N	0.01
5LR200.736	19.1	ANG	C4	1	38.29	15.35	QTZ	Y	NA	9.40
5LR200.737	19.2	FK	C4	1	33.34	6.34	QTZ	N	NA	6.10
5LR200.738	20.1	FK	B2	NA	23.22	7.59	QTZ	N	NA	2.00
5LR200.739	20.2	FK	B2	NA	24.47	3.83	QTZ	N	NA	1.20
5LR200.740	20.3	FK	B2	1	17.49	4.17	QTZ	N	NA	1.00
5LR200.741	20.4	FK	B2	1	13.51	3.43	QTZ	N	NA	0.30

CMPA Curation Number	HFM Item #	Item	Grid	Level	Max Length (mm)	Max Thickness (mm)	Raw Mat	Cortex	Burning	Mass (g)
5LR200.742	20.5	FK	B2	1	12.19	2.73	CH	N	Y	0.40
5LR200.743	21.1	FK	C3	NA	46.94	14.30	QTZ	Y	NA	21.50
5LR200.744	21.2	FK	D2	NA	30.85	7.58	QTZ	N	NA	3.50
5LR200.745	21.3	FK	C3	S	22.86	6.27	QTZ	N	NA	3.00
5LR200.746	21.4	FK	C3	1	28.70	10.95	QTZ	N	NA	4.00
5LR200.747	21.5	FK	C3	1	17.50	6.29	QTZ	N	NA	1.50
5LR200.748	21.6	FK	C3	3,1	17.51	4.08	QTZ	N	NA	0.60
5LR200.749	21.7	FK	D2	NA	18.91	4.37	QTZ	N	NA	1.20
5LR200.750	21.8	FK	C3	NA	17.30	3.50	QTZ	N	NA	0.80
5LR200.751	21.9	FK	C3	1	10.35	3.69	QTZ	N	NA	0.40
5LR200.752	21.11	FK	C3	1	18.89	3.16	QTZ	N	NA	0.70
5LR200.753	21.12	FK	C3	2	12.13	2.41	QTZ	N	NA	0.30
5LR200.754	21.13	FK	C3	S	14.93	2.41	QTZ	N	NA	0.50
5LR200.755	21.14	FK	C3	1	13.90	2.96	QTZ	N	NA	0.60
5LR200.756	21.15	FK	C3	NA	8.60	2.74	QTZ	N	NA	0.20
5LR200.757	21.16	FK	C3	1	10.84	1.73	CH	N	N	0.10
5LR200.758	21.17	FK	C3	1	13.35	2.49	CH	N	N	0.20
5LR200.759	22.1	FK	C2	1	24.70	7.15	QTZ	N	NA	3.30
5LR200.760	22.2	FK	C2	NA	19.11	2.16	QTZ	N	NA	0.70
5LR200.761	22.3	FK	C2	1	21.69	3.55	QTZ	N	NA	0.90
5LR200.762	22.4	FK	C2	NA	14.95	2.75	QTZ	N	NA	0.30
5LR200.763	22.5	FK	C2	NA	12.74	2.07	QTZ	N	NA	0.30
5LR200.764	22.6	FK	C2	NA	11.27	2.74	QTZ	N	NA	0.30
5LR200.765	22.7	FK	C2	1	12.14	1.90	CH	Y	N	0.10
5LR200.766	22.8	FK	C2	NA	10.58	1.74	QTZ	N	NA	0.10
5LR200.767	23.1	FK	S92-93	NA	33.18	5.35	CH	N	N	3.50
5LR200.768	23.2	ANG	S92-93	NA	12.04	3.90	CH	Y	Y	0.40
5LR200.769	23.3	FK	S92-93	NA	9.48	1.10	CHAL	N	N	0.01
5LR200.770	24.1	ANG	C18-19	2	19.25	11.23	CH	Y	N	1.90
5LR200.771	24.2	FK	C18-19	2	22.48	4.37	CH	N	N	1.70
5LR200.772	24.3	FK	C18-19	1	28.94	6.42	QTZ	N	NA	3.50
5LR200.773	24.4	ANG	C18-19	2	21.79	8.49	CH	N	N	2.40
5LR200.774	24.5	ANG	C18	2	21.07	4.16	PW	N	N	1.40
5LR200.775	24.6	FK	C18-19	1	14.99	3.14	QTZ	N	NA	0.80
5LR200.776	24.7	FK	C18	2	13.05	2.04	QTZ	N	NA	0.30
5LR200.777	24.8	FK	C19	1	30.01	5.02	CH	N	N	1.80
5LR200.778	24.9	FK	C18	2	18.93	4.88	CH	N	Y	1.10
5LR200.779	24.11	FK	C18	NA	18.48	4.40	CH	N	N	0.90
5LR200.780	24.12	FK	C18	1	17.03	8.35	CH	N	N	1.20
5LR200.781	24.13	FK	C18-19	1	13.88	4.21	CH	N	N	0.60
5LR200.782	24.14	FK	C18	NA	18.36	5.62	CH	N	N	1.40
5LR200.783	24.15	FK	C18	NA	15.14	3.12	CH	N	N	0.40
5LR200.784	24.16	FK	C18-19	1	17.66	3.21	CH	N	N	0.50
5LR200.785	24.17	FK	C19	1	21.52	4.17	CH	N	N	0.80
5LR200.786	24.18	ANG	C18	NA	17.12	6.71	CH	N	N	1.10
5LR200.787	24.19	FK	C18-19	1	14.61	3.53	CH	N	N	0.50
5LR200.788	24.21	FK	C18-19	1	11.37	2.27	CH	N	N	0.30
5LR200.789	24.22	FK	C19	1	16.43	2.37	CH	N	N	0.30
5LR200.790	24.23	FK	C18	2	18.30	3.72	CH	Y	N	0.70

CMPA Curation Number	HFM Item #	Item	Grid	Level	Max Length (mm)	Max Thickness (mm)	Raw Mat	Cortex	Burning	Mass (g)
5LR200.791	24.24	FK	C18	2	14.58	2.49	PW	N	N	0.30
5LR200.792	24.25	FK	C18-19	1	15.79	2.47	QTZ	N	N	0.30
5LR200.793	24.26	FK	C18	2	13.55	2.19	PW	N	N	0.40
5LR200.794	24.27	FK	C18	2	20.93	5.41	CHAL	N	N	1.20
5LR200.795	24.28	FK	C18	2	16.54	4.12	CH	N	N	0.70
5LR200.796	24.29	FK	C18	1	10.92	1.48	CH	N	N	0.01
5LR200.797	24.31	FK	C18-19	2	13.29	2.18	CH	N	N	0.30
5LR200.798	24.32	FK	C18-19	2	12.38	2.89	PW	N	N	0.30
5LR200.799	24.33	FK	C18	1	13.41	2.85	CH	Y	N	0.20
5LR200.800	24.34	FK	C18-19	2	16.76	2.28	CH	N	N	0.40
5LR200.801	24.35	FK	C18	2	13.79	1.72	PW	N	N	0.20
5LR200.802	24.36	FK	C18-19	2	22.64	2.12	PW	N	N	0.50
5LR200.803	24.37	FK	C18	NA	13.94	1.59	QTZ	N	NA	0.20
5LR200.804	24.38	FK	C18-19	2	19.54	2.51	PW	N	N	0.50
5LR200.805	24.39	FK	C18	NA	16.14	2.43	PW	N	N	0.30
5LR200.806	24.41	FK	C18-19	2	12.51	2.70	CH	N	N	0.40
5LR200.807	24.42	FK	C18	2	15.28	2.60	CH	N	N	0.40
5LR200.808	24.43	FK	C18	2	16.20	1.62	PW	N	N	0.20
5LR200.809	24.44	FK	C19	1	12.50	5.20	CHAL	Y	N	0.40
5LR200.810	24.45	FK	C19	NA	12.66	1.58	CH	N	Y	0.20
5LR200.811	24.46	FK	C19	S	14.94	2.35	CH	N	N	0.40
5LR200.812	24.47	FK	C18	1	12.41	2.74	CHAL	N	N	0.30
5LR200.813	24.48	FK	C18-19	NA	12.39	1.95	CH	N	N	0.20
5LR200.814	24.49	FK	C18	1	14.11	2.51	PW	N	N	0.50
5LR200.815	24.51	FK	C18	1	18.13	2.98	CHAL	N	N	0.60
5LR200.816	24.52	FK	C19	NA	15.24	2.70	QTZ	N	N	0.40
5LR200.817	24.53	FK	C18-19	1	12.69	2.86	CH	N	N	0.30
5LR200.818	24.54	ANG	C19	1	15.37	6.50	PW	N	N	0.40
5LR200.819	24.55	FK	C19	NA	13.84	2.01	QTZ	N	N	0.30
5LR200.820	24.56	FK	C18	2	14.05	2.88	CH	Y	Y	0.40
5LR200.821	24.57	FK	C18	2	12.80	3.46	PW	N	N	0.20
5LR200.822	24.58	FK	C18-19	2	14.27	2.38	PW	N	N	0.20
5LR200.823	24.59	FK	C18	2	10.60	2.22	PW	N	N	0.20
5LR200.824	24.61	FK	C19	NA	14.08	1.71	PW	N	N	0.20
5LR200.825	24.62	ANG	C19	1	13.26	7.59	CH	Y	N	0.60
5LR200.826	24.63	FK	C18-19	2	13.39	2.25	CH	N	N	0.30
5LR200.827	24.64	FK	C19	NA	11.09	2.27	CH	N	N	0.30
5LR200.828	24.65	FK	C18	NA	13.81	2.86	CH	N	Y	0.50
5LR200.829	24.66	FK	C18-19	2	10.74	1.72	CH	N	N	0.10
5LR200.830	24.67	FK	C18	NA	12.33	2.26	CH	N	N	0.30
5LR200.831	24.68	FK	C18-19	2	16.45	3.53	PW	N	N	0.50
5LR200.832	24.69	FK	C18-19	1	16.49	2.74	CH	N	N	0.50
5LR200.833	24.71	FK	C19	1	13.65	1.12	CH	N	N	0.20
5LR200.834	24.72	FK	C19	1	18.33	3.35	CH	Y	Y	0.90
5LR200.835	24.73	FK	C18	1	11.80	1.81	CH	N	N	0.20
5LR200.836	24.74	FK	C18-19	1	10.42	1.74	CH	N	N	0.10
5LR200.837	24.75	FK	C18	NA	15.66	1.71	CHAL	N	N	0.30
5LR200.838	24.76	FK	C18	1	11.07	1.83	CH	N	N	0.20
5LR200.839	24.77	FK	C19	1	11.35	1.61	CH	N	N	0.20

CMPA Curation Number	HFM Item #	Item	Grid	Level	Max Length (mm)	Max Thickness (mm)	Raw Mat	Cortex	Burning	Mass (g)
5LR200.840	24.78	FK	C19	1	9.76	2.84	CH	N	N	0.20
5LR200.841	24.79	FK	C18-19	2	10.38	1.26	QTZ	N	NA	0.01
5LR200.842	24.81	FK	C18	2	9.05	1.58	PW	N	N	0.10
5LR200.843	24.82	FK	C18	1	18.87	1.78	PW	N	N	0.20
5LR200.844	24.83	FK	C18-19	2	13.47	2.06	CH	N	N	0.20
5LR200.845	24.84	FK	C18	2	12.01	2.14	PW	N	N	0.20
5LR200.846	24.85	FK	C18	1	12.06	1.58	PW	N	N	0.10
5LR200.847	24.86	FK	C19	1	13.64	4.36	CH	N	Y	0.40
5LR200.848	24.87	FK	C19	NA	12.97	2.49	PW	N	N	0.30
5LR200.849	24.88	FK	C18	NA	13.61	2.87	PW	N	N	0.30
5LR200.850	24.89	FK	C18-19	NA	10.55	1.62	CH	N	N	0.10
5LR200.851	24.91	FK	C18	1	14.70	3.09	CHAL	Y	N	0.50
5LR200.852	24.92	FK	C18	2	9.98	1.72	PW	N	N	0.10
5LR200.853	24.93	FK	C18-19	1	13.61	2.99	CH	N	N	0.30
5LR200.854	24.94	FK	C-18	2	11.62	2.09	CH	N	N	0.20
5LR200.855	24.95	FK	C18	1	11.51	3.02	CH	N	N	0.30
5LR200.856	24.96	FK	C18-19	NA	11.57	2.52	CH	N	Y	0.10
5LR200.857	24.97	FK	C18-19	2	13.30	2.84	CH	N	N	0.20
5LR200.858	24.98	FK	C18	NA	12.39	1.12	CH	N	N	0.10
5LR200.859	24.99	FK	C18	NA	16.51	2.87	CH	N	N	0.20
5LR200.860	24.101	FK	C18-19	NA	10.51	2.37	CH	N	N	0.20
5LR200.861	24.102	FK	C18	2	12.10	2.64	PW	N	N	0.20
5LR200.862	24.103	FK	C18-19	1	10.25	2.03	CH	N	Y	0.10
5LR200.863	24.104	FK	C18-19	NA	8.88	2.94	CHAL	N	N	0.30
5LR200.864	24.105	FK	C19	1	13.41	1.08	CH	N	N	0.01
5LR200.865	24.106	FK	C18	1	10.20	2.01	PW	N	Y	0.20
5LR200.866	24.107	FK	C19	1	18.36	2.46	CHAL	N	N	0.20
5LR200.867	24.108	FK	C18	2	10.34	1.63	PW	N	N	0.20
5LR200.868	24.109	FK	C18	2	15.30	2.63	PW	N	N	0.40
5LR200.869	24.111	FK	C18-19	2	10.68	1.66	CH	N	N	0.20
5LR200.870	24.112	FK	C19	1	13.66	1.45	PW	N	N	0.10
5LR200.871	24.113	ANG	C19	1	12.68	5.31	CH	N	N	0.40
5LR200.872	24.114	FK	C18-19	NA	15.65	4.11	CHAL	N	N	0.20
5LR200.873	24.115	FK	C18	NA	11.23	1.65	CH	N	N	0.10
5LR200.874	24.116	FK	C18-19	2	12.39	2.10	CH	N	N	0.20
5LR200.875	24.117	FK	C19	1	9.93	1.44	CH	N	N	0.10
5LR200.876	24.118	FK	C18-19	NA	11.17	2.35	CH	Y	N	0.10
5LR200.877	24.119	FK	C18	1	11.99	2.81	CH	N	Y	0.30
5LR200.878	24.121	FK	C18-19	NA	11.44	3.45	CH	N	N	0.20
5LR200.879	24.122	FK	C19	1	13.15	2.46	CHAL	Y	N	0.20
5LR200.880	24.123	FK	C18-19	NA	9.05	1.60	CH	N	Y	0.10
5LR200.881	24.124	FK	C18	NA	10.93	1.54	CHAL	N	N	0.10
5LR200.882	24.125	FK	C18-19	2	12.47	1.26	CH	N	Y	0.10
5LR200.883	24.126	FK	C18	1	13.07	1.90	PW	N	N	0.20
5LR200.884	24.127	FK	C18-19	1	9.35	1.68	QTZ	N	NA	0.10
5LR200.885	24.128	FK	C18	2	11.57	1.47	CH	N	N	0.20
5LR200.886	24.129	FK	C18-19	NA	11.55	1.17	CH	N	N	0.01
5LR200.887	24.131	FK	C18	2	10.88	1.88	CH	N	N	0.10
5LR200.888	24.132	FK	C18-19	2	11.84	1.83	PW	N	N	0.10

CMPA Curation Number	HFM Item #	Item	Grid	Level	Max Length (mm)	Max Thickness (mm)	Raw Mat	Cortex	Burning	Mass (g)
5LR200.889	24.133	FK	C18-19	NA	8.85	1.43	CH	N	N	0.01
5LR200.890	24.134	FK	C18-19	1	10.67	2.61	QTZ	N	NA	0.20
5LR200.891	24.135	FK	C18-19	NA	10.50	1.69	CH	N	N	0.20
5LR200.892	24.136	FK	C18-19	NA	7.63	1.71	CH	N	N	0.01
5LR200.893	24.137	FK	C18-19	NA	8.47	1.07	QTZ	N	NA	0.01
5LR200.894	24.138	FK	C19	1	13.85	1.25	CH	N	N	0.10
5LR200.895	24.139	FK	C18-19	2	11.77	1.64	CH	N	Y	0.20
5LR200.896	24.141	FK	C18-19	NA	10.64	1.89	CH	N	Y	0.20
5LR200.897	24.142	FK	C18	2	11.53	1.66	CH	N	N	0.20
5LR200.898	24.143	FK	C18	1	11.66	2.34	CHAL	N	N	0.20
5LR200.899	24.144	FK	C18-19	NA	10.80	2.26	CH	N	N	0.10
5LR200.900	24.145	FK	C18-19	NA	10.45	2.25	CH	N	N	0.10
5LR200.901	24.146	FK	C19	1	10.87	1.82	CH	N	N	0.10
5LR200.902	24.147	FK	C18-19	2	13.04	1.91	CH	N	N	0.20
5LR200.903	24.148	FK	C18	1	10.00	2.16	CH	N	N	0.10
5LR200.904	24.149	FK	C18-19	1	8.94	1.60	CH	N	N	0.10
5LR200.905	24.151	FK	C18-19	NA	9.13	1.14	CH	N	N	0.01
5LR200.906	24.152	FK	C18	2	12.63	1.38	PW	N	N	0.20
5LR200.907	24.153	FK	C-18	NA	9.70	2.97	CH	N	N	0.20
5LR200.908	24.154	FK	C-18	NA	10.44	1.76	PW	N	N	0.20
5LR200.909	24.155	FK	C18-19	2	10.25	1.59	CH	N	Y	0.01
5LR200.910	24.156	FK	C18	1	9.88	1.98	CH	N	Y	0.10
5LR200.911	24.157	ANG	C18-19	NA	8.93	3.53	CH	N	N	0.10
5LR200.912	24.158	FK	C18-19	NA	10.19	1.31	CH	N	N	0.01
5LR200.913	24.159	FK	C19	2	11.66	1.82	QTZ	N	NA	0.20
5LR200.914	24.161	FK	C18-19	NA	8.96	1.43	CH	N	N	0.01
5LR200.915	24.162	FK	C18-19	1	11.74	1.48	CH	N	N	0.20
5LR200.916	24.163	FK	C19	1	11.12	1.91	CH	N	N	0.10
5LR200.917	24.164	FK	C18-19	NA	7.35	1.05	CHAL	N	N	0.01
5LR200.918	24.165	FK	C19	NA	10.61	2.22	CH	N	Y	0.20
5LR200.919	24.166	FK	C19	1	11.47	1.86	CH	N	N	0.10
5LR200.920	24.167	FK	C18	2	8.89	3.12	CH	N	N	0.20
5LR200.921	24.168	FK	C18	2	11.38	3.26	QTZ	N	NA	0.20
5LR200.922	24.169	FK	C18-19	NA	6.85	2.95	CH	N	N	0.10
5LR200.923	24.171	FK	C18-19	2	11.47	1.95	CH	N	N	0.20
5LR200.924	24.172	FK	C18	1	10.68	1.43	CH	N	N	0.01
5LR200.925	24.173	FK	C18-19	NA	11.44	1.35	CH	N	N	0.10
5LR200.926	24.174	FK	C18-19	NA	9.92	2.04	CH	N	Y	0.10
5LR200.927	24.175	FK	C18-19	NA	8.82	2.67	CH	N	N	0.10
5LR200.928	24.176	FK	C18	2	10.73	1.97	CH	N	Y	0.20
5LR200.929	24.177	FK	C18-19	NA	8.98	2.44	CH	N	N	0.20
5LR200.930	24.178	FK	C18-19	NA	8.07	1.43	PW	N	N	0.01
5LR200.931	24.179	FK	C18-19	NA	7.33	1.38	CH	N	N	0.01
5LR200.932	24.181	FK	C18-19	NA	8.21	1.32	CH	N	Y	0.10
5LR200.933	24.182	FK	C18-19	NA	9.88	1.98	CH	N	Y	0.10
5LR200.934	24.183	FK	C18-19	NA	9.85	1.26	CH	N	Y	0.10
5LR200.935	24.184	FK	C18-19	NA	8.07	1.52	CH	N	N	0.10
5LR200.936	24.185	FK	C18-19	NA	11.12	1.22	CH	N	Y	0.10
5LR200.937	24.186	FK	C19	1	8.18	1.80	CH	N	N	0.10

CMPA Curation Number	HFM Item #	Item	Grid	Level	Max Length (mm)	Max Thickness (mm)	Raw Mat	Cortex	Burning	Mass (g)
5LR200.938	24.187	FK	C18-19	NA	15.24	3.01	CH	N	Y	0.20
5LR200.939	24.188	FK	C18	2	10.00	0.92	CHAL	N	N	0.01
5LR200.940	24.189	FK	C18-19	NA	7.18	1.68	CH	N	N	0.10
5LR200.941	24.191	FK	C18-19	NA	7.47	1.19	CH	N	N	0.01
5LR200.942	24.192	FK	C18-19	NA	8.01	2.12	CHAL	N	N	0.01
5LR200.943	24.193	FK	C18-19	NA	8.21	2.53	CH	N	N	0.10
5LR200.944	24.194	FK	C18-19	NA	8.36	1.28	CH	N	N	0.01
5LR200.945	24.195	FK	C18-19	NA	9.44	1.28	CH	N	N	0.01
5LR200.946	24.196	FK	C18-19	NA	9.30	1.35	CH	N	N	0.01
5LR200.947	24.197	FK	C18-19	NA	6.29	2.04	CH	N	N	0.10
5LR200.948	24.198	FK	C18-19	NA	9.37	2.76	CHAL	N	N	0.10
5LR200.949	24.199	FK	C18-19	NA	9.27	1.68	CH	N	Y	0.10
5LR200.950	24.201	FK	C18-19	NA	9.49	1.31	CH	N	N	0.01
5LR200.951	24.202	FK	C18-19	NA	10.47	1.43	CH	N	N	0.01
5LR200.952	24.203	FK	C18-19	NA	10.81	1.91	CH	N	N	0.10
5LR200.953	24.204	FK	C18-19	NA	8.30	1.19	CH	N	Y	0.01
5LR200.954	24.205	FK	C18-19	NA	10.51	1.91	CHAL	N	Y	0.10
5LR200.955	24.206	FK	C18-19	NA	8.02	0.98	CHAL	N	N	0.01
5LR200.956	24.207	FK	C18	1	8.61	1.38	QTZ	N	NA	0.01
5LR200.957	24.208	FK	C18-19	NA	8.60	1.12	PW	N	N	0.01
5LR200.958	24.209	FK	C18-19	NA	8.56	2.47	CH	N	Y	0.10
5LR200.959	24.211	FK	C18-19	NA	7.89	1.40	CH	N	N	0.01
5LR200.960	24.212	FK	C18-19	NA	6.86	1.91	CH	N	N	0.01
5LR200.961	24.213	FK	C18-19	NA	7.23	1.41	CH	N	N	0.01
5LR200.962	24.214	FK	C18-19	NA	7.33	1.94	CH	N	Y	0.01
5LR200.963	24.215	FK	C18-19	NA	10.20	1.32	CH	N	N	0.01
5LR200.964	24.216	FK	C18-19	NA	10.59	2.30	QTZ	N	NA	0.20
5LR200.965	24.217	FK	C18-19	NA	9.13	1.99	CH	N	N	0.01
5LR200.966	24.218	FK	C18-19	NA	7.85	1.27	CH	N	N	0.01
5LR200.967	24.219	FK	C19	1	8.98	1.06	CH	N	N	0.01
5LR200.968	24.221	FK	C18-19	NA	8.49	1.06	QTZ	N	NA	0.01
5LR200.969	24.222	FK	C18-19	NA	6.29	1.72	PW	N	N	0.01
5LR200.970	24.223	FK	C18-19	NA	6.53	2.18	CHAL	N	N	0.10
5LR200.971	24.224	FK	C18-19	NA	6.37	0.77	CH	N	N	0.01
5LR200.972	24.225	FK	C18-19	NA	7.77	1.06	CH	N	N	0.01
5LR200.973	24.226	FK	C18-19	NA	10.06	1.71	CH	N	N	0.10
5LR200.974	24.227	FK	C18-19	NA	7.98	1.06	CH	N	Y	0.01
5LR200.975	24.228	FK	C18-19	NA	7.61	1.23	CH	N	N	0.01
5LR200.976	24.229	FK	C18-19	NA	7.20	1.92	CHAL	N	N	0.01
5LR200.977	24.231	FK	C18-19	NA	8.06	2.06	CH	N	Y	0.01
5LR200.978	24.232	FK	C18-19	NA	8.82	1.42	CH	N	N	0.01
5LR200.979	24.233	FK	C18-19	NA	7.96	1.03	PW	N	N	0.01
5LR200.980	24.234	FK	C18-19	NA	7.56	0.90	CH	N	N	0.01
5LR200.981	24.235	FK	C18-19	NA	10.82	1.75	CH	N	N	0.01
5LR200.982	24.236	FK	C18-19	NA	7.89	1.43	CH	N	Y	0.01
5LR200.983	24.237	FK	C18-19	NA	9.81	1.67	CH	N	Y	0.01
5LR200.984	24.238	FK	C18-19	NA	6.80	0.39	CH	N	N	0.01
5LR200.985	24.239	FK	C18-19	NA	8.24	1.13	CH	N	N	0.01
5LR200.986	24.241	FK	C18-19	NA	7.44	1.13	CH	N	N	0.01

CMPA Curation Number	HFM Item #	Item	Grid	Level	Max Length (mm)	Max Thickness (mm)	Raw Mat	Cortex	Burning	Mass (g)
5LR200.987	24.242	FK	C18-19	NA	10.73	1.61	CHAL	N	N	0.01
5LR200.988	24.243	FK	C18-19	NA	6.77	1.54	CH	N	N	0.01
5LR200.989	24.244	FK	C18-19	NA	8.47	1.97	QTZ	N	NA	0.10
5LR200.990	24.245	FK	C18-19	NA	9.74	0.75	PW	N	N	0.01
5LR200.991	24.246	FK	C18-19	NA	9.86	0.74	CH	N	N	0.01
5LR200.992	24.247	FK	C18-19	NA	7.36	1.20	CH	N	Y	0.01
5LR200.993	24.248	FK	C18-19	NA	8.09	1.56	CH	N	N	0.01
5LR200.994	24.249	FK	C19	1	12.07	1.34	CH	N	N	0.01
5LR200.995	24.251	FK	C18-19	NA	6.84	1.11	CH	N	N	0.01
5LR200.996	24.252	FK	C18-19	NA	10.60	1.50	CH	N	N	0.01
5LR200.997	24.253	FK	C18-19	NA	7.31	1.37	CHAL	N	N	0.01
5LR200.998	24.254	FK	C18-19	NA	7.52	0.83	CH	N	N	0.01
5LR200.999	24.255	FK	C18-19	NA	8.02	1.03	CHAL	N	N	0.01
5LR200.1000	24.256	FK	C18-19	NA	4.76	0.64	CH	N	N	0.01
5LR200.1001	24.257	FK	C18-19	NA	5.88	0.67	CHAL	N	N	0.01
5LR200.1002	24.258	FK	C18-19	NA	5.18	0.62	PW	N	N	0.01
5LR200.1003	24.259	FK	C18-19	NA	10.09	1.94	CHAL	N	N	0.01
5LR200.1004	24.261	FK	C18-19	NA	7.72	0.67	PW	N	N	0.01
5LR200.1005	24.262	FK	C18-19	NA	7.77	2.24	PW	N	N	0.01
5LR200.1006	24.263	FK	C18-19	NA	7.25	0.57	PW	N	N	0.01
5LR200.1007	24.264	FK	C18-19	NA	8.99	2.47	CH	N	N	0.10
5LR200.1008	24.265	FK	C18-19	NA	7.69	0.68	PW	N	N	0.01
5LR200.1009	24.266	FK	C18-19	NA	5.73	0.85	CH	N	N	0.01
5LR200.1010	24.267	FK	C18-19	NA	6.72	1.94	CH	N	Y	0.01
5LR200.1011	24.268	FK	C18-19	NA	5.86	1.32	PW	N	N	0.01
5LR200.1012	24.269	FK	C18-19	NA	5.92	0.92	CH	N	N	0.01
5LR200.1013	24.271	FK	C18-19	NA	7.29	1.17	PW	N	N	0.01
5LR200.1014	24.272	FK	C18-19	NA	6.50	1.20	CH	N	N	0.01
5LR200.1015	24.273	FK	C18-19	NA	5.53	0.82	CH	N	N	0.01
5LR200.1016	24.274	FK	C18-19	NA	6.95	1.18	PW	N	N	0.01
5LR200.1017	24.275	FK	C18-19	NA	5.78	0.90	CH	N	N	0.01
5LR200.1018	24.276	FK	C18-19	NA	7.81	1.96	PW	N	N	0.01
5LR200.1019	24.277	FK	C18-19	NA	7.68	1.07	CH	N	N	0.01
5LR200.1020	24.278	FK	C18-19	NA	8.60	1.24	CH	N	N	0.01
5LR200.1021	24.279	FK	C18-19	NA	8.66	0.80	CH	N	N	0.01
5LR200.1022	24.281	FK	C18-19	NA	5.81	1.29	CH	N	N	0.01
5LR200.1023	24.282	FK	C18-19	NA	8.54	1.35	CH	N	N	0.01
5LR200.1024	24.283	FK	C18-19	NA	9.73	1.32	PW	N	N	0.01
5LR200.1025	24.284	FK	C18-19	NA	8.30	1.16	PW	N	N	0.01
5LR200.1026	24.285	FK	C18-19	NA	5.95	0.86	CH	N	N	0.01
5LR200.1027	24.286	FK	C18-19	NA	5.35	0.67	CHAL	N	N	0.01
5LR200.1028	24.287	FK	C18-19	NA	5.89	0.87	CH	N	N	0.01
5LR200.1029	24.288	FK	C18-19	NA	6.68	1.37	CH	N	Y	0.01
5LR200.1030	24.289	FK	C18-19	NA	8.42	0.59	CH	N	N	0.01
5LR200.1031	24.291	FK	C18-19	NA	4.72	0.94	CH	N	N	0.01
5LR200.1032	24.292	FK	C18-19	NA	5.82	0.66	CH	N	N	0.01
5LR200.1033	24.293	FK	C18-19	NA	6.45	0.77	CH	N	N	0.01
5LR200.1034	24.294	FK	C18-19	NA	6.34	0.93	CH	N	N	0.01
5LR200.1035	24.295	FK	C18-19	NA	6.93	1.23	CH	N	N	0.01

CMPA Curation Number	HFM Item #	Item	Grid	Level	Max Length (mm)	Max Thickness (mm)	Raw Mat	Cortex	Burning	Mass (g)
5LR200.1036	24.296	FK	C18-19	NA	4.89	0.82	CHAL	N	N	0.01
5LR200.1037	24.297	FK	C18-19	NA	5.26	1.59	CH	N	N	0.01
5LR200.1038	24.298	FK	C18-19	NA	4.53	0.43	CH	N	N	0.01
5LR200.1039	24.299	FK	C18-19	NA	9.43	1.08	PW	N	N	0.01
5LR200.1040	24.301	FK	C18-19	NA	5.58	0.77	CH	N	N	0.01
5LR200.1041	24.302	FK	C18-19	NA	7.58	0.52	CH	N	N	0.01
5LR200.1042	24.303	FK	C18-19	NA	5.66	0.91	CH	N	N	0.01
5LR200.1043	24.304	FK	C18-19	NA	6.64	1.20	PW	N	N	0.01
5LR200.1044	24.305	FK	C18-19	NA	5.55	0.93	CH	N	N	0.01
5LR200.1045	24.306	FK	C18-19	NA	6.59	0.82	CH	N	N	0.01
5LR200.1046	24.307	FK	C18-19	NA	6.12	0.89	CH	N	Y	0.01
5LR200.1047	24.308	FK	C18-19	NA	9.04	0.53	CH	N	N	0.01
5LR200.1048	24.309	FK	C18-19	NA	7.22	0.88	CH	N	N	0.01
5LR200.1049	24.311	FK	C18-19	NA	7.73	0.48	CH	N	N	0.01
5LR200.1050	24.312	FK	C18-19	NA	6.34	1.18	CH	N	N	0.01
5LR200.1051	24.313	FK	C18-19	NA	6.14	1.15	CH	N	Y	0.01
5LR200.1052	24.314	FK	C18-19	NA	7.23	0.86	CH	N	Y	0.01
5LR200.1053	24.315	FK	C18-19	NA	6.16	1.66	CH	N	N	0.01
5LR200.1054	24.316	FK	C18-19	NA	4.62	0.51	CH	N	N	0.01
5LR200.1055	24.317	FK	C18-19	NA	4.86	0.58	CH	N	N	0.01
5LR200.1056	24.318	FK	C18-19	NA	5.21	0.66	CH	N	N	0.01
5LR200.1057	24.319	FK	C18-19	NA	7.32	1.41	CH	N	N	0.01
5LR200.1058	24.321	FK	C18-19	NA	5.98	1.99	CHAL	N	N	0.01
5LR200.1059	24.322	FK	C18-19	NA	5.78	0.63	CH	N	N	0.01
5LR200.1060	24.323	FK	C18-19	NA	6.05	1.39	CH	Y	N	0.01
5LR200.1061	24.324	FK	C18-19	NA	5.28	0.46	CH	N	N	0.01
5LR200.1062	24.325	FK	C18-19	NA	6.22	0.92	CH	N	N	0.01
5LR200.1063	24.326	FK	C18-19	NA	6.78	0.77	CH	N	N	0.01
5LR200.1064	24.327	FK	C18-19	NA	5.08	0.42	CH	N	N	0.01
5LR200.1065	24.328	FK	C18-19	NA	5.65	0.89	PW	N	N	0.01
5LR200.1066	24.329	FK	C18-19	NA	4.27	0.89	CH	N	N	0.01
5LR200.1067	24.331	FK	C18-19	NA	4.86	0.56	CH	N	N	0.01
5LR200.1068	24.332	FK	C18-19	NA	4.69	0.52	CH	N	N	0.01
5LR200.1069	24.333	FK	C18-19	NA	6.52	0.56	PW	N	N	0.01
5LR200.1070	24.334	FK	C18-19	NA	6.31	0.91	CH	N	N	0.01
5LR200.1071	24.335	FK	C18-19	NA	5.32	1.16	CH	N	N	0.01
5LR200.1072	24.336	FK	C18-19	NA	6.21	0.77	CH	N	N	0.01
5LR200.1073	24.337	FK	C18-19	NA	4.67	0.82	CH	N	N	0.01
5LR200.1074	24.338	FK	C18-19	NA	4.27	1.06	CH	N	Y	0.01
5LR200.1075	24.339	FK	C18-19	NA	4.26	0.95	PW	N	N	0.01
5LR200.1076	24.341	FK	C18-19	NA	5.82	1.37	CH	N	N	0.01
5LR200.1077	24.342	FK	C18-19	NA	5.94	0.55	CH	N	N	0.01
5LR200.1078	24.343	FK	C18-19	NA	4.87	0.40	CH	N	N	0.01
5LR200.1079	24.344	FK	C18-19	NA	4.26	0.67	CH	N	N	0.01
5LR200.1080	24.345	FK	C18-19	NA	4.65	0.51	CH	N	N	0.01
5LR200.1081	24.346	FK	C18-19	NA	3.22	0.80	CH	N	N	0.01
5LR200.1082	24.347	FK	C18-19	NA	6.24	1.33	CH	N	N	0.01
5LR200.1083	24.348	FK	C18-19	NA	5.02	0.64	CH	N	N	0.01
5LR200.1084	24.349	FK	C18-19	NA	3.49	0.72	CH	N	N	0.01

CMPA Curation Number	HFM Item #	Item	Grid	Level	Max Length (mm)	Max Thickness (mm)	Raw Mat	Cortex	Burning	Mass (g)
5LR200.1085	24.351	FK	C18-19	2	10.35	0.89	CH	N	N	0.01
5LR200.1086	NA	FK	D4	1	27.80	7.30	QTZ	N	NA	3.0
5LR200.1087	NA	FK	C3		22.80	7.00	QTZ	N	NA	2.6
5LR200.1088	NA	ANG	D2	1	44.00	10.80	QTZ	N	NA	14.6
5LR200.1089	NA	FK	C5	2.5"	21.50	4.20	CHAL	Y	N	1.9
5LR200.1090	NA	FK	A5	S	17.90	5.90	QTZ	N	NA	2.3
5LR200.1091	NA	FK	R92	1	23.30	2.50	CH	N	Y	1.2
5LR200.1092	NA	ANG	C2	1	35.20	13.20	QTZ	N	NA	7.8
5LR200.1093	NA	FK	C6	1	19.80	4.20	CH	N	N	1.5
5LR200.1094	NA	FK	E22		24.60	3.50	CH	N	N	1.4
5LR200.1095	NA	FK	C3	1	16.80	3.60	CHAL	N	N	1.1
5LR200.1096	NA	FK	C6		29.70	2.90	CHAL	N	N	1.1
5LR200.1097	NA	FK	M1	1	16.70	3.90	CH	N	N	0.8
5LR200.1098	NA	FK	D6		19.40	3.60	CH	N	N	1.3
5LR200.1099	NA	FK	R92	2	26.10	2.70	CH	N	N	1.5
5LR200.1100	NA	FK	E22	4"	20.70	4.00	CHAL	N	N	1.2
5LR200.1101	NA	ANG	C6		20.00	5.30	CH	N	Y	1.1
5LR200.1102	NA	FK	D5		31.20	6.90	CH	N	N	4.6
5LR200.1103	NA	FK	M1	2	22.30	5.20	QTZ	N	NA	1.5
5LR200.1104	NA	ANG	B20		13.40	7.50	CHAL	N	N	0.8
5LR200.1105	NA	FK	B92?	1	10.90	2.10	QTZ	N	NA	0.3
5LR200.1106	NA	FK	C6		16.00	2.30	CHAL	N	N	0.2
5LR200.1107	NA	FK	C4	1	15.50	4.80	CH	N	N	0.9
5LR200.1108	NA	FK	A5	1	15.40	2.70	QTZ	N	NA	0.5
5LR200.1109	NA	FK	C3	1	16.30	2.40	CH	N	N	0.4
5LR200.1110	NA	FK	M3		10.20	1.20	CHAL	N	N	0.1
5LR200.1111	NA	FK	B21	1	10.30	1.90	QTZ	N	NA	0.2
5LR200.1112	NA	FK	C6	1	12.50	2.90	CHAL	N	N	0.2
5LR200.1113	NA	FK	C6	1	12.70	1.70	CH	N	N	0.1

Appendix H: 5LR200 tool attributes and metrics. Flayharty (1972) original curation number is noted in table.

CPMA Curation Number	Flayharty/ 70s Excavation #	HFM Original Item #	Grid	Level	Feature	Trench	Max Length (mm)	Max Width (mm)	Thickness (mm)	Raw Mat	Color of Raw Mat	Mass (g)	Tool Type	Segment	Base	Notch
5LR200.01	14	1.2	B21	4'	11	3	21.2	13.5	4.3	chal	white	1.3	projectile point	all but complete	straight	side
5LR200.02	83	1.1	F39	1	39	1?	21.3	16.3	4.7	ch	brown	1.6	projectile point	all but complete	concave	not notched
5LR200.03	32	1.22	O96	1	12		15.3	20.0	3.6	pw	red brown	1.3	projectile point	base	straight	
5LR200.04	28	1.17	E22	2"	8		18.3	21.4	5	ch	gray	2.6	biface	midsection		
5LR200.05	31	1.4			35 or 36	1	9.7	10.6	2.4	ch	brown	0.3	projectile point	base	straight concave	side
5LR200.06	39	1.13		1	32	2	14.8	11.7	2.4	ch	white	0.5	projectile point	all but complete	straight	
5LR200.07	71	1.27	D2	1	2	6	9.5	9.0	2.1	chal	tan	0.2	unifacial tool	midsection		
5LR200.08	86	1.11		1	3		17.1	12.5	3.1	ch	tan	0.7	projectile point	all but complete	straight	
5LR200.09	78	1.28	D22		8		11.9	10.5	1.9	chal	tan	0.3	perforator	portion		
5LR200.10	84	1.19	D5	1	3		13.4	11.1	3.3	ch	gray	0.4	biface	tip		
5LR200.11	38	1.16	R92	1	32	1	11.2	14.4	2.1	ch	white and gray	0.4	projectile point	base	straight	
5LR200.12	50	1.23	O96	2	12		16.9	16.6	7	qtz	gray	1.6	biface	midsection		
5LR200.13	44	1.6	O96	2	12	1	13.8	12.8	3.8	qtz	gray	0.7	biface	radial split of midsection		
5LR200.14	34	1.14			32		10.0	9.4	1.7	ch	white and gray	0.1	projectile point	midsection		side
5LR200.15	79	1.8	O22		8		20.0	16.3	3.1	qtz	tan	1.0	projectile point	lateral section of base	straight	side
5LR200.16	89	1.7	M1	1	6		12.0	14.5	3.0	chal	white	0.6	projectile point	base	concave	side
5LR200.17	59	1.12	C18	1	10		11.4	10.1	1.8	pw	tan and red	0.3	projectile point	tip		
5LR200.18	55	1.5	G19	1			22.1	14.0	2.5	qtz	gray	0.7	projectile point	radial split	straight concave	not notched
5LR200.19	85	1.21	D5		3		9.4	9.4	2.0	ch	red brown	0.2	biface	midsection		
5LR200.20	35	1.15	R92	1	32		16.8	20.1	3.4	ch	white	1.5	projectile point	base	straight	
5LR200.21	36	1.18			32	2	13.0	7.5	1.6	ch	tan	0.1	biface	tip		
5LR200.22		1.29					10.6	8.7	2.6	ch	brown	0.1	biface	lateral section of midsection		
5LR200.23	42	1.25	R92		12		8.9	11.2	1.9	ch	white	0.2	biface	midsection		
5LR200.24		1.32	D5?	1	3		10.4	5.7	2.6	ch	white pink	0.2	biface	tip?		

CMPA Curation Number	Flayharty/70s Excavation #	HFM Original Item #	Grid	Level	Feature	Trench	Max Length (mm)	Max Width (mm)	Thickness (mm)	Raw Mat	Color of Raw Mat	Mass (g)	Tool Type	Segment	Base	Notch
5LR200.25	77	1.9	O22		8		12.0	8.3	2.2	ch	red	0.2	projectile point	tip		
5LR200.26	15	1.3	A21	1	11	5	11.9	11.3	2.6	ch	brown	0.4	projectile point	complete	straight concave	side
5LR200.27	1	1.33	A5	1			17.0	13.2	4.2	ch	white	1.0	edge modified flake			
5LR200.28	80	1.24	M3		7		10.6	11.3	2.2	chal	brown	0.3	biface	tip		
5LR200.29		1.36	M1	1	6		17.8	11.2	2.7	ch	tan	0.5	edge modified flake	complete		
5LR200.30		1.26	E22	4"	8		21.4	15.9	3.0	chal	light brown	1.0	edge modified flake	distal end		
5LR200.31		1.34	M1	1	6		40.4	27.3	26.3	ch	tan	34.2	core	complete		
5LR200.32		1.35	M1	1	6		34.6	28.7	19.3	ch	tan	19	core	complete		
5LR200.33	2	1.31	B5	S	5		52.7	34.5	11.2	qtz	tan	18.5	biface	end		
5LR200.34	58		C18	2	10		18.3	16.8	2.3	chal	yellow white	0.8	unifacial tool	tip		
5LR200.35	70		D3	2	2	1	36.7	27.4	8.5	qtz	light gray	8.1	edge modified flake			
5LR200.36	49		O96	2	12		22.4	18	7.1	qtz	light gray	2.8	biface	midsection		
5LR200.37	87		D23	2	9	1	53.6	26.9	20.3	chal	white and gray	30.2	scraper	complete		not notched
5LR200.38	88		D4	1	NA		44.5	35.5	17.0	qtz	gray	27.3	biface	complete		
5LR200.39	46/47 refit		O96	2	12		36.1	38.3	8.2	qtz	gray	9.8	biface	end		
5LR200.40	56		C19		10	1	22.6	26.2	5.5	ch	red/tan mottled with dendritic inclusion	3.1	edge modified flake	end		
5LR200.41	48		O96	2	12		33.3	16.4	7.7	qtz	gray	3.5	biface	end		
5LR200.42	76		D22	1	8		28.6	21.8	5.5	ch	tan with dark brown stripes	4.0	edge modified flake			
5LR200.43	54		C19	1	10		27.2	20.8	8.4	pw	orange brown	4.2	knife	tip		
5LR200.44	27			2	8		15.9	11.2	2.8	ch	matte gray	0.6	projectile point	all but complete	straight	not notched
5LR200.45	75		D22	S	8		29.9	12.8	3.9	chal	white	1.2	edge modified blade			
5LR200.46	25			S	8		43.9	18.2	4.4	chal	white and gray	3.2	edge			

CPA Curation Number	Flayharty/70s Excavation #	HFM Original Item #	Grid	Level	Feature	Trench	Max Length (mm)	Max Width (mm)	Thickness (mm)	Raw Mat	Color of Raw Mat	Mass (g)	Tool Type	Segment	Base	Notch
													modified blade			
5LR200.47	72		D2	1	2	T	41.5	13.8	6.1	ch	gray	3.7	edge modified blade			
5LR200.48	18		C3	1	2	T	25.5	16.0	3.0	qtz	gray	1.3	edge modified blade			
5LR200.49	41		R92	2	32	1	26.1	13.0	3.3	chal	tan	1.2	edge modified blade	complete		
5LR200.50	45		O96	2	12		21.2	9.5	3.4	chal	tan pink	0.6	edge modified blade			
5LR200.51	23		C4	1	NA	T	36.4	15.4	10.3	qtz	tan pink	5.1	edge modified blade			
5LR200.52	65		C6	1	4		27.8	15.4	3.7	ch	gray	1.4	edge modified blade	complete		
5LR200.53	69		C6	1	4		13.2	10.2	3.7	chal	dark gray	0.5	edge modified blade			
5LR200.54			M1	2	6		20.2	13.5	5.9	chal	tan with dendritic inclusion	1.1	scraper	end		
5LR200.55	53		C18	2	10		18.6	9.6	4.8	ch	red	0.6	biface	lateral margin		
5LR200.56	52			1	10		14.5	8.6	5.1	ch	red	0.5	biface	lateral margin		

Appendix I: 5LR200 photographs of all tools from excavated context and 2014 survey.





5LR200.006



5LR200.007



5LR200.008



5LR200.009



5LR200.010



5LR200.011



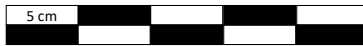
5LR200.012



5LR200.013



5LR200.014



5LR200.015



5LR200.016



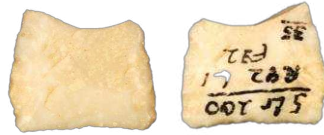
5LR200.017



5LR200.018



5LR200.019



5LR200.020



5LR200.021



5LR200.022



5LR200.023



5LR200.024



5LR200.025



5LR200.026



5LR200.027



5LR200.028



5LR200.029



5LR200.030



5LR200.031



5LR200.032





5LR200.037



5LR200.038



5LR200.039



5LR200.040



5LR200.041



5LR200.042



5LR200.043

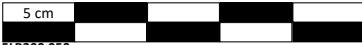


5LR200.044

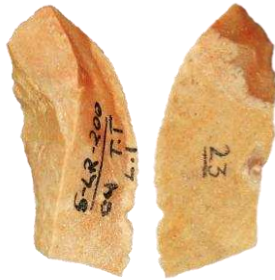




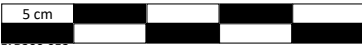
5LR200.049



5LR200.050



5LR200.051



5LR200.052



Below are Tools Collected in 2014 by the Colorado State University Field School

Not Used in this Analysis

Curated in the CSU Archaeological Repository, Department of Anthropology



Appendix J: 5LR289 photographs from 1982 excavation.



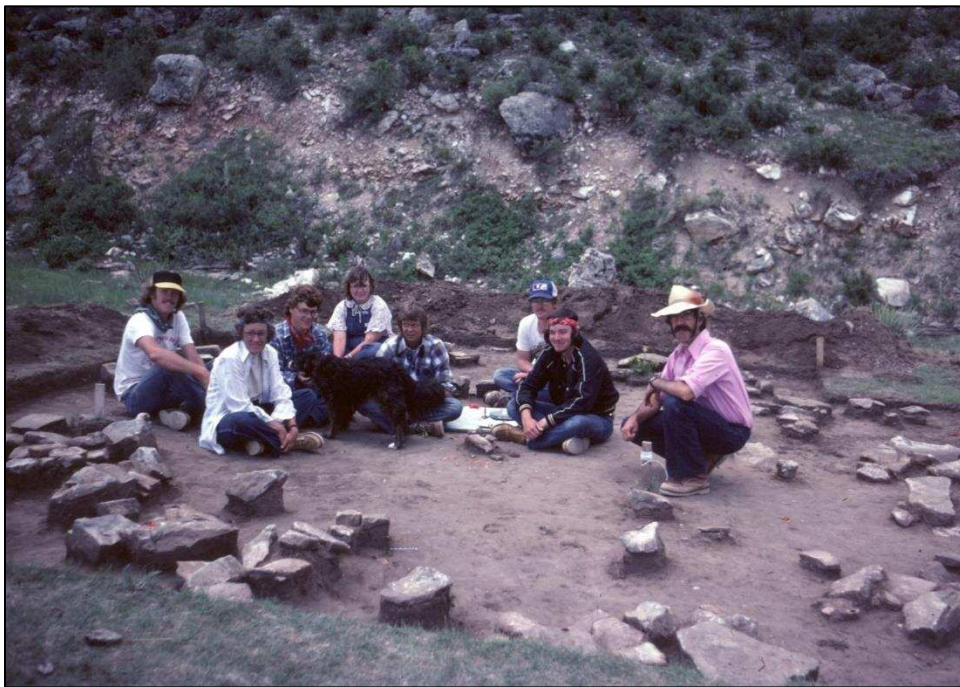
J.1 5LR289 site overview looking west.



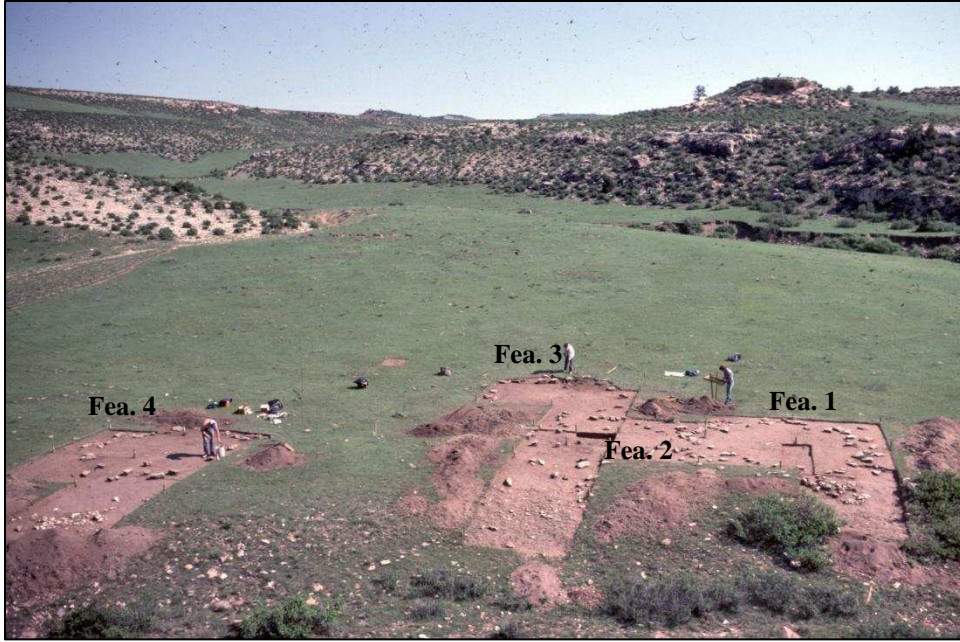
J.2 5LR289 excavation of Feature 5. Notice excavation is focused on interior space of ring.



J.3 5LR289 excavation of thermal feature in unknown ring. Likely Feature 6, a charcoal stain is noted on excavation map.



J.4 5LR289 1982 crew photo in unknown feature (likely Feature 1).



J.5 5LR289 site overview looking north. Features 1-4 are labeled on photo.



J.6 5LR289 feature profile, location is not known.



J.7 5LR289 overview of Features 1, 2, and 3. Image facing north/northeast.



J.8 5LR289 overview of Feature 7 (image left) and Feature 6 (image right) overview.



J.9 5LR289 site overview looking west. 1982 crew sitting in stone circles with Feature 1 upfront.



J.10 5LR289 overview of Features 6 (image left) and 5 (image right). Image facing north.



J.11 5LR289 overview of Features 7 (image left) and 6 (image right).



J.12 Overlooking 5LR289 feature excavations. Image facing east/northeast.

Appendix K: 5LR200 photographs from 1971 excavation.



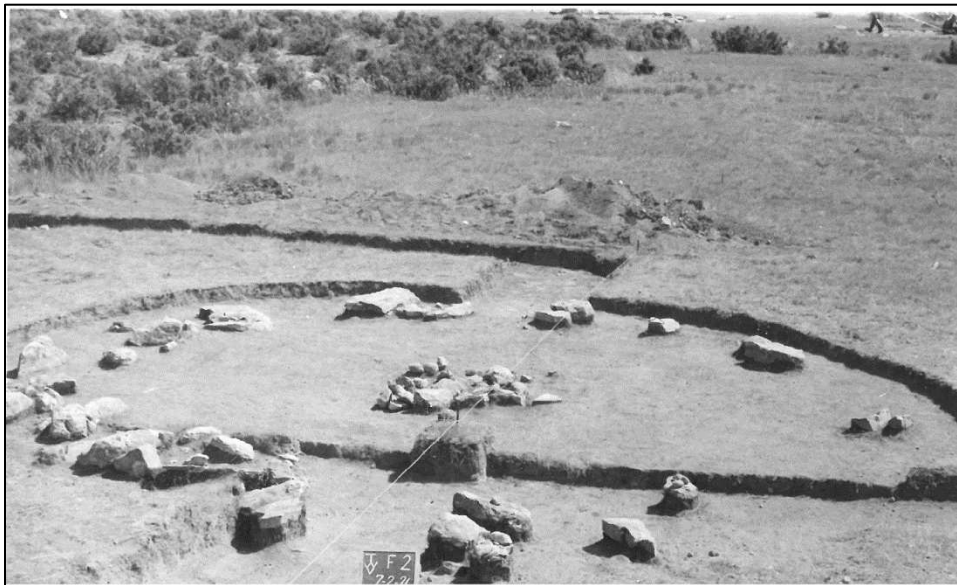
K.1: 5LR200 photograph of Feature 2. Thermal feature in center.



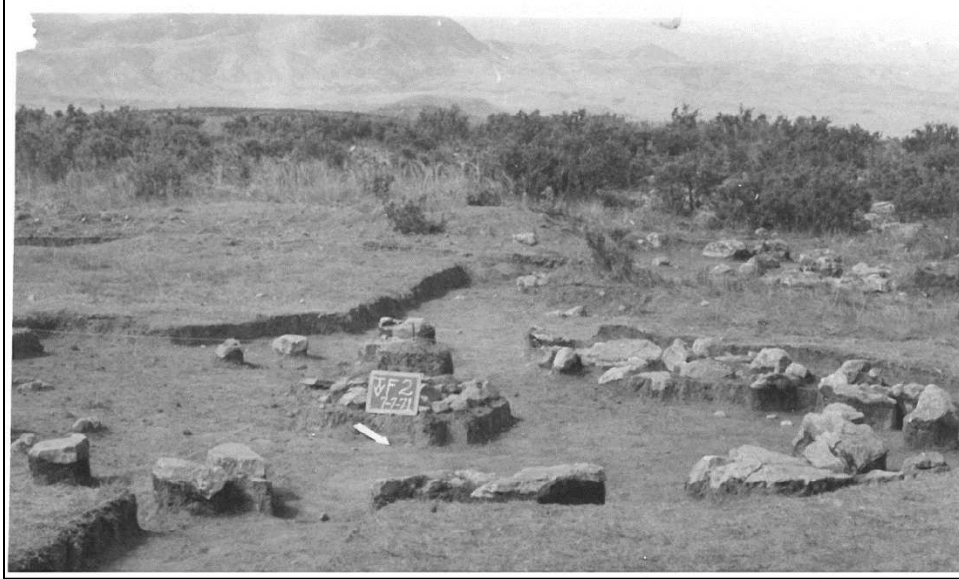
K.2: 5LR200 photograph of Feature 4 (front) and Feature 3 (back). Thermal feature in center of Feature 4.



K.3: Two crew members screen back dirt (likely Feature 2) while one crew member stands at photo stand (likely at site datum).



K.4: 5LR200 photograph of Feature 2. Thermal feature in center.



K.5: 5LR200 photograph of Feature 2. Thermal feature on pedestaled in center. White arrow points north.



K.6: 5LR200 excavation trench. Unknown location or feature.



K.7: 5LR200 excavation trench in unknown location.



K.8: 5LR200 crew member screens dirt at unknown feature.



K.9: 5LR200 two crew member screen dirt at unknown feature, possibly Feature 6 or 7.



K.10: 5LR200 excavation trench at unknown location.



K.11: 5LR200 two crew member screen dirt at unknown features.



K.12: 5LR200 Feature 1, level 1, concentration of rock. White arrow points north. Feature was determined to not be a stone ring.



K.13: 5LR200 Test trench 4. White arrow points north.

Appendix L: 5LR289 faunal data.

HFM #	Item	Grid	E/W	Grid	N/S	Level	Mass (g)	Element	Portion	Side	PF	DF	Burn	Spiral Fracture	Carni Mod	Cut	Max Length (mm)
46.137	bone	54	W	39	S	1	0.01	UN	US	N	5	5	1	0	0	0	3.0
46.169	bone	54	W	39	S	1	0.01	UN	US	N	5	5	1	0	0	0	3.1
46.174	bone	54	W	39	S	1	0.01	UN	US	N	5	5	1	0	0	0	3.2
46.129	bone	54	W	39	S	1	0.01	UN	US	N	5	5	1	0	0	0	3.5
46.141	bone	54	W	39	S	1	0.01	UN	US	N	5	5	1	0	0	0	3.8
46.158	bone	54	W	39	S	1	0.01	UN	US	N	5	5	1	0	0	0	3.8
46.139	bone	54	W	39	S	1	0.01	UN	US	N	5	5	1	0	0	0	3.8
46.76	bone	54	W	39	S	1	0.01	UN	US	N	5	5	1	0	0	0	4.7
46.149	bone	54	W	39	S	1	0.01	UN	US	N	5	5	1	0	0	0	4.7
32.4	bone	30	E	21	S	1	0.01	UN	US	N	5	5	0	0	0	0	4.7
46.161	bone	54	W	39	S	1	0.01	UN	US	N	5	5	1	0	0	0	5.0
46.168	bone	54	W	39	S	1	0.01	UN	US	N	5	5	1	0	0	0	5.0
46.145	bone	54	W	39	S	1	0.01	UN	US	N	5	5	1	0	0	0	5.4
46.166	bone	54	W	39	S	1	0.01	UN	US	N	5	5	1	0	0	0	5.5
46.173	bone	54	W	39	S	1	0.01	UN	US	N	5	5	1	0	0	0	5.5
38.2	bone	18	E	18	S	1	0.01	UN	US	N	5	5	0	0	0	0	5.7
46.167	bone	54	W	39	S	1	0.01	UN	US	N	5	5	1	0	0	0	5.9
33.1	bone	21	E	18	S	1	0.01	UN	US	N	5	5	2	0	0	0	5.9
46.162	bone	54	W	39	S	1	0.01	UN	US	N	5	5	1	0	0	0	5.9
46.156	bone	54	W	39	S	1	0.01	UN	US	N	5	5	1	0	0	0	6.0
46.171	bone	54	W	39	S	1	0.01	UN	US	N	5	5	1	0	0	0	6.2
36.35	bone	54	W	36	S	1	0.01	UN	US	N	5	5	0	0	0	0	6.2
40.13	tooth	54	W	33	S	NA	0.01	TFR	US	N	5	5	0	0	0	0	6.4
46.122	bone	54	W	39	S	1	0.01	UN	US	N	5	5	1	0	0	0	6.5
46.172	bone	54	W	39	S	1	0.01	UN	US	N	5	5	1	0	0	0	6.6
46.165	bone	54	W	39	S	1	0.01	UN	US	N	5	5	1	0	0	0	6.6
46.104	bone	54	W	39	S	1	0.01	UN	US	N	5	5	1	0	0	0	6.7
39.12	bone	12	W	27	S	NA	0.01	UN	US	N	5	5	0	0	0	0	6.7
46.157	bone	54	W	39	S	1	0.01	UN	US	N	5	5	1	0	0	0	6.7
46.127	bone	54	W	39	S	1	0.01	UN	US	N	5	5	1	0	0	0	6.8
46.85	bone	54	W	39	S	1	0.01	UN	US	N	5	5	1	0	0	0	6.8
46.106	bone	54	W	39	S	1	0.01	UN	US	N	5	5	1	0	0	0	6.9
46.142	bone	54	W	39	S	1	0.01	UN	US	N	5	5	1	0	0	0	6.9

HFM #	Item	Grid	E/W	Grid	N/S	Level	Mass (g)	Element	Portion	Side	PF	DF	Burn	Spiral Fracture	Carni Mod	Cut	Max Length (mm)
27.4	bone	17	W	27	S	1	0.01	UN	US	N	5	5	0	0	0	0	7.1
46.65	bone	54	W	39	S	1	0.01	UN	US	N	5	5	1	0	0	0	7.1
46.97	bone	54	W	39	S	1	0.01	UN	US	N	5	5	1	0	0	0	7.1
46.105	bone	54	W	39	S	1	0.01	UN	US	N	5	5	1	0	0	0	7.2
46.107	bone	54	W	39	S	1	0.01	UN	US	N	5	5	1	0	0	0	7.3
46.86	bone	54	W	39	S	1	0.01	UN	US	N	5	5	1	0	0	0	7.3
46.123	bone	54	W	39	S	1	0.01	UN	US	N	5	5	1	0	0	0	7.3
46.67	bone	54	W	39	S	1	0.01	UN	US	N	5	5	1	0	0	0	7.3
46.93	bone	54	W	39	S	1	0.10	UN	US	N	5	5	1	0	0	0	7.4
46.75	bone	54	W	39	S	1	0.01	UN	US	N	5	5	1	0	0	0	7.4
46.119	bone	54	W	39	S	1	0.01	UN	US	N	5	5	1	0	0	0	7.5
46.95	bone	54	W	39	S	1	0.01	UN	US	N	5	5	1	0	0	0	7.5
46.103	bone	54	W	39	S	1	0.01	UN	US	N	5	5	1	0	0	0	7.6
46.79	bone	54	W	39	S	1	0.01	UN	US	N	5	5	1	0	0	0	7.6
36.39	bone	54	W	36	S	1	0.01	UN	US	N	5	5	0	0	0	0	7.6
46.96	bone	54	W	39	S	1	0.01	UN	US	N	5	5	1	0	0	0	7.7
46.159	bone	54	W	39	S	1	0.01	UN	US	N	5	5	1	0	0	0	7.8
46.133	bone	54	W	39	S	1	0.01	UN	US	N	5	5	1	0	0	0	7.8
27.5	bone	17	W	27	S	1	0.01	UN	US	N	5	5	0	0	0	0	7.8
36.41	bone	54	W	36	S	1	0.01	UN	US	N	5	5	0	0	0	0	7.8
46.154	bone	54	W	39	S	1	0.01	UN	US	N	5	5	1	0	0	0	7.9
46.98	bone	54	W	39	S	1	0.01	UN	US	N	5	5	1	0	0	0	7.9
46.135	bone	54	W	39	S	1	0.01	UN	US	N	5	5	1	0	0	0	8.0
46.35	bone	54	W	39	S	1	0.10	UN	US	N	5	5	1	0	0	0	8.0
46.69	bone	54	W	39	S	1	0.01	UN	US	N	5	5	1	0	0	0	8.0
46.109	bone	54	W	39	S	1	0.01	UN	US	N	5	5	1	0	0	0	8.1
46.121	bone	54	W	39	S	1	0.01	UN	US	N	5	5	1	0	0	0	8.1
30.6	bone	15	W	25	S	1	0.01	UN	US	N	5	5	0	0	0	0	8.2
46.74	bone	54	W	39	S	1	0.01	UN	US	N	5	5	1	0	0	0	8.2
46.138	bone	54	W	39	S	1	0.01	UN	US	N	5	5	1	0	0	0	8.3
46.72	bone	54	W	39	S	1	0.01	UN	US	N	5	5	1	0	0	0	8.3
46.134	bone	54	W	39	S	1	0.01	UN	US	N	5	5	1	0	0	0	8.3
46.61	bone	54	W	39	S	1	0.10	UN	US	N	5	5	1	0	0	0	8.3
46.164	bone	54	W	39	S	1	0.01	UN	US	N	5	5	1	0	0	0	8.3

HFM #	Item	Grid	E/W	Grid	N/S	Level	Mass (g)	Element	Portion	Side	PF	DF	Burn	Spiral Fracture	Carni Mod	Cut	Max Length (mm)
46.101	bone	54	W	39	S	1	0.01	UN	US	N	5	5	1	0	0	0	8.3
40.18	bone	54	W	33	S	1	0.01	UN	US	N	5	5	1	0	0	0	8.4
46.82	bone	54	W	39	S	1	0.01	UN	US	N	5	5	1	0	0	0	8.4
46.87	bone	54	W	39	S	1	0.01	UN	US	N	5	5	1	0	0	0	8.5
46.113	bone	54	W	39	S	1	0.01	UN	US	N	5	5	1	0	0	0	8.5
36.36	bone	54	W	36	S	1	0.01	UN	US	N	5	5	0	0	0	0	8.5
46.131	bone	54	W	39	S	1	0.01	UN	US	N	5	5	1	0	0	0	8.6
46.147	bone	54	W	39	S	1	0.01	UN	US	N	5	5	1	0	0	0	8.6
46.151	bone	54	W	39	S	1	0.01	UN	US	N	5	5	1	0	0	0	8.6
46.94	bone	54	W	39	S	1	0.10	UN	US	N	5	5	1	0	0	0	8.7
46.117	bone	54	W	39	S	1	0.01	UN	US	N	5	5	1	0	0	0	8.9
46.99	bone	54	W	39	S	1	0.01	UN	US	N	5	5	1	0	0	0	8.9
46.83	bone	54	W	39	S	1	0.01	UN	US	N	5	5	1	0	0	0	8.9
46.152	bone	54	W	39	S	1	0.01	UN	US	N	5	5	1	0	0	0	8.9
46.62	bone	54	W	39	S	1	0.01	UN	US	N	5	5	1	0	0	0	9.0
46.148	bone	54	W	39	S	1	0.01	UN	US	N	5	5	1	0	0	0	9.0
46.155	bone	54	W	39	S	1	0.01	UN	US	N	5	5	1	0	0	0	9.0
46.143	bone	54	W	39	S	1	0.01	UN	US	N	5	5	1	0	0	0	9.0
46.153	bone	54	W	39	S	1	0.01	UN	US	N	5	5	1	0	0	0	9.1
33.3	bone	21	E	18	S	1	0.10	UN	US	N	5	5	0	0	0	0	9.1
46.63	bone	54	W	39	S	1	0.10	UN	US	N	5	5	1	0	0	0	9.1
46.84	bone	54	W	39	S	1	0.01	UN	US	N	5	5	1	0	0	0	9.1
36.28	bone	54	W	36	S	1	0.01	UN	US	N	5	5	0	0	0	0	9.2
43.1	bone	18	E	15	S	NA	0.30	UN	US	N	5	5	0	0	0	0	9.3
46.144	bone	54	W	39	S	1	0.01	UN	US	N	5	5	1	0	0	0	9.3
46.34	bone	54	W	39	S	1	0.10	UN	US	N	5	5	1	0	0	0	9.4
46.51	bone	54	W	39	S	1	0.20	UN	US	N	5	5	1	0	0	0	9.4
46.132	bone	54	W	39	S	1	0.01	UN	US	N	5	5	1	0	0	0	9.5
46.124	bone	54	W	39	S	1	0.01	UN	US	N	5	5	1	0	0	0	9.5
30.5	bone	15	W	25	S	1	0.01	UN	US	N	5	5	0	0	0	0	9.5
36.38	bone	54	W	36	S	1	0.01	UN	US	N	5	5	0	0	0	0	9.5
46.77	bone	54	W	39	S	1	0.01	UN	US	N	5	5	1	0	0	0	9.7
46.102	bone	54	W	39	S	1	0.01	UN	US	N	5	5	1	0	0	0	9.7
46.92	bone	54	W	39	S	1	0.10	UN	US	N	5	5	1	0	0	0	9.7

HFM #	Item	Grid	E/W	Grid	N/S	Level	Mass (g)	Element	Portion	Side	PF	DF	Burn	Spiral Fracture	Carni Mod	Cut	Max Length (mm)
46.71	bone	54	W	39	S	1	0.10	UN	US	N	5	5	1	0	0	0	9.7
34.1	bone	51	W	33	S	2	0.10	UN	US	N	5	5	0	0	0	0	9.8
46.118	bone	54	W	39	S	1	0.01	UN	US	N	5	5	1	0	0	0	9.9
46.163	bone	54	W	39	S	1	0.01	UN	US	N	5	5	1	0	0	0	10.1
46.115	bone	54	W	39	S	1	0.01	UN	US	N	5	5	1	0	0	0	10.2
46.146	bone	54	W	39	S	1	0.01	UN	US	N	5	5	1	0	0	0	10.2
46.57	bone	54	W	39	S	1	0.01	UN	US	N	5	5	1	0	0	0	10.2
46.68	bone	54	W	39	S	1	0.01	UN	US	N	5	5	1	0	0	0	10.2
46.66	bone	54	W	39	S	1	0.01	UN	US	N	5	5	1	0	0	0	10.2
46.33	bone	54	W	39	S	1	0.20	UN	US	N	5	5	1	0	0	0	10.3
46.136	bone	54	W	39	S	1	0.01	UN	US	N	5	5	1	0	0	0	10.4
34.2	bone	51	W	33	S	2	0.10	UN	US	N	5	5	0	0	0	0	10.5
46.78	bone	54	W	39	S	1	0.01	UN	US	N	5	5	1	0	0	0	10.7
46.114	bone	54	W	39	S	1	0.01	UN	US	N	5	5	1	0	0	0	10.8
36.37	bone	54	W	36	S	1	0.01	UN	US	N	5	5	0	0	0	0	10.8
46.73	bone	54	W	39	S	1	0.01	UN	US	N	5	5	1	0	0	0	10.8
46.64	bone	54	W	39	S	1	0.10	UN	US	N	5	5	1	0	0	0	11.0
44.1	bone	51	W	36	S	1	0.30	UN	US	N	5	5	0	0	0	0	11.1
46.36	bone	54	W	39	S	1	0.10	UN	US	N	5	5	1	0	0	0	11.1
46.111	bone	54	W	39	S	1	0.01	UN	US	N	5	5	1	0	0	0	11.2
36.23	bone	54	W	36	S	1	0.01	UN	US	N	5	5	0	0	0	0	11.2
46.37	bone	54	W	39	S	1	0.10	UN	US	N	5	5	1	0	0	0	11.2
46.108	bone	54	W	39	S	1	0.01	UN	US	N	5	5	1	0	0	0	11.2
46.52	bone	54	W	39	S	1	0.10	UN	US	N	5	5	1	0	0	0	11.3
46.59	bone	54	W	39	S	1	0.10	UN	US	N	5	5	1	0	0	0	11.3
46.125	bone	54	W	39	S	1	0.01	UN	US	N	5	5	1	0	0	0	11.3
46.81	bone	54	W	39	S	1	0.01	UN	US	N	5	5	1	0	0	0	11.4
30.2	bone	15	W	25	S	1	0.10	UN	US	N	5	5	0	0	0	0	11.7
48.5	bone	21	E	15	S	1	0.10	UN	US	N	5	5	0	0	0	0	11.8
36.32	bone	54	W	36	S	1	0.01	UN	US	N	5	5	0	0	0	0	12.0
46.49	bone	54	W	39	S	1	0.10	UN	US	N	5	5	1	0	0	0	12.0
46.41	bone	54	W	39	S	1	0.10	UN	US	N	5	5	1	0	0	0	12.3
46.43	bone	54	W	39	S	1	0.10	UN	US	N	5	5	1	0	0	0	12.3
46.126	bone	54	W	39	S	1	0.01	UN	US	N	5	5	1	0	0	0	12.4

HFM #	Item	Grid	E/W	Grid	N/S	Level	Mass (g)	Element	Portion	Side	PF	DF	Burn	Spiral Fracture	Carni Mod	Cut	Max Length (mm)
46.53	bone	54	W	39	S	1	0.10	UN	US	N	5	5	1	0	0	0	12.5
46.112	bone	54	W	39	S	1	0.01	UN	US	N	5	5	1	0	0	0	12.6
46.22	tooth	39	W	24	S	1	0.01	TFR	US	N	5	5	0	0	0	0	12.7
39.8	bone	12	W	27	S	NA	0.20	UN	US	N	5	5	0	0	0	0	12.8
36.18	bone	54	W	36	S	1	0.10	UN	US	N	5	5	0	0	0	0	12.8
46.29	bone	54	W	39	S	1	0.20	UN	US	N	5	5	1	0	0	0	12.8
46.89	bone	54	W	39	S	1	0.10	UN	US	N	5	5	1	0	0	0	12.9
46.116	bone	54	W	39	S	1	0.01	UN	US	N	5	5	1	0	0	0	13.0
46.21	bone	39	W	24	S	1	0.40	UN	US	N	5	5	0	0	0	0	13.0
36.31	bone	54	W	36	S	1	0.01	UN	US	N	5	5	0	0	0	0	13.0
46.39	bone	54	W	39	S	1	0.10	UN	US	N	5	5	1	0	0	0	13.1
46.45	bone	54	W	39	S	1	0.01	UN	US	N	5	5	1	0	0	0	13.2
46.47	bone	54	W	39	S	1	0.20	UN	US	N	5	5	1	0	0	0	13.3
36.25	bone	54	W	36	S	1	0.01	UN	US	N	5	5	0	0	0	0	14.0
39.11	bone	12	W	27	S	NA	0.10	UN	US	N	5	5	0	0	0	0	14.2
46.19	tooth	39	W	24	S	1	0.20	TFR	US	N	5	5	0	0	0	0	14.2
46.42	bone	54	W	39	S	1	0.01	UN	US	N	5	5	1	0	0	0	14.2
46.46	bone	54	W	39	S	1	0.10	UN	US	N	5	5	1	0	0	0	14.2
36.29	bone	54	W	36	S	1	0.10	UN	US	N	5	5	0	0	0	0	14.3
36.27	bone	54	W	36	S	1	0.10	UN	US	N	5	5	0	0	0	0	14.4
40.2	bone	54	W	33	S	1	0.30	UN	US	N	5	5	1	0	0	0	14.4
36.33	bone	54	W	36	S	1	0.01	UN	US	N	5	5	0	0	0	0	14.6
46.28	bone	54	W	39	S	1	0.10	UN	US	N	5	5	1	0	0	0	14.8
46.55	bone	54	W	39	S	1	0.30	UN	US	N	5	5	1	0	0	0	14.8
46.56	bone	54	W	39	S	1	0.20	UN	US	N	5	5	1	0	0	0	15.0
46.58	bone	54	W	39	S	1	0.10	UN	US	N	5	5	1	0	0	0	15.1
48.2	bone	21	E	15	S	2	0.60	UN	US	N	5	5	0	0	0	0	15.1
46.15	bone	39	W	24	S	1	0.50	UN	US	N	5	5	1	0	0	0	15.2
48.1	bone	21	E	15	S	2	0.20	UN	US	N	5	5	0	0	0	0	15.3
39.9	bone	12	W	27	S	NA	0.20	UN	US	N	5	5	0	0	0	0	15.4
46.14	bone	39	W	24	S	1	0.80	UN	US	N	5	5	1	0	0	0	15.5
34.3	bone	51	W	33	S	2	0.80	UN	US	N	5	5	0	0	0	0	15.6
39.4	bone	12	W	27	S	NA	0.60	UN	US	N	5	5	0	0	0	0	15.7
39.6	bone	12	W	27	S	NA	0.50	UN	US	N	5	5	0	0	0	0	15.7

HFM #	Item	Grid	E/W	Grid	N/S	Level	Mass (g)	Element	Portion	Side	PF	DF	Burn	Spiral Fracture	Carni Mod	Cut	Max Length (mm)
40.14	bone	54	W	33	S	1	0.01	UN	US	N	5	5	0	0	0	0	15.7
36.34	bone	54	W	36	S	1	0.01	UN	US	N	5	5	0	0	0	0	15.7
46.38	bone	54	W	39	S	1	0.20	UN	US	N	5	5	1	0	0	0	15.7
46.91	bone	54	W	39	S	1	0.10	UN	US	N	5	5	1	0	0	0	15.7
46.44	bone	54	W	39	S	1	0.10	UN	US	N	5	5	1	0	0	0	16.0
46.31	bone	54	W	39	S	1	0.20	UN	US	N	5	5	1	0	0	0	16.4
27.3	bone	17	W	27	S	1	0.10	UN	US	N	5	5	0	0	0	0	16.5
40.17	bone	54	W	33	S	1	0.01	UN	US	N	5	5	0	0	0	0	16.6
32.2	bone	30	E	21	S	1	0.10	UN	US	N	5	5	0	0	0	0	16.7
34.4	bone	51	W	33	S	2	0.40	UN	US	N	5	5	0	0	0	0	16.7
46.48	bone	54	W	39	S	1	0.20	UN	US	N	5	5	1	0	0	0	17.0
43.2	bone	18	E	15	S	NA	0.20	UN	US	N	5	5	0	0	0	0	17.1
46.25	bone	39	W	24	S	1	0.50	UN	US	N	5	5	0	0	0	0	17.1
35.2	tooth	21	E	21	S	1	0.20	TFR	US	N	5	5	0	0	0	0	17.2
36.21	bone	54	W	36	S	1	0.30	UN	US	N	5	5	0	0	0	0	17.4
32.1	bone	30	E	21	S	1	0.10	UN	US	N	5	5	0	0	0	0	17.5
46.32	bone	54	W	39	S	1	0.40	UN	US	N	5	5	1	0	0	0	17.6
36.15	bone	54	W	36	S	1	0.30	UN	US	N	5	5	0	0	0	0	17.7
46.54	bone	54	W	39	S	1	0.20	UN	US	N	5	5	1	0	0	0	17.7
36.24	bone	54	W	36	S	1	0.01	UN	US	N	5	5	0	0	0	0	18.0
40.16	bone	54	W	33	S	1	0.01	UN	US	N	5	5	0	0	0	0	18.1
30.3	tooth	15	W	25	S	1	0.30	TFR	US	N	5	5	0	0	0	0	18.6
46.27	bone	54	W	39	S	1	0.20	UN	US	N	5	5	1	0	0	0	18.6
40.15	bone	54	W	33	S	1	0.01	UN	US	N	5	5	0	0	0	0	18.7
46.128	bone	54	W	39	S	1	0.01	UN	US	N	5	5	1	0	0	0	19.0
46.26	bone	24	W	39	S	1	0.70	UN	US	N	5	5	1	0	0	0	19.1
48.3	bone	21	E	15	S	1	0.70	UN	US	N	5	5	0	0	0	0	19.4
48.4	bone	21	E	15	S	1	0.80	UN	US	N	5	5	0	0	0	0	19.6
36.11	bone	54	W	36	S	1	0.30	UN	US	N	5	5	0	0	0	0	20.0
36.16	bone	54	W	36	S	1	0.10	UN	US	N	5	5	0	0	0	0	20.0
46.5	bone	39	W	24	S	1	0.60	UN	US	N	5	5	0	0	0	0	20.4
36.26	bone	54	W	36	S	1	0.10	UN	US	N	5	5	0	0	0	0	20.6
32.3	bone	30	E	21	S	1	0.01	UN	US	N	5	5	0	0	0	0	20.7
47.1	bone	54	W	36	S	2	0.20	MD									20.9

HFM #	Item	Grid	E/W	Grid	N/S	Level	Mass (g)	Element	Portion	Side	PF	DF	Burn	Spiral Fracture	Carni Mod	Cut	Max Length (mm)
39.5	bone	12	W	27	S	NA	0.60	UN	US	N	5	5	0	0	0	0	20.9
46.88	bone	54	W	39	S	1	0.10	UN	US	N	5	5	1	0	0	0	20.9
36.19	bone	54	W	36	S	1	0.30	UN	US	N	5	5	0	0	0	0	21.0
40.11	bone	54	W	33	S	1	0.50	UN	US	N	5	5	0	0	0	0	21.0
46.24	bone	39	W	24	S	1	0.30	UN	US	N	5	5	0	0	0	0	21.8
40.12	bone	54	W	33	S	1	0.40	UN	US	N	5	5	0	0	0	0	21.8
38.1	bone	18	E	18	S	1	0.20	UN	US	N	5	5	0	0	0	0	21.9
39.1	bone	12	W	27	S	1	0.90	UN	US	N	5	5	0	0	0	0	22.7
46.13	bone	39	W	24	S	1	1.30	UN	US	N	5	5	1	0	0	0	22.8
36.12	bone	54	W	36	S	1	0.30	UN	US	N	5	5	0	0	0	0	22.9
40.1	bone	54	W	33	S	2	0.20	UN	US	N	5	5	0	0	0	0	23.2
39.3	bone	12	W	27	S	1	0.70	UN	US	N	5	5	0	0	0	0	23.9
30.4	bone	15	W	25	S	1	0.30	UN	US	N	5	5	0	0	0	0	24.1
39.7	bone	12	W	27	S	NA	0.40	UN	US	N	5	5	0	0	0	0	25.2
40.9	bone	54	W	33	S	1	0.70	UN	US	N	5	5	0	0	0	0	25.4
46.23	bone	39	W	24	S	1	0.50	UN	US	N	5	5	0	0	0	0	25.7
39.2	bone	12	W	27	S	1	2.00	UN	US	N	5	5	0	0	0	0	25.9
36.17	bone	54	W	36	S	1	0.30	UN	US	N	5	5	0	0	0	0	26.2
46.6	bone	39	W	24	S	1	1.60	UN	US	N	5	5	1	0	0	0	26.2
36.22	bone	54	W	36	S	1	0.10	UN	US	N	5	5	0	0	0	0	26.4
46.17	bone	36	W	24	S	1	1.30	UN	US	N	5	5	0	0	0	0	26.4
46.11	bone	39	W	24	S	1	1.30	UN	US	N	5	5	0	0	0	0	26.7
46.18	bone	36	W	24	S	1	1.00	UN	US	N	5	5	0	0	0	0	28.3
31.1	bone	15	W	27	S	1	0.80	UN	US	N	5	5	0	0	0	0	29.4
47.2	bone	54	W	36	S	2	2.90	RB	DS	N	5	5	1	0	0	0	30.2
36.13	bone	54	W	36	S	1	0.40	UN	US	N	5	5	0	0	0	0	31.0
40.6	bone	54	W	33	S	1	1.20	UN	US	N	5	5	0	0	0	0	31.9
36.14	bone	54	W	36	S	1	0.90	UN	US	N	5	5	0	0	0	0	32.6
40.8	bone	54	W	33	S	1	2.30	UN	US	N	5	5	0	0	0	0	32.8
27.2	bone	17	W	27	S	1	2.30	RB	DS	N	5	5	0	0	0	0	32.9
36.4	tooth	54	W	36	S	1	6.60	TFR	US	N	5	5	0	0	0	0	33.4
46.12	bone	39	W	24	S	1	1.50	UN	US	N	5	5	2	0	0	0	34.1
36.8	bone	54	W	36	S	1	1.30	UN	US	N	5	5	0	0	0	0	34.8
46.7	bone	39	W	24	S	1	2.80	UN	US	N	5	5	1	0	0	0	35.6

HFM #	Item	Grid	E/W	Grid	N/S	Level	Mass (g)	Element	Portion	Side	PF	DF	Burn	Spiral Fracture	Carni Mod	Cut	Max Length (mm)
36.5	bone	54	W	36	S	1	3.00	UN	US	N	5	5	0	0	0	0	36.3
40.3	bone	54	W	33	S	2	3.50	UN	US	N	5	5	0	0	0	0	36.4
40.4	bone	54	W	33	S	2	0.90	UN	US	N	5	5	0	0	0	0	36.8
46.1	bone	24	W	39	S	1	3.80	UN	US	N	5	5	1	0	0	0	39.9
36.9	bone	54	W	36	S	1	0.60	UN	US	N	5	5	0	0	0	0	40.1
46.4	bone	39	W	24	S	1	3.70	UN	US	N	5	5	0	0	0	0	40.8
27.1	bone	17	W	27	S	1	5.70	IM	US	N	5	5	0	0	0	0	41.1
35.1	bone	9	E	24	S	3	17.10	PHS	US	N	3	3	0	0	0	0	44.4
40.7	bone	54	W	33	S	1	2.80	UN	US	N	5	5	0	0	0	0	45.2
46.2	bone	39	W	24	S	1	0.80	UN	US	N	5	5	1	0	0	0	45.3
36.7	bone	54	W	36	S	1	2.00	UN	US	N	5	5	0	0	0	0	47.3
28.1	bone	18	E	12	S	1	1.80	RB	BL	N	5	5	0	0	0	0	50.1
46.16	bone	42	W	24	S	1	7.50	UN	US	N	5	5	0	0	0	0	51.1
46.9	bone	39	W	29	S	1	2.20	UN	US	N	5	5	0	0	0	0	51.5
40.5	bone	54	W	33	S	1	3.10	UN	US	N	5	5	0	0	0	0	56.8
36.6	bone	54	W	36	S	1	6.20	LB	US	N	5	5	0	0	0	0	57.2
42.1	bone	60	W	39	S	3	8.00	UN	US	N	5	5	0	0	0	0	57.6
36.1	bone	54	W	36	S	1	6.50	UN	US	N	5	5	0	0	0	0	61.6
31.2	bone	15	W	27	S	1	8.50	UN	US	N	5	5	1	0	0	0	61.8
37.1	bone	51	W	33	S	2	48.50	AS	CO	R	5	5	0	0	0	0	67.8
46.3	bone	29	W	39	S	1	3.90	UN	US	N	5	5	0	0	0	0	69.2
46.8	bone	39	W	24	S	1	21.20	RB	PR	L	5	5	0	0	0	0	73.6
41.1	bone	9	E	30	S	1	11.50	FM		L?			1				79.5
36.2	bone	54	W	36	S	1	14.80	LB	US	N	5	5	0	0	0	0	84.8
30.1	bone	15	W	25	S	1	7.00	LB	US	N	5	5	1	0	0	0	86.2
36.3	bone	54	W	36	S	1	6.80	LB	US	N	5	5	0	0	0	0	86.5
31.3	bone	15	W	27	S	1	17.30	LB	US	N	5	5	0	0	0	0	100.1
29.1	bone	NA	NA	NA	NA	1	8.50	RB	SHAFT	N	5	5	0	0	0	0	108.4

Appendix M: 5LR200 faunal data.

HFM #	Item	Grid	Level	T	Mass (g)	Element	Portion	Side	PF	DF	Burn	Spiral Fracture	Carni Mod	Cut	Max Length (mm)
30.1	bone	C2	.3'-.5'	NA	41.50	PHF	CO	N	3?	3?	0	0	0	0	61.2
45.1	bone	D2	3	4	0.30	UN	US	N	5	5	1	0	0	0	15.4
45.2	bone	D2	3	NA	0.80	UN	US	N	5	5	0	0	0	0	36.8
44.1	bone	D5	1	NA	24.40	FM	SH	L	5	5	0	1	0	0	101.4
29.1	tooth	D5	1	NA	0.20	UN	US	N	5	5	0	0	0	0	19.6
29.2	bone	D5	1	NA	1.80	UN	US	N	5	5	0	0	0	0	41.8
29.3	bone	D5	1	NA	0.50	UN	US	N	5	5	0	0	0	0	22.3
29.4	bone	D5	1	NA	1.00	UN	US	N	5	5	0	0	0	0	32.0
29.5	bone	D5	NA	NA	0.20	UN	US	N	5	5	0	0	0	0	11.7
29.6	tooth	D5	NA	NA	0.01	UN	US	N	5	5	0	0	0	0	11.7
33.1	bone	C5	NA	NA	9.10	LB	US	N	5	5	0	0	0	0	61.8
33.3	bone	C5	NA	NA	25.80	RD	PR	R	0	5	0	0	0	0	89.7
27.1	tooth	C5	NA	NA	0.01	TFR	US	N	5	5	0	0	0	0	10.1
33.2	bone	C5	1	2	18.10	UL	PR?	N	5	5	0	0	0	0	134.9
27.2	bone	C5	NA	NA	4.50	UN	US	N	5	5	0	0	0	0	60.1
27.15	bone	C5	NA	NA	1.70	UN	US	N	5	5	0	0	0	0	37.5
27.16	bone	C5	NA	NA	0.20	UN	US	N	5	5	0	0	0	0	32.3
27.6	bone	C5	NA	NA	0.40	UN	US	N	5	5	0	0	0	0	32.6
26.1	bone	C6	NA	NA	0.20	UN	US	N	5	5	0	0	0	0	19.0
26.11	bone	C6	NA	NA	0.10	UN	US	N	5	5	0	0	0	0	9.3
26.12	bone	C6	NA	NA	0.01	UN	US	N	5	5	0	0	0	0	7.8
26.2	bone	C6	NA	NA	0.20	UN	US	N	5	5	1	0	0	0	8.5
26.3	bone	C6	NA	NA	0.60	UN	US	N	5	5	2	0	0	0	19.9
26.4	bone	C6	NA	NA	0.50	UN	US	N	5	5	2	0	0	0	13.9
26.5	bone	C6	NA	NA	0.40	UN	US	N	5	5	2	0	0	0	14.9
26.6	bone	C6	NA	NA	0.10	UN	US	N	5	5	2	0	0	0	9.1
26.7	bone	C6	NA	NA	0.01	UN	US	N	5	5	2	0	0	0	10.2
26.8	bone	C6	NA	NA	0.70	UN	US	N	5	5	0	0	0	0	14.5
26.9	bone	C6	NA	NA	0.20	UN	US	N	5	5	0	0	0	0	12.4
40.1	bone	C6	3.5'	NA	0.10	UN	US	N	5	5	0	0	0	0	11.9
36.1	tooth	F8	NA	NA	0.30	TFR	US	N	5	5	0	0	0	0	12.6

HFM #	Item	Grid	Level	T	Mass (g)	Element	Portion	Side	PF	DF	Burn	Spiral Fracture	Carni Mod	Cut	Max Length (mm)
36.2	bone	F8	NA	NA	0.40	UN	US	N	5	5	0	0	0	0	16.5
43.1	tooth	D23	S	NA	0.50	TFR	US	US	5	5	0	0	0	0	20.9
33.4	bone	C5	NA	3	0.70	UN	US	N	5	5	0	0	0	0	33.4
33.5	bone	C5	NA	3	0.01	UN	US	N	5	5	0	0	0	0	12.6
33.7	bone	C5	NA	3	0.10	UN	US	N	5	5	0	0	0	0	9.0
33.8	bone	C5	NA	3	0.20	UN	US	N	5	5	0	0	0	0	14.3
33.9	tooth	C5	NA	3	0.10	UN	US	N	5	5	0	0	0	0	8.0
33.11	bone	C5	NA	NA	0.01		US	N	5	5	0	0	0	0	12.8
34.3	bone	C18-19	2	NA	1.00	MR	NA	NA	NA	NA	0	0	0	0	37.9
34.4	bone	C18-19	2	NA	2.60	MR	NA	NA	NA	NA	0	0	0	0	32.4
34.7	bone	C18-19	2	NA	1.40	MR	HRM?	?	5	5	0	0	0	0	25.0
34.9	bone	C18-19	2	NA	6.10	MR	CP	L	0	0	0	0	0	0	57.4
34.2	tooth	C18-19	2	NA	2.50	MUN	NA	NA	NA	NA	0	0	0	0	32.4
34.5	tooth	C18-19	2	NA	1.10	MUN	NA	NA	NA	NA	0	0	0	0	24.2
34.17	tooth	C18-19	2	NA	0.70	TFR	US	N	NA	NA	0	0	0	0	20.8
34.18	tooth	C18-19	2	NA	0.30	TFR	NA	NA	NA	NA	0	0	0	0	19.7
34.19	tooth	C18-19	2	NA	0.10	TFR	NA	NA	NA	NA	0	0	0	0	17.4
34.21	tooth	C18-19	NA	NA	0.20	TFR	NA	NA	NA	NA	0	0	0	0	12.3
34.22	tooth	C18-19	NA	NA	0.01	TFR	NA	NA	NA	NA	0	0	0	0	16.9
34.1	bone	C18-19	2	NA	0.40	UN	US	N	NA	NA	0	0	0	0	26.7
34.11	bone	C18-19	2	NA	0.40	UN	US	N	NA	NA	0	0	0	0	23.7
34.12	bone	C18-19	2	NA	0.01	UN	US	N	NA	NA	0	0	0	0	19.9
34.13	bone	C18-19	2	NA	0.30	UN	US	N	NA	NA	0	0	0	0	18.4
34.14	bone	C18-19	2	NA	0.40	UN	US	N	NA	NA	0	0	0	0	16.6
34.15	bone	C18-19	2	NA	0.90	UN	US	N	NA	NA	0	0	0	0	23.6
34.16	bone	C18-19	2	NA	0.30	UN	US	N	NA	NA	0	0	0	0	17.4
34.6	bone	C18-19	2	NA	0.30	UN	NA	NA	NA	NA	0	0	0	0	19.3
34.8	bone	C18-19	2	NA	0.30	UN	NA	NA	NA	NA	0	0	0	0	20.1
37.1	bone	B18	1	NA	0.10	UN	US	N	5	5	1	0	0	0	10.0
41.1	bone	C19	2	NA	0.60	UN	US	N	5	5	0	0	0	0	14.9
41.2	bone	C19	2	NA	0.01	UN	US	N	5	5	0	0	0	0	7.1
38.1	bone	C18	2	NA	0.60	UN	US	N	5	5	0	0	0	0	24.5

HFM #	Item	Grid	Level	T	Mass (g)	Element	Portion	Side	PF	DF	Burn	Spiral Fracture	Carni Mod	Cut	Max Length (mm)
38.11	bone	C18	2	NA	0.01	UN	US	N	5	5	0	0	0	0	6.8
38.12	bone	C18	2	NA	0.01	UN	US	N	5	5	0	0	0	0	8.5
38.13	bone	C18	2	NA	0.01	UN	US	N	5	5	0	0	0	0	5.6
38.14	bone	C18	2	NA	0.01	UN	US	N	5	5	0	0	0	0	6.6
38.15	bone	C18	2	NA	0.01	UN	US	N	5	5	1	0	0	0	9.2
38.16	bone	C18	2	NA	0.01	UN	US	N	5	5	1	0	0	0	6.5
38.17	bone	C18	2	NA	0.01	UN	US	N	5	5	1	0	0	0	7.8
38.2	bone	C18	2	NA	0.60	UN	US	N	5	5	0	0	0	0	25.8
38.3	bone	C18	2	NA	0.10	UN	US	N	5	5	0	0	0	0	16.7
38.4	bone	C18	2	NA	0.10	UN	US	N	5	5	0	0	0	0	25.5
38.5	bone	C18	2	NA	0.01	UN	US	N	5	5	0	0	0	0	15.0
38.6	bone	C18	2	NA	0.01	UN	US	N	5	5	0	0	0	0	17.7
38.7	bone	C18	2	NA	0.01	UN	US	N	5	5	0	0	0	0	7.2
38.8	bone	C18	2	NA	0.01	UN	US	N	5	5	0	0	0	0	11.5
38.9	bone	C18	2	NA	0.01	UN	US	N	5	5	0	0	0	0	6.8
39.1	bone	C18-19	1	NA	0.01	UN	US	N	5	5	1	0	0	0	15.6
42.1	bone	C19	1	NA	0.20	UN	US	N	5	5	0	0	0	0	21.3
34.23	bone	C18-19	NA	NA	0.01						0	0	0	0	9.7
32.1	bone	B21	0-.3'	3	0.10	UN	US	N	5	5	1	0	0	0	11.1
32.2	bone	B21	0-.3'	3	0.20	UN	US	N	5	5	1	0	0	0	11.9
32.3	bone	B21	0-.3'	3	0.40	UN	US	N	5	5	1	0	0	0	13.2
32.4	bone	B21	0-.3'	3	0.10	UN	US	N	5	5	1	0	0	0	11.7
32.5	bone	B21	0.3'	3	0.01	UN	US	N	5	5	1	0	0	0	8.8
28.1	bone	O96	2	NA	0.20	UN	US	N	5	5	0	0	0	0	20.8
28.2	bone	O96	1	NA	0.10	UN	US	N	5	5	0	0	0	0	13.6
44.2	bone	D6?	NA	NA	19.30	LB	US	N	5	5	0	0	0	0	113.3
44.5	bone	D6?	NA	NA	13.10	LB	US	N	5	5	0	0	0	0	90.6
44.3	bone	D6?	NA	NA	2.20	LB	US	N	5	5	0	0	0	0	69.4
44.4	bone	D6?	NA	NA	3.40	LB	US	N	5	5	0	0	0	0	51.0
31.1	bone	C3	1	NA	4.90	PHF	CO	N	2	3	0	0	0	0	42.9
44.11	bone	D6?	NA	NA	0.80	UN	US	N	5	5	0	0	0	0	22.1
25.1	bone	B20	4	5	0.40	UN	US	N	5	5	1	0	0	0	14.0

HFM #	Item	Grid	Level	T	Mass (g)	Element	Portion	Side	PF	DF	Burn	Spiral Fracture	Carni Mod	Cut	Max Length (mm)
25.2	tooth	B20	4	5	0.40	UN	US	N	5	5	0	0	0	0	25.1
27.11	bone	C5	NA	NA	0.20	UN	US	N	5	5	0	0	0	0	35.2
27.12	bone	C5	NA	NA	0.20	UN	US	N	5	5	0	0	0	0	15.2
27.13	tooth	C5	NA	NA	0.20	UN	US	N	5	5	0	0	0	0	17.6
27.14	bone	C5	NA	NA	0.01	UN	US	N	5	5	0	0	0	0	12.1
27.17	bone	C5	NA	NA	0.10	UN	US	N	5	5	0	0	0	0	20.6
27.18	bone	C5	NA	NA	0.01	UN	US	N	5	5	0	0	0	0	17.4
27.19	bone	C5	NA	NA	0.01	UN	US	N	5	5	0	0	0	0	7.3
27.21	bone	C5	NA	NA	0.01	UN	US	N	5	5	0	0	0	0	15.7
27.22	bone	C5	NA	NA	0.01	UN	US	N	5	5	0	0	0	0	12.9
27.23	bone	C5	NA	NA	0.01	UN	US	N	5	5	0	0	0	0	10.0
27.24	bone	C5	NA	NA	0.01	UN	US	N	5	5	0	0	0	0	9.3
27.25	bone	C5	NA	NA	0.01	UN	US	N	5	5	0	0	0	0	12.0
27.26	bone	C5	NA	NA	0.01	UN	US	N	5	5	0	0	0	0	7.9
27.27	bone	C5	NA	NA	0.01	UN	US	N	5	5	0	0	0	0	9.0
27.28	bone	C5	NA	NA	0.01	UN	US	N	5	5	0	0	0	0	8.1
27.5	bone	C5	NA	NA	0.70	UN	US	N	5	5	0	0	0	0	36.3
27.7	bone	C5	NA	NA	0.50	UN	US	N	5	5	0	0	0	0	22.5
27.8	bone	C5	NA	NA	0.20	UN	US	N	5	5	0	0	0	0	12.3
27.9	bone	C5	NA	NA	0.20	UN	US	N	5	5	0	0	0	0	14.5
33.6	tooth	C5	NA	NA	0.10	UN	US	N	5	5	0	0	0	0	12.9
44.13	bone	D6?	NA	NA	0.50	UN	US	N	5	5	0	0	0	0	19.3
44.14	bone	D6?	NA	NA	0.20	UN	US	N	5	5	0	0	0	0	18.3
44.15	bone	D6?	NA	NA	0.40	UN	US	N	5	5	0	0	0	0	14.0
44.16	bone	D6?	NA	NA	0.30	UN	US	N	5	5	0	0	0	0	23.0
44.17	bone	D6?	NA	NA	0.30	UN	US	N	5	5	0	0	0	0	17.2
44.18	bone	D6?	NA	NA	0.10	UN	US	N	5	5	0	0	0	0	21.3
44.19	bone	D6?	NA	NA	0.10	UN	US	N	5	5	0	0	0	0	18.0
44.21	bone	D6?	NA	NA	0.10	UN	US	N	5	5	0	0	0	0	16.0
44.22	bone	D6?	NA	NA	0.10	UN	US	N	5	5	0	0	0	0	18.9
44.23	bone	D6?	NA	NA	0.01	UN	US	N	5	5	0	0	0	0	20.1
44.24	bone	D6?	NA	NA	0.01	UN	US	N	5	5	0	0	0	0	17.2

HFM #	Item	Grid	Level	T	Mass (g)	Element	Portion	Side	PF	DF	Burn	Spiral Fracture	Carni Mod	Cut	Max Length (mm)
44.25	bone	D6?	NA	NA	0.01	UN	US	N	5	5	0	0	0	0	6.2
44.26	bone	D6?	NA	NA	0.01	UN	US	N	5	5	0	0	0	0	13.2
44.27	bone	D6?	NA	NA	0.01	UN	US	N	5	5	0	0	0	0	7.9
44.28	bone	D6?	NA	NA	0.01	UN	US	N	5	5	0	0	0	0	7.1
44.29	bone	D6?	NA	NA	0.01	UN	US	N	5	5	0	0	0	0	9.7
44.31	bone	D6?	NA	NA	0.01	UN	US	N	5	5	0	0	0	0	7.0
44.32	bone	D6?	NA	NA	0.01	UN	US	N	5	5	0	0	0	0	15.0
44.33	bone	D6?	NA	NA	0.01	UN	US	N	5	5	0	0	0	0	14.0
44.34	bone	D6?	NA	NA	0.01	UN	US	N	5	5	0	0	0	0	10.9
44.35	bone	D6?	NA	NA	0.01	UN	US	N	5	5	0	0	0	0	8.5
44.36	bone	D6?	NA	NA	0.01	UN	US	N	5	5	0	0	0	0	12.4
44.37	bone	D6?	NA	NA	0.01	UN	US	N	5	5	0	0	0	0	12.2
44.38	bone	D6?	NA	NA	0.01	UN	US	N	5	5	0	0	0	0	8.0
44.39	bone	D6?	NA	NA	0.01	UN	US	N	5	5	0	0	0	0	9.2
44.41	bone	D6?	NA	NA	0.01	UN	US	N	5	5	0	0	0	0	11.1
44.42	bone	D6?	NA	NA	0.01	UN	US	N	5	5	0	0	0	0	6.8
44.43	bone	D6?	NA	NA	0.01	UN	US	N	5	5	0	0	0	0	8.0
44.44	bone	D6?	NA	NA	0.01	UN	US	N	5	5	0	0	0	0	6.8
44.45	bone	D6?	NA	NA	0.01	UN	US	N	5	5	0	0	0	0	4.7
44.46	bone	D6?	NA	NA	0.01	UN	US	N	5	5	0	0	0	0	6.4
44.47	bone	D6?	NA	NA	0.01	UN	US	N	5	5	0	0	0	0	7.0
44.48	bone	D6?	NA	NA	0.01	UN	US	N	5	5	0	0	0	0	6.0
44.49	bone	D6?	NA	NA	0.01	UN	US	N	5	5	0	0	0	0	7.5
44.51	bone	D6?	NA	NA	0.01	UN	US	N	5	5	0	0	0	0	9.9
44.52	bone	D6?	NA	NA	0.01	UN	US	N	5	5	0	0	0	0	9.1
44.53	bone	D6?	NA	NA	0.01	UN	US	N	5	5	0	0	0	0	8.2
44.54	bone	D6?	NA	NA	0.01	UN	US	N	5	5	0	0	0	0	6.8
44.55	bone	D6?	NA	NA	0.01	UN	US	N	5	5	0	0	0	0	7.3
44.56	bone	D6?	NA	NA	0.01	UN	US	N	5	5	0	0	0	0	7.2
44.57	bone	D6?	NA	NA	0.01	UN	US	N	5	5	0	0	0	0	6.9
44.58	bone	D6?	NA	NA	0.01	UN	US	N	5	5	0	0	0	0	10.2
44.59	bone	D6?	NA	NA	0.01	UN	US	N	5	5	0	0	0	0	6.4

HFM #	Item	Grid	Level	T	Mass (g)	Element	Portion	Side	PF	DF	Burn	Spiral Fracture	Carni Mod	Cut	Max Length (mm)
44.6	bone	D6?	NA	NA	2.10	UN	US	N	5	5	0	0	0	0	27.2
44.61	bone	D6?	NA	NA	0.01	UN	US	N	5	5	0	0	0	0	4.3
44.7	bone	D6?	NA	NA	1.00	UN	US	N	5	5	0	0	0	0	41.2
44.8	bone	D6?	NA	NA	1.10	UN	US	N	5	5	0	0	0	0	31.3
44.9	bone	D6?	NA	NA	0.40	UN	US	N	5	5	0	0	0	0	20.3
46.1	bone	D6	NA	NA	0.30	UN	US	N	5	5	0	0	0	0	21.0
44.12	bone	D6?	NA	NA	0.50	UN	US	N	5	5	0	0	0	0	30.0
27.3	bone	C5	NA	NA	0.60	UN	US	N	5	5	0	0	0	0	47.3
27.4	bone	C5	NA	NA	1.80	UN	US	N	5	5	0	0	0	0	48.8